ParisTech
INSTITUT DES SCIENCES ET TECHNOLOGIES
PARIS INSTITUTE OF TECHNOLOGY

AgroParisTech
INSTITUT DES SCIENCES ET INDUSTRIES DU VIVANT ET DE L'ENVIRONNEMENT
PARIS INSTITUTE OF TECHNOLOGY FOR LIFE, FOOD AND ENVIRONMENTAL SCIENCES

Ecole Doctorale ABIES
Agriculture Agriculture Alimentation Food Biologie Biology Environnement Environment Santé Health

Doctorat ParisTech

T H È S E

Document Provisoire

pour obtenir le grade de docteur délivré par

L'Institut des Sciences et Industries du Vivant et de l'Environnement

(AgroParisTech)

Spécialité : Sciences et Procédés des Aliments et Bioproduits

Présentée et soutenue publiquement par

Alexandre RUELLAN

le 26 mai 2015

Conception raisonnée à l'aide de la formulation et du procédé d'un film souple biosourcé et biodégradable pour l'emballage alimentaire

Directrice de thèse : **Sandra DOMENEK**
Co-Directeur de thèse : **Cyrille SOLLOGOUB**
Co-encadrement de la thèse : **Violette DUCRUET, Alain GUINAULT**

Jury

M. Luc AVEROUS, Professeur, UMR 7515 ICPEES, Université de Strasbourg	Rapporteur
M. Jean-Marie RAQUEZ, Professeur, SMPC, Université de Mons (Belgique)	Rapporteur
M. Roland SEGUELA, Directeur de Recherche, UMR 5510 MATEIS, INSA de Lyon	Examinateur
M. Stéphane Bruzaud, Professeur, EA 4250 LIMATb, Université de Bretagne Sud	Examinateur
Mme Anne-Chrystelle DELAMOUR, Directeur R&D, Brodart Packaging	Membre invité
M. Alain GUINAULT, Ingénieur de Recherche, UMR 8006 PIMM, CNAM	Membre invité
Mme Sandra DOMENEK, Maître de Conférences HDR, UMR 1145 GENIAL, AgroParisTech	Directrice de thèse
M. Cyrille SOLLOGOUB, Maitre de Conférences, UMR 8006 PIMM, CNAM	Co-directeur de thèse

AgroParisTech
Nom de l'Unité de recherche
Adresse de l'Unité de recherche

RESUME

L'utilisation de ressources renouvelables et la production de matériaux biodégradables sont des solutions adaptées afin de diminuer l'impact environnemental du secteur des plastiques. Il existe donc une demande du marché pour des produits éco-responsables, à condition que ces derniers soient techniquement et économiquement concurrentiels par rapport aux matériaux classiquement utilisés. Dans le domaine de l'emballage alimentaire, une technique très employée permettant la réalisation de matériaux performants est la création de structures multicouches combinant avantageusement les propriétés de différents plastiques. Néanmoins, de tels matériaux multi-matières sont difficilement recyclables, leur biodégradabilité devient alors une propriété pertinente. Cette étude propose la réalisation de films souples biosourcés et biodégradables pour l'emballage alimentaire, à partir du polylactide et de coproduits de l'huilerie en tant qu'additifs, notamment les condensats de désodorisation. Parmi ces derniers, la solubilité partielle de leurs molécules ainsi que l'effet synergique des constituants liquides et solides à température ambiante, en fonction de la longueur et du degré d'insaturation de leurs chaînes alkyles, ont été montrés comme responsables de l'augmentation de la ductilité du PLA, permettant néanmoins de conserver sa vitrosité à température ambiante et son intéressante rigidité. L'ajout de PHBV au PLA formulé avec les coproduits de l'huilerie a également été étudié, engendrant principalement une amélioration significative de la tenue thermomécanique du matériau. Des essais d'accroissement d'échelle comprenant la production des granulés, l'extrusion à plat de films ainsi que leur impression sur des machines industrielles ont été réalisés. Enfin, avec l'aide du Laboratoire National de Métrologie et d'Essais (LNE), la conformité du film développé avec les exigences légales concernant les matières plastiques destinées au contact des aliments, mais également son aptitude à la biodégradation, ont été vérifiées.

ABSTRACT

The use of renewable resources and the production of biodegradable materials are appropriate solutions to reduce the environmental impact of the sector of plastics. There is thus a demand for eco-friendly products on the market provided they obtain performance equal or superior to synthetic materials currently used. One possibility, widely used in the food sector, to achieve efficient packaging film is the creation of multilayer structures by combining advantageous properties of different plastics. In this case, recycling of materials is difficult and the biodegradability of the packaging becomes relevant. This study proposes designing biobased and biodegradable films for food packaging from polylactide and co-products of the oil mill industry as additives, in particular the deodorization condensates. Among these lasts, the partial solubility of their molecules and the synergetic effect of the liquid and solid fat components at room temperature, depending on their alkyl chain length and unsaturation ratio, have both been observed to be responsible for the ductility increase, while the the higher than room temperature glass transition of PLA and its interesting rigidity were retained. Addition of PHBV to the formulated PLA with oil by-products has also been studied, mainly leading to a significative improvement in the thermomechanical resistance of the material. Scaled-up trials comprising the production of formulated pellets, cast extruded films and their printing using industrial devices were performed. Finally, with the help of the “Laboratoire National de Métrologie et d’Essais” (LNE), the compliance with requirements of Food Contact Material regulation of a formulated film of PLA, as well as its biodegradability, have both been proved.

PRODUCTION SCIENTIFIQUE

Brevet A. Ruellan (BRODART), A.C. Delamour (BRODART), V. Ducruet (INRA), S. Domenek (AGROPARISTECH), A. Guinault (CNAM), C. Sollogoub (CNAM), C. Alfos (ITERG), G. Chollet (ITERG). « Composition augmentant la ductilité d'un polymère thermoplastique ». Demande de brevet prioritaire n° FR1451772, le 04 mars 2014.

Chapitre A. Ruellan, V. Ducruet, S Domenek. Plasticization of poly(lactide). In book: Poly(lactic acid) Science and Technology. Processing, Properties, Additives and. Applications, Edition: 1st, Chapter: 5, pp.124-164, Publisher: RSC Polymer Chemistry Series., Editors: Alfonso Jimenez, Mercedes Peltzer, Roxana Ruseckaite.

Publication D. Rasselet, A. Ruellan, A. Guinault, G. Miquelard-Garnier, C. Sollogoub, B. Fayolle. Oxidative degradation of polylactide (PLA) and its effects on physical and mechanical properties. European Polymer Journal (Impact Factor: 3.24). 01/2014; 50:109–116

Publication A. Ruellan, A. Guinault, C. Sollogoub, V. Ducruet, S. Domenek, Solubility Factors as Screening Tools of Biodegradable Toughening Agents of Polylactide. J. Appl. Polym. Sci. 2015, Special Issue: Manufacturing of Advanced Biodegradable Polymeric Components. *Submitted.*

Publication A. Ruellan, A. Guinault, C. Sollogoub, G. Chollet, A. Ait-Mada, V. Ducruet, S. Domenek, Industrial vegetable oil by-products increase the ductility of polylactide. Express Polymer Letters 2015, *submitted.*

Communication orale A. Ruellan, A. Guinault, C. Sollogoub, S. Domenek, V. Ducruet. Amélioration de la ductilité du poly(lactide) par ajout de condensats de désodorisation d'huile végétale. Matériaux 2014, 24-28 novembre 2014, Montpellier, France.

Communication orale A. Ruellan, S. Domenek, C. Sollogoub, A. Guinault, V. Ducruet. Conception Raisonnée d'Emballages Alimentaires Biosourcés Biodégradables Multicouches (CREABIOM). Journée thématique du RMT ProPack Food "L'Emballage source d'innovation", 17 septembre 2014, Bourg en Bresse, France.

Communication par affiche A. Ruellan, A. Guinault, C. Sollogoub, V. Ducruet, S. Domenek. Influence of the plasticizer chemical structure on the toughening behaviour of PLA. 45 Journées de Calorimétrie et d' Analyse Thermique (JCAT 45), 20-23 mai 2014, Rouen, France.

Communication par affiche A. Kassouf, A. Ruellan, A. Guinault, J. Maalouly, H. Chebib, D. Rutledge, V. Ducruet. ATR-MIR spectroscopy coupled with independent components analysis for the identification of plasticizers in polylactide. The 4th International Conference on Biodegradable and Biobased Polymers (BIOPOL 2013), 2-4 octobre 2013, Rome, Italie.

Communication par affiche M. Boufarguine, A. Ruellan, S. Domenek, V. Ducruet, A. Guinault, G. Miquelard-Garnier, C. Sollogoub. PHBV as a functionnal component for improving ductility of PLA. The 4th International Conference on Biodegradable and Biobased Polymers (BIOPOL 2013), 2-4 octobre 2013, Rome, Italie.

Communication par affiche Damien Rasselet, A. Ruellan, A. Guinault, G. Miquelard-Garnier, C. Sollogoub, B. Fayolle. Thermo-oxidative degradation of polylactide (PLA) at low temperature: physical and mechanical aspects. The 4th International Conference on Biodegradable and Biobased Polymers (BIOPOL 2013), 2-4 octobre 2013, Rome, Italie.

Communication par affiche M. Boufarguine, A. Ruellan, A. Guinault, S. Domenek, V. Ducruet, G. Miquelard-Garnier, C. Sollogoub. PLA-PHBV FILMS : Microstructure effects on mechanical, gas barrier properties and thermoformability. 5^{th} International Symposium on Food Packaging (ILSI 2012). 14-16 novembre 2012, Berlin, Allemagne.

LISTE DES TABLEAUX

Table 1.1 Mechanical properties of PLA and main commodity plastics

Table 1.2 Solubility parameters of monomeric and oligomeric plasticizers

Table 1.3 Glass transition and mechanical properties of PLA plasticized with monomeric external plasticizers

Table 1.4 Glass transition and mechanical properties of PLA plasticized with polymeric external plasticizers

Table 1.5 Overview of physical ageing behaviour of PLA/plasticizer compounds

Tableau 2.1 Principales caractéristiques des polymères utilisés : teneur en L-lactide et hydroxyvalérate, masse molaire moyenne en nombre (M_n) et en poids (M_w) et température de transition vitreuse (T_g)

Tableau 2.2 Formule développée et masse molaire des additifs commerciaux utilisés comme plastifiants

Tableau 2.3 Composition relative des produits et coproduits de l'huilerie utilisés comme plastifiants

Tableau 2.4 Conditions opératoires de mélangeage par mélangeur interne

Tableau 2.5 Conditions opératoires du procédé de thermocompression

Tableau 2.6 Conditions opératoires de mise en œuvre par mélangeur interne et méthodologie de caractérisation

Tableau 2.7 Propriétés comparées des formulations témoins PLA/ATBC

Tableau 2.8 Conditions opératoires du procédé de mélangeage par extrusion bivis et des procédés d'extrusion monovis pour la réalisation de films PLA/CDHP/PHBV

Table 3.1 Processing conditions of blend compounding by twin screw extrusion

Table 3.2 Molar constant for the calculation of solubility values

Table 3.3 Extracted plasticizer contents, molar weight averages and dispersitiy of PLA/plasticizer formulations

Table 3.4 Physical data and computed solubility parameters of PLA and plasticizers

Table 3.5 Tensile testing results and T_g data of PLA/plasticizer formulations

Supporting information S4.1 Processing conditions of melt-mixing twin screw extrusion

Supporting information S4.2 Processing conditions of cast films extrusion

Supporting information S4.3 Used group contribution molar constants

Table 4.1 Composition of hydrogenated vegetable oils and vegetable oil deodorization condensates

Table 4.2 Physical properties and solubility parameters of fatty acids, mono-, di-, and tri-glycerides contained in the hydrogenated vegetable oils and oil deodorization condensates

Table 4.3 Mechanical and thermal properties of formulations

Table 5.1 PODC content and molar weight averages and dispersitiy of PLA and PLA/PODC formulations

Table 5.2 Composition of the PODC

Table 5.3 Physical properties of PLA 4060D and PLA 4060D /PODC films

Table 5.4 Physical properties of neat PLA 4042D and PLA 4042D/PODC sheets

Table 5.5 Overall migration tests in food simulants of PLA 4060D/PODC cast film

Table 6.1 Composition of the PODC

Table 6.2 Mechanical and thermal properties of PLA, PLA/PODC, PLA/PHBV and PLA/PODC/PHBV blends

Table 6.3 Volume relaxation kinetic parameters of PLA, PLA/PHBV, PLA/PODC and PLA/PODC/PHBV

LISTE DES FIGURES

Figure 1.1 Glass transition temperature depression of PLA/ATBC blends as function of ATB content

Figure 1.2 Strain at break values plotted against T_g

Figure 1.3 Glass transition temperature depression as a function of content average molecular weight of PEG

Figure 1.4 Stress-strain plots of initially amorphous neat PLA and amorphous PLA plasticized with 5 wt% and 7.5 wt % of PPG 400, PPG 1000, and PEG 600 **(A)** and for PLA plasticized with 10 wt% and 12.5 wt% of PPG 400, PPG 1000, and PEG 600 **(B)**

Figure 1.5 Stress-strain plots of initially semi-crystalline neat and plasticized PLA, plasticized at 5 wt%, 7.5 wt%, 10 wt% and 12.5 wt% of PEG 600 **(up)**, PPG 400 **(middle)** and PPG 1000 **(down)**

Figure 2.1 Mécanisme d'hydrolyse d'une fonction ester

Figure 2.2 Sécheurs de granulés
(a) Somos 60 L
(b) Motan 100 L

Figure 2.3 Hydrotracer Aboni FMX™

Figure 2.4 Masses molaires du PLA 4060D après extrusion bivis en fonction du temps de séchage préalable et de l'humidité résiduelle

Figure 2.5 **(a)** Mélangeur interne Haake Rheocord 9000
(b) Pales type « roller rotors »

Figure 2.6 **(a)** Presse chauffante Gibitre
(b) Principe de la thermocompression

Figure 2.7 Schéma du moule de thermocompression de plaques

Figure 2.8 Dimensions des éprouvettes utilisées selon la norme ISO 527-2

Figure 2.9 **(a)** Doseur d'alimentation de la résine thermoplastique et pompe pour additif liquide
(b) Extrudeuse bivis Thermo Haake Ptw 16D, L/D = 40:1

Figure 2.10 Schéma du profil de vis utilisé sur l'extrudeuse bivis Thermo Haake Ptw 16D, L/D = 40:1

Figure 2.11 Dispositif « burette chauffante » et son module de chauffe

Figure 2.12 Schéma d'une extrudeuse monovis équipée d'une filière plate et d'une calandre

Figure 2.13 Schéma d'une extrudeuse monovis équipée d'une filière gonflage de gaine

Figure 2.14 **(a)** Extrudeuse monovis Scamex Rheoscam 20 mm 12D
(b) Filière bandelette 40 mm large 1 mm entrefer fixe

Figure 2.15 Extrudeuse monovis Mapre E1 30-33D

Figure 2.16 **(a)** Filière plate 200 mm
(b) Calandreuse

Figure 2.17 **(a)** Système de gonflage de gaine Dr. Collin
(b) Bulle de [PLA 4060D + 10 %m CDHP]

Figure 2.18 Poinçon hélicoïdal « à canaux rayonnants » utilisé dans la filière gonflage de gaine

Figure 2.19 Vis Scamex 20-12D après essai d'extrusion de granulés [PLA 4060D + 15 %m CDHP]

Figure 2.20 Courbes rhéologiques à 100 et 130 °C du [PLA 4060D + 15 %m CDHP], géométrie plan/plan

Figure 2.21 Calandrage d'une feuille [90 %m (PLA 4060D + 10 %m CDHP) + 10 %m PHI 002] obtenue par extrusion monovis « procédé dryblend » en présence d'infondus PHBV

Figure 2.22 **(a)** Système d'extrusion/granulation Dr. Collin 35 mm L/D = 56:1
(b) Zone d'alimentation solide
(c) Granulateur

Figure 2.23 **(a)** Extrudeuse monovis Labtech Engineering 30 mm 30D et filière plate 350 mm
(b) Calandreuse
(c) Découpe des lisières du film
(d) Bobines réalisées

Figure 2.24 **(a)** Procédé d'impression flexographie
(b) Bobines imprimées

Figure 2.25 Etuve Memmert utilisée pour la cristallisation du PLA 4042D

Figure 2.26 Etuve FisherBrand utilisée pour le vieillissement des bandelettes de PLA 4060D

Figure 3.1 Chemical structures of PLA and plasticizers

Figure 3.2 Experimental T_g values of PLA/plasticizer formulations plotted with corresponding Fox equation

Figure 3.3 Typical stress/strain curves of PLA/plasticizer formulations

Figure 3.4 Picture of PLA + 15 wt% plasticizer samples after failure

Figure 3.5 SEM micrographs taken on the longitudinal surface of PLA + 15wt% plasticizer samples near the breaking zone after failure

Supporting information S4.4 Stress/strain curves of PLA blends with free fatty acids, hydrogenated vegetable oils (HPO and HCO), unsaponifiable compounds (squalene, α-tocopherol), and vegetable oil deodorization condensates (palm oil PODC, olive oil OODC, soybean oil SODC and rapeseed oil RODC)

Supporting information S4.5 Thermograms of free fatty acids, hydrogenated vegetable oils (HPO and HCO), unsaponifiable compounds (squalene, α-tocopherol), and vegetable oil deodorization condensates (palm oil PODC, olive oil OODC, soybean oil SODC and rapeseed oil RODC)

Supporting information S4.6 Thermograms of PLA blends with free fatty acids, hydrogenated vegetable oils (HPO and HCO), unsaponifiable compounds (squalene, α-tocopherol), and vegetable oil deodorization condensates (palm oil PODC, olive oil OODC, soybean oil SODC and rapeseed oil RODC)

Supporting information S4.7 PLA + 10 wt% PODC blend stretched at 100 % strain

Figure 4.1 SEM micrographs of blends with PLA at 10 wt%
(a) C16:0
(b) C18:1
(c) PODC

Figure 4.2 Optical micrographs of uniaxially stretched PLA and PLA blends with free fatty acids (C16:0, C18:1) and palm oil deodorization condensate (PODC) at different strain

Figure 4.3 Principal components projection plot of F1 and F2 of the data set

Figure 4.4 Loadings plot of the Principal Components Analysis of the dataset

Figure 5.1 Thermogravimetric curves of neat PLA 4060D pellets, neat PODC and PLA 4060D/PODC blend pellets

Figure 5.2 Stress-strain curves of PLA 4060D and PLA 4060D/PODC films

Figure 5.3 Heatflow (exo-up) of PLA 4060D and PLA4060D/PODC films measured by MDSC

Figure 5.4 Heatflow (exo-up) of neat PODC, PLA 4042D and PLA 4042D/PODC sheets measured by DSC

Figure 5.5 Stress-strain curves of neat PLA 4042D and PLA 4042D/PODC sheets

Figure 5.6 E' and E" curves of PLA 4042D and PLA4042D/PODC sheets measured by DMA

Figure 5.7 Physical aspect change of PLA 4060D/PODC cast film after testing during 10 days at 40 °C in ethanol 50 vol% and acetic acid 3 vol%

Figure 5.8 Biodegradation curves of cellulose reference and PLA 4060D/PODC cast film

---

Figure 6.1 Cast extruded films stored at 40°C during one month
(a) [PLA + 10 wt% PODC]
(b) [90 wt% (PLA + 10 wt% PODC) + 10 wt% PHBV]

Figure 6.2 DSC heating scans of PLA and PLA blends after physical aging at Tg -15 °C for different times

Figure 6.3 PODC contents of PLA/PODC and PLA/PHBV/PODC films determined from thermogravimetric analyses in function of the aging time

Figure 6.4 Dependence of **(a)** Enthalpy loss (δ_H) and **(b)** Peak temperature (T_p) during physical aging of neat PLA, PLA/PODC, PLA/PHBV and PLA/PODC/PHBV films at $T_a = T_g$ - 15 °C as a function of log ($_{\text{aging time (h)}}$)

Figure 6.5 Typical stress/strain curves of neat PLA, PLA/PHBV and PLA/PODC/PBHV films upon physical aging

Figure 6.6 break Mechanical properties of neat PLA, PLA/PHBV and PLA/PODC/PHBV films as function of the aging time
(a) Elongation at break
(b) Young modulus
(c) Stress at yield

Figure 6.7 SEM micrographs of the surface of stretched until breakage samples

ABREVIATIONS

ACP	Analyse en composantes principales
AGM	Acétyl glycérol monolaurate
ATBC	Acétyl tributyl citrate
ATEC	Acétyl triéthyl citrate
CDHP	Condensat de désodorisation d'huile de palme
CED	Densité d'énergie cohésive
d/ρ	Densité
DBM	Diéthyl bishydroxyméthyl malonate
DBM-A-8 (ou **18**)	Diéthyl bishydroxyméthyl malonate-adipoyl dichloride (m=8 ou 18)
DBM-S-4 (ou **7**)	Diéthyl bishydroxyméthyl malonate-succinyl dichloride (m=4 ou 7)
DBS	Dibutyl sebacate
Dehydat VPA 1726	Glucose monoester (Henkel)
DINCH	Di(isononyl) cyclohexane-1,2-dicarboxylate
DMTA ou **DMA**	Analyse thermomécanique dynamique
DOA	Dioctyl adipate
DOP	Dioctyl phtalate
DSC	Calorimétrie différentielle à balayage
E *(MPa)*	Module d'Young ou module élastique
E'' *(MPa)*	Module de perte
$\mathbf{E_D}$	Energie de dispersion
$\mathbf{E_H}$	Energie de liaison hydrogène
$\mathbf{E_P}$	Energie d'interaction polaire
EPE19	Polymère tribloc PEG-b-PPG-b-PEG (Pluronic L35) avec PEG 1900 $g.mol^{-1}$ et PPG 950 $g.mol^{-1}$
EPO	Huile de palme epoxydée

ESO	Huile de soja epoxydée
FDA	Food and Drug Administration
FT-IR	Infra-Rouge à Transformée de Fourier
GMS	Glycérol monostéarate
GTA	Glycérine triacétate ou triacétine
HSP	Paramètres de solubilité de Hansen
l *(m)*	Epaisseur
LA	Acide lactique
LDPE	Polyéthylène basse densité
Loxiol GMS 95	Ester d'acide gras (Henkel)
HDPE	Polyéthylène haute densité
MAF	Fraction amorphe mobile
MDSC	Calorimétrie différentielle à balayage à température modulée
$\mathbf{M_n}$ *(g.mol^{-1})*	Masse molaire moyenne en nombre
M-PEG	Poly(éthylène glycol) monolaurate
$\mathbf{M_w}$ *(g.mol^{-1})*	Masse molaire moyenne en poids
OLA	Oligomères d'acide lactique
OTR *(m^3.m^{-2}.s^{-1})*	Vitesse de transmission de l'oxygène
PA G206/2 (ou **5 ou** 7)	Polyadipate Glyplast® 206/2 (5 ou 7)
PBA	Poly(butylène adipate)
PBAT	Poly(butylène adipate-co-téréphtalate)
PBOH	Poly(1,3-butanediol)
PCL	Polycaprolactone
PDEA	Poly(diéthylène adipate)
PDLA	Poly(D-acide lactique)/ Poly(D-lactide)
P(D,L)LA	Poly(D,L-acide lactique)/ Poly(D,L-lactide)

PDLLA-b-PEG750	Poly(D,L-lactide-b-éthylène glycol) avec M_w du PEG = 750 $g.mol^{-1}$
PEA	Poly(éthylène adipate)
PEG	Poly(éthylène glycol)
PEGCA	Poly(éthylèneglycol-co-acide citrique)
PEG-CH_3	Poly(éthylène glycol) monométhylether
PES	Poly(éthylène succinate)
PET	Poly(éthylène téréphtalate)
PHA	Poly(hexaméthylène adipate)
PHA(s)	Polyhydroxyalcanoate(s)
PHB	Polyhydroxybutyrate
PHBV	Poly(hydroxybutyrate-co-hydroxyvalérate)
PID37	Polysorb® ID 37
PLA	Poly(acide lactique) ou polylactide
PP	Polypropylène
PS	Polystyrène
PVC	Poly(chlorure de vinyle)
QSAR	Quantitative Structure-Activity Relationship
R	Constante universelle des gaz parfaits
RAF	Fraction amorphe rigide
RH *(%)*	Humidité relative
Rikemal PL-710	Diglycérine tetraacétate
RPE	Résonance paramagnétique électronique
SEC	Chromatographie d'exclusion stérique
t et **dt** *(s)*	Temps et sa dérivée
T et **dT** *(°C)*	Température et sa dérivée
tan δ	Tangente de l'angle de perte

TBC	Tributyl citrate
T_c *(°C)*	Température de cristallisation
TEC	Triéthyl citrate
TBC-E	Oligomères de tributylcitrate diéthylène glycol
T_f ou **T_m** *(°C)*	Température de fusion
T_g *(°C)*	Température de transition vitreuse
[THTDP][DE]	Trihexyl tetradécyl phosphonium decanoate
[THTDP][BF4]	Trihexyl tetradécyl phosphonium tetrafluoroborate
UNIFAP	Universal Functional Activity coefficient for Polymers
V_f	Fraction de volume libre
V_a *($cm^3.mol^{-1}$)*	Volume molaire du composé a
ΔCp *($J.g^{-1}.K^{-1}$)*	Saut de chaleur spécifique
ΔH_c ($J.g^{-1}$)	Enthalpie de cristallisation
ΔH_m *($J.g^{-1}$)*	Enthalpie de fusion
$\Delta H_{m\ 100\%}$ *($J.g^{-1}$)*	Enthalpie de fusion du polymère 100% cristallin
ε *(%)*	Elongation à la rupture
σ *(MPa)*	Contrainte au seuil
χ	Paramètre d'interaction de Flory-Huggins
ΔG_{mix} *(J)*	Enthalpie libre de mélange de Gibbs
n_a	Fraction molaire du composé a
ϕ_a	Fraction volumique du compose a
ω_a	Fraction massique du composé a
z	Facteur de coordination
ε_{ab}	Energie nette d'interaction entre les composés a et b
ΔE *($kJ.mol^{-1}$)*	Energie de cohésion
ΔH_{vap} *($kJ.mol^{-1}$)*	Enthalpie de vaporisation

δ_a *(J.cm^{-3})$^{1/2}$*	Paramètre de solubilité d'Hildebrand du composé a
δ_D *(J.cm^{-3})$^{1/2}$*	Paramètre d'interaction de Hansen de l'énergie dispersive
δ_P *(J.cm^{-3})$^{1/2}$*	Paramètre d'interaction de Hansen des contributions polaires
δ_H *(J.cm^{-3})$^{1/2}$*	Paramètre d'interaction de Hansen des liaisons hydrogènes
χ_c *(%)*	Taux de cristallinité

TABLE DES MATIERES

INTRODUCTION GENERALE 1

CHAPITRE 1 - LITERATURE REVIEW: PLASTICIZATION OF POLY(LACTIDE) 11

ABSTRACT 13

1.1. INTRODUCTION 14

1.2. PRINCIPLES OF PLASTICIZING 15

1.3. PLASTICIZER PERMANENCE, MIGRATION AND INTERACTION WITH CONTACT MEDIA 21

1.4. PLA PLASTICIZERS: PROPERTIES, EFFECTS AND PROCESSABILITY 27

1.4.1. Plasticizer Impact on Mechanical Properties 27

1.4.1.1. Monomeric Plasticizers *27*

1.4.1.2. Oligomeric Plasticizers *34*

1.4.1.3. Mixed Plasticizers *45*

1.4.2. Plasticizers as Processing Aids 45

1.5. LONG-TERM STABILITY OF PLASTICIZED PLA 48

1.5.1. Physicochemical Studies of Long-term Stability 48

1.5.2. Chemical Stability and Degradation 54

1.6. PLA PLASTICIZERS DERIVED FROM BIOMASS 56

1.7. OTHER SOLUTIONS FOR PLA TOUGHENING 56

1.7.1. Deformation behaviour of amorphous glassy polymers through damage mechanisms 60

1.7.2. Principles of toughening 61

1.7.3. Examples of toughen polylactide 62

1.8. CONCLUSION 63

REFERENCES 65

CHAPITRE 2 – MATERIAUX, MATERIELS ET PROCEDES DE MISE EN ŒUVRE 75

2.1. MATERIAUX 78

2.1.1. Polymères 78

2.1.2. Additifs 78

2.2. METHODES EXPERIMENTALES 81

2.2.1. Séchage des granulés de PLA 81

2.2.1.1. Description des sécheurs à granulés *81*

2.2.1.2. Protocole expérimental de séchage des granulés *82*

2.2.2. Mise en forme des mélanges et des plaques à l'échelle laboratoire 84

2.2.2.1. Description du mélangeur interne *84*

2.2.2.2. Protocole expérimental d'utilisation du mélangeur interne *85*

2.2.2.3. Description de la presse chauffante *86*

2.2.2.4. Protocole expérimental de thermocompression *87*

2.2.2.5. Validation du protocole de mélangeage à l'échelle laboratoire *88*

2.2.3. Mise en forme des mélanges et des films à l'échelle semi-pilote 91

2.2.3.1. Principe de l'extrusion bivis *91*

2.2.3.2. Description de l'extrudeuse bivis *91*

2.2.3.3. Protocole expérimental d'extrusion bivis *94*
2.2.3.4. Principe de l'extrusion monovis *94*
2.2.3.5. Description de la ligne d'extrusion de bandelettes *96*
2.2.3.6. Description de la ligne d'extrusion de films à plat et films soufflés *97*
2.2.3.7. Protocole expérimental d'extrusion de bandelettes *99*
2.2.3.8. Protocoles expérimentaux d'extrusion de films à plat et films soufflés *101*
2.2.4. Mise en forme des mélanges et des films à l'échelle pilote 105
2.2.4.1. Description de la ligne d'extrusion bivis *105*
2.2.4.2. Protocole expérimental d'extrusion bivis *106*
2.2.4.3. Description de la ligne d'extrusion de films à plat *107*
2.2.4.4. Protocole expérimental d'extrusion de films à plat *108*
2.2.5. Impression par flexographie encres à l'eau à l'échelle pilote 109
2.2.6. Conditionnement d'échantillons en étuve 110
2.2.6.1. Méthode de cristallisation du PLA 4042D *110*
2.2.6.2. Méthode de vieillissement accéléré des échantillons de PLA 4060D *111*

TABLEAU SYNOPTIQUE DES MATERIAUX, MATERIELS, PROCEDES DE MISE EN ŒUVRE ET CARACTERISATIONS UTILISES **112**

REFERENCES **113**

CHAPITRE 3 - SOLUBILITY FACTORS AS SCREENING TOOLS OF BIODEGRADABLE TOUGHENING AGENTS OF POLYLACTIDE **115**

ABSTRACT **118**

3.1. INTRODUCTION **119**

3.2. EXPERIMENTAL **121**
3.2.1. Materials 121
3.2.2. Samples preparation 122
3.2.3. Characterization of PLA films 122
3.2.3.1. Extraction of the plasticizer from the formulated PLA *122*
3.2.3.2. Size exclusion chromatography (SEC) *123*
3.2.3.3. Differential Scanning calorimetry (DSC) *124*
3.2.3.4. Tensile Tests *124*
3.2.3.5. Scanning electron microscopy (SEM) *125*
3.2.3.6. Calculation of the solubility parameters *122*

3.3. RESULTS AND DISCUSSION **128**
3.3.1. Analysis of plasticizer content and average molecular weight of the compounded PLA 128
3.3.2. Miscibility study 129
3.3.3. Tensile properties of plasticized PLA 131

3.4. CONCLUSION **137**

ACKNOWLEDGEMENTS **137**

REFERENCES **138**

CHAPITRE 4 - INDUSTRIAL VEGETABLE OIL BY-PRODUCTS INCREASE THE DUCTILITY OF POLYLACTIDE **141**

ABSTRACT **144**

4.1. INTRODUCTION **145**

4.2. EXPERIMENTAL 147
4.2.1. Materials 147
4.2.2. Film fabrication 148
4.2.3. Characterization 150
4.2.3.1. Composition of HPO, HCO, RODC, SODC, OODC and PODC 150
4.2.3.2. Calculation of molar volume and solubility parameters in PLA 153
4.2.3.3. Differential Scanning Calorimetry (DSC) 154
4.2.3.4. Tensile tests 155
4.2.3.5. Uniaxial deformation under optical microscopy 155
4.2.3.6. Scanning Electron Microscopy (SEM) 155
4.2.3.7. Principal Component Analysis (PCA) 156
4.3. RESULTS AND DISCUSSION 156
4.3.1. Effects of free fatty acids, glycerides, α-tocopherol and squalene on PLA ductility 156
4.3.2. Properties of PLA blends with vegetable oil deodorization condensates 162
4.3.3. Study of the deformation mechanisms involved in PLA/oil deodorization condensates blends 163
4.3.4. Role of the chemical composition of deodorization condensates in ductility improvement 166
4.4. CONCLUSIONS 169
ACKNOWLEDGEMENTS 169
REFERENCES 170

CHAPITRE 5 - BIOBASED AND BIODEGRADABLE BY-PRODUCT OF OIL INDUSTRY AS TOUGHENING AGENT OF POLYLACTIDE 175
ABSTRACT 178
5.1. INTRODUCTION 179
5.2. EXPERIMENTAL 181
5.2.1. Materials 181
5.2.2. Polymer processing 181
5.2.3. Characterization 183
5.2.3.1. Composition of the PODC 183
5.2.3.2. Weighting of PODC content from the formulated PLA materials 183
5.2.3.3. Size Exclusion Chromatography 184
5.2.3.4. Differential Scanning Calorimetry (DSC and MDSC) 185
5.2.3.5. Tensile tests 186
5.2.3.6. Dynamic Mechanical Analysis (DMA) 186
5.2.3.7. Oxygen permeability 186
5.2.3.8. Biodegradation 186
5.2.3.9. Migration of PODC in food simulants 187
5.2.3.10. Sensorial testing 188
5.3. RESULTS AND DISCUSSION 189
5.3.1. Processability of PLA/PODC blends and effects of the process on molecular weight of PLA and PODC contents 189
5.3.2. Thermal and mechanical properties of amorphous PLA 4060D/PODC blends 192
5.3.3. Oxygen barrier properties of amorphous PLA 4060D/PODC films 195
5.3.4. Aging of amorphous PLA 4060D/PODC films at ambient conditions 195
5.3.5. Effect of crystallization of PLA 4042D/PODC blends on thermal and mechanical properties 196

5.3.6. Compliance of PLA 4060D/PODC film with requirements of Food Contact Material regulation 200
5.3.7. Biodegradation of the PLA 4060D/PODC cast extruded film 202
5.4. CONCLUSION 203
ACKNOLEWDGEMENTS 203
REFERENCES 204

CHAPITRE 6 - PHYSICAL AGING AND ITS EFFECT ON MECHANICAL PROPERTIES OF TOUGHENED PLA FILMS 209
ABSTRACT 212
6.1. INTRODUCTION 213
6.2. EXPERIMENTAL 215
6.2.1. Materials 215
6.2.2. Processing 215
6.2.3. Physical Aging 217
6.2.4. Characterization 217
6.2.4.1. Differential Scanning Calorimetry (DSC) 217
6.2.4.2. Tensile tests 218
6.2.4.3. Scanning Electron Microscopy (SEM) 218
6.2.4.4. Quantification of the PODC content 218
6.3. RESULTS AND DISCUSSION 219
6.3.1. Thermal and mechanical properties of PLA/PHBV/PODC blends 219
6.3.2. Effect of aging time on volume relaxation kinetic 220
6.3.3. Mechanical properties evolution upon physical aging 224
6.3.4. Deformation and fracture behavior variations during physical aging 228
6.4. CONCLUSION 231
ACKNOWLEDGEMENT 232
REFERENCES 233

CONCLUSION GENERALE 239

PERSPECTIVES 245

INTRODUCTION GENERALE

Introduction générale

Il existe aujourd'hui une préoccupation croissante en matière d'environnement. Cette tendance se traduit par une demande citoyenne de produits « verts ». Néanmoins, ces produits éco-responsables doivent posséder des performances égales ou supérieures aux matériaux synthétiques communément utilisés afin d'être concurrentiels.

Actuellement, dans le secteur de l'emballage alimentaire, une des possibilités très employée permettant de réaliser des films d'emballage performants est la création de structures multicouches en associant avantageusement les propriétés de différentes matières plastiques. Dans ce cas précis, le recyclage de ces produits multi-matières est difficile et la biodégradabilité de l'ensemble s'avère être une propriété pertinente.

D'autre part, dans l'hypothèse où l'on souhaite diminuer l'impact environnemental des emballages plastiques, la substitution du carbone fossile par l'utilisation de la biomasse renouvelable promet des gains substantiels. Parmi les différentes matrices biosourcées et biodégradables, les polyesters montrent un bon potentiel pour la fabrication de matériaux d'emballage. On retient notamment le polylactide (PLA) qui est déjà disponible sur le marché en grands volumes. Ce polymère est d'autant plus intéressant qu'il peut être mis en forme sur des équipements d'extrusion classiques.

Néanmoins, bien que le PLA possède beaucoup des exigences nécessaires aux thermoplastiques pour le packaging, ce polymère connu depuis les années 1970 souffre d'une trop faible élongation à la rupture lors d'une déformation mécanique, ce qui limite d'une façon substantielle son développement.

La solution la plus couramment utilisée pour améliorer la ductilité des matériaux polymères consiste en l'adjonction d'additifs plastifiants. Cette étape est généralement réalisée à l'aide

de produits pétrochimiques ne permettant pas de conserver les avantages écologiques du produit, et ce d'autant plus qu'un plastifiant est usuellement ajouté en quantité élevée (entre 10 %m et 30 %m). Par ailleurs, l'adjonction d'un plastifiant dans un matériau polymère tend généralement à diminuer sa température de transition vitreuse (T_g) ainsi que sa rigidité, caractéristiques physiques du matériau souvent primordiales pour l'application visée. En effet, dans le cas d'un PLA amorphe ou faiblement cristallin, il importe que la T_g du matériau formulé soit suffisamment haute pour que les granulés ou les bobines de film ne souffrent pas de phénomènes de « thermo-collage » lors du stockage parfois rudimentaire. De plus, il est primordial que la rigidité du film reste suffisante pour correspondre à une utilisation normale par les consommateurs, le produit ne devant pas facilement subir de déformations permanentes pouvant nuire à l'emballage, tant sur l'aspect de la conservation de l'aliment que sur celui de l'esthétique.

D'autre part, la mise sur le marché de nouveaux emballages alimentaires ou de nouvelles molécules est soumise à une réglementation très stricte au niveau Européen. Les risques d'utilisation d'une nouvelle substance chimique entrant dans la composition d'un emballage, d'un point de vue de l'exposition du consommateur (migration, exposition, etc…) et de sa toxicité, doivent être évalués de manière très stricte. Ces substances autorisées sont ensuite classées dans une liste : la Liste Positive (règlement CE 1935/2004).

Enfin, bien que le prix du PLA, grâce aux volumes de production en constante croissance, ne soit devenu que récemment concurrentiel pour s'attribuer des parts de marchés significatives, le coût de l'additif doit rester maîtrisé pour ne pas faire augmenter le tarif du produit final.

Le projet BIP-ADEME 2010-2014 « Conception Raisonnée d'Emballages Alimentaires BIOdegradables Multicouches » (CREABIOM), porté par le groupe Brodart, société familiale française centenaire spécialisée dans l'impression et la transformation d'emballages souples et

semi-rigides destinés pour 80 % à l'agro-alimentaire, a réuni 6 partenaires au sein d'un consortium. Les objectifs du groupe Brodart de se prémunir envers les futures mesures environnementales sur le conditionnement alimentaire, d'être acteur dans le développement de nouvelles solutions au niveau de la transformation et de prévoir les prochains investissements/évolutions machine en fonction des développements biosourcés en cours, ont conduit à la création d'un poste de doctorant CIFRE pendant 36 mois dont les résultats sont présentés dans ce document.

Concernant la fabrication de films multicouches incluant des polymères compostables, plusieurs pistes avaient déjà été testées par Brodart, notamment des solutions à base de PLA et de NatureFlex™ sur base papier, ainsi que l'enduction des composés biosourcés, solutions ne permettant pas d'obtenir de réponse satisfaisante aux niveaux de la tenue du packaging, de la perméabilité (remplacement de l'aluminium), ni sur les possibilités de complexage encore non industrielles dans le domaine des biosourcés. Ainsi, pour réussir le développement de nouveaux films utilisant des matériaux biosourcés dans différentes applications alimentaires telles que l'emballage de fromages ou de barres céréalières, le suremballage de café, le céllophanage et les intercolis, Brodart a dressé le cahier de charges suivant : un produit transparent, souple; imprimable, résistant à la déchirure, ayant une basse température de scellage (70-80 °C), une aptitude à la surgélation (-18 °C) et à la stérilisation (120 °C), une faible épaisseur (12-40 µm), ne dégageant pas ou peu d'odeurs, apte au contact gras, sec, humide et acide, ayant une capacité d'adsorption d'eau mais une importante barrière aux arômes.

Il serait très difficile pour un matériau de réunir autant de caractéristiques. Le complexage, opération couteuse mais très versatile, faisant intervenir des adhésifs ou liants afin d'assurer l'adhésion des couches des films et/ou des traitements de surface (chimique, Corona, flammage, etc…), pourra être utilisé par Brodart afin de compléter les caractéristiques

techniques du matériau développé selon l'application souhaitée. Pour cela, les matériaux compléxés seront, dans la mesure du possible, biosourcés et biodégradables (cellulose, paraffine, etc.).

De manière générale, l'objectif de ces travaux de recherche a été défini comme la recherche d'une source biosourcée, stable et peu onéreuse d'additifs biodégradables et aptes au contact alimentaire, permettant l'obtention d'un film de PLA souple de faible épaisseur à l'aide des procédés de plasturgie classiques, utilisable en tant que matrice complexable, dont les propriétés mécaniques et thermiques seront compatibles avec une transformation industrielle classique (impression, perforation, découpe, pliage, etc.) et une utilisation de commodité par les utilisateurs.

Les coproduits de l'huilerie alimentaire, marchandises faiblement valorisées, peuvent constituer une intéressante voie de substitution aux additifs et plastifiants issus de la pétrochimie. A titre d'exemple, les études préliminaires au projet ont estimé que les tocophérols et polyphénols issus des procédés de raffinage de l'huile possèderaient des propriétés antioxydantes, pouvant limiter la dégradation des polymères lors de la polymérisation et/ou du procédé. Les cires, lipides et phospholipides auraient potentiellement des propriétés plastifiantes et/ou d'aides aux procédés, permettant ainsi de diminuer les températures de mise en forme et de maîtriser les cristallinités. Les standolies, à savoir des lipides complexes, pourraient également posséder des propriétés anti-chocs. Cependant, des verrous technologiques tels que la stabilité thermique des intrants lors du procédé ou la maîtrise de la pureté des coproduits ont été identifiés.

Aidé de l'Institut des Corps Gras (ITERG), partenaire du projet CREABIOM spécialisé dans les huiles et matières grasses d'origines végétales et animales, une étape de sélection réalisée au cours de cette thèse, a permis de discriminer les condensats de désodorisation d'huiles

végétales (extrants issus d'un procédé de distillation utilisant la vapeur d'eau haute température) comme source de nombreuses molécules d'intérêt, notamment des acides gras libres saturés et insaturés, des glycérides, des stérols et autres composés hydrocarbonés. Par ailleurs, ce procédé étant récurrent dans le raffinage des huiles alimentaires avant leur mise sur le marché, l'approvisionnement en grandes quantités a été jugé comme potentiellement aisé. En outre, les conditions de désodorisation ayant une incidence sur les qualités organoleptiques de l'huile commercialisée, ce procédé est généralement très rigoureux, conduisant à une bonne reproductibilité des coproduits formés. Enfin, cette distillation étant réalisée sur la quasi-totalité des huiles, quelle qu'en soit la source végétale, un large panel en termes de composition et concentration en corps gras et dérivés est disponible. Une étude sur le choix d'une source végétale générant un condensat de désodorisation au profil adéquat a été réalisée et les effets sur les propriétés thermomécaniques du PLA étudiés.

Par ailleurs, afin de pallier à la faible stabilité thermomécanique du PLA, nous avons opté pour l'utilisation de poly(hydroxyalcanoates) (PHAs), dont les formes les plus disponibles sur le marché, le poly(3-hydroxybutyrate) (PHB) et le poly(3-hydroxybutyrate-co-valérate) (PHBV), peuvent également être mises en forme sur des équipements de plasturgie existants et se distinguent par une très grande cristallinité qui donne lieu à une bonne stabilité thermique en dessous de leur point de fusion. Ces polymères sont issus de biotechnologies de pointe, lesquelles présentent la particularité de produire des bioplastiques à partir de ressources diverses, telles que les amidons issus de céréales, mais également d'huile ou de déchets. Ces productions bactériennes sont aujourd'hui relativement réduites en volume. Veolia Environnement, partenaire du projet CREABIOM et leader dans le domaine de l'assainissement municipal et industriel, a pour cela lancé un programme de développement industriel visant à produire des PHAs à partir de boues de station d'épuration. Cette

production devrait à terme valoriser une ressource non alimentaire ne mobilisant pas de terres arables et être localisée sur tout le territoire français.

Afin de mener à bien l'ensemble de ces développements, ce travail de thèse s'est inscrit dans le cadre de deux équipes de recherche :

- Le laboratoire des Matériaux Industriels Polymères du Cnam, partie intégrante de l'équipe « Architecture, propriétés et procédés des polymères » (ArPE) au sein de l'UMR 8006 « Procédés et Ingénierie en Mécanique et Matériaux » (PIMM) du centre de Paris d'Arts et Métiers ParisTech dont la recherche s'attache à comprendre la relation entre les procédés, la microstructure et les propriétés des polymères (amorphes, semi-cristallins et réseaux réticulés, dont les élastomères) et de matériaux polymères multiphasés (composites, polymères micro (ou nano) chargés, mélanges de polymères, etc.). De ce fait, il dispose notamment des principaux équipements de transformation rencontrés dans l'industrie des polymères (extrusion, injection, thermoformage, compression des thermoplastiques) à l'échelle laboratoire (1 à 10-15 $kg.h^{-1}$).

  Et,

- L'équipe « Interaction Matériaux Milieu au Contact » (I2MC) au sein de l'UMR 1145 « Génie Industriel Alimentaire » (GENIAL), dont l'objectif est de comprendre les mécanismes qui contrôlent les propriétés barrière ou de sélectivité des matériaux au contact notamment de produits alimentaires. Pour cela, l'équipe dispose de nombreux moyens de caractérisation physicochimiques (MDSC, ATG, perméamètre, etc.) et de chimie analytique (SEC, GC, GC-MS, ATR-IR, etc.)

Ce mémoire est organisé en 6 chapitres s'articulant autour de 5 publications scientifiques publiées, soumises ou en passe de l'être. L'ensemble est encadré par une introduction générale et une conclusion s'ouvrant sur des propositions et perspectives de recherche.

- L'étude bibliographique (publication n°1, parue) présentée au chapitre 1, est consacrée à l'étude de l'amélioration de la ductilité du PLA via son additivitation et plus spécifiquement au travers de sa plastification externe. Les principes physiques, les théories relatives à la solubilité, les effets sur la processabilité, la modification des propriétés thermomécaniques ainsi que l'évolution des caractéristiques des matériaux au cours du temps sont étudiés. Ce chapitre bibliographique contient et complète le chapitre "Plasticization of Poly(lactide)" paru dans Poly(lactic acid) Science and Technology : Processing, Properties, Additives and Applications, Alfonso Jiménez, Mercedes Peltzer & Roxana Ruseckaite (Eds). RSC Polymer Chemistry Series. 2014.

- Le second chapitre présente succinctement les matériaux, les matériels et les étapes d'optimisation des procédés de mise en œuvre utilisés au cours du projet. Ces différentes phases ont été menées en vue de l'établissement d'une formulation de granulés, la réalisation de films fins selon les procédés de plasturgie conventionnels et leur transformation.

Les résultats expérimentaux sont présentés en 4 chapitres successifs :

- Le troisième chapitre (publication n°2, soumise) aborde l'effet de la solubilité des additifs plastifiants calculée par les méthodes de Hansen et de Hildebrand, sur les propriétés thermomécaniques du PLA, en vue de la discrimination de plastifiants biosourcés et biodégradables. Ce chapitre contient la publication "Solubility Factors as Screening Tools of Biodegradable Toughening Agents of Polylactide" soumise pour publication au mois de février 2015 à la revue scientifique internationale Journal of

Applied Polymer Science pour le Special Issue “Manufacturing of Advanced Biodegradable Polymeric Components”.

- Le quatrième chapitre (publication n°3, soumise) est consacré à l’étude des effets de la composition des condensats de désodorisation d’huile végétale sur la modification des propriétés mécaniques et thermiques du PLA. Pour cela, quatre condensats de sources végétales différentes (olive, colza, palme et soja) et leurs principaux constituants (acides gras libres, stérols, composés hydrocarbonés) ont été mélangés au PLA par extrusion bivis à des concentrations allant jusqu’à 20 %m. Une Analyse en Composantes Principales (ACP) a notamment été réalisée afin de réduire le nombre de variables et d’identifier des critères d’efficacité. Ce chapitre contient la publication “Industrial vegetable oil by-products increase the ductility of polylactide” soumise pour publication au mois de mars 2015 à la revue scientifique internationale Express Polymer Letters.

- Le cinquième chapitre (publication n°4, non soumise) est centré sur la caractérisation du PLA additivé à 10 %m de condensat de désodorisation d’huile de palme, produit sélectionné grâce à la précédente étude. Pour cela, deux grades ont été utilisés : le PLA 4060D, résine amorphe ne pouvant cristalliser en conditions normales, et le PLA 4042D, grade semi-cristallin. Les effets du condensat sur la processabilité, les propriétés thermomécaniques, le vieillissement, la cristallisation, l’aptitude au contact alimentaire et la biodégradabilité ont été analysés. Ce chapitre contient la publication “Biobased and biodegradable by-product of oil industry as toughening agent of polylactide” qui sera proposée très prochainement à la revue scientifique internationale Journal of Applied Polymer Science.

- Le sixième et dernier chapitre (publication n°5, non soumise) amorce l'étude des effets du condensat de désodorisation d'huile de palme et ceux du PHBV (3 % HV) sur la relaxation du PLA vitreux à une température proche de T_g. Les paramètres cinétiques de relaxation enthalpique ont été calculés et l'évolution des propriétés mécaniques en traction uniaxiale ainsi que les mécanismes de déformation associés ont été observés. Sous reserve de conforter les résultats présentés dans ce manuscrit à l'aide d'analyses complémentaires, l'article "Physical aging and its effect on mechanical properties of toughened PLA films" devrait être dans les prochaines semaines proposé pour publication à une revue scientifique internationale à comité de lecture.

CHAPITRE 1

TABLE OF CONTENTS

ABSTRACT **13**

1.1. INTRODUCTION **14**

1.2. PRINCIPLES OF PLASTICIZING **12**

1.3. PLASTICIZER PERMANENCE, MIGRATION AND INTERACTION WITH CONTACT MEDIA **21**

1.4. PLA PLASTICIZERS: PROPERTIES, EFFECTS AND PROCESSABILITY **27**

1.4.1. Plasticizer Impact on Mechanical Properties 27

1.4.1.1. Monomeric Plasticizers *27*

1.4.1.2. Oligomeric Plasticizers *34*

1.4.1.3. Mixed Plasticizers *45*

1.4.2. Plasticizers as Processing Aids 45

1.5. LONG-TERM STABILITY OF PLASTICIZED PLA **48**

1.5.1. Physicochemical Studies of Long-term Stability 48

1.5.2. Chemical Stability and Degradation 54

1.6. PLA PLASTICIZERS DERIVED FROM BIOMASS **56**

1.7. OTHER SOLUTIONS FOR PLA TOUGHENING **60**

1.7.1. Deformation behaviour of amorphous glassy polymers through damage mechanisms 60

1.7.2. Principles of toughening 61

1.7.3. Examples of toughen polylactide 62

1.8. CONCLUSION **63**

REFERENCES **65**

Chapitre 1 - Literature Review: Plasticization of Poly(lactide)

Alexandre Ruellan[a,b,c], Violette Ducruet[d], Sandra Domenek[b]

[a] *Arts et Métiers ParisTech, Laboratoire PIMM, 21 rue Pinel, F-75013 Paris.*
[b] *AgroParisTech, Ingénierie Procédés Aliments, 1 avenue des Olympiades, F-91300 Massy.*
[c] *Brodart Packaging, Département R&D, 1 rue du Stand, F-10700 Arcis-Sur-Aube.*
[d] *INRA, Ingénierie Procédés Aliments, 1 avenue des Olympiades, F-91300 Massy.*

Abstract

External plasticization is a widely applied technique to improve PLA processability and toughness. Keys to successful plasticization of PLA are the miscibility of the plasticizer and its permanence in the polymer structure to ensure long-term stability of the material. To provide rules for successful plasticizing of PLA, a brief reminder of physicochemical mechanisms behind plasticization is given and the main theories allowing for the calculation of solubility parameters are summarized. To make use of this approach, a number of solubility parameters were gathered for potential PLA plasticizers. This chapter provides furthermore a comprehensive overview of literature results on glass transition temperatures and mechanical properties obtained for PLA and PLA nanocomposites mixed with monomeric and polymeric plasticizers. Additionally, physical and chemical long-term stability of plasticized materials is detailed. Finally, novel strategies of compounding PLA with additives derived from by-products of agriculture and food industries and the use of low or no-miscible toughening agents are briefly discussed.

1.1. Introduction

Poly(lactic acid) (PLA) offers the opportunity to replace petroleum-based commodity plastics in a cost-effective way because of its numerous advantages, such as ease of processing, satisfying mechanical properties, glass transition higher than room temperature, ability for heat sealing, high transparency, gloss, printing ability, etc.[1]

PLA is, however, a rigid and brittle polymer with medium tensile strength but low deformation at break. **Table 1.1** gives main characteristics of PLA compared to petrochemical commodity plastics. Furthermore, PLA exhibits slow crystallization rate.[2] Plasticization is a widely used technique to increase polymer ductility. Furthermore, it can also improve processability, for example by melting point depression, improving crystallization rates and change service applications by a decrease of the glass transition temperature. It affects moreover other properties, such as optical clarity, electric conductivity or resistance to abiotic or biological degradation. In consequence a large literature addresses the plasticizing of PLA with a number of different molecules and processes used.

Table 1.1 Mechanical properties of PLA and main commodity plastics

	T_g *(°C)*	**E** *(GPa)*	**σ** *(MPa)*	**E** *(%)*
PET	70 ─ 80	2.8 ─ 4.1	275	60 ─ 165
PS	105	2.9	45	3
HDPE	-125	0.4 ─ 0.95	10 ─ 60	400 ─ 1,800
LDPE	-130	0.1 ─ 0.9	9 ─ 15	100 ─ 800
PP	-20 ─ -5	0.9	31 ─ 45	20
PLA	58 ─ 60	2 ─ 3	40 ─ 70	10

Data compiled from ref [1a, 1c, 3]

Plasticizers can be classified as internal or external plasticizers: internal plasticizers can be co-polymerized into the polymer structure or react with the original polymer; external plasticizers are not chemically attached to the polymer chain by covalent bonds. They are typically high boiling point liquids having a molecular mass lower than 600 g mol^{-1}. This chapter seeks to give an overview of recent results in order to provide the reader with some simple guidelines to successfully plasticizing PLA with external plasticizers.

1.2. Principles of Plasticizing

Plasticization can be explained by several theories[4] which are initially based on physical observations such as the decrease of elastic moduli, viscosity or glass transition temperature. Since the beginning of the 1940's, scientists have elaborated different theories which all tried to clarify critical phenomena observed in plasticized polymer materials.

First works[5] modeled the small plasticizer molecules as being partly attached to the macromolecules with a pending portion acting as lubricants. Thereby, plasticizer molecules should have a specific chemical structure in order to create points of attraction with the polymer chains and leave an unattached portion. Then, this lubrication model was extended with the notion of voids filled by plasticizer between the macromolecules, establishing a structure of parallel alternate layers of polymers lubricated by strata made of plasticizers, which break intermolecular bonds between polymer chains. Furthermore, for Houwink[6] the quantity of broken links between macromolecules was dependent on the swelling rate induced by the dissolving ability of the plasticizer, which is higher when the respective polarities of polymer and plasticizer are similar.

Afterwards, based on the hypothesis that the elasticity development in plasticized PVC was due to the enhancement of micro-Brownian motions of the polymer,[7] Doolittle,[8] Stickney and Cheyney[9] and Alfrey et al.[10] developed the Gel Theory. They considered that the mechanical properties of a polymer were due to the elastic resistance of entangled segments of the macromolecules structured as a three-dimensional network. The plasticizer molecules which are dissolved into the polymer matrix break some points of attachment between macromolecules leading to an easier glide. Moreover, due to the dynamic equilibrium between plasticizers and polymer chains, phenomena of aggregation and disaggregation of cohesion links between macromolecules occur. However, due to the too high cohesion forces

existing inside the polymer crystallites, these events only happen in the amorphous regions of the polymer network.[11] The main effect of the addition of plasticizers to a polymer can also be rationalized as an increase in free volume of the system. The Free Volume Theory relies on the assumption that the free volume (*i.e.* not occupied space) of a polymer system can be decomposed into interstitial free volumes, distributed continuously in space and a discontinuous distribution of holes. The Free Volume Theory has been principally developed to describe the transport of small molecules in solid matrices. The Cohen–Turnbull–Fujita model[12] describes successfully the dependence of diffusivity in swollen polymer systems in assuming that the free volume of the binary system is the sum of the fractional free volume of the polymer and of the solvent. The solvent has thus a large contribution to the free volume of the system. The main action of plasticizers is to increase the free volume of the polymer/ plasticizer system by augmenting the space between polymer chains in spreading them apart. They form secondary bonds with the polymer and reduce secondary bonds between polymer chains. Fox and Flory postulated the Free Volume Theory for plasticizing after they studied viscosity, thermal expansion coefficients and specific volume of polymers, as a function of temperature,[13] and showed that viscosity at the glass transition temperature was similar for all polymers.[14] To explain this phenomenon, Williams[15] related the viscosity to the volume between macromolecules. He concluded that for the glass transition to take place, a proper volume between macromolecules, regardless of their chemical structure, has to be reached. It was later estimated[16] for all polymers to be 0.0646 $cm^3.g^{-1}$. Thereby, above this volume, enough energy and space are available for configurational changes, and below T_g the amorphous structure is frozen. Increasing free volume allows for more mobility of the macromolecular chain and affects in consequence the relaxation properties of the polymer in lowering the energy needed (*i.e.* the glass transition temperature) to enable the motion of the macromolecules segments. It explains typical plasticizer effects, such as increased ductility,

lowered glass transition temperature, raised crystallization rates, changed optical and conductivity properties, etc. A plasticizer needs thus to be bulky to develop large free volume, molecules should be miscible to permit introduction into the system and to avoid phase separation, and have preferentially low volatility to prevent loss during ageing.

The inverse effect of plasticizing is sometimes observed when a small quantity of plasticizer is added to the polymer not allowing for sufficient swelling of the amorphous phase. In this case, the free volume increase allows the amorphous phase to gain more order and to enhance the size and the number of the hypothetical crystallites.[17] This results in stronger elastic moduli and higher tensile strength, opposite effects to the expected ones, being called antiplasticization.

The choice of a plasticizer is mainly ruled by its compatibility with the polymer material involved. In fact, as explained by the plasticization theories, plasticizer molecules have to deeply penetrate into the macromolecules network and remain stable inside. Thereby, the initial emulsion during the mixing process using an extruder or roll mixers requires a thermodynamically favorable plasticizer/polymer pair. In order to quantify the compatibility, several approaches have been developed.[4] The most complex ones are the QSAR (Quantitative Structure-Activity Relationship)[18] or UNIFAP (Universal Functional Activity coefficient for Polymers),[19] which are highly effective, but need extensive amounts of data and consequently might be uncomfortable to employ in a first approach.

Another way[20] is the determination of the Flory–Huggins interaction parameter noted χ. It is a dimensionless semi-empirical constant which can depict the compatibility level between a plasticizer and a polymer. The lower the χ value is, the better the compatibility. The highest value for a plasticizer to be considered as compatible enough with the polymer is 0.5. This theory is based on the Gibbs free energy of mixing equation[21] and can be expressed as:

$$\Delta G_{mix} = \Delta H_{mix} - T\Delta S_{mix} \quad \textbf{(1.1)}$$

$$\frac{\Delta G_{mix}}{RT} = n_a \ln \phi_a + n_b \ln \phi_b + \chi \phi_a \phi_b \left(n_a + n_b \frac{V_b}{V_a}\right) \quad \textbf{(1.2)}$$

$$\chi = \frac{z\Delta\varepsilon_{ab}}{RT} \quad \textbf{(1.3)}$$

$$\Delta\varepsilon_{ab} = \left(\frac{\varepsilon_{aa}+\varepsilon_{bb}}{2}\right) - \varepsilon_{ab} \quad \textbf{(1.4)}$$

where ΔG_{mix} is the Gibbs free energy of mixing, n_a and n_b are respectively the mole fractions of plasticizer and polymer, φ_a and φ_b are respectively the volume fractions of plasticizer and polymer, χ is the Flory–Huggins interaction parameter, z is the coordination number and ε_{aa}, ε_{bb}, ε_{ab} are respectively the net energy associated to the contacts established between pure plasticizer molecules, pure polymer molecules and their mixture.

Another useful tool is the Hildebrand solubility theory, which is applicable to apolar and moderately polar systems. For strongly polar systems, it is unable to correctly qualify the compatibility between components.[22] However, the massive amount of interaction parameters data obtained in recent decades, and mainly the Small's method[23] allowing to assess them, make this theory quite efficient and readily applicable. The Hildebrand solubility parameter (δ) can be defined as the square root of the cohesive energy density (CED) and is measured in $(MJ.m^{-3})^{0.5}$. This parameter indicates the polarity level of the component and goes from 12 $(MJ.m^{-3})^{0.5}$ for nonpolar components to 23 $(MJ.m^{-3})^{0.5}$ for water. The larger the difference between the plasticizer and the polymer solubility parameters is, the lower their compatibility.

$$\delta = \sqrt{\frac{\Delta E}{V_m}} = \sqrt{\frac{\Delta H_{vap} - RT}{V_m}} \quad \textbf{(1.5)}$$

where ΔE is the cohesive energy, V_m is the molar volume and ΔH_{vap} is the heat of vaporization.

Another interesting way to predict compatibility, and probably the most useful theory for PLA, has been developed by Hansen.[24] He assumed that the cohesive energy (derived from the free energies of vaporization of solvents as the Flory–Huggins parameter χ and Hildebrand's δ) could be split into three terms, each representing a kind of contribution: the dispersion energy (E_D), the polar cohesion energy (E_P) and the hydrogen bonding energy (E_H). Then, divided by the molar volume, the cohesive energy becomes:

$$\frac{\Delta E}{V_m} = \delta^2 = \delta_D^2 + \delta_P^2 + \delta_H^2 \qquad \textbf{(1.6)}$$

where δ_D, δ_P and δ_H are respectively the interaction parameters of dispersive energy, polar interaction and hydrogen bonding.

The strength of this theory relies in the three-dimensional interpretation related to this method. In fact, each of the three contribution parameters can be considered as a coordinate in space. Since the plasticizer and the polymer both have some specific contribution parameters, it is therefore possible to calculate the spatial distance between them and so determine their thermodynamical similarity degree. Thereby, the acceptance degree of the polymer, which partly depends on its molecular weight or its crystallinity degree, can be defined as a sphere radius. The plasticizers whose coordinates are located inside the sphere are dissolving or swelling the polymer whereas those outside are not miscible within the polymer matrix. Another interesting point is that compounds with identical solubility parameters according to Hildebrand's theory are now able to be distinguished.[25] Finally, once again, the closer both plasticizer and polymer coordinates are, the better the compatibility:

$$distance = \left[4\left(\delta_{D\,Plast} - \delta_{D\,Pol}\right)^2 + \left(\delta_{P\,Plast} - \delta_{P\,Pol}\right)^2 + \left(\delta_{H\,Plast} - \delta_{H\,Pol}\right)^2\right]^{1/2} \qquad \textbf{(1.7)}$$

Note that the factor ‘‘4’’ is used to obtain a convenient fit to experimental data. Moreover, as for Hildebrand’s solubility parameter, it is possible to calculate the Hansen parameters using a similar increment method as Small’s or van Krevelen approaches.

Some solubility parameters and molar volume values[24b] for the main plasticizers chemical families are given in **Table 1.2**. Regarding the Hansen parameters data table, the relative energy difference (RED) between PLA and molecules has been calculated by dividing the distance by the PLA solubility sphere radius.[25] Therefore, closer from zero the value is, the better the miscibility. Furthermore, a distance value higher than 1 means that the molecule is out of the PLA solubility sphere and it will not be miscible within the PLA matrix.

On the other hand, the molar volume informs on the diffusion ability of the molecule getting into the polymer network.[25] The smaller it is, the faster the molecule is likely to diffuse. Thereby, a molecule having a low molar volume and a high distance value will exude out of PLA and induce poor ageing properties. Moreover, according to the free volume theory, a plasticizer with a high molar volume would be more efficient. Taking into account these indications, molecules such as di(ethyl-hexyl) phthalate (DEHP), tricresyl phosphate or triisooctyl trimellitate would potentially be good plasticizers for PLA. Finally, comparing the solubility values obtained for Hildebrand and Hansen theories, respectively, some differences can be noticed. For example, according to Hildebrand, tributyl citrate (TBC) and butyl benzoate would have nearly the same compatibility with PLA, whereas Hansen theory says that butyl benzoate would be almost ‘‘twice as compatible’’ as TBC. Nevertheless, the Hansen theory usually provides more reliable indications for PLA compatibilities than Hildebrand’s.[25]

1.3. Plasticizer Permanence, Migration and Interaction with Contact Media

Miscibility of plasticizers with the polymer matrix and their diffusion rate inside the structure are important for their permanence. Migration means removing the plasticizer from the material, being extracted into a neighboring gas (evaporation), liquid or solid phase (extraction), and it is one of the toughest challenges in the choice or development of an external plasticizer.

The physicochemical mechanism behind the migration is the transport (diffusion) of molecules in solid phases and the partitioning with the neighboring phase. Therefore, the plasticizer should have low vapor pressure and diffusion rate in the polymer. Plastic materials are often in contact with stationary or flowing liquids or with solid materials to where plasticizers can be leached out. Besides the technological problems raised by leaching out of the plasticizer, there are evident potential risks for health and the environment. PLA is furthermore a biodegrading polymer, and consequently the plasticizer becomes inevitably freed in end-of-life treatments, such as composting. These problems are addressed in PLA plasticizing by using plasticizers admitted for food contact materials and, preferentially, biodegradable by themselves. To decrease migration problems and increase permanence, the rate of transport of the molecules inside the polymer matrix has to be slowed down. This can be achieved by using high molecular mass plasticizers, as diffusivity decreases with increasing molecular mass.[26]

In the case of small plasticizers, the considered molecules need to be miscible, *i.e*. to present strong intermolecular forces with the polymer. In the case of partial miscibility, phase separation occurs when the miscibility limit of the plasticizer is exceeded and pure plasticizer phase and enriched polymer phase are observed. Thus, two glass transitions can be observed, one of the plasticizer enriched or pure plasticizer phase and one of the polymer containing the

plasticizer at its miscibility limit. This can give rise to the presence of plasticizer droplets on the surface especially during ageing. Polymeric plasticizers, possessing the advantage of low volatility and high permanence, have, however, the drawback of low miscibility and reduced efficiency. Compared to monomeric plasticizers, they have fewer chain ends per mass of plasticizer and develop lower free volume. Branched structures will bring more free volume to the system and will be often more efficient in increasing polymer mobility inside the material than linear molecules of same molecular weight. An interesting result was obtained recently by Fang et al.[26c] who showed that the introduction of flexible chemical structures near the center of mass of a molecule can have a tremendous impact on the diffusion coefficient. In the case of biphenyls, it was found that the addition of one -CH_2 group between benzene rings diminished the diffusion coefficient by one order of magnitude. However, compatibility with the target polymer needs to be ensured for example by using those methods of solubility prediction discussed earlier.

Table 1.2 Solubility parameters of monomeric and oligomeric plasticizers

	Reference			Hildebrand solubility parameter		Hansen solubility parameters[24b]					Physical properties[27]			Food Contact Safety[28]	
Chemical family	**Name**	**Abbreviation**	**Cas N°**	**δ** *$(MJ.m^{-3})^{0.5}$*	**Difference**	**δ_D** *$(MJ.m^{-3})^{0.5}$*	**δ_P** *$(MJ.m^{-3})^{0.5}$*	**δ_H** *$(MJ.m^{-3})^{0.5}$*	**Distance**	**Relative Energy Difference** *(Distance / radius)*	**Molecular weight** *$(g.mol^{-1})$*	**Molar volume** *$(cm^3.mol^{-1})$*[24b]	**Boiling point at 760 mmHg** *(°C)*	**Approval**	**Specific migration limit** *$(mg.kg^{-1})$*
	Polylactide	PLA	33135-50-1	21.9	-	18.6[25]	9.9[25]	6.0[25]	-	(radius 10.7)[25]	-	-	-	Yes	60
Citrates	Triethyl citrate	TEC	77-93-0	20.4	1.5	16.5	4.9	12.0	8.9	0.83	276	243	294	Yes	60
	Tributyl citrate	TBC	77-94-1	19.8	2.1	16.6	3.8	10.1	8.4	0.78	360	346	325	No	-
	Acetyl triethyl citrate	ATEC	77-89-4	19.0	2.9	16.6	3.5	8.6	8.0	0.75	318	280	327	No	-
	Acetyl tributyl citrate	ATBC	77-90-7	18.4	3.5	16.7	2.5	7.4	8.4	0.79	402	384	441	Yes	60
Polycitrates	Tri(tributyl citrate)	TBC-3	-	18.6[29]	1.5[29]	-	-	-	-	-	980	-	-	No	-
	Hepta(tributyl citrate)	TBC-7	-	18.6[29]	1.5[29]	-	-	-	-	-	2,240	-	-	No	-
Adipates	Dioctyl adipate	DOA	123-79-5	17.6	4.3	16.7	2.0	5.1	8.8	0.82	370	400	398	No	-
	Bis(2-ethylhexyl) adipate	DEHA	103-23-1	17.6	4.3	16.7	2.0	5.1	8.8	0.82	370	400	374	Yes	18
	Diisobutyl adipate	DiBA	141-04-8	18.0	3.9	16.7	2.5	6.2	8.3	0.78	258	270	293	No	-
	Diisononyl adipate	DiNA	33703-08-1	17.0	4.9	16.2	1.8	4.9	9.5	0.89	398	434	405	No	-
Polyadipates	Poly(ethylene adipate)	PEA	-	18.9[30]	0.3[30]	-	-	-	-	-	2,000	-	-	No	-
	Poly(butylene adipate)	PBA	-	18.1[30]	1.1[30]	-	-	-	-	-	2,000	-	-	No	-
	Poly(hexalethylene adipate)	PHA	-	17.6[30]	1.6[30]	-	-	-	-	-	2,000	-	-	No	-
	Poly(diethylene adipate)	PDEA	-	18.1[30]	1.1[30]	-	-	-	-	-	2,000	-	-	No	-
	Glyplast® 2006/2		-	21.9[31]	2.0[31]	-	-	-	-	-	M_n = 1,532	-	-	No	-
	Glyplast® 206/7		-	22.9[31]	3.0[31]	-	-	-	-	-	M_n = 2,565	-	-	No	-
Phthalates	Dioctyl phthalate	DOP	117-84-0	18.3	3.6	16.6	7.0	3.1	5.7	0.54	390	377	230	No	-
	Ditridecyl phthalate	DtDP	119-06-2	17.6	4.4	16.6	5.4	1.9	7.3	0.68	530	558	508	No	-
	Dimethyl phthalate	DMP	131-11-3	22.1	0.1	18.6	10.8	4.9	1.4	0.13	194	163	284	No	-
Sebacates	Dimethyl sebacate	DMS	106-79-6	18.1	3.8	16.6	2.9	6.7	8.1	0.76	230	233	288	No	-
	Dibutyl sebacate	DBS	109-43-3	17.8 17.7[32]	4.1 5.4[32]	16.7	4.5	4.1	6.9	0.64	314	339	345	Yes	60
	Di-(2-ethyl hexyl) sebacate	DEHS	122-62-3	17.5	4.4	16.8	1.0	4.7	9.7	0.91	424	469	551	No	-
Phosphates	Tributyl phosphate	TBPA	126-73-8	18.0	3.9	16.3	6.3	4.3	6.1	0.57	266	274	289	No	-
	Tricresyl phosphate	TCPA	1330-78-5	23.1	1.2	19.0	12.3	4.5	2.9	0.27	368	316	438	No	-
	Trioctyl phosphate	TOPA	1806-54-8	17.7	4.2	16.2	5.9	4.2	6.5	0.61	434	470	414	No	-
	Triphenyl phosphate	TPPA	115-86-6	22.2	0.3	20.1	6.4	6.8	4.7	0.44	326	272	447	No	-
Maleates	Dibutyl maleate	DBM	105-76-0	19.0	2.9	16.5	6.1	7.2	5.8	0.54	228	230	280	No	-
Azelates	Di-(2-Ethyl Hexyl) Azelate	DEHAz	103-24-2	17.4	4.5	16.7	1.4	4.8	9.4	0.88	412	450	417	No	-
Trimellitates	Triisooctyl trimellitate	TiOT	27251-75-8	17.8	4.1	16.6	6.0	2.5	6.6	0.62	547	553	585	No	-
	Triisononyl trimellitate	TiNT	53894-23-8	17.7	4.2	16.6	5.7	2.2	6.9	0.65	588	603	617	No	-
Stearates	Butyl stearate	BS	123-95-5	15.4	6.5	14.5	3.7	3.5	10.6	0.99	340	382	343	Yes	60
Cinnamates	Ethyl cinnamate	EC	103-36-6	20.6	1.4	18.4	8.2	4.1	2.6	0.2	176	167	270	No	-
Benzoates	Benzyl benzoate	BzB	120-51-4	21.3	0.6	20.0	5.1	5.2	5.6	0.52	212	191	324	No	-
	Butyl benzoate	BuB	136-60-7	19.9	2.0	18.3	5.6	5.5	4.4	0.41	178	178	250	Yes	60
Acetates	Glycerol triacetate (triacetin)	GTA	102-76-1	19.4	2.5	16.5	4.5	9.1	7.5	0.70	218	188	258	No	-
	Diethylene glycol butyl ether acetate	DEGBEA	124-17-4	18.4	3.5	16.0	4.1	8.2	8.1	0.76	204	208	240	No	-
	2-Ethyl hexyl acetate	EHA	103-09-3	16.9	5.1	15.8	2.9	5.1	9.0	0.84	172	196	200	No	-
Polymalonates	Diethyl bishydroxymethyl malonate	DBM	20605-01-0	20.2[33]	0.1[32]	-	-	-	-	-	220	180	350	No	-
	DBM / adipoyl dichloride copolymer	DBM-A-8	-	18.7[32]	1.4[32]	-	-	-	-	-	M_n = 2,500 M_w = 4,200	-	-	No	-
	DBM / adipoyl dichloride copolymer	DBM-A-18	-	18.7[32]	1.4[32]	-	-	-	-	-	M_n = 5,300 M_w = 8,900	-	-	No	-
	DBM / succinyl dichloride copolymer	DBM-S-4	-	18.4[32]	1.7[32]	-	-	-	-	-	M_n = 1,300 M_w = 1,800	-	-	No	-
	DBM / succinyl dichloride copolymer	DBM-S-7	-	18.4[32]	1.7[32]	-	-	-	-	-	M_n = 2,100 M_w = 3,500	-	-	No	-
Poly(ethylene glycol)	Ethylene glycol	EG	107-21-1	33.0	11.0	17.0	11.0	26.0	20.3	1.90	62	56	197	Yes	30
	Diethylene glycol	DEG	111-46-6	29.1	7.2	16.6	12.0	20.7	15.4	1.44	106	95	245	Yes	30
	Triethylene glycol	TEG	112-27-6	27.5	5.6	16.0	12.5	18.6	13.9	1.30	150	114	286	Yes	60
	Tetraethylene glycol	PEG 200	112-60-7	24.3 23.5[32]	2.4 0.4[32]	16.6	5.7	16.8	12.3	1.15	194	175	314	Yes	60
	Poly(ethylene glycol) 400	PEG 400	25322-68-3	22.5[32]	0.6[32]	-	-	-	-	-	400	-	-	Yes	60
	Poly(ethylene glycol) 800	PEG > 800	25322-68-3	20.6	1.3	16.6	7.3	9.8	6.1	0.57	> 800	-	-	Yes	60
	Poly(ethylene glycol) 1000	PEG 1000	25322-68-3	21.9[32]	1.2[32]	-	-	-	-	-	1,000	-	-	Yes	60
	Poly(ethylene glycol)	PEG	25322-68-3	22.1	0.2	17.0	11.0	8.9	4.5	0.42	> 10,000	-	-	Yes	60

Table 1.2 Solubility parameters of monomeric and oligomeric plasticizers (continued)

	Reference			Hildebrand solubility parameter		Hansen solubility parameters[24b]					Physical properties[27]			Food Contact Safety[28]	
Chemical family	**Name**	**Abbreviation**	**Cas N°**	**δ** *$(MJ.m^{-3})^{0.5}$*	**Difference**	**δ_D** *$(MJ.m^{-3})^{0.5}$*	**δ_P** *$(MJ.m^{-3})^{0.5}$*	**δ_H** *$(MJ.m^{-3})^{0.5}$*	**Distance**	**Relative Energy Difference** *(Distance / radius)*	**Molecular weight** *$(g.mol^{-1})$*	**Molar volume** *$(cm^3.mol^{-1})$*[24b]	**Boiling point at 760 mmHg** *(°C)*	**Approval**	**Specific migration limit** *$(mg.kg^{-1})$*
	Acetyl glycerol monolaurate	AGM	-	18.5[32]	4.6[32]	-	-	-	-	-	358	-	-	No	-
	Poly(1.3-butanediol)	PBOH	-	21.3[32]	1.8[32]	-	-	-	-	-	M_w = 2,100	-	-	No	-
Biobased	Limonene	Li	6876-12-6	17.8	4.1	17.2	1.8	4.3	8.7	0.82	136	-	75	No	-
	Glycerol	Gly	56-81-5	36.2	14.3	17.4	12.1	29.3	23.5	2.20	92	73	290	Yes	60
	Oleic acid	OA	112-80-1	17.4	4.5	16.0	2.8	6.2	8.8	0.82	282	317	390	Yes	60
	Castor oil	CO	8001-79-4	18.2	3.7	13.6	6.0	10.5	11.6	1.09	-	-	-	Yes	60
	Linseed oil	LO	8001-26-1	14.4	7.5	13.5	3.5	3.7	12.3	1.15	-	-	-	No	-
	Lactic acid	LA	50-21-5	34.1	12.21	17.0	8.3	28.4	22.7	2.1	90	72	227	Yes	60

The compatibility of the plasticizer in the PLA matrix, the morphological stability of the plasticized material and the prevention of the plasticizer migration from the material bulk should be optimized as leaching out of additives from materials could impact the media in contact. This is of particular importance where food packaging applications are concerned, because food safety has to be ensured and contamination risks should be minimized. As with all substances intentionally added to the packaging polymer, the choice of plasticizer must comply with the European Commission regulation EU 10/2011 on plastic materials intended to come into contact with food. This regulation establishes a positive list of these compounds authorized for use in plastic formulations and manufacturing and provides migration limits for quite a number of molecules. **Table 1.2** gives information on the regulatory status of the different plasticizers described. In comparison with other additives used in packaging materials, plasticizers focus attention as they need to be used in high amounts in glassy polymers, up to 50 wt% in PVC and up to 30 wt% in PLA to reach the expected mechanical properties.

With respect to migration during food contact, obviously cyclic lactide monomers, oligolactic acid additives and linear oligolactic acid could be considered as ideal plasticizers in comparison to traditional approaches, as they have a similar structure to the polylactide chain and they are, thus, not expected to cause new toxic migrants.[34] On the contrary, these low molecular mass molecules can diffuse rapidly in the bulk of the polymer and cause contamination problems to the media in contact with the polymer. As an example, lactide is an environmentally degradable, non-toxic additive that is well known as a good plasticizing agent for PLA, but its rather fast migration rate results in a stiff material with time and it can easily contaminate the processing equipment.[35]

Thus, controlling the degradation rate, the release of degradation products and other migrants are key issues during the design of plasticized polymers. Few studies related the influence of

plasticizer structure on the migration (*i.e*. leach out) phenomena in contact with food or simulants (according to the regulation EU 10/2011). In general, large leaching out of plasticizer is expected when phase separation occurs and that plasticizer diffuses in the bulk to reach the material's surface, as was shown for PEG, for example.[36]

Non-intentional plasticization could occur during food storage. In fact, polymers used in packaging are not inert and mass transfers occur between them and foodstuff, even in the case of glassy polymers like PET or PVC.[37] On one hand, sorption of organic compounds into packaging such as aroma compounds could impact food quality. On the other hand, a number of studies showed that the sorption of flavor molecules can change the properties of the packaging material by swelling and/or plasticization. Plasticization and solvent-induced crystallization of PLA by ethyl acetate were observed using high ethyl acetate activities 0.5 and 0.2, respectively.[38] For example, Colomines et al.[38a] found that T_g decreased from 50.9 °C to 16.9 °C after 3 days of contact at 0.5 activity. Recently Salazar et al.[39] showed that a small plasticization of PLA occurs even at very low concentration (< 200 ppm) in vapor contact with aroma compounds like ethyl esters. Benzaldehyde, an aromatic molecule, showed high interaction with PLA compared to ethyl esters, although the latter have a more similar chemical structure. Furthermore, this aldehyde played a synergy role towards the low interacting molecules present in the mixture and augmented their solubility in the polymer. The good solubility of benzaldehyde in PLA was in accordance with the prediction of the Hansen solubility (high δ_D) parameters and could be compared with the good miscibility of PLA with aromatic solvents.

1.4. PLA Plasticizers: Properties, Effects and Processability

The first goal of plasticizing a polymer is, as discussed, the improvement in the mechanical properties, mainly the increase in the elongation at break and the decrease of T_g to render the polymer more flexible at service conditions. In this respect, many different molecules have been tested as PLA plasticizers. But there have been only a few reviews on the subject, such as Saeidlou et al.[2] and Liu and Zhang.[1b] To get a clear picture on the main findings and advances in PLA plasticizing, we choose to separate the discussion of literature results in systems using monomeric and polymeric molecules. The discussion is supported by tables gathering main literature results for either monomeric (**Table 1.3**) or polymeric (**Table 1.4**) plasticizers. In the aim of creating bio-based polymer materials, the use of additives derived from renewable resources, often being co-products of agriculture or food industry, has conceptual importance. To highlight these novel approaches, we voluntarily separated these novel plasticizers into a specific section 1.6 "PLA Plasticizers Derived From Biomass".

1.4.1. Plasticizer Impact on Mechanical Properties

1.4.1.1. Monomeric Plasticizers

Table 1.3 gathers the main literature results on PLA plasticized with monomeric external plasticizers. It shows furthermore that different chemical families have been used, where by far the most prominent family is those of citrates. Adipates have also attracted some interest. Both chemical families present good compatibility with PLA, but, according to their solubility parameters (**Table 1.2**) they are not highly miscible in PLA. They will swell PLA rather than dissolve it and a risk of bleeding out is present. Molecules with closer solubility parameters, such as DBS[32] (sebacate) and DEHP[40] (phthalate) have been used with success in increasing tensile properties. The molecule with a priori the highest miscibility, LA is evidently a very

good plasticizer for PLA, increasing the most the elongation at break, but it is characterized by low permanence due to its relatively high volatility.[35]

Miscibility is one of the key factors for the successful increase of tensile properties and decrease of T_g. Most literature studies used a maximum plasticizer concentration of 20 wt%, which allowed for the fabrication of a priori fully miscible blends. Correlation between yield stress and plasticizer concentration is a sign of miscible blends, as yield stress can serve as a measurement of macromolecular mobility.[41] Miscibility limits in PLA observed by some authors were 5 wt% DOA measured by DSC,[42] 10 wt% DINCH (by DSC and FESEM),[43] 20 wt% for DBS (DSC)[32] and GMS 15 wt% (DSC).[44] Furthermore, below 10 wt% DOA, Muriaru et al.[42] observed a decrease in the impact strength, explained by the antiplasticization effect.

A detailed investigation of miscibility can be undertaken for ATBC, where most data are available, using T_g as a descriptor and using DSC as analysis technique. The main research interest in ATBC stems from the fact that it proves most efficient in T_g depression and increase in elongation at break. Its branched structure allows apparently to bring sufficiently free volume to the polymer. Maximum ε values reach almost the one obtained by LA, but permanence of ATBC is supposed to be higher. **Figure 1.1** plots together the results of Baiardo et al.[45] with those from other authors. The continuous line represents the Fox Equation, which is often used for the description of the T_g decrease of miscible blends:

$$\frac{1}{T_g} = \frac{\omega_1}{T_{g_1}} + \frac{\omega_2}{T_{g_2}} \quad \textbf{(1.8)}$$

where ω_1 and ω_2 are the weight fractions of plasticizer and polymer, and T_{g1} and T_{g2} are the glass transition temperature of plasticizer and polymer, respectively.

One of the advantages of the Fox Equation is that it does not contain adjustable parameters. An agreement of experimental data with the prediction supports the conclusion of the high miscibility. Data from different authors are consistent and show that up to 45 wt% of ATBC content in PLA, the Fox Equation is applicable. At concentrations equal to or higher than 60 wt%, ATBC phase separation is evidenced in a miscible PLA/ATBC blend of stable composition and a pure ATBC phase. Consequently two T_g values can be measured, where the high temperature transition becomes independent of the ATBC content and the low temperature transition corresponds to the T_g of pure ATBC.[45] These observations prove the phase separation in the blend at ATBC concentrations higher than 45 wt%, which leads to the formation of a pure ATBC phase.

DSC is not a very sensitive technique to determine phase separation, as micro-domains of a certain size (420 nm)[32] need to be formed before being significant in the heat flow signal. Courgneau et al.[46] probed phase separation in PLA/ATBC blends with the help of Electron Spin Resonance (ESR). This non-invasive technique detects the local mobility of spin probes, generally stable nitroxyl radicals. ESR spectra allow reorientation dynamics of the spin probes in the material to be measured and therefore to conclude on domains of different mobility. By exposition of ATBC-plasticized PLA samples to vapors of two different spin probes at high temperature (70 °C for 29 days), the authors were able to assess mobility differences of the probes with penetration depth into the polymer. PLA/ATBC samples were found to be homogenous up to a concentration of 9 wt%. The sample at 17 wt% showed mobility differences between sample surface and bulk, indicating a micro-phase separation at the sample surface.

Table 1.3 Glass transition and mechanical properties of PLA plasticized with monomeric external plasticizers

Plasticizer	**Process**	**M_w** or **M_n** *($g.mol^{-1}$)*	**Content** (wt%)	**T_g** *(DSC) (°C)*	**σ** *(MPa)*	**E** *(MPa)*	**ε** *(%)*	**Ref.**
LA	-	144	1.3	-	51.7	1,993	3	47
			17.3	-	15.8	820	288	
			19.2	32 ─ 40	29.2	658	536	
			25.5	-	16.8	232	546	
PLA (blank)	MM+E	M_w = 137,000	0	59.1	51.7	-	7	48
TEC		276	10	42.1	28.1	-	21.3	
			20	32.6	12.6	-	382	
TBC		360	10	40.4	22.4	-	6.2	
			20	17.6	7.1	-	350	
ATEC		318	10	50.8	34.5	-	10	
			20	30	9.6	-	320	
ATBC		402	10	25.4	17.7	-	2.3	
			20	17	9.2	-	420	
PLA	TS	M_n = 74,000	0	54	57	3,750	5	35
Loxiol GMS 95		-	2.5	-	52	3,400	15	
			5	-	48	3,200	7	
			10	45	45	3,000	8	
Dehydat VPA 1726 (GME)		-	2.5	-	53	3,300	5	
			5	-	47	3,000	6	
			10	40	38	2,500	13	
PLA	IM+E	M_w = 49,000	0	58	-	2,050 ± 44	9 ± 2	49
Glycerol		92	10	54	-	-	-	
			20	53	-	-	-	
TBC		360	10	51	-	-	-	
			20	46	-	-	-	
PLA	TS	-	0	60 *(onset)*	66	3,300	2	45
			5	49	53	3,200	5	
ATBC		402	10	41	50	2,900	7	
			12.5	26	18	100	218	
			15	27	21	100	299	
			20	24	23	100	298	
PLA (blank)	IM	M_w = 100,000	0	54 *(DMA)*	-	-	-	50
			15	29	-	-	-	
TBC		360	20	16	-	-	-	
			25	1	-	-	-	
			15	29	-	-	-	
GTA		218	20	21	-	-	-	
			25	10	-	-	-	
			30	0	-	-	-	
PLA (blank)	TS	M_w = 100,000	0	54	-	-	6	51
GTA		218	11	29	-	-	355	
TBC		360	12	29	-	-	350	
PLA	TS	M_w = 100,000	0	52	-	-	-	52
TBC		360	15	25	-	-	-	
DBM		220	15	29	-	-	-	
PLA	IM	M_w = 74,000	0	59.2	64 ± 1.5	2,840 ± 50	3 ± 0.3	32
DBS		314	10	39.9	39.2 ± 4	2,000 ± 80	2.3 ± 0.2	
			20	-66.9 and 26.1	23.1 ± 0.9	430 ± 50	269 ± 6	
AGM		358	10	45.8	52.1 ± 4	2,240 ± 100	32 ± 2.1	
			20	-65.8 and 24.3	27.1 ± 3.1	35 ± 5	335 ± 2.3	
PLA	C	M_n = 63,000	0	58.2	-	-	-	53
DOA		371	10	40.8	-	-	-	
			20	40.1	-	-	-	
PLA	TS+I	-	0	-	69.2 ± 0.41	3,680 ± 130	6.0 ± 0.29	54
			2	-	64.3 ± 0.68	3,490 ± 70	8.8 ± 1.78	
ATEC		318	5	-	57.8 ± 1.32	3,460 ± 50	5.2 ± 0.34	
			10	-	50.1 ± 0.28	3,150 ± 80	6.1 ± 1.30	
PLA	IM	M_n = 74,500	0	62	66 ± 2	1,020 ± 100	11 ± 3	42
			10	44	51 ± 1	970 ± 70	11 ± 4	
ATBC		402	15	32	37 ± 1	590 ± 50	221 ± 8	
			20	38	30 ± 1	270 ± 20	317 ± 4	
DOA		371	5	49	-	-	-	
			10	45	29 ± 2	720 ± 90	36 ± 5	
			15	45	22 ± 1	710 ± 50	77 ± 44	
			20	45	21 ± 1	670 ± 120	78 ± 33	
GTA		218	10	48	38 ± 3	760 ± 140	8 ± 2	
			15	45	31 ± 5	590 ± 110	223 ± 19	
			20	29	24 ± 1	10 ± 3	443 ± 13	

Table 1.3 Glass transition and mechanical properties of PLA plasticized with monomeric external plasticizers (continued)

Plasticizer	Process	M_w or M_n *(g.mol^{-1})*	Content (wt%)	T_g *(DSC) (°C)*	σ *(MPa)*	E *(MPa)*	ε *(%)*	Ref.
PLA[a]	TS	M_n = 107,000	0	61.7	79 ± 2	1,870 ± 60	5.63 ± 0.03	40
			5	52.3	71 ± 2	1,720 ± 40	6.20 ± 0.12	
DOP		390	7.5	40.9	65 ± 1	1,660 ± 120	6.35 ± 0.02	
			10	41.6	60 ± 2	1,480 ± 140	147 ± 5	
			12.5	40.4	44 ± 1	1,330 ± 180	221 ± 11	
			15	41.3	46 ± 2	1,300 ± 90	225 ± 9	
PLA	IM	M_n = 63,000	0	58.2	47 ± 5	2000 ± 200	6 ± 2	31
DOA		371	10	40.8	27 ± 4	1600 ± 100	259 ± 64	
			20	40.1	17 ± 1	1400 ± 100	295 ± 89	
PLA	IM	M_n = 81,000	0	61	52 ± 2	1800 ± 150	6 ± 1	55
TBC		360	20	20	20 ± 1	9 ± 1	320 ± 20	
PLA	IM	M_n = 142,000	0	59.4	69.5 ± 0.6	-	4 ± 1	43
			3	55.2	-	-	-	
			5	49.8	-	-	-	
DINCH		425	8	49.7	-	-	-	
			10	49.8	41.1 ± 0.2	-	129 ± 20	
			20	49.9	30.1 ± 0.1	-	200 ± 16	
TBC		360	10	38.5	57.1 ± 0.4	-	7 ± 1	
			20	24.0	37.2 ± 1.2	-	300 ± 15	
PLA[b]	TS	M_w = 204,453	0	58.01	41.7	3364	1.27	56
			12.44	41.12	38.3	2542	2.14	
TEC[c]		360	12.99	37.61	12.4	1248	> 100.2	
			15.58	32.1	6.4	53	> 100.16	
			22.52	21.74	9.9	55	> 102.77	
PLA[d]		M_w = 204,453	0	-	41.69	3364	1.27	
			12.44	39.45	41.95	2301	3.43	
TEC[e]		360	12.99	36.7	19.97	1337	> 99.98	
			15.58	30.37	7.67	313	> 100.03	
			22.52	33.95	11.95	159	100.08	
PLA	IM	-	0	60.7	-	-		57
[THTDP][DE]		655	5	49.5	-	-	brittle[f]	
			10	45.1	-	-		
[THTDP][BF_4]		571	5	55.9	-	-	ductile[f]	
			10	54.5	-	-		
PLA	IM	M_n = 90,500	0	58	47 ± 7	1,291 ± 60	8 ± 5	58
			2.5	52	40 ± 8	1,300 ± 69	4 ± 1	
			5	47.3	41 ± 9	1,306 ± 64	8 ± 3	
ATBC		402	9	41.5	30 ± 5	1,039 ± 55	16 ± 10	
			13	35.1	22 ± 4	615 ± 41	300 ± 179	
			17	28.6	-	69 ± 18	503 ± 45	
PLA[g]	IM	M_n = 90,500	0	58	46 ± 8	1,216 ± 106	5 ± 2	38b
ATBC		402	17	25.1	20 ± 2	347 ± 21	59 ± 24	
PLA	TS	M_w = 121,400	0	58.6	69.8 ± 3.2	1,777 ± 42	5.7 ± 0.3	44
			5	52.7	44.8 ± 1.3	1,570 ± 44	4.5 ± 0.5	
			10	52.5	41.9 ± 4.6	1,200 ± 12	7.6 ± 2.4	
GMS		358	15	52.3	39.7 ± 1.0	1,270 ± 36	11.0 ± 5.0	
			20	51.9	35.1 ± 2.1	1,210 ± 17	9.5 ± 6.5	
			25	52.1	32.4 ± 1.8	1,190 ± 24	11.0 ± 3.1	
			30	51.5	29.9 ± 2.6	695 ± 38	45 ± 16	
PLA	IM	M_n = 96,000	0	58	63 ± 4	2,400 ± 100	49 ± 9	59
ATBC		402	20	33	50 ± 5	2,400 ± 200	158 ± 27	
PLA/D43B[h] (3%)		-	0	58	59 ± 3	2,800 ± 100	3 ± 0.2	
D43B[h]+ATBC		-	20	34	37 ± 5	1,900 ± 300	167 ± 55	
PLA	TS	M_n = 100,000	0	60	49 ± 4	3,100 ± 150	3.4 ± 0.9	
ATBC		402	20	38	16 ± 2	1,000 ± 140	143 ± 14	
PLA/D43B[h] (3%)		M_n = 59,000	0	57	56 ± 5	3,400 ± 200	2.3 ± 0.3	
D43B[h]+ATBC		-	20	31	34 ± 7	2,100 ± 300	163 ± 35	

TS twin screw extrusion, IM internal mixer, E single screw extrusion, I injection molding, C casting, MM manual mixing, [a]crosslinked PLA, [b]aged 10 days, [c]aged 20 days, [d]aged 24 days, [e]aged 32 days, [f]behavior assessed by 3-point bending test, [g]semicrystalline samples (degree de crystallinity 30 %), [h]Montmorillonite Dellite 43B

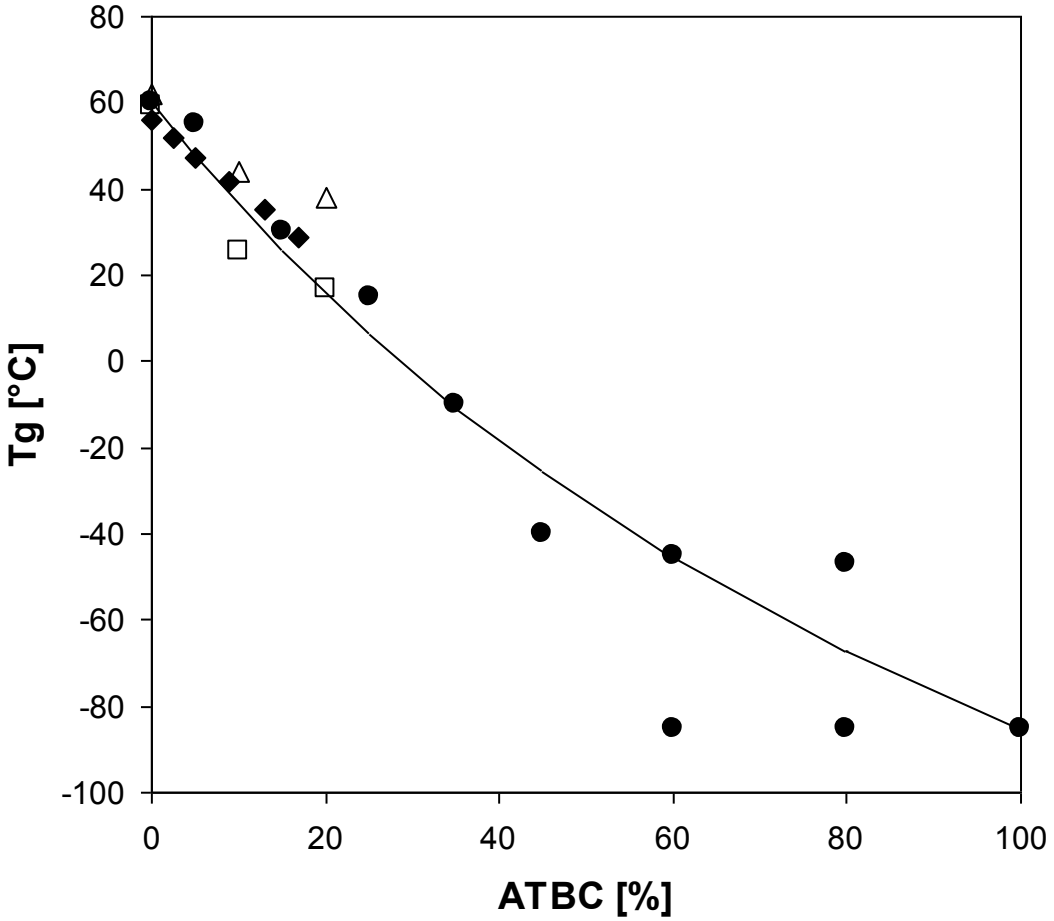

Figure 1.1 Glass transition temperature depression of PLA/ATBC blends as function of ATB content
● Data Ref.[45], ♦ Data Ref.[58], □ Data Ref.[48], Δ Data Ref.[42].
The straight line represents the Fox Equation, modelled with the parameters given by Ref.[45].

Another interesting feature of PLA plasticizing can be observed in **Figure 1.2**, which plots ε values against T_g. In the case of the poorly compatible plasticizer GMS, even though some decrease in T_g is reached, not much gain in ε can be obtained. Comparing di(octyl adipate), DOA, with ATBC shows that in the high T_g range, DOA outperforms ATBC. Apparently the more linear molecule DOA is able to bring more mobility to the macromolecular chains, which probably shows the importance of the molecular volume of the molecule. Indeed, DOA is bulkier than ATBC, although having lower molecular weight. Once the ATBC content reaches a critical limit, this leads to some increase in ε in the low T_g range. ATBC outperforms DOA, which cannot reach low T_g due to the miscibility limit. Moreover,

properties change close to T_g = 40 °C, which means that the measuring temperature of the tensile testing (23 °C according to ASTM-D683) becomes to be close to the glass transition range of the material. However, ATBC, although it is the monomeric plasticizer yielding the highest increase in ε (**Table 1.3**) barely yields doubled impact strength.[42] However, DOA, even if not miscible with PLA produced an almost ten-fold gain in impact strength.[42]

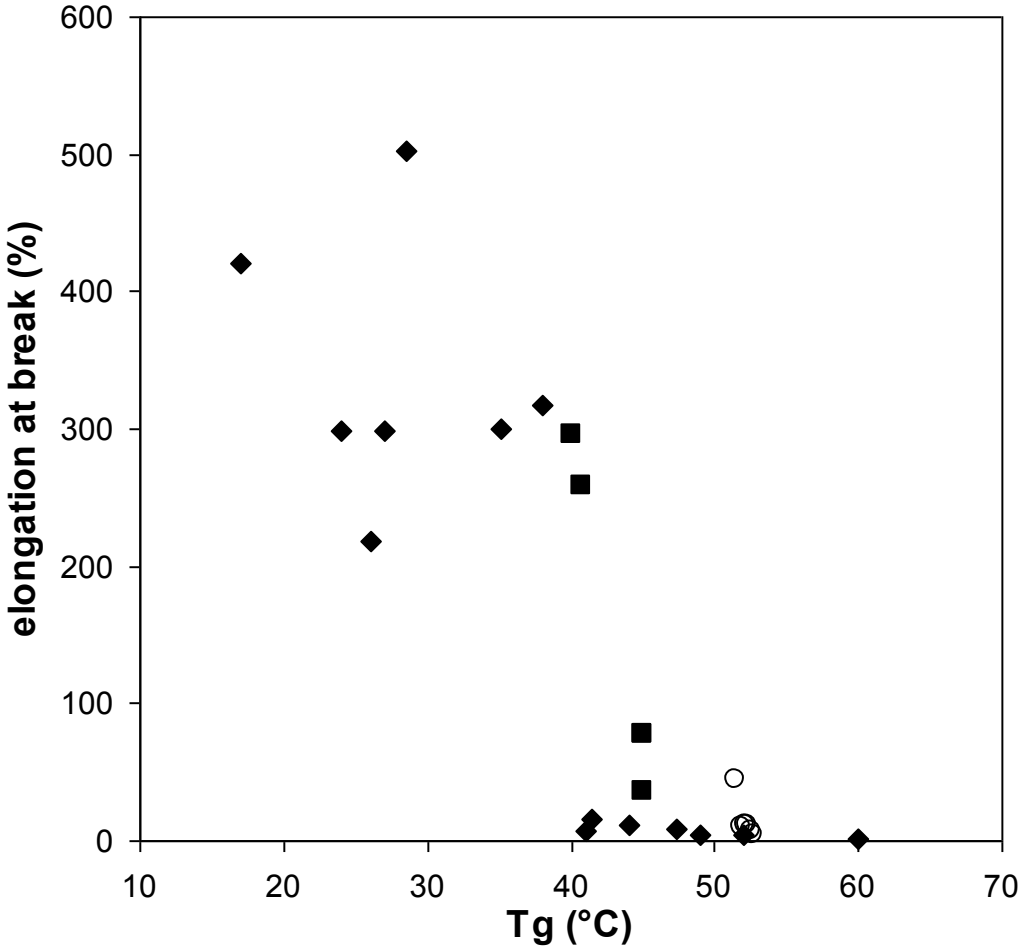

Figure 1.2 Strain at break values plotted against T_g

◆ ATBC[42, 45, 48, 58], ■ DOA[31, 42], ○ GMS[44]

1.4.1.2. Oligomeric Plasticizers

The main drawback of monomeric plasticizers is their tendency to migrate from the polymer or to be leached out by contacting media. In anticipation of permanence problems caused by monomeric plasticizers, oligomeric plasticizers have attracted the main research interest for toughening PLA. Furthermore, polymeric plasticizers often bring additional increase in impact strength. Drawbacks in the use of polymeric plasticizers have already been discussed and are, to sum up, the lower miscibility with the polymer, in consequence the higher propensity to phase separation, and lower efficiency in T_g depression. **Table 1.4** displays a literature overview of the work carried out on oligomeric plasticizers. It shows the different chemical families studied, which are mainly oligomers of glycols, citrates, adipates and malonates. These molecules (except glycol) proved already to be interesting monomeric plasticizers.

The influence of the molecular weight on plasticizing efficiency and miscibility is an important point for oligomeric plasticizers. Solubility parameters have been used as a tool for prediction and explication of these properties. They are generally efficient to discriminate different chemical structures of oligomers, but not able to assess the influence of the increase in chain length for a given oligomer. For example, the solubility parameters were calculated for a series of TBC oligomers with increasing chain length. They were constant upon increase of monomer units up to n = 7, but the efficiency in T_g and melting point depression decreased.[29] Similar results were found in the case of DBM oligoesters and DBM oligoesteramides.[33, 52] Polar amide groups introduced to the oligomeric chain of oligoesteramides increased plasticizing efficiency, which shows the importance of polar interactions and hydrogen bonding. These polar groups permitted the solubility coefficient to approach PLA[52] and, in consequence, blends had higher stability compared to oligoesters.[33, 52] The use of citric acid branched with PEG, both individually good plasticizers, as

macromolecular plasticizer was also evaluated.[60] Miscibility was rather poor between PLA and PEG-co-citric acid, and only a small decrease in T_g was observed. However, the highly branched structure brought significantly higher impact strength to PLA.

The miscibility of polyadipates with PLA was also investigated in the function of M_n. It decreased with increasing chain length. The largest molecule certainly has the least efficiency in T_g depression, but all oligomers produced large gains in PLA ductility.[53, 61] A trade-off in oligomer chain length needs to be found between plasticizing efficiency and miscibility. Excellent properties were also obtained for different polyester adipates (PEA, PBA and PHA, see **Table 1.4**).[30] The best result was shown by a PLA/PEA blend having elongation at break of 800 % and relatively high tensile strength (24.8 MPa).[30] The solubility parameter δ calculated at 180 °C explained the miscibility differences between PEA and PHA, but not between PBA and PDEA. Although δ values were equal, PBA was found to be only partially miscible, while the PDEA was fully miscible. The authors proposed that the higher configurational entropy of PDEA compared to PBA might be the reason for enhanced miscibility, by inducing higher entropy gain upon mixing.

Table 1.4 Glass transition and mechanical properties of PLA plasticized with polymeric external plasticizers

Plasticizer	**Process**	**M_w** or **M_n** *($g.mol^{-1}$)*	**Content** *(wt%)*	**T_g** *(DSC)* *(°C)*	**σ** *(MPa)*	**E** *(MPa)*	**ε** *(%)*	**Ref.**
PLA	TS	M_n = 74,000	0	54	57	3,750	5	35
PEG 1500		M_w = 1,500	2.5	-	50	3,200	5	
			5	-	44	2,500	7	
			10	28	38	1,300	40	
PLA	IM+E	M_w = 49,000	0	58	-	2,050 ± 44	9 ± 2	49
OLA		-	10	37	-	1,256 ± 38	34 ± 4	
			20	18	-	744 ± 22	200 ± 24	
M-PEG		M_w = 400	10	34	-	1,571 ± 51	18 ± 2	
			20	21	-	1,124 ± 33	142 ± 19	
PEG 400		M_w = 400	10	30	-	1,488 ± 39	26 ± 5	
			20	12	-	976 ± 31	160 ± 12	
PEG 1500		M_w = 1,500	10	41	-	-	-	
			20	30	-	-	-	
PLA	TS	M_w =100,000	0	54	-	-	6	29
			10	38	-	-	-	
TBC-3 oligomer		980	15	33	-	-	-	
			20	30	-	-	-	
TBC-7 oligomer		2,240	15	43	-	-	-	
PLA	TS	M_w = 100,000	0	52	-	-	-	33
DBM		220	15	29	-	-	-	
DBM-A-8 oligomer		M_n =4,200	15	42	-	-	-	
DBM-A-18 oligomer		M_n = 5,300	15	39	-	-	-	
DBM-S-4 oligomer		M_n = 1300	15	36	-	-	-	
DBM-S-7 oligomer		M_n = 2,100	15	40	-	-	-	
PLA	TS	M_w = 160,000	0	58	53 ± 2	2,200 ± 50	14 ± 1	62
PEG 8000		M_w = 8,000	10	36	23 ± 1	950 ± 30	200 ± 10	
			15	30	16 ± 1	630 ± 20	260 ± 10	
			20	21	5 ± 1	180 ± 20	300 ± 20	
			30	9	-	5 ± 1	500 ± 20	
PLA	TS	M_w = 190,000	0	60	68 ± 2	2,500 ± 200	3 ± 0,5	63
PEG 8000		M_w = 8,000	10	39	26 ± 1	900 ± 50	180 ± 10	
			20	21	4 ± 0.5	150 ± 20	260 ± 20	
			30	12	-	20 ± 2	300 ± 30	
PLA	TS	M_w = 84,000	0	60 *(onset)*	66	3,300	2	45
PEG 400		M_w = 400	5	40	42	2,500	2	
			10	23	33	1,200	140	
			12.5	22	19	500	115	
			15	20	19	600	88	
			20	19	16	500	71	
PEG 1500		M_w = 1,500	5	46	52	2,900	4	
			10	42	47	2,800	5	
			12.5	30	19	700	194	
			15	27	24	800	216	
			20	20	22	600	235	
PEG 10000		M_w = 10,000	5	49	54	2,800	2	
			10	42	49	2,800	3	
			15	36	42	2,500	4	
			20	34	22	700	130	
PLA	TS	M_n= 81,800	0	55	-	-	-	64
PEG 1000		M_w = 1,000	20	15	-	-	-	
PLA+CNa^+-3%/PEG		-	20	14	-	-	-	
PLA+C30B-3%/PEG		-	20	16	-	-	-	
PLA+C25A-3%/PEG		-	20	16	-	-	-	
PLA+C20A-3%/PEG		-	20	16	-	-	-	
PLA	IM	M_w = 160,000	0	56	-	-	-	65
PEG 1500		M_w = 1,500	10	45	-	-	-	
PLA+C25A-3%/PEG		-	10	44	-	-	-	
PLA	IM	M_n = 85,000	0	58	-	-	-	66
PLA+C30B-3%	IM	-	0	58	-	-	-	
PLA+C30B-3%	MB+IM	-	0	61	-	-	-	
PLA+C30B-3%/PEG	MB+IM	M_w = 1,000	20	26	-	-	-	

Table 1.4 Glass transition and mechanical properties of PLA plasticized with polymeric external plasticizers (continued)

Plasticizer	Process	M_w or M_n *(g.mol^{-1})*	Content *(wt%)*	T_g *(DSC) (°C)*	σ *(MPa)*	E *(MPa)*	ε *(%)*	Ref.
PLA		M_n = 81,800	0	49.7	-	-	-	
PEG 1000		M_w = 1,000	20	23.4	-	-	-	
PLA+C20A-3%/PEG	IM	-	20	28.2	-	-	-	67
PLA+C25A-3%/PEG		-	20	25.8	-	-	-	
PLA+C30B-3%/PEG		-	20	27.2	-	-	-	
PLA		M_w = 166,000	0	57	47	-	18	
PEG 400		M_w = 400	5	-	-	-	-	
			10	-	-	-	300	
PEG 600	IM	M_w = 600	5	47	39	-	25	
			10	36	18	-	550	68
PEG-CH_3		M_w = 550	5	43	35	-	22	
			10	32	20	-	550	
PEG-CH_3		M_w = 750	5	-	35	-	> 30	
			10	-	18	-	550	
PLA		M_w = 108,000	0	55.7	41.4 ± 1.5	-	64 ± 42	
PPG 425		M_w = 425	5	44.5	31.3 ± 1.2	-	19 ± 8	
			7.5	38.5	29.0 ± 2.1	-	107 ± 50	
			10	33.1	17.4 ± 2.0	-	524 ± 66	
			12.5	26.8	6.0 ± 0.4	-	702 ± 31	
PPG 1000	IM	M_w = 1,000	5	44.8	32.3 ± 1.8	-	44 ± 3	
			7.5	39.0	28.4 ± 1.3	-	329 ± 20	69
			10	34.0	23.1 ± .09	-	473 ± 111	
			12.5	32.0	16.1 ± 1.6	-	496 ± 70	
PEG 600		M_w = 600	5	42.8	30.3 ± 1.8	-	67 ± 33	
			7.5	37.8	25.7 ± 0.2	-	360 ± 25	
			10	31.3	17.5 ± 1.7	-	427 ± 42	
			12.5	28.0	5.1 ± 0.8	-	622 ± 75	
PLA^{sc}		M_w = 108,000	0	56	55	-	10	
PPG 425		M_w = 425	5	38	30	-	40	
			7.5	35	25	-	40	
			10	-	19	-	65	
			12.5	-	19	-	65	
PPG 1000	IM	M_w = 1,000	5	41	28	-	35	
			7.5	39.5	19	-	45	70
			10	-	19	-	90	
			12.5	-	19	-	105	
PEG 600		M_w = 600	5	38	32	-	20	
			7.5	35	20	-	25	
			10	-	19	-	25	
			12.5	-	15	-	15	
PLA		M_w = 180,000	0	61.8	65	2,600	5	
PLA-MMT-Na-3%		-	0	66.2	56	2,450	5	
PEG	IM	M_w = 1,000	10	41.3	38	1,500	220	71
PLA-MMT-Na-3%		-	10	40.2	30	1,400	180	
Rikemal PL-710		-	10	42.4	45	2,400	5	
PLA-MMT-Na-3%		-	10	43.5	39	1,900	7	
PLA		M_w = 74,000	0	59.2	64 ± 1.5[b]	2,840 ± 50	3 ± 0.3	
			10	47,6	56,3 ± 1.9[b]	2,350 ± 50	3 ± 0.3	
PBOH		M_w = 2,100	20	-48.5 and 30.1	30.2 ± 1.1[b]	350 ± 20	302.5 ± 32	
			30	29.4 and -45.0	25.2 ± 1.8[b]	300 ± 50	390 ± 35	
PEG 200	IM	M_w = 200	10	35.8	30 ± 4.1[b]	1,700 ± 100	2 ± 0.6	32
PEG 400		M_w= 400	10	37.1	39 ± 0.3[b]	1,920 ± 53	2.4 ± 0.3	
			20	-50.2 and 18.6	16 ± 0.3[b]	630 ± 20	21.2 ± 2.3	
PEG 1000		M_w = 1,000	10	40.2	39.6 ± 5[b]	1,970 ± 120	2.7 ± 0.3	
			20	-62.7 and 22.4	21.6 ± 0.4[b]	290 ± 50	200 ± 13	
			30	29.9 and -68.9	4.7 ± 0.2[b]	420 ± 40	1.5 ± 0.2	
PLA		-	0	-	69.2 ± 0.41	3,680 ± 130	6.0 ± 0.29	
PEG	TS+I	M_w = 3,350	2	-	60.5 ± 0.76	3,700 ± 140	10.5 ± 4.6	54
			5	-	54.5 ± 0.96	3,560 ± 100	9.1 ± 7.2	
			10	-	44.8 ± 0.97	3,020 ± 70	39.9 ± 37.2	
PLA		M_n = 97,000	0	64	67	840	1	
PEA		M_n = 2,000	20	36	24.8	375	815	
PBA	IM	M_n = 2,000	20	47	42.6	675	428	30
PHA		M_n = 2,000	20	55	36.8	710	19	
PDEA		M_n = 2,000	20	34	17.7	257	705	

Table 1.4 Glass transition and mechanical properties of PLA plasticized with polymeric external plasticizers (continued)

Plasticizer	**Process**	**M_w** or **M_n** ($g.mol^{-1}$)	**Content** *(wt%)*	**T_g** *(DSC)* *(°C)*	**σ** *(MPa)*	**E** *(MPa)*	**ε** *(%)*	**Ref.**
PLA		M_n = 63,000	0	58 *(DMA)*	-	2,000	6	
PA G206/2	IM	M_n = 1,532	10	44	-	1,600	5	
			20	27	-	250	480	61a
PA G206/7		M_n = 2,565	10	44	-	1,700	8	
			20	32	-	400	480	
PLA		M_n = 63,000	0	58.2	47 ± 5	2,000 ± 200	6 ± 2	
PA G206/2	IM	M_n = 1,532	10	39.5	34 ± 2	1,600 ± 100	5 ± 1	
			20	25.4	25 ± 4	200 ± 100	485 ± 65	31
PA G206/7		M_n = 2,565	10	42.1	36 ± 2	1,700 ± 0.2	7 ± 5	
			20	30.6	28 ± 2	500 ± 100	491 ± 34	
PLA		M_n = 63,000	0	58	-	-	-	
PA G206/7	IM	M_n = 2,565	15	37.6	-	660	250	
			20	31.1	-	300	310	61b
PLA-C30B-3%/G206/7		-	15	37.7	-	720	150	
			20	30.5	-	400	200	
PLA		M_n = 63,000	0	58				
PA G206/2		M_n = 1,532	15	33	-	430	320	
C30B-2.1%/G206/2		-	15	33	-	470	250	
PA G206/5	IM	M_n = 2,209	15	34	-	520	320	72
C30B-2.1%/G206/5		-	15	35	-	550	230	
PA G206/7		M_n = 2,565	15	36	-	620	320	
C30B-2.1%/G206/7		-	15	35	-	630	230	
PLA		M_n = 90,500	0	58	47.1 ± 6.9	1,291 ± 60	8 ± 5	
			2.5	48	41.1 ± 8.8	1,335 ± 143	5 ± 1	
	IM		5	40.5	38.1 ± 7.2	1,338 ± 84	5 ± 2	58
PEG 300		M_n = 300	9	39.5	29.6 ± 2.8	908 ± 36	7 ± 2	
			13	39	18.1 ± 1.5	547 ± 34	99 ± 43	
			17	38	15.8 ± 1.2	323 ± 44	137 ± 34	
PLA		M_w = 104,000	0	64 *(DMA)*	61	-	6	
PPG		M_w = 1,000	10	50	51	-	7	
			15	50	54	-	7	
EPE11	IM	M_w = 1,180	10	49	56	-	7	73
			15	48	32	-	510	
EPE19		M_w = 1,940	10	46	21	-	460	
			15	43	22	-	510	
PLA		-	0	61	74	1,700	5	
PEG 1000	IM	M_w = 1,000	15	-	42	1,100	120	60
PEGCA		-	15	52	40	1,300	230	
PLA		-	0	59.98	-	-	-	
C30B-3%	TS	-	0	61.1	-	-	-	74
PEG		-	20	29.4	-	-	-	
C30B-3%/PEG		-	20	33.5	-	-	-	
PLA		-	0	62	49	4,300	1.8	
			5	46	53	3,000	2.9	
PEG	-	M_w = 1,000	10	38	51	3,300	3.1	75
			15	33	29	2,100	4.2	
			20	33	22	1,900	15.4	
PLA		M_n = 98,000	0	59.2	-	2,500	8	
	IM		15	38.9	-	1,600	180	76
OLA		M_n = 957	20	33.7	-	750	300	
			25	25.8	-	250	310	

The most investigated family of polymeric plasticizers is polyethylene glycols (PEGs). These linear polymers can have favorable solubility parameters (**Table 1.2**) and they are commercially available in a large range of chain lengths. Depending on the molecular weight average, PEGs can be a crystalline solid (M_w > 1500 Da), waxy (M_w ≈ 1000 Da) or liquid (M_w < 1000 Da) at room temperature.[45] PEGs are capable of greatly enhancing the toughness of PLA. **Table 1.4** shows that PEG of small chain length (M_w = 300 Da[58] or 400 Da[45], for example) raises steeply from the brittle behavior of PLA to a maximum value, while PEG of longer chain length (M_w = 8000 Da,[62] *e.g.*) yields a more gradual property change. Insight into the influence of chain length on PEG miscibility with PLA can be gained from the T_g data of Pillin et al.[32] and Baiardo et al.[45] in comparison to values of different literature sources (**Figure 1.3**).

The miscibility limit of PEG in a M_n range of 200 Da to M_n = 3,400 Da was established at 20 wt% with the help of DSC measurements.[32, 45] PEG with M_n = 10,000 Da demixed already at 15 wt%.60 Hu et al.[62-63] showed miscibility of PEG 8000 with PLA up to 30 wt% with the help of DSC and DMA measurements. Courgneau et al.[58] found exudation of PEG 300 already after 9 wt% with the help of DMA measurements. In their follow-up paper Courgneau et al.[46] used ESR to observe exudation of PEG 300 from the film samples already at 9 wt% PEG 300. However, their samples needed to be stored at a temperature higher than T_g for several weeks in order to allow sorption of the ESR spin probes. Therefore, the differences between observations of different research teams might be linked to ageing. Instabilities in the PLA/PEG system will be discussed in more detail in Section 1.5 ‘‘longterm stability’’.

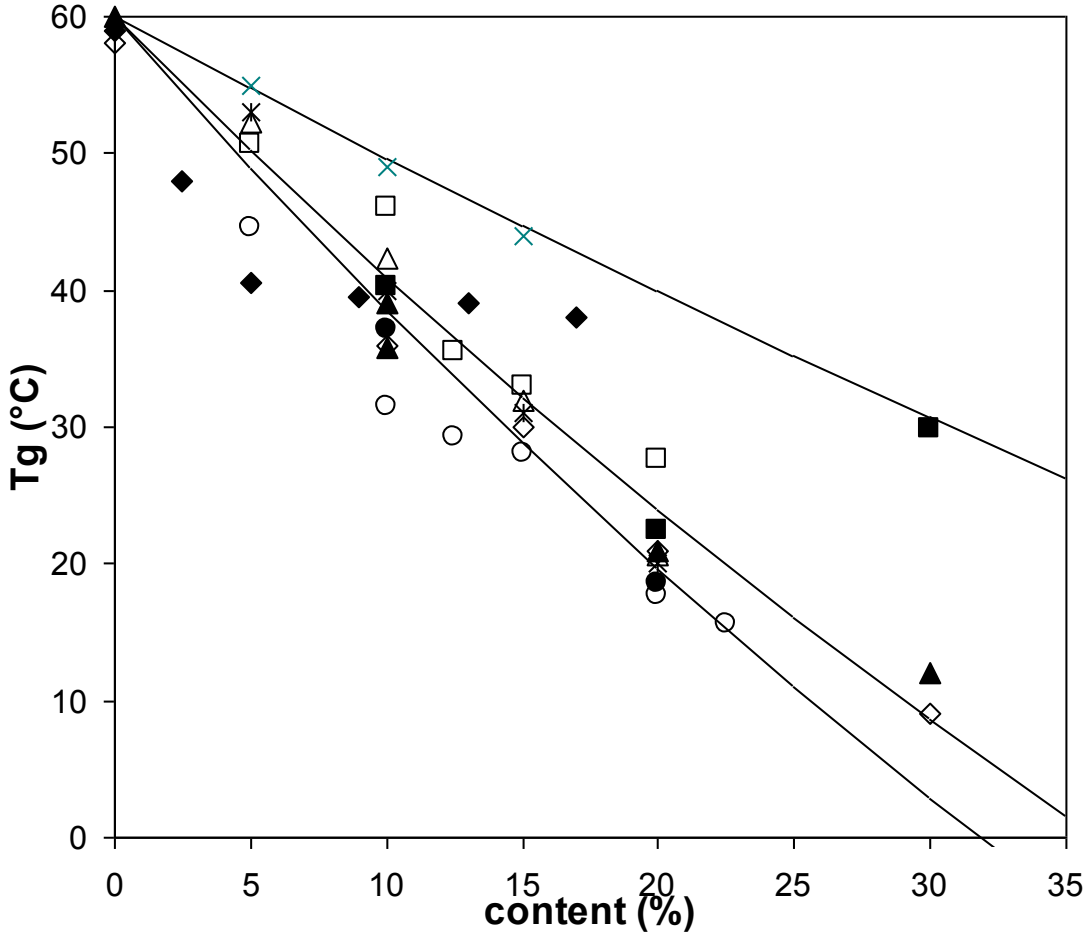

Figure 1.3 Glass transition temperature depression as a function of content average molecular weight of PEG ▲ PEG 200,[32] ◆ PEG 300,[58] ● PEG 400,[32] ○ PEG 400,[45] ■ PEG 1000,[32] □ PEG 1500,[45] ✶ PEG 2000,[45] △ PEG 3400,[45] ◇ PEG 8000,[62] × PEG 10000.[45]

The straight lines correspond to the Fox Equation for PEG having M_w of 10,000 ; 8,000 and 400 (upper to lower).

PPGs and their copolymers were studied in comparison to PEGs and showed good ability to increase PLA toughness.[55, 69-70, 73, 75] PPGs have the advantage that their T_g is lower and even at M_w = 1,000 Da they are viscous liquids at room temperature. Therefore T_g depression after the addition of PPGs is more efficient compared to PEG,[70] **Table 1.4**. Miscibility of PPG 400 with PLA was found for all the studied concentrations up to 12.5 wt%, while phase separation was found at 12.5 wt% in the PLA/PPG 1,000 blend.[69-70] Using the PLA/PEG and two PLA/PPG systems, Kulinski at al.[69] and Piorkowska et al.[70] investigated the combined effect

of the plasticizer content and crystallization on PLA. **Figure 1.4**, reprinted from Ref.[69], shows the stress/strain curves of neat and plasticized amorphous PLA. Plasticizing improved drawability and decreased yield stress due to enhanced macromolecular mobility. In the case of drawing PLA in the glassy state (neat or 5 wt% plasticizer) the plastic deformation was caused by crazing. Beginning with 7.5 wt% of plasticizer, T_g approached drawing temperature and the blends crystallized resulting in strain hardening (**Figure 1.4**). PPG 1000 separated from the amorphous PLA at 12.5 wt% and formed small droplets in the polymer, a phenomenon that was accelerated by the PLA crystallization during drawing. These liquid inclusions did, most interestingly, not downgrade drawability, but seemed to be beneficial by the plasticizer accumulation in the amorphous phase due to expulsion of their molecules from the originating crystallites.[69]

The effect of crystallization on PLA drawability is generally negative,[38b, 70] but it enhances other important properties, such as modulus, heat stability and barrier properties. The plasticizer separated in the amorphous phase during PLA crystallization accumulates at the crystalline phase boundary,[68] broadening the glass transition region. In the case of the PLA/PPG and PLA/PEG systems, different consequences were observed. In the case of PLA/PPG 400, the T_g value of the amorphous phase decreased due to the increase of the amount of plasticizer in the amorphous phase. In the case of PLA/PPG 1000 and PLA/PEG 600, the T_g value increased after PLA crystallization. Phase separation of the plasticizer was observed for every composition, but separate liquid inclusions inside the amorphous PLA matrix were revealed uniquely for PPG 1000.[70]

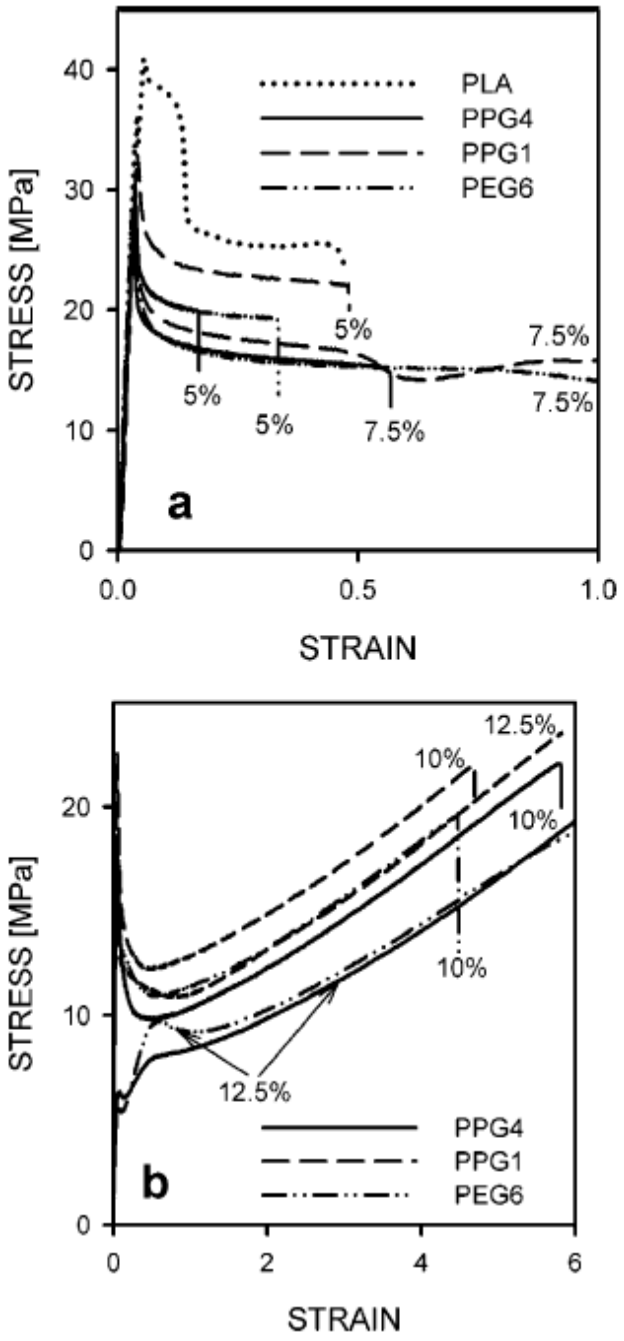

Figure 1.4 Stress-strain plots of initially amorphous neat PLA and amorphous PLA plasticized with 5 wt% and 7.5 wt % of PPG 400, PPG 1000, and PEG 600 **(A)** and for PLA plasticized with 10 wt% and 12.5 wt% of PPG 400, PPG 1000, and PEG 600 **(B)**

Reprinted with permission from Kulinski et al., Biomacromolecules, 2006, 7, 2128.[69]

Figure 1.5 plots the stress/strain curves of the corresponding samples. Both PPGs are far more efficient in preserving high elongation at break even for semi-crystalline PLA. Yielding in PLA/PPG 400 and PLA/PEG 600 disappeared at a plasticizer content of 7.5 wt%. At high contents, flow stress decreased without further ε increase. Cracks propagated preferentially through interspherulitic crazes, as the interspherulitic boundaries were the weakest element. PEG 600 accumulation in front of a growing spherulite was higher compared to PPG 400, which explained the earlier fracture of PLA/PEG 600. In the case of PPG 1000, extensive yielding was observed. The phase separation of PPG 1000 in droplets prevented the accumulation of the plasticizer in the amorphous phase and resulted in comparatively higher T_g of PLA. This more uniform distribution of PPG 1000 apparently enhanced drawability.[69-70] In summary, the accumulation of plasticizer can importantly weaken tensile properties in plasticized amorphous PLA. Solid inclusions and crystallizing plasticizers (such as PEG with high M_w) also deteriorate properties, while small inclusions of a liquid plasticizer phase can be beneficial for drawability.

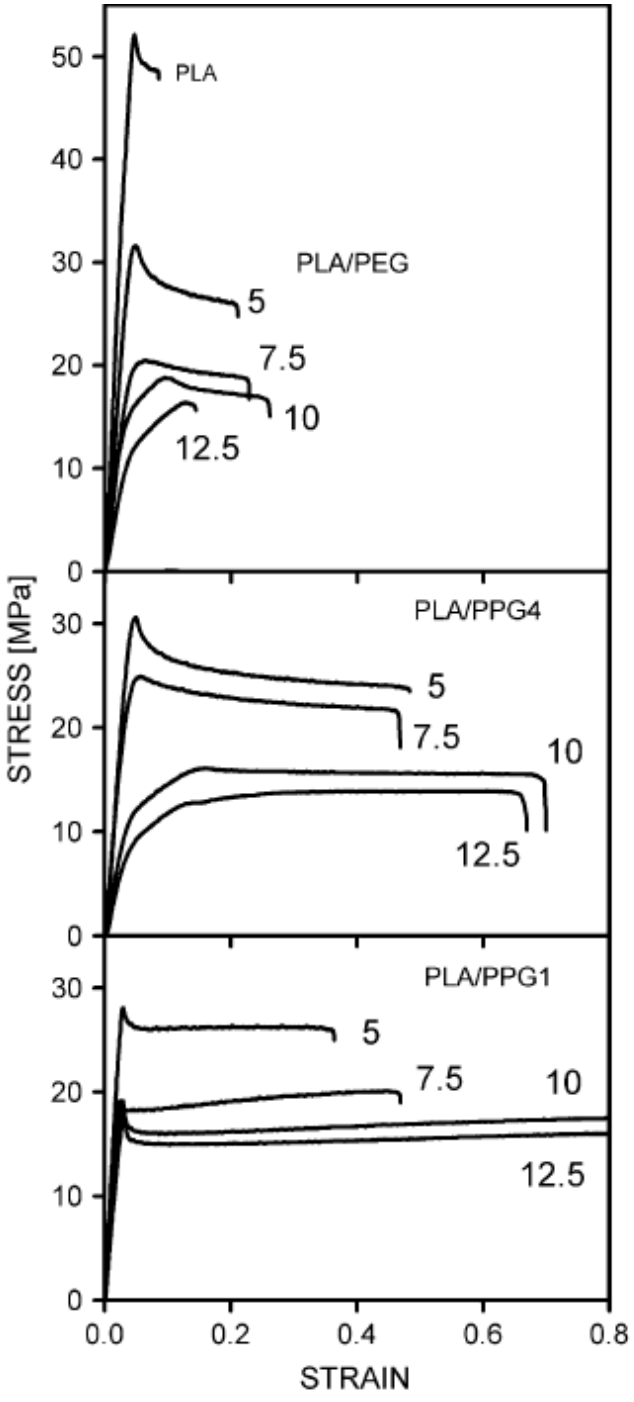

Figure 1.5 Stress-strain plots of initially semi-crystalline neat and plasticized PLA, plasticized at 5 wt%, 7.5 wt%, 10 wt% and 12.5 wt% of PEG 600 **(up)**, PPG 400 **(middle)** and PPG 1000 **(down)**

Reprinted from Piorkowska et al., Polymer, 2006, 47, 7178[70] with permission from Elsevier.

1.4.1.3. Mixed Plasticizers

Knowledge from extensive studies of PVC plasticizing and results obtained from the different studies on plasticized PLA render evident the complementary character of monomeric and polymeric plasticizers. In fact, most PVC plasticizing techniques rely on mixtures of primary and secondary plasticizers. Primary plasticizers are soluble at high concentrations and secondary plasticizers show a limited compatibility, but they are blended with primary plasticizers to improve product properties or reduce the cost. The use of a plasticizer mixture in PLA formulations has not been extensively reported.[55, 77] Mixtures of TBC and different PLA-b-PEG copolymers were studied to combine the positive effect of TBC on ε and the increase in σ given by the copolymer.[55] Among different copolymer structures, the linear molecule (PDLLA-b-PEG750) was one of the most successful. Furthermore, the use of the copolymers increased the impact strength in samples that did not break during testing. The use of a mixed plasticizer of GTA and oligomeric poly(1,3-butylene glycol adipate) showed moderate Tg depression (**Table 1.4**) but substantial increase in elongation at break (Tg = 52 °C, ε = 320 %).[77] The topographic AFM analysis revealed a fine ‘‘network’’ of crystalline lamellae all over the sample, the strands of which grew thinner when the plasticizer quantity increased. This morphology contributed to the high elongation at break values, although samples were clearly crystalline. Unfortunately, the authors gave no comment on the miscibility of the plasticizer and PLA, so a comparison of this system with the phase separated PPG system[69-70] cannot be drawn. Both approaches produced systems with high elongation at break and tensile strength. The use of plasticizer mixtures seems therefore a promising way to tune PLA mechanical .properties.

1.4.2. Plasticizers as Processing Aids

Different properties of plasticizers are useful in the aim of easing PLA processing. Melting point depression and reduction of T_g results in decreasing the processing temperature. T_g

depression was extensively discussed in previous sections. In the limit of miscibility, melting point depression is also efficient to speed up crystallization rates. Furthermore, plasticizers decrease polymers melt viscosity and allow better flow in the different process equipment. Some data are available on the melt viscosity of plasticized PLA, not aimed at foaming or spinning applications. Examples show the effect of the most popular PLA plasticizers, *i.e.* citrate derivatives and PEG. In general, PLA exhibits shear thinning behavior in the high shear range and plasticizers decrease the viscosity values at all shear rates. Liu et al.[78] tested apparent viscosity of PLA plasticized with ATBC using a capillary rheometer and observed shear thinning all over the used apparent shear rate range (100 to 1000 s^{-1}). Apparent melt viscosity at 165 °C decreased from 1,789 $Pa.s^{-1}$ at 100 s^{-1} apparent shear rate to approximately 400 $Pa.s^{-1}$ at 1,000 s^{-1} apparent shear rate. The addition of 3 wt% ATBC decreased the apparent melt viscosity at 100 s^{-1} apparent shear rate to 1,350 $Pa.s^{-1}$, shear thinning curves being parallel to neat PLA. The melt flow rate and melt flow volume of PLA/ATBC in a twin screw extruder were examined by Scatto et al.[59] The authors found a significant increase in melt flow rate from 3.8 to 10.7 g (10 min^{-1}) for neat and PLA containing 20 wt% ATBC, respectively. Melt flow rate was furthermore found independent from the twin screw speed. Impact of plasticizers on zero shear viscosity of PLA in the Newtonian plateau was investigated for ATEC,[54] PEG 1000[75] and PEG 3350.[54] The authors showed an important decrease of zero shear viscosity upon blending with PEG, from 5,000 to approximately 800 $Pa.s^{-1}$ for 10 wt% PEG 3350[54] and from 870 to 310 $Pa.s^{-1}$ for 10 wt% PEG 1000.[75] In both cases the decrease in the curve leveled off at about 20 wt% of PEG, when the miscibility limit was reached. ATEC gives a higher zero shear viscosity decrease from 5,000 to approximately 100 $Pa.s^{-1}$ for 10 wt% ATEC.[54]

The decreased viscosity of the plasticized melt also helps greatly in the incorporation of fillers. Plasticizers have been used as processing aids for the fabrication of PLA

nanocomposites by melt inclusion techniques. PEG is the plasticizer mostly used as a processing aid for the preparation of PLA nanocomposites. PEG has the ability to preferentially intercalate between layers of the silicates and thereby help nanoclay exfoliation.[60, 64-67, 79] Due to this preferential intercalation, PEG permits the opening of the tactoid structure of non-organomodified clays, such as Cloisite® Na^+.[64] It was observed that at high nanoclay loads, T_g of PLA increased because of the depletion of PEG from the polymer phase by intercalation between nanoclay stacks.[64] The preferential intercalation of PEG depends on the type of modification of the clay, where the most apolar structures present the lowest efficiency.[67] In organomodified nanoclays, for example Cloisite® 20A and Cloisite® 30B, co-intercalation of PLA with PEG during melt compounding can be found.[67] PEG is clearly a processing aid for the successful production of PLA/clay nanocomposites.

Polyadipates were also shown to be good processing aids for exfoliation of layered aluminosilicates.[61b, 72] On the contrary to PEG oligomers, polyadipates show no preferential interaction with the nanoclays.[72] Polyadipates of different chain length are able to swell nanoclays, as observed for Cloisite® 30B.[72] The higher molecular weight polyadiapate (M_n = 3,460 Da) was found to be slightly less efficient than the smaller oligomer (M_n = 2,400 Da). However, the second has the advantage of lower migration propensity due to increased chain length.[72] Scatto et al.[59] not only showed the interest of ATBC as an aid for exfoliation of layered nanoclays in PLA but worked on different processing techniques and concluded that the best method for the nanoclay introduction is by forming a previous mixture with the plasticizer. The comparison between mixing in an internal mixer and by twin-screw extrusion showed the superiority of this latter processing for nanoclay dispersion.

1.5. Long-term Stability of Plasticized PLA

The long-term stability of plasticized materials is a major concern for their successful application and it can be depreciated by chemical degradation of the polymer and/or plasticizer or by physical changes in the bulk properties of materials.

1.5.1. Physicochemical Studies of Long-term Stability

Physical ageing is commonly understood as a phenomenon occurring during storage of a polymer below its glass transition, where only restricted motion as rotation of small groups of atoms and vibration and rotation motion of chemical bonds along the polymer chain is permitted. Consequently, the polymer relaxes slowly to its equilibrium, causing changes in bulk properties, such as volume or enthalpy.[80] Above the glass transition temperature, the amorphous phase is thought to be in its equilibrium and no ageing caused by relaxation phenomena is thought to occur, although for semi-crystalline polymers it has been shown that the constrained amorphous phase close to the crystalline lamellae may give rise to ageing effects.[80] However, in the case of semi-crystalline polymers phenomena like cold crystallization can occur.

Most studies on ageing effects of PLA including physical phenomena were carried out by storage of samples in ambient conditions with minor control of environmental parameters, although most of the authors are careful in sealing the samples in polyethylene bags to protect from ambient humidity. This method is of main interest as it corresponds to real conditions plasticized PLA materials might experience during their storage and service time, noting that major PLA applications correspond to the use at ambient temperature. The distance between glass transition temperature and ageing temperature varied among studies and often even changed during the experiment time. Therefore all the above-mentioned physical phenomena

can be expected. **Table 1.5** gives an overview of different studies available and sums up very briefly the main physical changes of the samples observed for each experiment.

Within the family of monomeric plasticizers, the long-term stability of GTA and TBC was investigated.[43, 51] Phase separation and cold crystallization were evidenced in all cases, where ageing was carried out very close to T_g or even at T_g (**Table 1.5**). Storage of PLA/GTA and PLA/TBC at ambient conditions resulted in substantial chain scission of PLA (M_w divided by 5 after 123 days).[51] The authors suggested that the hygroscopic character of the plasticizers permitted the water sorption in the film triggering PLA hydrolysis. The chain scission then caused some increase in crystallinity, decrease in T_g and embrittlement of the aged material. Furthermore, plasticizers exuded during storage causing the material surface to become sticky.[51] Immersion of PLA/TBC films in water showed the gradual loss of TBC and the increase of T_g. Upon material storage in dry environment, cold crystallization of PLA was still observed and the T_g increased with time.[43] DINCH, although it was much less efficient than TBC to depress T_g, had higher permanence in the PLA structure upon immersion in water and during ageing in dry conditions over 4 months almost no change in T_g was detected.[43] Due to the large difference in T_g of the initial blend, the storage of PLA/TBC was carried out inside the glass transition range, while the PLA/DINCH was glassy, where transport phenomena are strongly slowed down.

With respect to polymeric plasticizers, the PLA/PEG system received some interest in ageing studies. A common result of all of them is that PEG/PLA blends are not stable. In the case of PEG with small M_n and waxy at room temperature, phase separation by ageing was observed.[65, 74, 81] Pluta et al.[81] undertook an extensive study of ageing of PLA/PEG 1000 and PLA/nanoclay/PEG 1000 systems for 1 to 4 years below glass transition temperature. They investigated first the evolution of M_n, which showed that the ageing of 1 year decreased importantly the macromolecular chain length to only 18 % of the initial value. A small

quantity of organomodified nanoclay seemed meanwhile to have a positive effect on the chemical stability, as M_n decreased less in that case. Due to the substantial decrease of the macromolecular chain length, samples were highly crystalline and brittle after 4 years of storage. Interestingly, T_g after 4 years was higher than after one year, which was the effect of phase separation inside the sample and migration of PEG 1000 onto the sample surface. The authors evaluated the amount of PEG 1000 leached out by diffusion and reported that approximately 7.4 % of PEG was lost from the bulk. It gathered on the sample surface forming a crystalline layer. The dispersion of nanoclays at low concentration (< 10 wt%) inside PLA delayed the PEG 1000 diffusion, most probably due to the increase in the tortuosity of the molecules' pathway. Furthermore, the PEG 1000 diffusion from the PLA/Cloisite® 30B/PEG 1000 system was always low. A retention effect due to interactions of hydroxyl groups of PEG and ammonium cations contained in the organomodifier was proposed. Besides diffusion, the nanoclays hindered also the phase separation while preferential PEG/nanoclay interactions depleted the amorphous phase of the blends. The effect is that the PEG-rich phase in the nanocomposites always had higher T_g compared to the blank sample.[81] Another study of physical ageing in PLA/Cloisite® 30B nanocomposites plasticized with PEG 1000 for one year in the glassy state showed that the initially almost fully exfoliated structure of Cloisite® 30B recovered a tactoid structure after ageing for one year.[74] Due to the phase segregation taking place the clay galleries got depleted again and recovered an aggregated structure.

Table 1.5 Overview of physical ageing behaviour of PLA/plasticizer compounds

	Plasticizer	**t_a** *(d)*	**T_a** *(°C)*	**T_g** *(°C)*	**Note**	**Ref.**
PLA	GTA	123	RT	29	M_w degradation, T_g decrease, cold crystallization, phase separation, migration	51
	TBC	123	RT	29	Cold crystallization	
PLA	DBM	120	22	29	Phase separation, cold crystallization	33
	DBM-A	120	22	39	No phase separation	
PLA	TBC-E	120	22	33	Phase separation	29
PLA	TBC	120	RT	24.0	T_g increase, cold crystallization, embrittlement	43
	DINCH	120	RT	49.9	No T_g change, embrittlement	
PLA, 13 % D	PEG 8 000	75	23	9	PEG crystallization as long as T_a>T_g, thus gradual increase of T_g, embrittlement	62
PLA, 5 % D	PEG 8 000	125	23	12	Phase separation, increase of T_g, low crystallization of PEG, embrittlement	63
PLA	PEG 10000	60	20	50.5	No change in T_g	82
				32.0	T_g increase, cold crystallization, embrittlement	
				25.0	T_g increase, cold crystallization, PEG crystallization, embrittlement	
	PEPG 12000	60	RT	50.9	No change in T_g	
				23.4	T_g increase, cold crystallization, phase separation, embrittlement	
PLA	PEG 1500	90	RT	44.8	T_g increase, cold crystallization	65
PLA-C25A-3%	PEG 1500	90	RT	44.0	T_g increase, cold crystallization	
PLA	PEG 1000	365	RT	29.4	T_g increase, small enthalpic relaxation peak, phase separation	74
PLA-C30B-3%	PEG 1000	365	RT	33.5	T_g increase, enthalpic relaxation, phase separation, tactoid clay structure increase	
PLA	PEG 1000	1460	4	23.4	T_g increase, cold crystallization phase separation, crystalline PEG layer outside	81
PLA-C20A-10%	PEG 1000			27.6	T_g increase, smaller cold crystallization, phase separation delay by clay presence	
PLA-C25A- 10% PLA-C30B- 10%				28.5	T_g increase, cold crystallization reduced by clay presence, phase separation delayed, all samples show strong embrittlement	
PLA	PA G206/2	150	28	39.5	No change in T_g, no phase separation	61a
				25.4	Cold crystallization, embrittlement, increase in barrier properties	
PLA	PA G206/7	60	RT	37.6	No T_g change	61b
PLA-C30B-3%				37.7	No T_g change, cold crystallization, embrittlement, increase in barrier properties	
PLA	OLA	90	25	38.9	No change in T_g, embrittlement, increase in barrier properties	76

In the case of PEG 8000, being a crystalline solid at room temperature, crystallization of the plasticizer inside the PLA matrix was observed as long as the storage temperature was higher than glass transition.[62-63, 82] The crystallization depleted the amorphous phase from the plasticizer, which caused the T_g to rise. At the point at which the T_g became higher than the storage temperature, the crystallization of PEG 8000 ceased.[62] The material simultaneously experienced an increase of the glassy modulus by the reinforcing effect of PEG 8000 crystals. At high PEG 8000 concentrations (30 wt%), an influence of PLA stereo-regularity on the PLA/PEG 8000 mixing behavior could be observed. While PLA with low stereo-regularity/PEG 8000 showed miscibility at room temperature, PLA with higher stereo-regularity readily phase separated.[63] In this case, phase separation, characterized by the appearance of two glass transition temperatures, was the primary ageing mechanism and completed after 48 h. No crystallization of PEG 8000 was observed.[63]

Faced with long-term instability of PLA/PEG blends, alternatives were studied and PPGs were considered good candidates. Jia et al.[82] tested the ageing of a PEG-PPG (PEPG 12000) copolymer against PEG 1000. PEG 1000 showed crystallization of PEG, as discussed earlier. The PEPG 12000 blend phase separated gradually over time. In the case of ageing in the glassy state, the authors reported the important increase of the enthalpic relaxation peak resulting in the drastic reduction of elongation at break.

The positive effect of increasing the chain length of oligomers on the longterm stability of plasticized PLA was shown in the case of oligomeric TBC,[29] malonates,[33] lactic acid[76] and adipates.[61] The ageing of PLA/TBC-E-3 (3 sub-units) near T_g showed phase separation and cold crystallization with time, but the material became non-sticky on the surface even after 4 months, showing the lower trend of the oligomer to migrate to the polymer surface.[29] The strategy of increasing M_n for long-term stability was successful in the case of malonate oligomers.[33] While DBM yielded phase separation, embrittlement, cold crystallization of PLA

and migrated to the surface of the polymer, the oligomers (n = 8) were very stable for an ageing period of 4 months without cold crystallization and changes in T_g. The ageing of PLA/ OLA blends was done at temperatures at or slightly lower than T_g forcing minor decrease in ε.[76] The strongest embrittlement occurred upon storage at temperatures below T_g. In this case, ε decreased from almost 200 % to nearly the value of neat PLA (5 %) and enthalpic relaxation could be observed. A very interesting result was obtained by measuring the oxygen barrier properties of films during ageing. Plasticizing generally decreases barrier properties due to bringing free volume to the polymer, but ageing let the barrier properties increase again. In fact, PLA blends containing 20 wt% OLA (T_g = 34 °C, T_a = 25 °C, **Table 1.5**) almost recovered the barrier properties of the neat PLA. The authors suggested that PLA experienced a gradual structure rearrangement causing densification, but without crystallization.[76] The same research group investigated the ageing of PLA plasticized with polyadipates of different M_n at T_g or below.[61] Ageing at T_g let cold crystallization of PLA happen, causing the elastic modulus to rise and drawability to decrease. Phase separation in the material was solely observed for the addition of the lowest M_n polyadipate at 20 wt%. All samples showed exudation to the sample surface, which became sticky with time. In a follow-up study, the ageing of PLA/polyadipates was carried out for 2 months at temperatures slightly below T_g (**Table 1.5**). Interestingly, putting both studies together, the enthalpic relaxation peak was seen only for the 10 wt% blend with a difference of T_g - T_a = 14 °C.[61a] The 15 wt% blend with a distance of T_g - T_a = 12 °C and the 20 wt% blend having a difference of T_g - T_a = 6 °C showed no enthalpic relaxation.[61b] Nevertheless, an increase in barrier properties was observed. The oxygen transmission rate thus seems a very fine probe for densification phenomena occurring during physical ageing. The absence of change in oxygen barrier properties over two months of storage of the PLA/ Cloisite® 30B/polyadipate ternary

nanocomposite proved that the delay of ageing brought by nanoclays applied also to polyadipate plasticizers.[61b]

1.5.2. Chemical Stability and Degradation

Plasticizers are additives that could be present up to 30 wt% in PLA formulations. Their impact on the chemical ageing of PLA could be considered by either a negative or a positive role depending on their chemical architecture and hydrophilicity and also on their use in medical or commodity applications.

Lim et al.[83] showed that the melt mixing of PLA with additives often results in a decrease of the molecular weight, which can be due to the high sensitivity of PLA to the thermo-mechanical input, to the moisture and/or to transesterification reactions with additives. Furthermore, water should be considered and controlled as being a third active component during PLA plasticization process and acting in chemical ageing. Interchange reactions in polyesters are rapid in the melt during processing and in particular the mechanism of transesterification, which is an associative-type mechanism where bonds breaking and formation occur simultaneously. Jamshidi et al.[84] proved that low-molecular-weight compounds associated with the polymer seemed to play an important role in lowering its M_n at high temperatures. These molecules were identified as water, monomers, oligomers and polymerization catalysts. Afterwards Hyon et al.[85] and Cam and Marucci[86] showed the negative impact of residual monomers on the thermal stability of polylactides, but otherwise cyclic or aliphatic monomers are viewed as efficient plasticizers. Thus, removal of the non-polymeric contents and blocking the hydroxyl end-group enhanced the thermal stability of polymers. Obviously, the presence of plasticizers with ester-groups, –OH or –COOH derived groups could emphasize the degradation routes by transesterification.

Murariu et al.[42] studied the stability of a PLA grade (L/D isomer ratio 96/4, high molecular weight) when melt-mixed with selected plasticizers, namely DOA, GTA, ATBC up to 20 wt%. In particular, molecular weight parameters (number average molar mass, M_n, and dispersity, M_w/M_n) of neat PLA and plasticized PLA were determined. The authors concluded that no major decrease in the M_n of PLA was observed whatever the plasticizer. However, they were careful to use moderate and controlled mixing conditions by using an internal mixer and they specified that plasticizers were carefully dried under vacuum before blending with dry PLA. Careful drying is necessary due to the risk of hydrolysis reactions of ester linkages depending on residual water content and/or plasticizer leading to reduction in molecular weight. Minimizing moisture content by intensively drying all components represents a first step to reduce losses by hydrolysis and to preserve the polyester molecular weight as high as possible.

In the same manner, Courgneau et al.[58] showed that when PLA is extensively dried, only a slight decrease in molecular weight is observed after melt blending at 160 °C. The addition of plasticizer brings about a notable decrease (40 %) in M_w in the case of 9 wt% PEG. The addition of PEG results in the molecular weight decrease, which may be due to the degradation of PLA chains coupled to main chain scission and transesterification reactions between PLA and PEG. ATBC, on the contrary, does not induce a decrease in M_n at low contents and the addition of this plasticizer up to 17 wt% PLA results only in a slight decrease in M_n.[58]

1.6. PLA Plasticizers Derived from Biomass

One interesting way to modify the mechanical properties and preserve the environmentally friendly aspect of polylactide is by introducing bio-based compounds within the PLA matrix. Furthermore, the use of non-edible biomass could constitute a wide source of additives, and could provide an economically viable way to get added-value from residues.[87] Numerous studies to transform biomass by-products of the agriculture and food industries have been conducted recently[88] and some eco-friendly products have been successfully used to plasticize vitreous polymers, such as PVC.[89] Nevertheless, due to the large diversity of molecules constituting a product issued from the biomass, isolating one of them is often costly and renders the process economically uncompetitive. Two main approaches using biobased products to enhance PLA mechanical properties are currently investigated and examples of each one are given below.

The first approach can be summed up by the use of specific molecules extracted from the biomass. Thus, the chosen molecules, according to the classical plasticization concepts, have to be highly miscible within the polymer network to dissolve and/or swell it. Among bio-based molecules, Jacobsen et al.[35] investigated the plasticizing efficiency of glucose-monoester and partial fatty acids esters. However, no significant improvement in plasticization was observed. An eventual explanation of this result could be the poor miscibility of those molecules in PLA inducing a non-homogeneous material. Martin et al.[49] studied the plasticization ability of glycerol and OLA. The first one exhibited a poor compatibility with PLA since T_g was only decreased by 5 °C for a PLA/glycerol blend 80/20 wt%. On the contrary, adding 20 wt% of OLA strongly diminished the T_g to 18 °C, improved ε to 200 % and greatly reduced the elastic modulus from 2,050 to 744 MPa. More recently, Azwar et al.[90] proposed the use of liquefied wood flour and liquefied rice bran (obtained by acid-catalyzed reaction) to plasticize polylactide. They showed that liquefied wood flour,

mainly constituted by low-molecular-weight polyols and mono/disaccharides was able to penetrate the matrix. Indeed, the T_g was decreased below room temperature (*i.e.* to 27 °C and 12 °C for 90/10 wt% and 70/30 wt% of PLA/additive blends, respectively). Furthermore, by adding 30 wt% of this product ε rose to 300 %. Liquefied rice bran did not show any of these plasticizing abilities. According to size exclusion chromatography (SEC) study, the authors assumed that the liquefied rice bran was composed of too high molecular weight oligosaccharides to permit an efficient plasticizing effect. Limonene, which is a common by-product of citrus juice processing,[91] has also been used as plasticizer for PLA. In fact, Arrieta et al.[92] showed that the T_g of PLA was lowered by up to 30 °C (from 60.3 °C to 30.2 °C) when adding 15 wt% of limonene, and ε improved up to 150 %. Blends containing 20 wt% of limonene were also prepared, exhibiting a T_g value slightly higher than the previous blend (33.8 °C) and ε = 165 %, very close to the previous result. These last observations could possibly point out the miscibility limit of limonene in PLA. Moreover, Sawalha et al.[93] studied the effect of the incorporation of volatile alkanes on the PLA morphology. They also observed the plasticizing efficiency of limonene. Although the amount of limonene remaining in the PLA matrix was unknown, they noticed that the T_g was lowered to 30 °C, while ε was enhanced up to 200 %. The compatibility of limonene and PLA can be explained by the Hansen solubility parameters (HSP). Indeed, the limonene parameters are (δ_D = 17.2; δ_P = 1.8; δ_H = 4.3)[24b] and those for PLA are (δ_D = 18.6; δ_P = 9.9; δ_H = 6.0).[25] This confers limonene compatibility with PLA similar to ATBC or DOA. Recent researches to study positive effects, such as antioxidant and plasticizing properties, have been conducted among bio-based additives. Lopez-Rubio et al.[94] investigated β-carotene (which is a well-known natural antioxidant[95] and UV absorber[96]) by adding 0.4 wt% into PLA. They reported a nucleating effect and a decrease in cold crystallization temperature from 113.5 °C to 80.5 °C. They also observed a significant improvement in elongation at break from 13 % to 250 %. Furthermore,

the tensile modulus was lowered from 2,060 MPa to 570 MPa, meaning that β-carotene could exhibit good plasticizing efficiency. Nevertheless, another hypothetical explanation of these effects could come from the eventual residues of solvent remaining in the PLA matrix after casting. Hwang et al.[97] tested α-tocopherol and resveratrol, which are natural antioxidant molecules, present in soybean, cotton-seed, sunflower and grapes. They added both additives to PLA in several proportions representing a constant total quantity of 5 wt%. Nevertheless, no plasticizing abilities were observed, since the T_g values and ductility showed no significant changes.

The second strategy consists of improving the PLA ductility by using products that are directly issued from low-cost biomass derivatives but have only partial miscibility with PLA. In this case, the mechanical properties improvement is partly based on the modification of the polymer breakage behavior. In fact, when products with low compatibility are incorporated within PLA, some micro-voids can be formed during the tensile deformation. They appear at the interface between PLA and non-dissolved additive droplets, resulting in a stress whitening phenomenon.[68, 70] In this case, a ductility improvement and a decrease in tensile strength while T_g remains relatively high can be observed. Piorkowska et al.[70] who investigated blends of PLA and PPG rationalized this behavior by a local plasticization of PLA due to the presence of micro-droplets of the additive in the polymer structure. Moreover, the presence of these droplets in the polymer matrix might enable dissipation of the fracture energy through the interfaces between matrix and droplets, raising the maximum absorbable energy of the material.[70] Additives that involve such mechanisms to increase the polymer ductility are sometimes called toughening agents. More details about such mechanisms are given in Section 1.7 “Other Solutions for PLA Toughening”.

Epoxidized vegetable oils have received much recent interest. It has been shown that functional groups, such as ester or epoxy, could be degraded by micro-organisms,[87] making

epoxidized vegetable oils interesting additives to maintain biodegradability of blends with PLA. In particular, epoxidized soybean oil (ESO), which has also been used as an effective plasticizer for PVC,[98] was studied. Ali et al.[99] reported that blending ESO with PLA reduced T_g by about 4 °C, 8 °C and 9 °C for 95/5 wt%, 80/20 wt% and 70/30 wt% blends, respectively. Partial miscibility of epoxy resins with thermoplastic polyesters with carboxyl end groups could be explained by hydrogen bonding between ester groups or the terminal hydroxyls of PLA with the epoxy group of the additive.[100] Regarding ductility, a maximum enhancement was obtained for the 80/20 wt% blend exhibiting nearly 40% elongation at break, while 90/10 wt% and 70/30 wt% blends showed values around 20 %. The 95/5 wt% PLA/ESO blend did not point to any ductility improvement to values for neat PLA (ε = 5 %), but stress at yield was lowered from 60 MPa to 45 MPa. Al-Mulla et al.[101] showed that modified montmorillonites with fatty nitrogen compounds obtained from vegetable oils could enhance the ductility of PLA/ESO blends by increasing their compatibility. Xiong et al.[102] studied a 90/10 wt% PLA/ESO blend but did not report a ductility increase. However, they noticed some decrease in T_g (no values mentioned) and a slight depression in elastic moduli and tensile strength from 3,020 MPa and 69 MPa to 2,730 MPa and 62 MPa, respectively. Xu et al.[100b] introduced ESO at five concentrations into PLA (3, 6, 9, 12 and 15 wt%) and did not notice ductility improvements while tensile modulus and tensile strength decreased. Based on the same principles, epoxidized palm oil (EPO) was studied, partly because of the great economic importance of palm oil production.[103] Silverjah et al.[104] mixed EPO with PLA and observed an important increase in ductility, while T_g was reduced only by a few degrees and micro-voids were noticed. Indeed, the PLA containing 5 wt% of EPO exhibited a T_g value of 56.8 °C and ε up to 100 %, while neat PLA was measured at 63.5 °C and 6.3 %, respectively. In another study,[105] same authors examined the effect of the EPO epoxy content and observed that the higher it was, the more important was the improvement in mechanical properties. Al-

Mulla et al.[106] also reported elongation at break of 210 % for blends of PLA/EPO (80/20 wt%), which decreased with higher contents of EPO. In general terms, an ideal concentration of 20 wt% of epoxidized oils was found to maximize the ductility enhancement. Furthermore, the authors also found that a higher thermal stability was obtained when adding EPO to PLA, probably due to reduced heat sensitivity.[107]

1.7. Other solutions for PLA toughening

In order to supplement this survey on PLA plasticization, a short overview of the use of immiscible components as additives to enhance the PLA ductility is presented. As previously mentioned in section 1.6 "PLA Plasticizers Derived from Biomass", such involved deformation mechanisms do not rely on free volume improvement but mainly on damage mechanisms, often resulting in stress-whitening.

1.7.1. Deformation behaviour of amorphous glassy polymers through damage mechanisms

The literature on polymer deformation generally depicts two mechanisms for failure: shear yielding and crazing. Both mechanisms can occur and mostly depend on temperature, strain rate, and stress state.[108] In fact, shear bands and crazes propagate via highly cooperative segmental rotation of isomers;[109] the yield criterion for glassy polymers is based on 1) the activation energy for conformational relaxation and 2) the intermolecular segmental cohesive energy[110] holding the material together, result of intermolecular forces of attraction such as van der Waals forces, hydrogen bonding, etc.[111]

Shear yielding is generally associated to plasticity and locates in high stress concentration zones.[112] It generates shear bands under an angle of 45 ° to the deformation axis due to displacement of a part of the material in relation to another. The involved plastic deformation is related to the material softening right after yielding.[113] Two types of shear bands can be

distinguished: fine bands and coarse bands.[114] Generally, fine ones slowly propagate and allow greater deformation. According to Friedrich,[115] intersection between shear bands may constitute a weakness point promoting crazing.

Crazing is due to microvoids (cavitation) appearance in regions of stress concentrations perpendicularly to the deformation axis because deformation is constrained laterally, resisting to Poisson contraction: the density of the material decreases with increasing strain.[116] Crazes look like a fissure whose edges are connected by extensively stretched macromolecules called fibrils and are capable of bearing a load.[117] In fact, crazing is a mode of plastic deformation rather than mechanical cracking.[118] Further stretching however leads to fibrils breakdown and formation of a microcrack[113, 119] growing until it reaches a critical size; at which point catastrophic failure takes place.[120] Note that creation of voids is generally associated to optical whitening of the deformed material[121] as sometimes observed using low miscible products and depicted along previous sections.

1.7.2. Principles of toughening

Toughening of brittle polymers by dint of inclusion of micrometric particles (generally rubbery polymers) can be an effective alternative to plasticization. Cavitation due to a high level of hydrostatic stress in the particles, resulting from an important contrast between mechanical properties of the matrix and the particles, as well as debonding of interfaces,[122] can delay the final breakage. In fact, multiplying cracks may lead to higher energy absorption, increasing the maximum damaging capacity of the material.[123] Note that according to Gent,[124] cavitation is favored when particles have internal flaws. Besides, at low deformation rate, cavitation points may geometrically organize trough dilatational bands named “croids”,[125] which preferentially develop plasticity. Particles also can stop cracks propagation preventing early breakage[126] provided good interface cohesion between particles and matrix is present.[127]

On the other hand, particles may also relieve the stress triaxiality and favor shear yielding over crazing of the matrix.[128] Studies have shown that predominance between shear yielding and crazing is influenced by the size of the particles: small ones promote yielding[129] because they harder cavitate.[130] On the opposite, the size does not appear to have a significant effect on the yield stress[131] despite the macroscopic cavitation stress inversely increases with size.[124] Note that for maximal efficiency, the particle cavitation stress has to be close to the local yield stress of the material.[132] Furthermore, the interparticle distance also influence the deformation mechanism: close enough particles which cavitate will allow the matrix to be in a plane stress state able to develop greater plastic deformation through shearing.[131] On the opposite, adding a too important quantity of toughening agents may decrease mechanical properties: cavitation of aggregated particles leads to the creation of a big size weakness area from which a crack may grow.[133]

1.7.3. Examples of toughen polylactide

Many different polymers have been tried out to toughen PLA. Few examples given below were selected to illustrate come specific points previously approached. Lu et al.[134] observed that large amounts of poly(ethylene succinate) (PES), a highly ductile polyester, had to be used to significantly increase the ductility of blends. In fact, the elongation at break was around 15 % for PLLA/PES 80/20, and further increased to around 145 % for PLLA/PES 60/40. Bad compatibility of both materials was probably the cause of lately enhanced properties. Noda et al.[135] used polyhydroxyalkanoates (PHAs) copolymers, namely Nodax, varying the weight content up to 60 %. Important gain in energy at break and substantial ductile plastic deformation up to 100 % were observed for blends containing 10 and 20 wt% of Nodax. Clear sign of extensive crazing through whitening was pointed. In another study, Kowalczyk et al.[136] added poly(1,4-cis-isoprene), natural rubber immiscible with PLA. Crazing initiation and cavitation of particles, which further promote shear yielding, allowed

reaching ε ≈ 100 %. Poly(butylene adipate-co-terephthalate) (PBAT) was also used up to 20 wt% in PLA.[137] Tensile behavior changed from brittle to ductile fracture showing a distinct yielding and stable neck growth and getting ε = 200 %. A biodegradable poly(ether)urethane elastomer having a partial miscibility with PLA[138] added up to 30 wt% decreased crystallinity degree of PLA. Shear yielding and ductile fracture up to ε = 360 % were obtained. Shape memory effect after heating was surprisingly observed blending a polyamide elastomer with PLA.[139] The high compatibility of the dispersed phase working as plasticizer by decreasing the glass transition of PLA promoted orientation and reorganization of PLA molecules in the lower temperature. Shibata et al.[140] used poly(butylene succinate-co-l-lactate) (PBSL) to enhance the PLA ductility. They observed that addition of a plasticizer, however at insufficient content to turn the PLA ductile, significantly improved the blend mechanical properties by bettering miscibility. Natural rubber grafted with poly(vinyl acetate) copolymer to improve miscibility was blended with PLA.[141] Because of bettered compatibility, reduction of the rubber particles diameter was obtained and enhancement of toughness and ductility of PLA was therefore observed. Reactive blending of acrylonitrile–butadiene–styrene copolymer (ABS) with PLA using a compatibilizer was conducted[142] to overcome the thermodynamic immiscibility of both materials: the size of ABS domains was significantly decreased, bettering the ductility.

1.8. Conclusion

Plasticization of PLA has proved to be very effective in improving mechanical and other important properties. The type and quantity of the external plasticizer depends on the target application of the compounded PLA-based material. Very schematically, if the service-life of the material is intended to be short, or even if the first service of the polymer is degradation, as in many biomedical applications, the use of a monomeric plasticizer bearing no toxicological risk is preferable. Monomeric plasticizers have generally higher efficiency in T_g

depression and drawability increase. The use of solubility parameters is a good guide for choosing the adequate molecule, but other factors, such as molar volume, should be taken into account. At equal molar volume, the molecule with smaller molecular weight will be more efficient by the higher number of terminal groups at an equal mass concentration. Their drawback is the small permanence, so if the service-life of the material should be long (typically several years), such as in most commodity applications, polymeric plasticizers are very likely preferable. In this case, miscibility prediction by solubility parameters often fails, as the underlying models cannot take into account the effect of the macromolecular chain length. Partial miscibility between the polymeric plasticizers and PLA is not negative for properties in any case, though. It has been shown that inclusions of small droplets of liquid plasticizers within a certain proportion (typically below 20 wt%) can have a positive impact on drawability. The molecules function in this case as toughening agents and involved mechanisms are likely similar to the one of impact modifier immiscible components Many novel attempts to toughen PLA with molecules derived from biomass and not necessarily miscible with the polymer rely on this mechanism. More research needs to be carried out on the topic.

Finally, PVC plasticizing technology frequently uses mixtures of monomeric and polymeric plasticizers. This approach has the potential to increase PLA toughness in combining efficiencies of both types of plasticizer. Monomeric plasticizers help to increase miscibility of polymeric molecules with the polymer matrix. This strategy has been attempted very rarely for PLA, but the pioneering studies show very promising results. Another approach to solve permanence and miscibility problems is the use of internal plasticizers, which are grafted on the polymer chain or copolymerized into it.

REFERENCES

1. **(a)** Auras, R. A.; Harte, B.; Selke, S.; Hernandez, R., Mechanical, physical, and barrier properties of poly (lactide) films. *Journal of Plastic Film and Sheeting* 2003, *19* (2), 123-135.
(b) Mark, J. E., *The Polymer Data Handbook*. Oxford University Press Inc: New York, USA, 1999.

2. Saeidlou, S.; Huneault, M. A.; Li, H.; Park, C. B., Poly(lactic acid) crystallization. *Progress in Polymer Science* 2012, *37* (12), 1657-1677.

3. Liu, H. Z.; Zhang, J. W., Research Progress in Toughening Modification of Poly(lactic acid). *J. Polym. Sci. Pt. B-Polym. Phys.* 2011, *49* (15), 1051-1083.

4. Wypych, G., *Handbook of plasticizers*. ChemTech Publishing: Toronto-Scarborough, 2004.

5. Kirkpatrick, A., Some Relations Between Molecular Structure and Plasticizing Effect. *Journal of applied physics* 1940, *11* (4), 255-261.

6. Houwink, R., In *Proc. XI Int. Cong. Pure Appl. Chem*, London, 1947; pp 575-583.

7. **(a)** Mead, D. J.; Tichenor, R. L.; Fuoss, R. M., Electrical Properties of Solids. XII. Plasticized Polyvinyl Chloride1. *Journal of the American Chemical Society* 1942, *64* (2), 283-291.
(b) Aiken, W.; Alfrey, T.; Janssen, A.; Mark, H., Creep behavior of plasticized vinylite VYNW. *Journal of Polymer Science* 1947, *2* (2), 178-198.

8. **(a)** Doolittle, A. K., Mechanism of Solvent Action. *Industrial & Engineering Chemistry* 1944, *36* (3), 239-244.
(b) Doolittle, A. K., Mechanism of Solvent Action.Influence of Molecular Size and Shape on Termperature Dependence of Solvent Ability. *Industrial & Engineering Chemistry* 1946, *38* (5), 535-540.
(c) Doolittle, A. K., *The Technology of Solvents and Plasticizers*. John Wiley & Sons: New York, 1954.
(d) Doolittle, A. K., Mechanism of Plasticization. In *Plasticizer Technology*, F, B. P., Ed. Reinhold: New York, 1965.

9. Stickney, P. B.; Cheyney, L. E., Plasticizers for rubbers and resins. *Journal of Polymer Science* 1948, *3* (2), 231-245.

10. Alfrey Jr, T.; Wiederhorn, N.; Stein, R.; Tobolsky, A., Some studies of plasticized polyvinyl chloride. *Journal of Colloid Science* 1949, *4* (3), 211-227.

11. Moorshead, T. C., Advances in PVC Compounding and Processing. Sons, M. K., Ed. London, 1962.

12. **(a)** Cohen, M. H.; Turnbull, D., Molecular transport in liquids and glasses. *J. Chem. Phys.* 1959, *31*, 1164.
(b) Fujita, H., Diffusion in polymer-diluent systems. In *Fortschritte Der Hochpolymeren-Forschung*, Springer Berlin / Heidelberg: 1961; Vol. 3, pp 1-47.

13. **(a)** Flory, P. J., Viscosities of Linear Polyesters. An Exact Relationship between Viscosity and Chain Length. *Journal of the American Chemical Society* 1940, *62* (5), 1057-1070.
(b) Fox, T. G.; Flory, P. J., Viscosity - Molecular Weight and Viscosity + Temperature Relationships for Polystyrene and Polyisobutylene1,2. *Journal of the American Chemical Society* 1948, *70* (7), 2384-2395.

14. Fox, T. G.; Flory, P. J., Second-Order Transition Temperatures and Related Properties of Polystyrene. I. Influence of Molecular Weight. *Journal of applied physics* 1950, *21* (6), 581-591.

15. Williams, M. L.; Landel, R. F.; Ferry, J. D., The Temperature Dependence of Relaxation Mechanisms in Amorphous Polymers and Other Glass-forming Liquids. *Journal of the American Chemical Society* 1955, *77* (14), 3701-3707.

16. Ueberreiter, K.; Kanig, G., Self-plasticization of polymers. *Journal of Colloid Science* 1952, *7* (6), 569-583.

17. Kern Sears, J.; Darby, J. R., *The Technology of Plasticizers*. John Wiley & Sons: New York, 1982.

18. Todeschini, R.; Consonni, V., *Handbook of Molecular Descriptors*. Weinheim, 2000.

19. Oishi, T.; Prausnitz, J. M., Estimation of Solvent Activities in Polymer Solutions Using a Group-Contribution Method. *Industrial & Engineering Chemistry Process Design and Development* 1978, *17* (3), 333-339.

20. Flory, P. J., *Principles of Polymer Chemistry*. Cornell University Press: New York, 1953.

21. **(a)** Huggins, M. L., Solutions of Long Chain Compounds. *The journal of Chemical Physics* 1941, *9* (5), 440.
(b) Flory, P. J., Thermodynamics of High Polymer Solutions. *The journal of Chemical Physics* 1941, *9* (8), 660.
(c) Flory, P. J., Thermodynamics of High Polymer Solutions. *The journal of Chemical Physics* 1942, *10* (1), 51-61.

22. Abboud, J.-L. M.; Notari, R., Critical compilation of scales of solvent parameters. Part I. Pure, non-hydrogen bond donor solvents. *Pure Applied Chemistry* 1999, *71* (4), 645-718.

23. **(a)** Small, P. A., Some factors affecting the solubility of polymers. *Journal of Applied Chemistry* 1953, *3* (2), 71-80.
(b) van Krevelen, D. W.; Klaas, N. T., *Properties of polymers: Their Correlation with Chemical Structure, their Numerical Estimation & Prediction from Additive Group Contributions*. Elsevier Publishing: Amsterdam, 1972.
(c) Fedors, R. F., A method for estimating both the solubility parameters and molar volumes of liquids. *Polymer Engineering & Science* 1974, *14* (2), 147-154.

24. **(a)** Hansen, C. M., "The Three Dimensional Solubility Parameter-Key to Paint Component Affinities" : I. Solvents, Plasticizers, Polymers and Resins. *Journal of Paint Technology* 1967, *39*, 104 & 505.
(b) Hansen, C. M., *Hansen Solubility Parameters: A User's Handbook*. CRC Press: Boca Raton, Florida, 2007.

25. Abbott, S. J., Chemical Compatibility of Poly (Lactic Acid) : A practical Framework using Hansen Solubility parameters. In *Poly(lactic acid): Synthesis, Structures, Properties, Processing, and Applications*, Wiley: 2010; pp 83-93.

26. **(a)** Berens, A. R., Vinyl chloride monomer in PVC: from problem to probe. *Pure Appl. Chem.* 1981, *53* (2), 365-375.
(b) Dole, P.; Feigenbaum, A. E.; Cruz, C. D. L.; Pastorelli, S.; Paseiro, P.; Hankemeier, T.; Voulzatis, Y.; Aucejo, S.; Saillard, P.; Papaspyrides, C., Typical diffusion behaviour in packaging polymers – application to functional barriers. *Food Additives & Contaminants* 2006, *23* (2), 202-211.
(c) Fang, X.; Domenek, S.; Ducruet, V.; Réfrégiers, M.; Vitrac, O., Diffusion of Aromatic Solutes in Aliphatic Polymers above Glass Transition Temperature. *Macromolecules* 2013, *46* (3), 874-888.
(d) Piringer, O. G.; Baner, A. L., *Plastic Packaging: Interactions with Food and Pharmaceuticals*. Wiley-VCH: Weinheim, 2008.

27. www.chemspider.com. (accessed 09/09/2013).

28. Brouillet, S.; Fugit, J.-L., Solutions to reduce release behavior of plasticizers out of PVC-made equipments: binary blends of plasticizers and thermal treatment. *Polymer Bulletin* 2009, *62* (6), 843-854.

29. Ljungberg, N.; Wesslen, B., Tributyl citrate oligomers as plasticizers for poly (lactic acid): thermo-mechanical film properties and aging. *Polymer* 2003, *44* (25), 7679-7688.

30. Okamoto, K.; Ichikawa, T.; Yokohara, T.; Yamaguchi, M., Miscibility, mechanical and thermal properties of poly(lactic acid)/polyester-diol blends. *European Polymer Journal* 2009, *45* (8), 2304-2312.

31. Martino, V. P.; Jimenez, A.; Ruseckaite, R. A., Processing and Characterization of Poly(lactic acid) Films Plasticized with Commercial Adipates. *Journal of Applied Polymer Science* 2009, *112* (4), 2010-2018.

32. Pillin, I.; Montrelay, N.; Grohens, Y., Thermo-mechanical characterization of plasticized PLA: Is the miscibility the only significant factor? *Polymer* 2006, *47* (13), 4676-4682.

33. Ljungberg, N.; Wesslén, B., Thermomechanical film properties and aging of blends of poly(lactic acid) and malonate oligomers. *Journal of Applied Polymer Science* 2004, *94* (5), 2140-2149.

34. Andersson, S. R.; Hakkarainen, M.; Albertsson, A. C., Tuning the Polylactide Hydrolysis Rate by Plasticizer Architecture and Hydrophilicity without Introducing New Migrants. *Biomacromolecules* 2010, *11* (12), 3617-3623.

35. Jacobsen, S.; Fritz, H. G., Plasticizing polylactide—the effect of different plasticizers on the mechanical properties. *Polymer Engineering & Science* 1999, *39* (7), 1303-1310.

36. Hu, Y., Hu, Y. S., Topolkaraev, V., Hiltner, A., Baer, E., Crystallization and phase separation in blends of high stereoregular poly(lactide) with poly(ethylene glycol). *Polymer* 2003, *44*, 5681-5689.

37. Ducruet, V.; Vitrac, O.; Saillard, P.; Guichard, E.; Feigenbaum, A.; Fournier, N., Sorption of aroma compounds in PET and PVC during the storage of a strawberry syrup. *Food Additives & Contaminants* 2007, *24* (11), 1306-1317.

38. **(a)** Colomines, G.; Ducruet, V.; Courgneau, C.; Guinault, A.; Domenek, S., Barrier properties of poly(lactic acid) and its morphological changes induced by aroma compound sorption. *Polymer International* 2010, *59* (6), 818-826.
(b) Courgneau, C.; Domenek, S.; Lebossé, R.; Guinault, A.; Avérous, L.; Ducruet, V., Effect of crystallization on barrier properties of formulated polylactide. *Polymer International* 2012, *61* (2), 180-189.

39. Salazar, R.; Domenek, S.; Courgneau, C.; Ducruet, V., Plasticization of poly(lactide) by sorption of volatile organic compounds at low concentration. *Polymer Degradation and Stability* 2012, *97* (10), 1871-1880.

40. Yang, S.-L.; Wu, Z.-H.; Meng, B.; Yang, W., The effects of dioctyl phthalate plasticization on the morphology and thermal, mechanical, and rheological properties of chemical crosslinked polylactide. *Journal of Polymer Science Part B: Polymer Physics* 2009, *47* (12), 1136-1145.

41. Galeski, A., *Mechanical Properties of Polymers Based on Nanostructure and Morphology*. Taylor & Francis Group: London, New York, Singapore, 2005.

42. Murariu, M.; Da Silva Ferreira, A.; Alexandre, M.; Dubois, P., Polylactide (PLA) designed with desired end-use properties: 1. PLA compositions with low molecular weight ester-like plasticizers and related performances. *Polymers for Advanced Technologies* 2008, *19* (6), 636-646.

43. Wang, R.; Wan, C.; Wang, S.; Zhang, Y., Morphology, mechanical properties, and durability of poly(lactic acid) plasticized with Di(isononyl) cyclohexane-1,2-dicarboxylate. *Polymer Engineering & Science* 2009, *49* (12), 2414-2420.

44. Ge, H.; Yang, F.; Hao, Y.; Wu, G.; Zhang, H.; Dong, L., Thermal, mechanical, and rheological properties of plasticized poly(L-lactic acid). *Journal of Applied Polymer Science* 2013, *127* (4), 2832-2839.

45. Baiardo, M.; Frisoni, G.; Scandola, M.; Rimelen, M.; Lips, D.; Ruffieux, K.; Wintermantel, E., Thermal and mechanical properties of plasticized poly(L-lactic acid). *Journal of Applied Polymer Science* 2003, *90* (7), 1731-1738.

46. Courgneau, C.; Vitrac, O.; Ducruet, V.; Riquet, A.-M., Local demixion in plasticized polylactide probed by electron spin resonance. *Journal of Magnetic Resonance* 2013, *233* (0), 37-48.

47. Sinclair, R. G., The Case for Polylactic Acid as a Commodity Packaging Plastic. *Journal of Macromolecular Science, Part A* 1996, *33* (5), 585-597.

48. Labrecque, L. V.; Kumar, R. A.; Davé, V.; Gross, R. A.; McCarthy, S. P., Citrate esters as plasticizers for poly(lactic acid). *Journal of Applied Polymer Science* 1997, *66* (8), 1507-1513.

49. Martin, O.; Averous, L., Poly(lactic acid): plasticization and properties of biodegradable multiphase systems. *Polymer* 2001, *42* (14), 6209-6219.

50. Ljungberg, N.; Wesslén, B., The effects of plasticizers on the dynamic mechanical and thermal properties of poly(lactic acid). *Journal of Applied Polymer Science* 2002, *86* (5), 1227-1234.

51. Ljungberg, N.; Andersson, T.; Wesslén, B., Film extrusion and film weldability of poly(lactic acid) plasticized with triacetine and tributyl citrate. *Journal of Applied Polymer Science* 2003, *88* (14), 3239-3247.

52. Ljungberg, N.; Wesslen, B., Preparation and properties of plasticized poly(lactic acid) films. *Biomacromolecules* 2005, *6* (3), 1789-1796.

53. Martino, V.; Ruseckaite, R.; Jiménez, A., Thermal and mechanical characterization of plasticized poly (L-lactide-co-D,L-lactide) films for food packaging. *Journal of Thermal Analysis and Calorimetry* 2006, *86* (3), 707-712.

54. Li, H.; Huneault, M. A., Effect of Nucleation and Plasticization on the Crystallization of Poly(Lactic Acid). *Polymer* 2007, *48*, 6855-6866.

55. Lemmouchi, Y.; Murariu, M.; Dos Santos, A. M.; Amass, A. J.; Schacht, E.; Dubois, P., Plasticization of poly(lactide) with blends of tributyl citrate and low molecular weight poly(D,L-lactide)-b-poly(ethylene glycol) copolymers. *European Polymer Journal* 2009, *45* (10), 2839-2848.

56. Sierra, J.; Noriega, M.; Cardona, E.; Ospina, S. In *Relationship between properties, citrate content and postproduction time for a plasticized polylactic acid*, ANTEC 2010, Orlando, Florida USA, 16-20 May 2010; Society of Plastics Engineers: Orlando, Florida USA, 2010.

57. Park, K.; Ha, J. U.; Xanthos, M., Ionic liquids as plasticizers/lubricants for polylactic acid. *Polymer Engineering & Science* 2010, *50* (6), 1105-1110.

58. Courgneau, C.; Domenek, S.; Guinault, A.; Averous, L.; Ducruet, V., Analysis of the Structure-Properties Relationships of Different Multiphase Systems Based on Plasticized Poly(Lactic Acid). *Journal of Polymers and the Environment* 2011, *19* (2), 362-371.

59. Scatto, M.; Salmini, E.; Castiello, S.; Coltelli, M.-B.; Conzatti, L.; Stagnaro, P.; Andreotti, L.; Bronco, S., Plasticized and nanofilled poly(lactic acid)-based cast films: Effect of plasticizer and organoclay on processability and final properties. *Journal of Applied Polymer Science* 2013, *127* (6), 4947-4956.

60. Gui, Z.; Xu, Y.; Gao, Y.; Lu, C.; Cheng, S., Novel polyethylene glycol-based polyester-toughened polylactide. *Materials Letters* 2012, *71* (0), 63-65.

61. **(a)** Martino, V. P.; Ruseckaite, R. A.; Jimenez, A., Ageing of poly(lactic acid) films plasticized with commercial polyadipates. *Polymer International* 2009, *58* (4), 437-444.
(b) Martino, V. P.; Ruseckaite, R. A.; Jiménez, A.; Averous, L., Correlation between Composition, Structure and Properties of Poly(lactic acid)/Polyadipate-Based Nano-Biocomposites. *Macromolecular Materials and Engineering* 2010, *295* (6), 551-558.

62. Hu, Y.; Rogunova, M.; Topolkaraev, V.; Hiltner, A.; Baer, E., Aging of poly(lactide)/poly(ethylene glycol) blends. Part 1. Poly(lactide) with low stereoregularity. *Polymer* 2003, *44*, 5701-5710.

63. Hu, Y.; Hu, Y. S.; Topolkaraev, V.; Hiltner, A.; Baer, E., Aging of poly(lactide)/poly(ethylene glycol) blends. Part 2. Poly(lactide) with high stereoregularity. *Polymer* 2003, *44* (19), 5711-5720.

64. Paul, M.-A.; Alexandre, M.; Degee, P.; Henrist, C.; Rulmont, A.; Dubois, P., New nanocomposite materials based on plasticized poly(l-lactide) and organo-modified montmorillonites: thermal and morphological study. *Polymer* 2003, *44* (2), 443-450.

65. Pluta, M., Morphology and properties of polylactide modified by thermal treatment, filling with layered silicates and plasticization. *Polymer* 2004, *45* (24), 8239-8251.

66. Paul, M.-A.; Delcourt, C.; Alexandre, M.; Degée, P.; Monteverde, F.; Rulmont, A.; Dubois, P., (Plasticized) Polylactide/(Organo-)Clay Nanocomposites by in situ Intercalative Polymerization. *Macromolecular Chemistry and Physics* 2005, *206* (4), 484-498.

67. Pluta, M.; Paul, M.-A.; Alexandre, M.; Dubois, P., Plasticized polylactide/clay nanocomposites. I. The role of filler content and its surface organo-modification on the physico-chemical properties. *Journal of Polymer Science Part B: Polymer Physics* 2006, *44* (2), 299-311.

68. Kulinski, Z.; Piorkowska, E., Crystallization, structure and properties of plasticized poly(l-lactide). *Polymer* 2005, *46* (23), 10290-10300.

69. Kulinski, Z.; Piorkowska, E.; Gadzinowska, K.; Stasiak, M., Plasticization of poly(L-lactide) with poly(propylene glycol). *Biomacromolecules* 2006, *7* (7), 2128-2135.

70. Piorkowska, E.; Kulinski, Z.; Galeski, A.; Masirek, R., Plasticization of semicrystalline poly(L-lactide) with poly(propylene glycol). *Polymer* 2006, *47* (20), 7178-7188.

71. Shibata, M.; Someya, Y.; Orihara, M.; Miyoshi, M., Thermal and mechanical properties of plasticized poly(L-lactide) nanocomposites with organo-modified montmorillonites. *Journal of Applied Polymer Science* 2006, *99* (5), 2594-2602.

72. Martino, V. P.; Jiménez, A.; Ruseckaite, R. A.; Avérous, L., Structure and properties of clay nano-biocomposites based on poly(lactic acid) plasticized with polyadipates. *Polymers for Advanced Technologies* 2011, *22* (12), 2206-2213.

73. Kowalczyk, M.; Pluta, M.; Piorkowska, E.; Krasnikova, N., Plasticization of polylactide with block copolymers of ethylene glycol and propylene glycol. *Journal of Applied Polymer Science* 2012, *125* (6), 4292-4301.

74. Gumus, S.; Ozkoc, G.; Aytac, A., Plasticized and unplasticized PLA/organoclay nanocomposites: Short- and long-term thermal properties, morphology, and nonisothermal crystallization behavior. *Journal of Applied Polymer Science* 2012, *123* (5), 2837-2848.

75. Sungsanit, K.; Kao, N.; Bhattacharya, S. N., Properties of linear poly(lactic acid)/polyethylene glycol blends. *Polymer Engineering and Science* 2012, *52* (1), 108-116.

76. Burgos, N.; Martino, V. P.; Jimenez, A., Characterization and ageing study of poly(lactic acid) films plasticized with oligomeric lactic acid. *Polymer Degradation and Stability* 2013, *98* (2), 651-658.

77. Ren, Z. J.; Dong, L. S.; Yang, Y. M., Dynamic mechanical and thermal properties of plasticized poly(lactic acid). *Journal of Applied Polymer Science* 2006, *101* (3), 1583-1590.

78. Liu, B.; Jiang, L.; Zhang, J., Study of Effects of Processing Aids on Properties of Poly(lactic acid)/Soy Protein Blends. *Journal of Polymers and the Environment* 2011, *19* (1), 239-247.

79. Rodriguez-Llamazares, S.; Rivas, B. L.; Perez, M.; Perrin-Sarazin, F., Poly(ethylene glycol) as a compatibilizer and plasticizer of poly(lactic acid)/clay nanocomposites. *High Perform. Polym.* 2012, *24* (4), 254-261.

80. Hutchinson, J. M., Physical aging of polymers. *Progress in Polymer Science* 1995, *20* (4), 703-760.

81. Pluta, M.; Paul, M.-A.; Alexandre, M.; Dubois, P., Plasticized polylactide/clay nanocomposites. II. The effect of aging on structure and properties in relation to the filler content and the nature of its organo-modification. *Journal of Polymer Science Part B: Polymer Physics* 2006, *44* (2), 312-325.

82. Jia, Z. Y.; Tan, J. J.; Han, C. Y.; Yang, Y. N.; Dong, L. S., Poly(ethylene glycol-co-propylene glycol) as a Macromolecular Plasticizing Agent for Polylactide: Thermomechanical Properties and Aging. *Journal of Applied Polymer Science* 2009, *114* (2), 1105-1117.

83. Lim, L. T.; Auras, R.; Rubino, M., Processing technologies for poly(lactic acid). *Progress in Polymer Science* 2008, *33* (8), 820-852.

84. Jamshidi, K.; Hyon, S. H.; Ikada, Y., Thermal characterization of polylactides. *Polymer* 1988, *29* (12), 2229-2234.

85. Hyon, S. H.; Jamshidi, K.; Ikada, Y., Effects of residual monomer on the degradation of DL-lactide polymer. *Polymer International* 1998, *46* (3), 196-202.

86. Cam, D.; Marucci, M., Influence of residual monomers and metals on poly (l-lactide) thermal stability. *Polymer* 1997, *38* (8), 1879-1884.

87. Rahman, M.; Brazel, C. S., The plasticizer market: an assessment of traditional plasticizers and research trends to meet new challenges. *Progress in Polymer Science* 2004, *29* (12), 1223-1248.

88. **(a)** Briones, R.; Serrano, L.; Labidi, J., Valorization of some lignocellulosic agro-industrial residues to obtain biopolyols. *Journal of Chemical Technology & Biotechnology* 2012, *87* (2), 244-249.
(b) Kurimoto, Y.; Koizumi, A.; Doi, S.; Tamura, Y.; Ono, H., Wood species effects on the characteristics of liquefied wood and the properties of polyurethane films prepared from the liquefied wood. *Biomass and Bioenergy* 2001, *21* (5), 381-390.
(c) Lee, S.-H.; Yoshioka, M.; Shiraishi, N., Liquefaction and product identification of corn bran (CB) in phenol. *Journal of Applied Polymer Science* 2000, *78* (2), 311-318.
(d) Lee, S.-H.; Teramoto, Y.; Shiraishi, N., Acid-catalyzed liquefaction of waste paper in the presence of phenol and its application to Novolak-type phenolic resin. *Journal of Applied Polymer Science* 2002, *83* (7), 1473-1481.

89. Yin, B.; Hakkarainen, M., Oligomeric isosorbide esters as alternative renewable resource plasticizers for PVC. *Journal of Applied Polymer Science* 2011, *119* (4), 2400-2407.

90. Azwar, E.; Yin, B.; Hakkarainen, M., Liquefied biomass derived plasticizer for polylactide. *Journal of Chemical Technology & Biotechnology* 2012, *88* (5), 897-903.

91. Perez, A. G.; Luaces, P.; Oliva, J.; Rios, J. J.; Sanz, C., Changes in vitamin C and flavour components of mandarin juice due to curing of fruits. *Food Chemistry* 2005, *91* (1), 19-24.

92. Arrieta, M. P.; Lopez, J.; Ferrandiz, S.; Peltzer, M. A., Characterization of PLA-limonene blends for food packaging applications. *Polymer Testing* 2013, *32* (4), 760-768.

93. Sawalha, H.; Schroën, K.; Boom, R., Mechanical properties and porosity of polylactide for biomedical applications. *Journal of Applied Polymer Science* 2008, *107* (1), 82-93.

94. Lopez-Rubio, A.; Lagaron, J. M., Improvement of UV stability and mechanical properties of biopolyesters through the addition of beta-carotene. *Polymer Degradation and Stability* 2010, *95* (11), 2162-2168.

95. Telfer, A.; Dhami, S.; Bishop, S. M.; Phillips, D.; Barber, J., beta-Carotene Quenches Singlet Oxygen Formed by Isolated Photosystem II Reaction Centers. *Biochemistry* 1994, *33* (48), 14469-14474.

96. Ivanov, V. B.; Shlyapintokh, V. Y., Stabilization of polymers against the effect of light by means of antioxidants. *Polymer Degradation and Stability* 1990, *28* (3), 249-273.

97. Hwang, S. W.; Shim, J. K.; Selke, S. E. M.; Soto-Valdez, H.; Matuana, L.; Rubino, M.; Auras, R., Poly(L-lactic acid) with added α-tocopherol and resveratrol: optical, physical, thermal and mechanical properties. *Polymer International* 2012, *61* (3), 418-425.

98. Ishiaku, U. S.; Shaharum, A.; Ismail, H.; Ishak, Z. A. M., The effect of an epoxidized plasticizer on the thermo-oxidative ageing of poly(vinyl chloride)/epoxidized natural rubber thermoplastic elastomers. *Polymer International* 1998, *45* (1), 83-91.

99. Ali, F.; Chang, Y.-W.; Kang, S. C.; Yoon, J. Y., Thermal, mechanical and rheological properties of poly (lactic acid)/epoxidized soybean oil blends. *Polymer Bulletin* 2009, *62* (1), 91-98.

100. (a) Kim, S.; Jo, W.; Kim, J.; Lim, S.; Choe, C., The effect of crystalline morphology of poly (butylene terephthalate) phases on toughening of poly(butylene terephthalate)/epoxy blends. *Journal of Materials Science* 1999, *34* (1), 161-168.
(b) Xu, Y. Q.; Qu, J. P., Mechanical and Rheological Properties of Epoxidized Soybean Oil Plasticized Poly(lactic acid). *Journal of Applied Polymer Science* 2009, *112* (6), 3185-3191.
(c) Yew, G. H.; Mohd Yusof, A. M.; Mohd Ishak, Z. A.; Ishiaku, U. S., Water absorption and enzymatic degradation of poly(lactic acid)/rice starch composites. *Polymer Degradation and Stability* 2005, *90* (3), 488-500.

101. Al-Mulla, E. A. J.; Suhail, A. H.; Aowda, S. A., New biopolymer nanocomposites based on epoxidized soybean oil plasticized poly(lactic acid)/fatty nitrogen compounds modified clay: Preparation and characterization. *Industrial Crops and Products* 2010, *33* (1), 23-29.

102. Xiong, Z.; Yang, Y.; Feng, J.; Zhang, X.; Zhang, C.; Tang, Z.; Zhu, J., Preparation and characterization of poly(lactic acid)/starch composites toughened with epoxidized soybean oil. *Carbohydr. Polym.* 2012, *92* (1), 810-816.

103. Wan Rosli, W. D.; Kumar, R. N.; Mek Zah, S.; Hilmi, M. M., UV radiation curing of epoxidized palm oil-cycloaliphatic diepoxide system induced by cationic photoinitiators for surface coatings. *European Polymer Journal* 2003, *39* (3), 593-600.

104. Silverajah, V. S. G.; Ibrahim, N. A.; Zainuddin, N.; Yunus, W.; Abu Hassan, H., Mechanical, Thermal and Morphological Properties of Poly(lactic acid)/Epoxidized Palm Olein Blend. *Molecules* 2012, *17* (10), 11729-11747.

105. Silverajah, V. S. G.; Ibrahim, N. A.; Yunus, W.; Abu Hassan, H.; Woei, C. B., A Comparative Study on the Mechanical, Thermal and Morphological Characterization of Poly(lactic acid)/Epoxidized Palm Oil Blend. *Int. J. Mol. Sci.* 2012, *13* (5), 5878-5898.

106. Al-Mulla, E. A. J.; Yunus, W.; Ibrahim, N. A. B.; Ab Rahman, M. Z., Properties of epoxidized palm oil plasticized polytlactic acid. *Journal of Materials Science* 2010, *45* (7), 1942-1946.

107. Lee, S. N.; Lee, M. Y.; Park, W. H., Thermal stabilization of poly(3-hydroxybutyrate) by poly(glycidyl methacrylate). *Journal of Applied Polymer Science* 2002, *83* (13), 2945-2952.

108. Ishikawa, M.; Ogawa, H.; Narisawa, I., Brittle fracture in glassy polymers. *Journal of Macromolecular Science, Part B* 1981, *19* (3), 421-443.

109. Sternstein, S. S., Mechanical Properties of Glassy Polymers. In *Treatise on Materials Science & Technology*, Schultz, J. M., Ed. Elsevier: 1977; Vol. Volume 10, Part B, pp 541-598.

110. Matsuoka, S.; Hale, A., Cooperative relaxation processes in polymers. *Journal of Applied Polymer Science* 1997, *64* (1), 77-93.

111. Narisawa, I.; Yee, A., Crazing and Fracture of Polymers. In *Materials Science and Technology*, Wiley-VCH Verlag GmbH & Co. KGaA: 2006.

112. Kramer, E. J., The growth of shear bands in polystyrene. *Journal of Polymer Science: Polymer Physics Edition* 1975, *13* (3), 509-525.

113. Estevez, R.; Tijssens, M. G. A.; Van der Giessen, E., Modeling of the competition between shear yielding and crazing in glassy polymers. *Journal of the Mechanics and Physics of Solids* 2000, *48* (12), 2585-2617.

114. Han, C. D., Shear yielding and shear bands. In *Plastic deformation of amorphous and semi-crystalline materials*, Escaig, B.; G'Sel, C., Eds. Les Editions de Physique: Paris, 1984; Vol. 23.

115. Friedrich, K., Crazes and shear bands in semi-crystalline thermoplastics. In *Crazing in Polymers*, Kausch, H. H., Ed. Springer Berlin Heidelberg: 1983; Vol. 52-53, pp 225-274.

116. Kambour, R. P., Refractive indices and compositions of crazes in several glassy polymers. *Journal of Polymer Science Part A: General Papers* 1964, *2* (9), 4159-4163.

117. Sauer, J. A.; Marin, J.; Hsiao, C. C., Creep and Damping Properties of Polystyrene. *Journal of Applied Physics* 1949, *20* (6), 507-517.

118. Lampman, S., Crazing and Fracture. In *Characterization and Failure Analysis of Plastics*, A S M International: 2003; pp 204-210.

119. Beahan, P.; Bevis, M.; Hull, D., The morphology of crazes in polystyrene. *Philosophical Magazine* 1971, *24* (192), 1267-1279.

120. **(a)** Kambour, R. P., Mechanism of fracture in glassy polymers. II. Survey of crazing response during crack propagation in several polymers. *Journal of Polymer Science Part A-2: Polymer Physics* 1966, *4* (1), 17-24.
(b) Rabinovitz, S.; Beardmore, P., Craze Formation and Fracture in Glassy Polymers. In *Critical Reviews in Macromolecular Science*, Chemical Rubber Company ed.; Baer, E., Ed. CRC Press: 1972; Vol. 1.

121. Géhant, S.; Schirrer, R., Multiple light scattering and cavitation in two phase tough polymers. *Journal of Polymer Science Part B: Polymer Physics* 1999, *37* (2), 113-126.

122. **(a)** Dompas, D.; Groeninckx, G.; Isogawa, M.; Hasegawa, T.; Kadokura, M., Toughening behaviour of rubber-modified thermoplastic polymers involving very small rubber particles: 3. Impact mechanical behaviour of poly(rmvinyl chloride)/methyl methacrylate-butadiene-styrene graft copolymer blends. *Polymer* 1994, *35* (22), 4760-4765.
(b) González-Montiel, A.; Keskkula, H.; Paul, D. R., Impact-modified nylon 6/polypropylene blends: 3. Deformation mechanisms. *Polymer* 1995, *36* (24), 4621-4637.

123. Flexman, E. A., Impact behavior of nylon-66 compositions: Ductile-brittle transitions. *Polymer Engineering & Science* 1979, *19* (8), 564-571.

124. Gent, A. N.; Lindley, P. B., *Internal Rupture of Bonded Rubber Cylinders in Tension*. 1959; Vol. 249, p 195-205.

125. Lazzeri, A.; Bucknall, C. B., Dilatational bands in rubber-toughened polymers. *Journal of Materials Science* 1993, *28* (24), 6799-6808.

126. Jang, B. Z.; Uhlmann, D. R.; Sande, J. B. V., Rubber-toughening in polypropylene. *Journal of Applied Polymer Science* 1985, *30* (6), 2485-2504.

127. Wu, S., Phase structure and adhesion in polymer blends: A criterion for rubber toughening. *Polymer* 1985, *26* (12), 1855-1863.

128. Bucknall, C. B., *Toughened plastics*. Elsevier Applied Science Publishers, Limited: 1977.

129. Jang, B. Z.; Uhlmann, D. R.; Sande, J. B. V., The rubber particle size dependence of crazing in polypropylene. *Polymer Engineering & Science* 1985, *25* (10), 643-651.

130. Fond, C.; Schirrer, R., A Mechanical Model for the Onset of Damage in Rubber Modified Amorphous Polymers. *J. Phys. IV France* 1996, *06* (C6), C6-375-C6-384.

131. Borggreve, R. J. M.; Gaymans, R. J.; Luttmer, A. R., Influence of structure on the impact behaviour of nylon-rubber blends. *Makromolekulare Chemie. Macromolecular Symposia* 1988, *16* (1), 195-207.

132. Dompas, D.; Groeninckx, G.; Isogawa, M.; Hasegawa, T.; Kadokura, M., Toughening behaviour of rubber-modified thermoplastic polymers involving very small rubber particles: 2. Rubber cavitation behaviour in poly(vinyl chloride)/methyl methacrylate-butadiene-styrene graft copolymer blends. *Polymer* 1994, *35* (22), 4750-4759.

133. George, J.; Prasannakumari, L.; Koshy, P.; Varughese, K. T.; Thomas, S., Tensile Impact Strength of Blends of High-Density Polyethylene and Acrylonitrile-Butadiene-Rubber: Effect of Blend Ratio and Compatibilization. *Polymer-Plastics Technology and Engineering* 1995, *34* (4), 561-579.

134. Lu, J.; Qiu, Z.; Yang, W., Fully biodegradable blends of poly(l-lactide) and poly(ethylene succinate): Miscibility, crystallization, and mechanical properties. *Polymer* 2007, *48* (14), 4196-4204.

135. Noda, I.; Satkowski, M. M.; Dowrey, A. E.; Marcott, C., Polymer Alloys of Nodax Copolymers and Poly(lactic acid). *Macromolecular Bioscience* 2004, *4* (3), 269-275.

136. Kowalczyk, M.; Piorkowska, E., Mechanisms of plastic deformation in biodegradable polylactide/poly(1,4-cis-isoprene) blends. *Journal of Applied Polymer Science* 2012, *124* (6), 4579-4589.

137. Jiang, L.; Wolcott, M. P.; Zhang, J., Study of Biodegradable Polylactide/Poly(butylene adipate-co-terephthalate) Blends. *Biomacromolecules* 2005, *7* (1), 199-207.

138. Li, Y.; Shimizu, H., Toughening of Polylactide by Melt Blending with a Biodegradable Poly(ether)urethane Elastomer. *Macromolecular Bioscience* 2007, *7* (7), 921-928.

139. Zhang, W.; Chen, L.; Zhang, Y., Surprising shape-memory effect of polylactide resulted from toughening by polyamide elastomer. *Polymer* 2009, *50* (5), 1311-1315.

140. Shibata, M.; Teramoto, N.; Inoue, Y., Mechanical properties, morphologies, and crystallization behavior of plasticized poly(l-lactide)/poly(butylene succinate-co-l-lactate) blends. *Polymer* 2007, *48* (9), 2768-2777.

141. Chumeka, W.; Tanrattanakul, V.; Pilard, J.-F.; Pasetto, P., Effect of Poly(Vinyl Acetate) on Mechanical Properties and Characteristics of Poly(Lactic Acid)/Natural Rubber Blends. *Journal of Polymers and the Environment* 2013, *21* (2), 450-460.

142. Li, Y.; Shimizu, H., Improvement in toughness of poly(l-lactide) (PLLA) through reactive blending with acrylonitrile–butadiene–styrene copolymer (ABS): Morphology and properties. *European Polymer Journal* 2009, *45* (3), 738-746.

CHAPITRE 2

TABLE DES MATIERES

2.1. MATERIAUX **78**

2.1.1. Polymères 78
2.1.2. Additifs 78

2.2. METHODES EXPERIMENTALES **81**

2.2.1. Séchage des granulés de PLA 81
2.2.1.1. Description des sécheurs à granulés *81*
2.2.1.2. Protocole expérimental de séchage des granulés *82*

2.2.2. Mise en forme des mélanges et des plaques à l'échelle laboratoire 84
2.2.2.1. Description du mélangeur interne *84*
2.2.2.2. Protocole expérimental d'utilisation du mélangeur interne *85*
2.2.2.3. Description de la presse chauffante *86*
2.2.2.4. Protocole expérimental de thermocompression *87*
2.2.2.5. Validation du protocole de mélangeage à l'échelle laboratoire *88*

2.2.3. Mise en forme des mélanges et des films à l'échelle semi-pilote 91
2.2.3.1. Principe de l'extrusion bivis *91*
2.2.3.2. Description de l'extrudeuse bivis *91*
2.2.3.3. Protocole expérimental d'extrusion bivis *94*
2.2.3.4. Principe de l'extrusion monovis *94*
2.2.3.5. Description de la ligne d'extrusion de bandelettes *96*
2.2.3.6. Description de la ligne d'extrusion de films à plat et films soufflés *97*
2.2.3.7. Protocole expérimental d'extrusion de bandelettes *98*
2.2.3.8. Protocoles expérimentaux d'extrusion de films à plat et films soufflés *101*

2.2.4. Mise en forme des mélanges et des films à l'échelle pilote 105
2.2.4.1. Description de la ligne d'extrusion bivis *105*
2.2.4.2. Protocole expérimental d'extrusion bivis *106*
2.2.4.3. Description de la ligne d'extrusion de films à plat *107*
2.2.4.4. Protocole expérimental d'extrusion de films à plat *108*

2.2.5. Impression par flexographie encres à l'eau à l'échelle pilote 109

2.2.6. Conditionnement d'échantillons en étuve 110
2.2.6.1. Méthode de cristallisation du PLA 4042D *110*
2.2.6.2. Méthode de vieillissement accéléré des échantillons de PLA 4060D *111*

TABLEAU SYNOPTIQUE DES MATERIAUX, MATERIELS, PROCEDES DE MISE EN ŒUVRE ET CARACTERISATIONS UTILISES **112**

REFERENCES **113**

Chapitre 2 – Matériaux, matériels et procédés de mise en œuvre

Le but de cette section est de présenter les matériaux, les matériels et les procédés de mise en œuvre utilisés dans les chapitres/publications suivants. Ces derniers ont requis différentes étapes d'optimisation qui ne peuvent être intégrées dans les publications, mais nécessitent d'être exposées pour clarifier l'ensemble du développement entrepris. En effet, cette thèse de doctorat sous contrat Cifre s'est inscrite dans le projet de recherche CREABIOM, présenté en introduction, ayant pour objectif de développer à l'échelle laboratoire puis à l'échelle pilote, voire industrielle, un film de PLA biosourcé et biodégradable présentant une ductilité fortement améliorée.

L'approche choisie a consisté en l'additivation du PLA par des coproduits de l'huilerie se présentant sous forme liquide, cireuse ou solide. Puis dans un second temps, nous avons étudié l'ajout de polyhydroxyalcanoates (PHAs) en vue d'améliorer les propriétés thermomécaniques des formulations. Ainsi, nous exposons dans cette partie les différents outils nécessaires à l'incorporation de ces derniers dans le PLA, ceux liés à la mise en forme des films à l'échelle laboratoire puis aux échelles semi-pilote et pilote. Nous montrons également les méthodes développées pour la mise au point des paramètres de chacune des étapes.

Ainsi, avec les matériels disponibles dans les différents laboratoires et sites mis à disposition pour ces travaux, il a été nécessaire de réaliser le séchage des granulés, l'additivation du PLA par mélangeur interne et par extrusion bivis, la mise en forme de plaques et de bandelettes pour la caractérisation initiale puis la mise en forme de films par extrusion filière plate et extrusion soufflage de gaine. D'autre part, des tests spécifiques au projet ont également été mis en place comme l'imprimabilité, la cristallisation ou le vieillissement en étuve afin d'évaluer la stabilité des formulations qui feront notamment l'objet des chapitres 5 et 6.

2.1. Matériaux

2.1.1. Polymères

Les polylactides de référence INGEO PLA 4060D et PLA 4042D étudiés lors de cette thèse ont été fournis par NatureWorks sous forme de granulés. La teneur en acide lactique de forme L de ces polymères est respectivement de 89 ± 1 % et 96 ± 0.5 %, selon les fiches techniques. Le poly(hydroxybutyrate-co-valérate) (PHBV) de référence PHI 002 a été fourni par NaturePlast. Le taux de co-monomère hydroxyvalérate est de 3%, selon les données fournisseur. Pour chacun des polymères, les masses molaires ont été évaluées par chromatographie d'exclusion stérique et les températures de transition vitreuse par analyse calorimétrique différentielle à balayage (**Tableau 2.1**).

Tableau 2.1 Principales caractéristiques des polymères utilisés : teneur en L-lactide et hydroxyvalérate, masse molaire moyenne en nombre (M_n) et en poids (M_w) et température de transition vitreuse (T_g)

Référence	**Teneur en L-acide lactique** *(%)*	**Teneur en hydroxyvalérate** *(%)*	**M_n** *($g.mol^{-1}$)*	**M_w** *($g.mol^{-1}$)*	**T_g** *(°C)*
PLA 4060D	89 ± 1	-	109 000	243 000	57
PLA 4042D	96 ± 0.5	-	112 000	198 000	59
PHI 002	-	3	255 000	517 000	3

2.1.2. Additifs

Huit types d'additifs commerciaux, employés en tant que plastifiants, ont été utilisés lors de ce travail. L'acétyl tributyl citrate (ATBC), le poly(éthylène glycol) (PEG 400), le dioctyl adipate (DOA), le squalène, l'α-tocophérol, l'acide palmitique (C16:0) et l'acide oléique (C18:1) ont été fournis par Sigma Aldrich (France). Le Polysorbid® 37 (PID37) a quant à lui été fourni par la société Roquette Frères (France). Ils ont été mélangés au PLA 4060D à des teneurs comprises entre 5 et 20 % en poids. Les caractéristiques de ces additifs sont rassemblées dans le **Tableau 2.2**.

Tableau 2.2 Formule développée et masse molaire des additifs commerciaux utilisés comme plastifiants

Additif	**Formule développée**	**Masse molaire** *(g.mol^{-1})*
ATBC	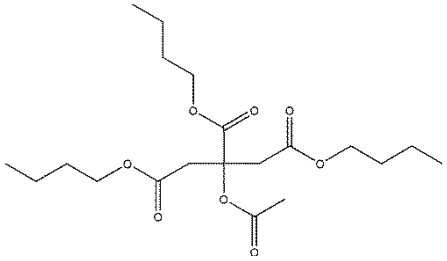	402
PEG 400 *(n = 6 à 7)*	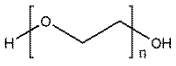	370 à 414
DOA	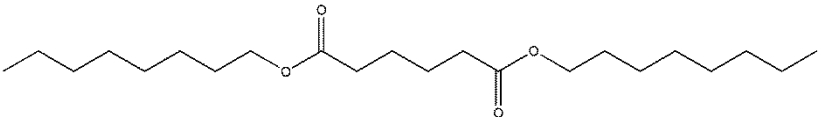	370
PID37 *(n = 2 à 4)*	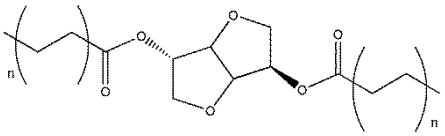	342 à 454
Squalene	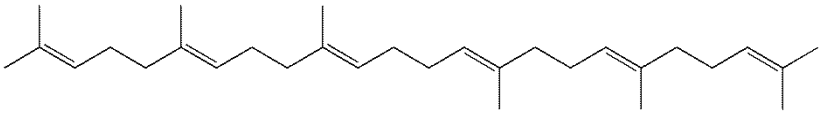	410
α-tocophérol	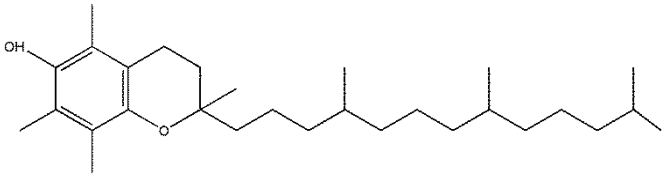	430
Acide palmitique	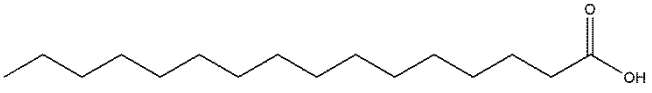	256
Acide oléique	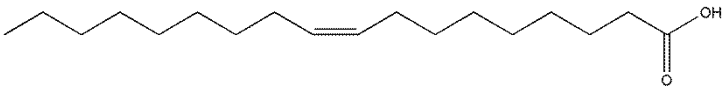	282

D'autre part, l'Institut des Corps Gras (ITERG) nous a fourni différents produits et coproduits de l'huilerie, également utilisés en tant que plastifiants. Leur composition est fournie dans le **Tableau 2.3**.

Tableau 2.3 Composition relative des produits et coproduits de l'huilerie utilisés comme plastifiants (informations fournies par l'ITERG)

	Type		HPH	HCH	CDHC	CDHS	CDHO	CDHP
Composition glycéridique *(%)*	Acides gras libres		0,0	39,0	43,1	39,2	95,4	0,0
	Monoglycerides		0,2	11,2	2,9	2,0	1,7	0,0
	Diglycerides		10,6	2,7	9,0	8,4	2,2	0,0
	Triglycerides		88,9	12,2	16,8	33,5	0,7	100,0
	Stérols (α-tocophérol)		0,0	25,7	9,8	1,6	0,0	0,0
	Hydrocarbures (Squalène)		0,0	0,0	13,8	13,0	0,0	0,0
	Non identifiés		0,3	9,2	4,6	2,3	0,0	0,0
Indice d'acide *(mg KOH,g^{-1})*			0,1	0,1	65,3	68,4	47,7	201,0
Indice de saponification *(mg KOH,g^{-1})*			198,6	255,2	125,1	157,9	162,2	205,7
Teneur en eau *(%)*			0,11	0,10	0,55	0,34	0,37	0,16
Composition en acides gras *(%)*	Acide caproïque	C6:0	0,0	0,0	0,0	0,0	0,0	0,5
	Acide caprylique	C8:0	0,0	0,0	0,0	0,0	0,0	6,8
	Acide caprique	C10:0	0,0	0,0	0,1	0,0	0,0	5,7
	Acide laurique	C12:0	0,0	0,8	0,0	0,4	0,5	47,5
	Acide myristique	C14:0	0,0	0,4	0,0	1,3	1,2	18,1
	Acide palmitique	C16:0	7,4	12,3	11,3	49,8	43,6	9,4
	Acide palmitoléique	C16:1	0,0	0,0	0,0	0,2	0,0	0,0
	Acide stéarique	C18:0	3,4	4,1	2,5	4,1	53,8	10,8
	Acide oléique	C18:1	27,3	21,7	69,5	35,2	0,0	1,0
	Acide linoléique	C18:2	42,4	49,7	10,9	7,8	0,0	0,0
	Acide linolénique	C18:3	1,5	6,4	0,6	0,3	0,0	0,0
	Acide arachidique	C20:0	0,5	0,3	0,4	0,3	0,5	0,1
	Acide eicosénoïque	C20:1	0,3	0,2	0,4	0,1	0,0	0,0
	Acide béhénique	C22:0	1,0	0,5	0,0	0,0	0,1	0,0
	Acide lignocérique	C24:0	0,5	0,2	0,1	0,0	0,1	0,0
	Non identifiés		0,2	15,7	3,4	4,2	0,5	0,1
Nombre moyen de carbone de la chaîne alkyle			17,1	13,0	17,9	17,7	17,8	16,9
Nombre moyen d'insaturation de la chaîne alkyle			0,0	0,0	1,4	1,5	1,0	0,5

huile de palme hydrogénée (HPH) ; huile de coprah hydrogénée (HCH) ; condensat de désodorisation d'huile de colza (CDHC) ; condensat de désodorisation d'huile de soja (CDHS) ; condensat de désodorisation d'huile d'olive (CDHO) ; condensat de désodorisation d'huile de palme (CDHP)

2.2. Méthodes expérimentales

2.2.1. Séchage des granulés de PLA

Le PLA est un polyester sensible à la dégradation hydrolytique : il est essentiel de le sécher avant toute transformation thermique afin d'en minimiser l'effet.[1]

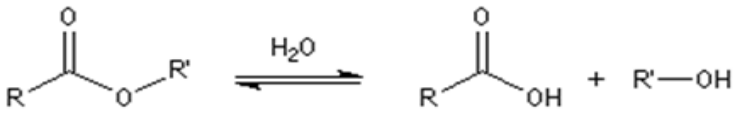

Figure 2.1 Mécanisme d'hydrolyse d'une fonction ester

2.2.1.1. Description des sécheurs à granulés

Deux sécheurs à granulés ont été utilisés durant l'étude : le principal est un sécheur d'une capacité de 60 L de marque Somos du laboratoire PIMM. Le second est un sécheur d'une capacité de 100 L appartenant au centre technique MateriaNova, prestataire lors de la phase de scale-up.

(a) 

(b) 

Figure 2.2 Sécheurs de granulés **(a)** Somos 60 L et **(b)** Motan 100 L

Ces sécheurs disposent d'un dispositif de dessiccation permettant d'assurer le séchage des granulés sous air sec et ainsi atteindre de basses teneurs en humidité résiduelle. La température et le temps de séchage, paramètres dépendant du polymère, doivent faire l'objet

d'une étude tant ce critère est crucial pour la qualité finale des films de polylactide. Cette humidité résiduelle après séchage est contrôlée par dosage chimique lors du chauffage d'une quantité déterminée de granulés (160 °C dans le cas du PLA 4060D et 180 °C pour le PLA 4042D). Cette analyse est réalisée grâce à l'utilisation d'un Hydrotracer ABONI FMX™ (**Figure 2.3**)

Figure 2.3 Hydrotracer Aboni FMX™

2.2.1.2. Protocole expérimental de séchage des granulés

Le polylactide utilisé pour la quasi-totalité du projet de recherche est un grade amorphe (PLA 4060D), sa tenue thermomécanique est principalement gouvernée par sa température de transition vitreuse ($T_g \approx 60$ °C). De ce fait, afin d'éviter tout phénomène de collage thermique des granulés lors de l'étape de séchage, nous avons choisi de ne pas dépasser cette température et avons fixé la consigne à 60 °C. Le seul paramètre d'étude est alors le temps de séchage.

Après optimisation, le temps de séchage retenu est de *24 heures, permettant d'atteindre une humidité résiduelle du PLA d'environ 350 ppm*, valeur proche du seuil préconisé par le fournisseur NatureWorks.[2]

Pour l'optimisation de ce paramètre, une étude a été menée. Dans le sécheur à granulés Somos Dryer 60 L (**Figure 2.2a**) produisant de l'air sec à 60 °C, cinq paniers contenant chacun 1 kg de granulés PLA 4060D préalablement exposés à l'humidité ambiante pendant un mois, ont été mis à sécher. Après différents temps de séchage, l'humidité des granulés a été mesurée par Hydrotracer Aboni FMX™ (**Figure 2.3**), puis une étape d'extrusion bivis a été réalisée (extrudeuse bivis Thermo Haake Ptw, **Figure 2.9**, vitesse de rotation de vis 300 rpm, débit 0,6 $kg.h^{-1}$, température uniforme 190 °C) et les masses molaires après extrusion déterminées par chromatographie d'exclusion stérique (colonnes PL Gel Mixed-C et PLGel 100 Å, solvant chloroforme 1 $mL.min^{-1}$, calibration polystyrène, détecteur réfractométrique). Les masses molaires du PLA 4060D avant séchage et extrusion ont également mesurées : M_n = 139 500 $g.mol^{-1}$, M_w = 263 000 $g.mol^{-1}$, I = 1,87. Les résultats sont exposés dans la **Figure 2.4**.

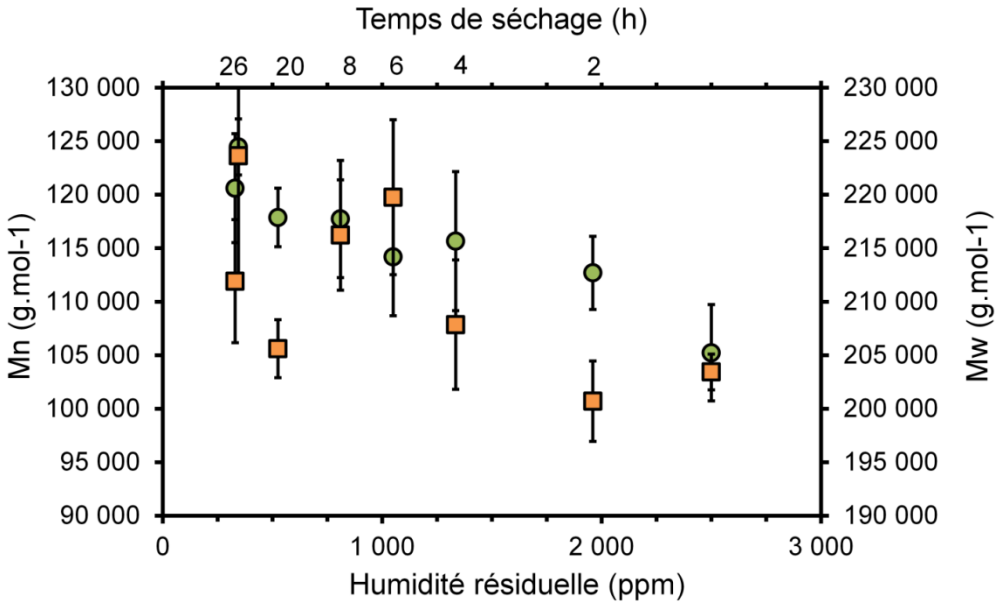

Figure 2.4 Masses molaires du PLA 4060D après extrusion bivis en fonction du temps de séchage préalable et de l'humidité résiduelle

(○) Mn ; (□) Mw

2.2.2. Mise en forme des mélanges et des plaques à l'échelle laboratoire

Pour caractériser les propriétés mécaniques des PLA additivés, il est notamment nécessaire de disposer de plaques ou de films. Le mélangeur interne est un appareil très utilisé pour l'additivation ou le mélangeage des polymères à l'échelle laboratoire. Son intérêt réside dans les faibles quantités de matière à mettre en œuvre et les temps de manipulation relativement courts, permettant des études préliminaires. Les inconvénients étant la faible quantité de matière obtenue et la nécessité de mettre en œuvre les mélanges recueillis par une étape de thermocompression pour être ensuite testés.

2.2.2.1. Description du mélangeur interne

Le mélangeur interne utilisé (Haake Rheocord 9000, **Figure 2.5**) est constitué d'une chambre d'un volume effectif de 69 cm^3 thermorégulée par trois résistances électriques chauffantes et un jet d'air comprimé. Deux éléments contrarotatifs de malaxage pales type « roller rotors » (**Figure 2.5b**) permettent de brasser la matière thermoplastique chauffée à l'intérieur de la chambre de mélangeage. Le programme des conditions opératoires (vitesse de rotation des pales, durée de mélangeage et température de chauffe) est asservi numériquement.

(a)  **(b)** 

Figure 2.5 (a) Mélangeur interne Haake Rheocord 9000 et **(b)** Pales type « roller rotors »

2.2.2.2. Protocole expérimental d'utilisation du mélangeur interne

Cette technique nécessite une optimisation de la température de la cuve, de la vitesse des rotors, du temps de brassage et des moments d'introduction de l'additif pour permettre un bon mélangeage en minimisant la dégradation.

Une première étude a été conduite afin de déterminer les paramètres optimaux de conduite du procédé de mélangeage à partir de granulés de PLA 4060D préalablement séchés pendant 24 h à 60 °C. Les produits ont été jugés macroscopiquement par observation visuelle de la coloration finale du matériau (apparition d'un jaunissement du PLA) et l'odeur dégagée lors du procédé de mise en œuvre. Une appréciation qualitative allant de « produit très dégradé » à « produit non dégradé » a été attribuée. Le **Tableau 2.4** présente les conditions opératoires et les appréciations données. Les conditions *mélangeage pendant 8 min à 180 °C à une vitesse de rotation des pales de 60 rpm* ont été retenues.

Tableau 2.4 Conditions opératoires de mélangeage par mélangeur interne

Temps *(min)*	**Température** *(°C)*	**Vitesse de rotation** *(rpm)*	**Aspect final du matériau**
15	160	30	Très dégradé
12	170	50	Dégradé
10	180	60	Moyennement dégradé
8	180	60	Faiblement dégradé
6	200	80	Moyennement dégradé
4	220	80	Moyennement dégradé

La seconde étude a porté sur l'introduction de l'additif. Conformément au protocole en vigueur au sein du laboratoire, une seringue en verre permettant l'introduction des additifs liquides a été utilisée pour les études préliminaires d'additivation du PLA par mélangeur interne. Ci-après est décrit le mode opératoire utilisé :

- Début introduction additif à t_0 + 2 min (couple moteur du mélangeur stable indiquant la plastification thermique ou fusion de la matrice PLA amorphe ou semi-cristalline),

- Goutte à goutte continu de $t_0 + 2$ à $t_0 + 6$ min (permettant de ne pas saturer localement la matrice en additif par une introduction trop rapide),
- Fin introduction additif à $t_0 + 6$ min (les deux dernières minutes du procédé permettent d'homogénéiser l'ensemble de la matrice additivée).

Une fois l'étape de mélangeage terminée, le matériau est collecté par raclage de l'intérieur de la chambre et de la surface des pâles à l'aide de spatules en laiton. Le matériau est placé dans un emballage métallisé hermétiquement scellé afin d'éviter sa reprise en humidité.

2.2.2.3. Description de la presse chauffante

Une presse hydraulique de laboratoire de marque Gibitre, avec force de verrouillage 20 tonnes, équipée de plans avec chauffage électrique de 250 x 250 mm a été utilisée (**Figure 2.6**).

(a)

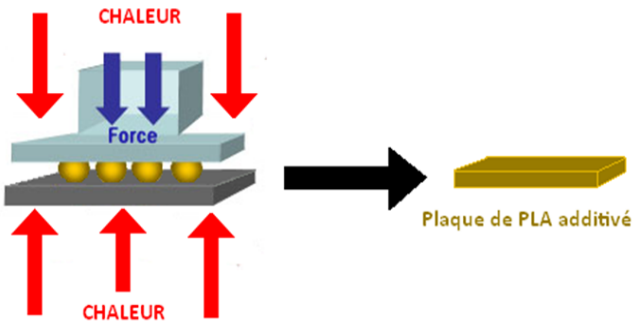

(b)

Figure 2.6 (a) Presse chauffante Gibitre et **(b)** Principe de la thermocompression

Afin de réaliser les plaques, un moule constitué de deux éléments plans en acier de 25 x 30 cm recouverts d'un film antiadhésif, et d'un cadre carré en aluminium d'épaisseur 1 mm ayant une section creuse interne de 10 cm de côté a été fabriqué (**Figure 2.7**).

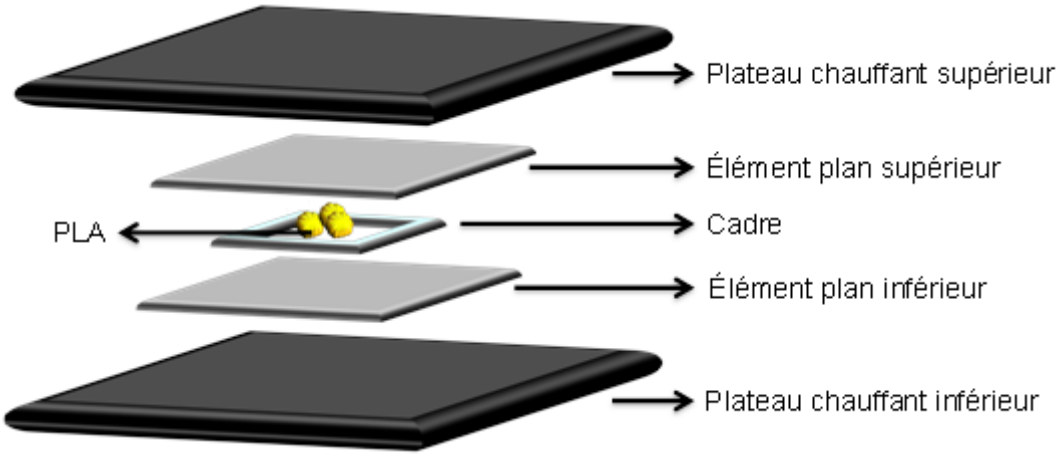

Figure 2.7 Schéma du moule de thermocompression de plaques

2.2.2.4. Protocole expérimental de thermocompression

La résine thermoplastique est déposée au centre du cadre, lui-même placé entre les éléments plans en acier. Le tout est positionné entre les deux plateaux chauffants de la presse. Le moule représente un volume de 10 cm^3. La densité du PLA est d'environ 1,3 soit une capacité maximale de 13 g de matière. Un excès de résine thermoplastique PLA (environ 15 g à 17 g) est utilisé lors de chaque essai, l'excédent permettant d'assurer un remplissage optimal du moule lors de la montée en pression. La matière en excès est évacuée par 4 canaux préalablement creusés à la surface du cadre.

Comme pour les autres techniques, les températures et durées des différentes phases du procédé de compression doivent être optimisés. Différentes conditions opératoires ont été testées en vue d'optimiser le protocole de mise en forme par thermocompression (**Tableau 2.5**). Les essais ont été menés sur des granulés de PLA 4060D préalablement séchés puis additivés en mélangeur interne avec 5 %m de condensat de désodorisation d'huile d'olive. La durée de

ramollissement correspond à la phase pendant laquelle le matériau est placé dans le moule entre les mâchoires chauffantes sans pression appliquée. La résine thermoplastique est lentement aplatie par le seul poids exercé par l'élément plan supérieur du moule lors de la diminution de viscosité due à l'élévation de température. Cette première étape permet d'évacuer une partie de l'air présent entre les granulés solides. La durée de montée en pression correspond au temps mis pour atteindre la pression maximale (220 bar) lors de la fermeture des mâchoires de la presse. Lorsque la thermocompression est terminée, la pression est relâchée et le moule est placé sur une grille en acier. L'ensemble est refroidi par un jet continu d'air comprimé directement sur le moule. Une fois la température revenue à l'ambiante (≈ 3 min), le moule est ouvert et la plaque thermoplastique est désolidarisée du cadre. Les conditions *durée de ramollissement 2 minutes, durée de montée en pression jusqu'à 220 bar 2 minutes* ont été retenues.

Tableau 2.5 Conditions opératoires du procédé de thermocompression

Température *(°C)*	**Durée de ramollissement** *(min)*	**Durée de montée en pression** *(min)*	**Homogénéité de l'épaisseur** *(mm)*	**Aspect final du matériau**
160	4	1	± 0,25 mm	Bulles d'air
170	3	1	± 0,15 mm	Bulles d'air
180	2	2	± 0,10 mm	Pas de bulles d'air
190	1,5	2,5	± 0,10 mm	Pas de bulles d'air
210	1	2	± 0,10 mm	Pas de bulles d'air Aspect ≈ jaune

2.2.2.5. Validation du protocole de mélangeage à l'échelle laboratoire

Une étude[3] menée au cours d'une précédente thèse de doctorat à AgroParisTech, sous la direction du D[r] V. Ducruet, présente des similitudes quant au protocole développé pour l'additivation liquide du PLA amorphe par mélangeur interne. Nous avons souhaité valider le procédé de mélangeage choisi en préparant différentes formulations PLA/ATBC similaires à celles déjà réalisées, dont les propriétés mécaniques mesurées en traction uniaxiale et les masses molaires mesurées par chromatographie d'exclusion stérique ont été publiées dans

Ref[4]. Les conditions opératoires de mise en œuvre et les méthodologies de caractérisation des formulations sont présentées dans le **Tableau 2.6**. Les dimensions des éprouvettes mécaniques utilisées sont présentées en **Figure 2.8**. Les propriétés mécaniques et les masses molaires mesurées sont données dans le **Tableau 2.7**.

Tableau 2.6 Conditions opératoires de mise en œuvre par mélangeur interne et méthodologie de caractérisation

Conditions opératoires et caractéristiques	**Etude de Courgneau et al.[4]**	**Formulations testées**
Taux d'énantiomères (L-lactide) du PLA selon le fournisseur *(%)*	8	11
Masse molaire (M_n) du PLA avant mélangeage *($g.mol^{-1}$)*	90 000	105 000
Conditions de séchage des granulés	80 °C pendant 12 h sous pression réduite	60 °C pendant 24 h sous air sec
Méthode de mélangeage	Mélangeur interne	Mélangeur interne
Conditions opératoires de mélangeage	160 °C pendant 15 min à 60 rpm	180 °C pendant 8 min à 60 rpm
Méthode de réalisation des plaques	Presse chauffante	Presse chauffante
Conditions opératoires de réalisation des films	3 min à 185 °C sans pression, puis augmentation régulière jusqu'à 150 bars pendant 2 min	2 min à 180 °C sans pression, puis augmentation régulière jusqu'à 220 bars pendant 2 min
Epaisseur des films obtenus	100 µm	1 000 µm
Profil des éprouvettes pour essais traction uniaxiale	Haltère type 1BA	Haltère type 5A
Vitesse de traction uniaxiale	5 $mm.min^{-1}$	25 $mm.min^{-1}$
Méthode de mesure des masses molaires	Chromatographie d'exclusion stérique (SEC)	Chromatographie d'exclusion stérique (SEC)
Méthode de calibration de chromatographie	Standards polystyrène	Standards polystyrène
Solvant de chromatographie	Chloroforme	Tetrahydrofurane

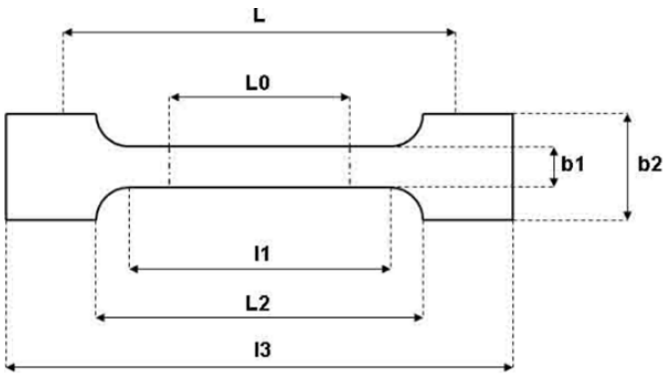

Forme	**L** *(mm)*	**L0** *(mm)*	**l1** *(mm)*	**l3** *(mm)*	**b1** *(mm)*	**b2** *(mm)*
Haltère	L2 + 2 ; L2 = 58 ± 2	25 ± 0,5	30 ± 0,5	> 75	5 ± 0,5	10 ± 0,5
Haltère	50 ± 2	20 ± 0,5	25 ± 1	> 75	4 ± 0,1	12,5 ± 1

Figure 2.8 Dimensions des éprouvettes utilisées selon la norme ISO 527-2

Tableau 2.7 Propriétés comparées des formulations témoins PLA/ATBC

Formulation	Propriétés	Etude de Courgneau et al.[4]	Formulations testées
PLA	Elongation à la rupture *(%)*	8 ± 5	5 ± 1
	Module d'Young* *(MPa)*	1 290 ± 60	1 660 ± 35
	Contrainte à l'écoulement *(MPa)*	47 ± 7	65 ± 4
	Masse molaire en nombre (M_n) *($g.mol^{-1}$)*	70 200	77 500
	Masse molaire en poids (M_w) *($g.mol^{-1}$)*	223 450	207 600
PLA + 5 %m ATBC	Elongation à la rupture *(%)*	8 ± 3	4 ± 1
	Module d'Young* *(MPa)*	1 305 ± 65	1 540 ± 30
	Contrainte à l'écoulement *(MPa)*	41 ± 9	57 ± 3
	Masse molaire en nombre (M_n) *($g.mol^{-1}$)*	98 900	88 000
	Masse molaire en poids (M_w) *($g.mol^{-1}$)*	228 100	211 700
PLA + 10 %m ATBC	Elongation à la rupture *(%)*	16 ± 10	4 ± 2
	Module d'Young* *(MPa)*	1 040 ± 55	1 405 ± 35
	Contrainte à l'écoulement *(MPa)*	30 ± 55	53 ± 3
	Masse molaire en nombre (M_n) *($g.mol^{-1}$)*	76 650	88 100
	Masse molaire en poids (M_w) *($g.mol^{-1}$)*	182 500	210 900
PLA + 15 %m ATBC	Elongation à la rupture *(%)*	300 ± 179	430 ± 110
	Module d'Young* *(MPa)*	615 ± 40	255 ± 20
	Contrainte à l'écoulement *(MPa)*	22 ± 4	30 ± 2
	Masse molaire en nombre (M_n) *($g.mol^{-1}$)*	57 550	94 900
	Masse molaire en poids (M_w) *($g.mol^{-1}$)*	123 900	221 800

** mesures réalisées sans extensomètre*

Bien que les deux grades de PLA utilisés soient différents (propriétés mécaniques et masses molaires), les tendances observées sont similaires. Les deux essais montrent des effets de plastification externe apparaissant à des taux supérieurs à 10 %m d'ATBC. Les propriétés mécaniques deviennent alors comparables : le matériau développe une importante ductilité ($\varepsilon > 300$ %) et la rigidité diminue de manière importante ($E < 600$ MPa). D'autre part, les masses molaires des formulations réalisées selon le procédé de mise en œuvre développé au cours de cette étude montrent des effets de dégradation moindres que les formulations obtenues selon la méthode de mélangeage de Courgneau et al.[4] Bien que la température de chauffe choisie soit de 20 °C supérieure, la diminution du temps de séjour de 15 à 8 minutes semble être bénéfique.

2.2.3. Mise en forme des mélanges et des films à l'échelle semi-pilote

Cette phase a pour but d'utiliser des outils industriels de taille laboratoire que l'on dénomme semi-pilote. Ainsi, le mélangeur interne est remplacé par une extrudeuse double vis (bivis) alors que le procédé de thermocompression est remplacé par l'extrusion monovis filière plate de bandelettes ou de films, ou par l'extrusion soufflage de gaine. Deux lignes d'extrusion monovis ont été utilisées dans le cadre de cette étude. La première est une ligne dédiée à la production de bandelettes, dont l'intérêt est la faible consommation de matière (environ 1 kg de matière suffit), nous permettant de vérifier l'extrudabilité des formulations et de préparer des éprouvettes pour les travaux sur le vieillissement des formulations (chapitre 6). La seconde est une ligne dédiée à la production de films à plat et de films soufflés pour validation des formulations en vue de leur capacité à être extrudées par ces techniques au niveau industriel.

2.2.3.1. Principe de l'extrusion bivis

Une extrudeuse bivis est une machine de transformation des matières thermoplastiques permettant le mélangeage intime en continu de différents composants. La matière thermoplastique chauffée fluide est mélangée par cisaillement aux autres composés introduits dans le système par l'intermédiaire de doseurs, de pompes ou d'autres dispositifs. L'ensemble est convoyé de manière continue par l'action rotative engrenante des deux vis sans fin jusqu'à la filière. La matière sort sous forme d'un ou plusieurs joncs en fonction de la filière utilisée, refroidis puis granulés par un appareillage additionnel. Les granulés thermoplastiques obtenus sont ensachés dans un sac métallisé hermétiquement scellé.

2.2.3.2. Description de l'extrudeuse bivis

L'appareil utilisé dans le cadre de cette étude est une extrudeuse bivis Thermo Haake Ptw16-40D (**Figure 2.9**), possédant deux vis corotatives engrenantes et interpénétrées, au sein d'un

fourreau chauffant permettant une régulation en 7 points de la température. Le diamètre des vis est de 16 mm avec un rapport L/D = 40:1. Le profil des vis est ajustable par changement des éléments constitutifs. Le profil de vis retenu pour l'ensemble du projet est présenté en **Figure 2.10** : les éléments d'alimentation sont constitués d'un pas de vis large engendrant un faible cisaillement afin de ne pas générer de bourrage, les éléments de malaxage engendrent un cisaillement important et permettant un brassage plus intime de la matière et donc une meilleure distribution, et les éléments de convoyage génèrent un cisaillement intermédiaire et permettent le transport de la matière. L'alimentation des plastifiants liquides est assurée par une pompe comme montré sur la **Figure 2.9**. L'alimentation du plastifiant est réalisée après plastification préalable du polymère (**Figure 2.10**).

(a)  **(b)** 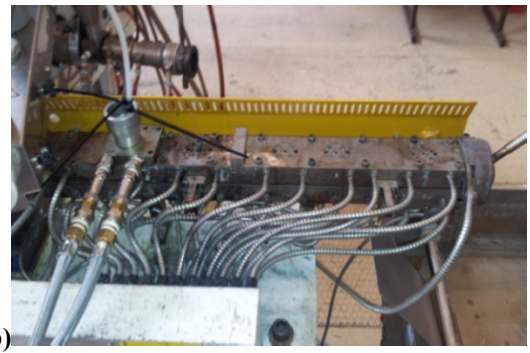

Figure 2.9 (a) Doseur d'alimentation de la résine thermoplastique et pompe pour additif liquide et **(b)** Extrudeuse bivis Thermo Haake Ptw 16D, L/D = 40:1

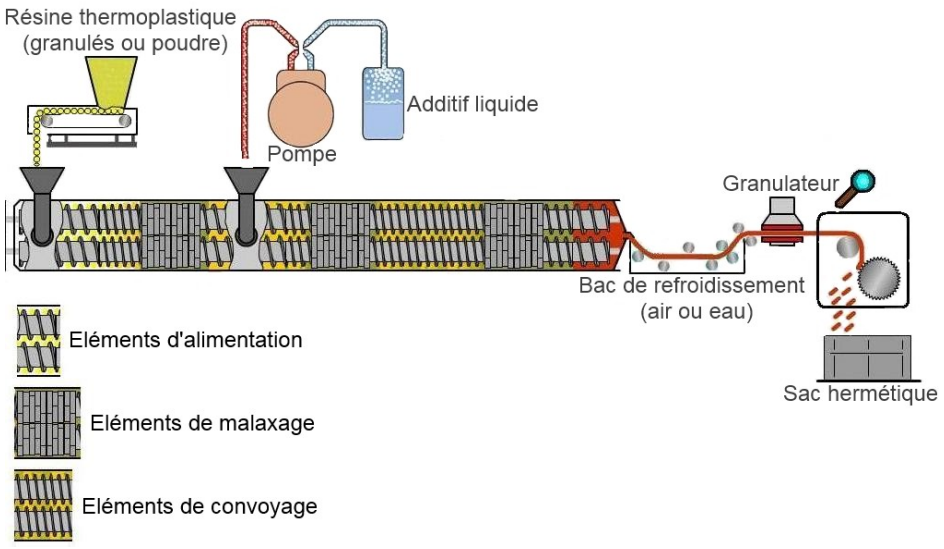

Figure 2.10 Schéma du profil de vis utilisé sur l'extrudeuse bivis Thermo Haake Ptw 16D, L/D = 40:1

A contrario, afin de pouvoir procéder à l'introduction d'additifs fusibles solides à température ambiante (tels que des corps gras à chaines courtes et/ou saturées) de manière précise et régulière, nous avons développé un système permettant de fondre l'additif et contrôler le débit d'introduction (**Figure 2.11**), l'utilisation de la pompe liquide étant impossible pour cause de refroidissement des additifs engendrant leur solidification à l'intérieur du système. Pour cela, un dispositif métallique, semblable à une burette, constitué d'un réservoir en acier inoxydable chauffé par deux résistances électriques, équipé à sa base d'un robinet métallique permettant de délivrer un goutte-à-goutte régulier et facilement contrôlable, a été fabriqué. L'additif solide à température ambiante est placé dans le réservoir chauffant. Une fois l'additif fondu et sa température stable et homogène, le robinet est ouvert jusqu'à l'obtention d'un goutte-à-goutte régulier. Le débit massique est déterminé par pesées successives et la fréquence de chute des gouttes correspondante est notée. Une fois le réglage d'ouverture du robinet effectué, le débit massique est contrôlé régulièrement par mesure de la fréquence de chute des gouttes (la masse de chaque goutte étant constante puisque fonction de la tension superficielle du liquide elle-même dépendante de la température vérifiée constante). La quantité totale d'additif délivré est également mesurée par différence entre la masse initiale et la masse finale d'additif dans le réservoir.

Figure 2.11 Dispositif « burette chauffante » et son module de chauffe

2.2.3.3. Protocole expérimental d'extrusion bivis

Les granulés de PLA préalablement séchés sont introduits dans la 1ère zone de l'extrudeuse moyennant un doseur à granulés permettant de régler un débit de l'ordre de 600 $g.h^{-1}$. Le débit de la pompe ou de la burette, selon le cas, est réglé pour obtenir les proportions massiques voulues. La vitesse de rotation des vis d'extrusion a été fixée dans tous les cas à 300 rpm, alors que les profils de température ont été ajustés en fonction des mélanges (voir chapitres 4 à 6). Par exemple, le mélange [PLA + 10 %m CDHP] a été extrudé avec le profil de température qui suit :

Fourreau : 180 – 185 - 180 – 170 – 160 – 150 Filière jonc : 140°C

Les deux premières zones de température fixées à 180 et 185°C permettent une plastification rapide du PLA. L'introduction de l'additif est réalisée au niveau de la 3ème zone. Les températures des zones suivantes sont adaptées pour conserver la plastification du PLA sans toutefois trop chauffer, afin d'éviter tout phénomène d'exsudation prononcée du plastifiant, voire sa dégradation. Les joncs produits sont ensuite refroidis par air comprimé (le passage dans un bac à eau étant proscrit pour le PLA) et ensuite coupés sous forme de granulés par un granulateur de marque Scamex.

2.2.3.4. Principe de l'extrusion monovis

L'extrusion monovis est un procédé qui permet, par l'action d'une vis sans fin tournant dans un fourreau thermorégulé, de plastifier en continu des matériaux thermoplastiques. La matière plastifiée est alors modelée sous la forme voulue par l'adjonction d'une filière également thermorégulée, puis refroidie et plus ou moins étirée selon l'épaisseur finale désirée.

L'utilisation d'une filière plate conduit à la formation continue d'une feuille d'épaisseur contrôlée mais de largeur fixe définie par les dimensions de la filière utilisée. Directement en

sortie de filière, la feuille subit une étape de calandrage permettant d'en diminuer l'épaisseur par action conjointe de l'écrasement de la matière entre les cylindres et étirage contrôlé par leur vitesse de rotation. Le refroidissement de la matière est assuré par la régulation thermique des rouleaux par circulation interne d'eau froide. Le film obtenu est embobiné.

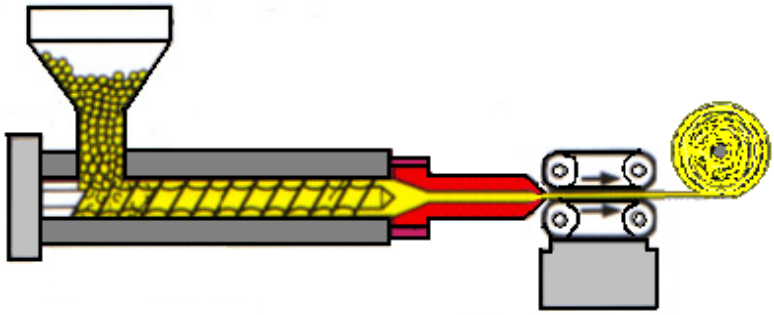

Figure 2.12 Schéma d'une extrudeuse monovis équipée d'une filière plate et d'une calandre

Sur le schéma ci-dessus, la matière thermoplastique initialement sous forme de granulés (jaune) est placée dans la trémie. La rotation de la vis sans fin assure l'alimentation et permet de convoyer longitudinalement la matière dans le fourreau chauffant (gris) jusque dans la filière plate (rouge) créant notamment de la chaleur par dissipation visqueuse. La matière sort sous forme d'une feuille aplatie et étirée par les rouleaux de la calandreuse.

Les équipements de type gonflage de gaine sont constitués d'une filière annulaire (le poinçon) possédant en son centre un système de soufflage d'air permettant de gonfler la gaine de résine thermoplastique. Les dimensions telles que l'épaisseur et la largeur de la gaine sont directement proportionnelles au diamètre du poinçon, au coefficient de gonflage de la gaine et à la vitesse de tirage. Une fois la gaine gonflée et stabilisée (la bulle), celle-ci est pincée par deux rouleaux afin d'être dégonflée et aplatie. Pour obtenir un film, la gaine aplatie peut être ouverte et/ou divisée en deux par découpe au niveau d'une ou des deux tranches. Contrairement au principe d'extrusion à travers une filière plate induisant un étirage uniaxial

du film lors de l'étape de calandrage, l'extrusion de type gonflage de gaine engendre un étirage biaxial de la matière pouvant modifier les propriétés du matériau final.

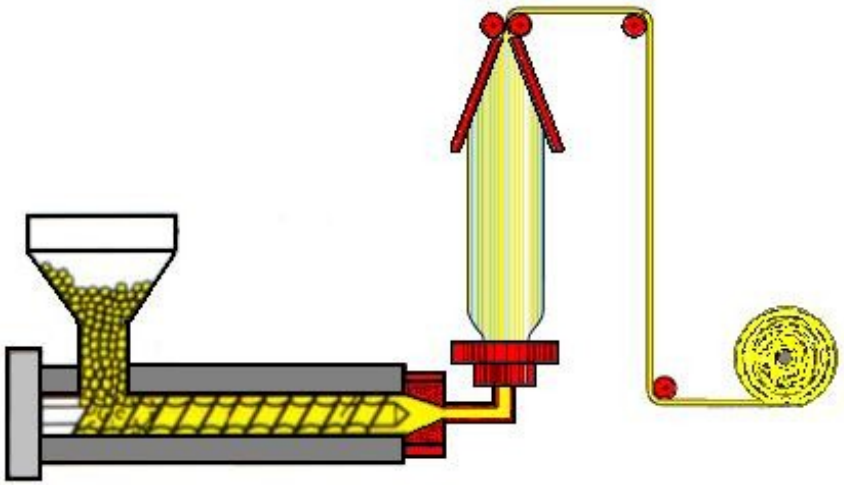

Figure 2.13 Schéma d'une extrudeuse monovis équipée d'une filière gonflage de gaine

2.2.3.5. Description de la ligne d'extrusion de bandelettes

La ligne d'extrusion de bandelettes utilisée dans le cadre de ces travaux est constituée i) d'une extrudeuse monovis de marque Scamex équipée d'une vis de diamètre 20 mm et de rapport L/D = 12:1 au sein d'un fourreau chauffant permettant une régulation de température en 3 points et capable de délivrer un débit matière entre 0.1 et 2 kg.h^{-}1 (**Figure 2.14a**) et ii) d'une filière bandelette d'une largeur 40 mm et 1 mm d'entrefer non modifiable (**Figure 2.14b**).

(a) 

(b) 

Figure 2.14 (a) Extrudeuse monovis Scamex Rheoscam 20 mm 12D et **(b)** Filière bandelette 40 mm large 1 mm entrefer fixe

2.2.3.6. Description de la ligne d'extrusion de films à plat et films soufflés

Pour ces deux méthodes de fabrication de films, une extrudeuse monovis de marque Mapre, appartenant au laboratoire PIMM, équipée d'une vis de diamètre 30 mm ayant un rapport L/D = 33:1 au sein d'un fourreau permettant une régulation de température en 6 points, capable de délivrer un débit matière entre 1 et 10 $kg.h^{-1}$a été utilisée (**Figure 2.15**).

Figure 2.15 Extrudeuse monovis Mapre E1 30-33D

La ligne d'extrusion de film à plat comprend une filière plate et une calandre. La filière plate utilisée pour la réalisation des films laboratoire possède une largeur d'ouverture de 200 mm et un entrefer réglable de 300 à 2 000 µm (**Figure 2.16a**). La calandre utilisée est dotée de trois rouleaux thermorégulés et permet une vitesse de tirage jusqu'à 10 $m.min^{-1}$ (**Figure 2.16b**).

(a) 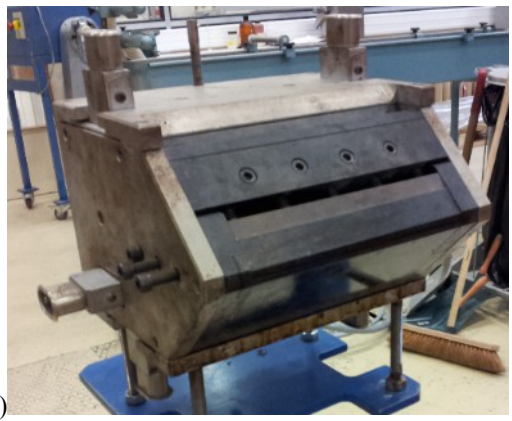 (b) 

Figure 2.16 (a) Filière plate 200 mm et **(b)** Calandreuse

L'unité de soufflage de gaine de marque Dr. Collin (**Figure 2.17**) comprend i) une filière équipée d'un poinçon de 50 mm de diamètre et d'entrefer fixe 0,8 mm de type hélicoïdale à canaux rayonnants (**Figure 2.18**). Ce système permet de dévier la matière thermoplastique dans le sens axial et la répartir sur l'ensemble de la circonférence du poinçon, superposant ainsi plusieurs veines de matière. Cette architecture permet notamment d'éviter les lignes de ressoudure du flux. ii) un dispositif de refroidissement par l'intermédiaire d'un anneau de refroidissement, iii) deux rouleaux dont un caoutchouté et un second poli capable d'étirer le film tout en conservant l'air à l'intérieur de la gaine et iv) un dispositif d'enroulage du film produit.

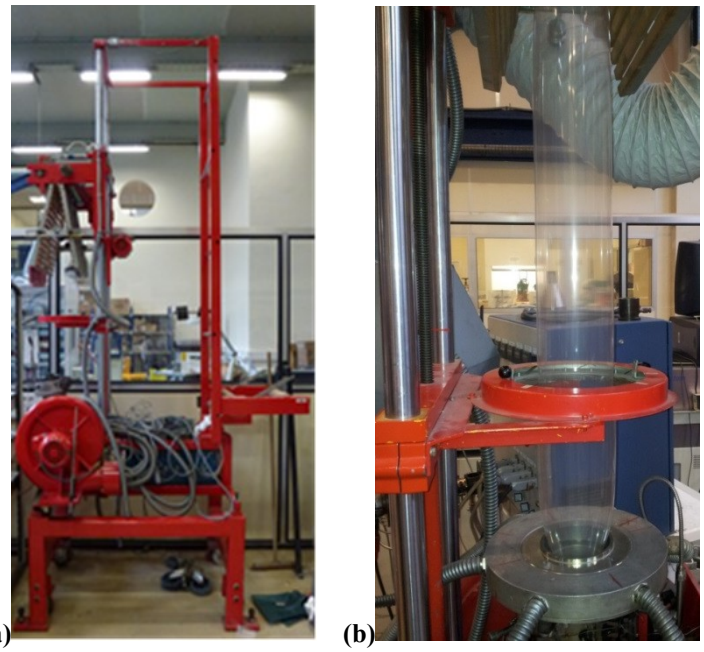

Figure 2.17 (a) Système de gonflage de gaine Dr. Collin, **(b)** Bulle de [PLA 4060D + 10 %m CDHP]

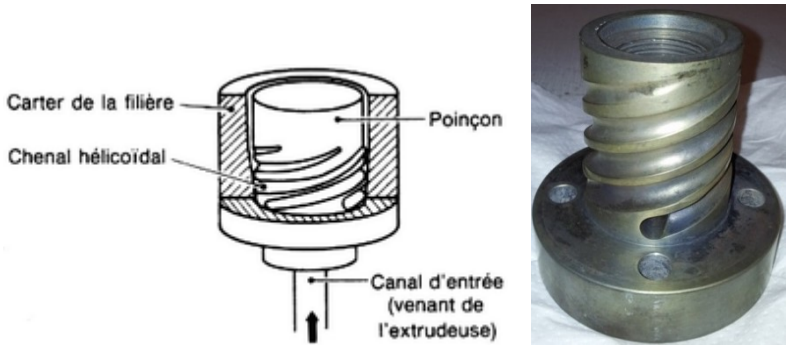

Figure 2.18 Poinçon hélicoïdal « à canaux rayonnants » utilisé dans la filière gonflage de gaine

2.2.3.7. Protocole expérimental d'extrusion de bandelettes

La température de la matière constitue un facteur clé du procédé d'extrusion monovis : une matière trop froide entraîne la présence « d'infondus » créant des défauts dans le film final, tandis qu'une température trop élevée engendre une matière trop fluide, potentiellement dégradée, ne pouvant être mise en forme en sortie de filière. La résine polylactide (PLA 4060D) employée au cours de la quasi-totalité de cette étude est amorphe. Le profil de température d'extrusion est alors fonction de la viscosité de la matière, elle-même dépendante du degré de plastification du polymère. De façon empirique, le profil de température utilisé pour extruder une matrice plastifiée est celui employé pour la matière non additivée auquel est soustraite la diminution de température de transition vitreuse liée à la présence d'un plastifiant. Ainsi, de manière très générale, la température de mise en œuvre est comprise entre T_f + 20 à + 50 °C ou T_g + 100 à + 150 °C. D'autre part, il est nécessaire que la pression de remplissage de la filière soit suffisamment élevée. Elle est assurée par le convoyage longitudinal continu de la matière entraînée par la contrainte de frottement de la vis en rotation. Si la contrainte de frottement est insuffisante, l'alimentation de la filière est perturbée et ne permet pas la réalisation d'un film homogène.

Les essais préliminaires d'extrusion de bandelettes ont été conduits sur trois résines thermoplastiques de PLA 4060D contenant respectivement 5, 10 et 15 % en masse de condensat de désodorisation d'huile de palme (CDHP), additif sélectionné pour sa capacité à augmenter de manière significative la ductilité du PLA.**chapitres 4-6**

Ainsi, nous avons optimisé les profils de température suivants pour la ligne d'extrusion de bandelettes, avec 5 et 10 %m CDHP, à une vitesse de 105 rpm :

Fourreau 175 - 158- 155 filière 160 °C

L'échantillon [PLA 4060D + 15 %m CDHP] a néanmoins montré de nombreux problèmes de stabilité du procédé dus à un mauvais convoyage de la matière dans l'extrudeuse. Il en a été de même pour les formulations à base de condensat d'huile d'olive quelques soient les proportions.

Figure 2.19 Vis Scamex 20-12D après essai d'extrusion de granulés [PLA 4060D + 15 %m CDHP]

Bien que la viscosité de la matière soit un facteur important, nous avons constaté que l'exsudation de l'additif semble l'élément critique empêchant l'extrusion de l'échantillon [PLA 4060D + 15%m CDHP]. En effet, la miscibilité entre le PLA (≈ hydrophile) et l'additif utilisé (≈ hydrophobe) est faible.[chapitre 4] En conséquence, lors de la plastification thermique des granulés additivés dans l'extrudeuse, une partie de l'additif exsude et lubrifie le contact entre la vis et la matière. Lorsque le taux initial d'additif dans les granulés est trop élevé (≈ 15 %m CDHP), l'exsudation interdit une contrainte de frottement suffisante entre la vis et la matière et gêne le convoyage dans l'extrudeuse monovis et le bon remplissage de la filière.

Afin de caractériser le phénomène d'exsudation, nous avons tenté de reproduire les effets de cisaillement et de chauffage similaires à ceux rencontrés dans la zone d'alimentation de l'extrudeuse (1ère zone). Pour cela, nous avons utilisé un rhéomètre équipé de deux plateaux rotatifs plan/plan préchauffés. Le cisaillement rencontré dans l'extrudeuse est mimé par l'utilisation du mode de déformation continu du rhéomètre (5 s^{-1}).

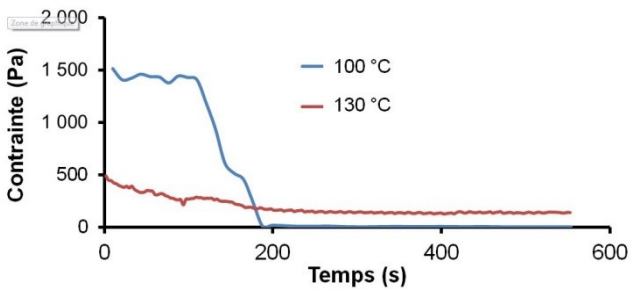

Figure 2.20 Courbes rhéologiques à 100 et 130 °C du [PLA 4060D + 15 %m CDHP], géométrie plan/plan

L'essai réalisé à 100 °C montre une chute brutale de la contrainte mesurée, attribuée à la lubrification de l'interface matière/plateau due à l'exsudation de l'additif lors de la plastification thermique du PLA. Cette exsudation est visible à la surface de l'échantillon via la présence de petites gouttes d'additif. Une fois l'essai terminé, nous obtenons une galette de PLA n'offrant plus aucune adhérence à la surface métallique des plateaux rotatifs. L'essai réalisé à 130°C montre une contrainte initiale plus faible que l'essai effectué à 100 °C, ceci signifiant que le plastifiant a déjà exsudé lors du chauffage préalable de la matière avant essai. Bien que la contrainte finale soit plus élevée que celle mesurée pour l'essai à 100 °C (pouvant s'expliquer par une matrice PLA moins visqueuse à 130 °C qu'à 100 °C, plus encline à se déformer), la viscosité n'est cependant pas suffisante pour générer une pression adéquate de remplissage de la filière. Nous avons ensuite choisi de poursuivre le développement du projet en utilisant le mélange [PLA + 10 %m CDHP], ce dernier présentant le meilleur compromis en termes d'amélioration des propriétés mécaniques et de processabilité.**chapitre 4**

2.2.3.8. Protocoles expérimentaux d'extrusion de films à plat et films soufflés

Pour la réalisation à l'échelle semi-pilote d'un film d'environ 25 µm d'épaisseur et de 15 cm de largeur par extrusion monovis avec filière plate, les conditions opératoires optimisées sont les suivantes :

- Extrudeuse : *Mapre. E1 30-33D. Filtres + deux mélangeurs statiques SMX™*
- Vitesse rotation vis : *30 rpm*
- Débit : ≈ *3 kg.h^{-1}*
- Profil de température extrudeuse: *170/165/160/155/150/145 °C*
- Température filière : *140 °C*
- Entrefer filière : *550 µm*
- Vitesse calandrage : *10 m.min^{-1}*.

Le problème est plus complexe en soufflage de gaine. Les essais témoins menés au laboratoire en utilisant du PLA 4060D non additivé n'ont pas permis l'obtention d'une bulle stable. Ceci est néanmoins conforme à nos attentes puisque le PLA est connu pour son problème de « melt strength » non adapté à ce type d'extrusion.[chapitre 5] Des sociétés commercialisent des additifs pour régler ce problème, il s'agit notamment des Biostrength™ d'Arkema et des Paraloid™ BPMS250 de Dow.

Des essais d'extrusion ont toutefois été réalisés avec le PLA additivé de CDHP. Dans le cas de la réalisation d'un film [PLA 4060D + 10 %m CDHP] de 25µm d'épaisseur et de 15 cm de large (gaine monoface) via l'utilisation de la filière gonflage de gaine, les conditions opératoires optimisées qui suivent ont permis de produire une gaine de qualité présentant un taux de gonflage de l'ordre de 2 :

- Extrudeuse : *Mapre 30D, L/D = 330:1. Filtres + deux mélangeurs statiques SMX™*
- Vitesse rotation vis : *30 rpm*
- Débit : ≈ *3 kg.h^{-1}*
- Profil de température extrudeuse: *140/145/150/155/155/155 °C*
- Filière : *gonflage de gaine Dr. Collin (poinçon diamètre 50 mm et entrefer 0,8 mm)*
- Température filière : *155°C*
- Entrefer filière : *800 µm*
- Vitesse tirage rouleaux : *2,4*
- Coefficient gonflage : *2.0 à 2.5.*

Ceci signifierait donc que notre additif, outre son rôle d'agent plastifiant, est également un bon « processing aid », à condition qu'il ne démixe pas de manière excessive.

Pour finir, des extrusions ont également été réalisées dans le cas du mélange ternaire [90 %m (90 %m PLA + 10 %m CDHP) + 10 %m PHBV] dont l'intérêt est présenté et détaillé dans le chapitre 6. Pour cela, deux méthodologies d'incorporation du PHBV au mélange PLA/CDHP ont préalablement été étudiées :

- « Procédé bivis » : le mélangeage à l'état fondu est réalisé par extrusion bivis. Ainsi, 10 %m de granulés PHI 002 sont mélangés à l'état fondu avec 90 %m de granulés [PLA 4060D + 10 %m CDHP] issus d'une précédente étape d'extrusion bivis.

Dans ce cas, les granulés finaux obtenus [90 %m (PLA 4060D + 10 %m CDHP) + 10 %m PHI 002] doivent subir une étape d'extrusion monovis ultérieure pour être mis sous forme de films.

- « Procédé dryblend » : le mélangeage à l'état fondu de 10 %m de granulés PHI 002 avec 90 %m de granulés [PLA 4060D + 10 %m CDHP] est directement réalisé au cours de l'étape d'extrusion monovis du film. Les granulés de PHI 002 sont introduits dans la trémie de l'extrudeuse monovis aux côtés des granulés de [PLA 4060D + 10 %m CDHP].

Ce procédé permet d'éviter une étape d'extrusion bivis supplémentaire et ainsi potentiellement diminuer les dégradations thermiques associées.

Pour chaque procédé de mélangeage décrit ci-avant, les conditions opératoires d'extrusion des films en filière plate (filière largeur 200 mm) et en soufflage de gaine ont été optimisées. Elles sont récapitulées dans le **Tableau 2.8**.

Tableau 2.8 Conditions opératoires du procédé de mélangeage par extrusion bivis et des procédés d'extrusion monovis pour la réalisation de films PLA/CDHP/PHBV

Procédé	**Profil température** *(°C)*	**Vitesse rotation vis** *(rpm)*	**Débit** *($kg.h^{-1}$)*
Procédé bivis	160 / 165 / 155 / 150 / 140 / 135 Filière 130	300	1.1
Extrusion monovis à plat *granulés issus du procédé bivis*	180 / 180 / 180 / 185 / 190 / 190 Filière 170	30	2.8
Extrusion monovis gonflage *granulés issus du procédé bivis*	180 / 180 / 180 / 185 / 190 / 190 Filière 150	30	2.8
Extrusion monovis à plat *procédé dryblend*	180 / 180 / 180 / 185 / 190 / 190 Filière 170	30	3.1
Extrusion monovis gonflage *procédé dryblend*	180 / 180 / 180 / 185 / 190 / 190 Filière 150	30	3.2

Néanmoins, nous avons observé qu'occasionnellement le « procédé dryblend » pouvait conduire au relargage de granulés infondus de PHBV pouvant obstruer la filière et/ou générer des défauts dans la plaque de matière calandrée en sortie de filière, provoquant alors des ruptures de flux et/ou déchirements du filmcomme observé sur la **Figure 2.21**.

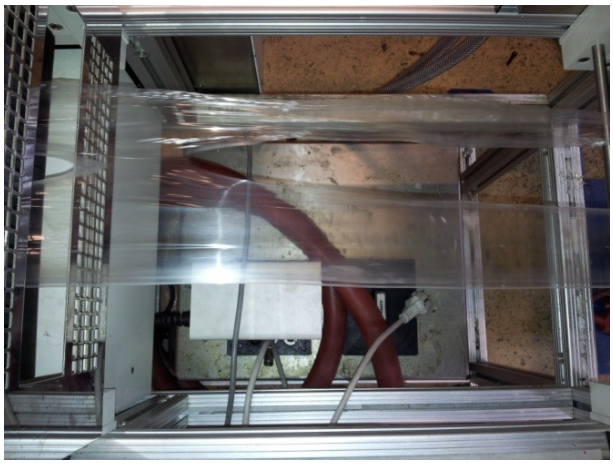

Figure 2.21 Calandrage d'une feuille [90 %m (PLA 4060D + 10 %m CDHP) + 10 %m PHI 002] obtenue par extrusion monovis « procédé dryblend » en présence d'infondus PHBV

Dès lors, nous avons opté pour la réalisation de granulés du mélange ternaire [90 %m (90 %m PLA + 10 %m CDHP) + 10 %m PHBV] par extrusion bivis préalablement à la réalisation de films par extrusion monovis.

2.2.4. Mise en forme des mélanges et des films à l'échelle pilote

L'objectif de cette partie est de valider les essais préalablement réalisés à l'échelle semi-pilote au PIMM sur des équipements de taille pilote, dont les capacités de production se rapprochent de celles de l'industrie. Conformément à ce qui a été présenté précédemment, ces essais de validation ont été réalisés sur le mélange ternaire [90 %m (90 %m PLA + 10 %m CDHP) + 10 %m PHBV].

2.2.4.1. Description de la ligne d'extrusion bivis

Ci-après sont mentionnées les caractéristiques techniques des équipements de la ligne pilote utilisée appartenant à la société prestataire MateriaNova (Ghislenghien, Belgique).

- Sécheur granulés : *Motan, capacité 100 L, Débit air 50 $m^3.h^{-1}$*
- Pompe chauffante : *PuMelt d280 Robatech, 20-180 °C, débit 1-40 $kg.h^{-1}$*
- Extrudeuse bivis : *Dr. Collin, Vis diamètre 35, rapport L/D 56.*
  Profil de vis non communiqué
- Tapis de refroidissement et granulateur : *Dr. Collin*

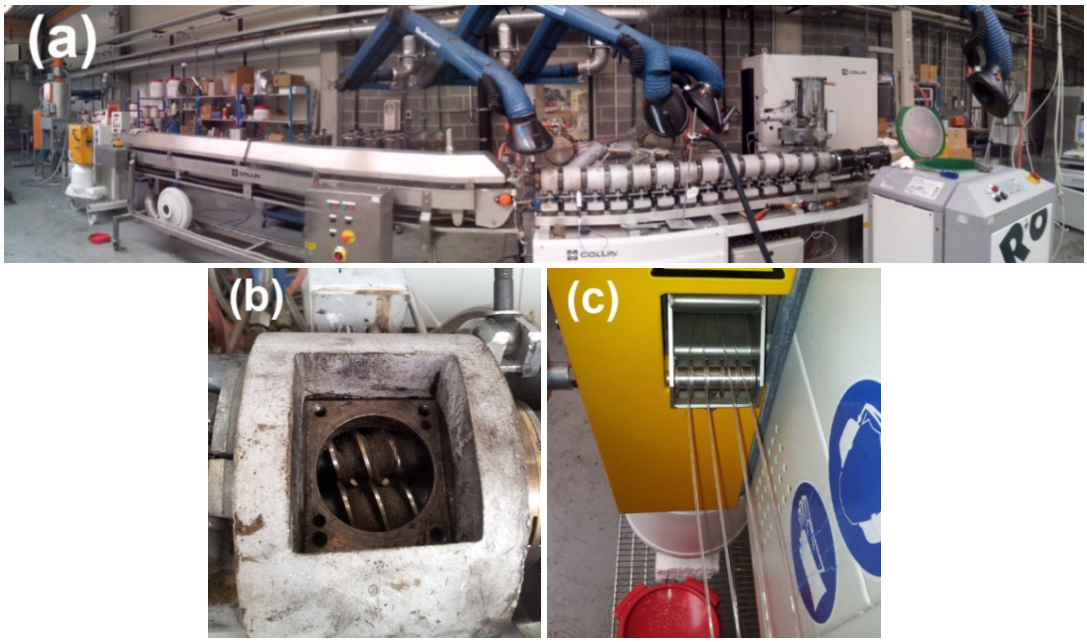

Figure 2.22 (a) Système d'extrusion/granulation Dr. Collin 35 mm L/D = 56:1,
(b) Zone d'alimentation solide, **(c)** Granulateur

2.2.4.2. Protocole expérimental d'extrusion bivis

Les essais ont été réalisés chez la société prestataire MateriaNova (Ghislenghien, Belgique). Les granulés PLA/CDHP/PHBV ont été réalisés en une seule étape d'extrusion bivis moyennant les conditions suivantes :

- Séchage des granulés : *PLA 4060D pendant 24 h à 60 °C*
  PHI 002 pendant 24 h à 80 °C
- Profil de température extrudeuse : *60/195/195/160/160/155/155/155/170/170/165/160/150/150 °C*
- Température filière : *150 °C*
- Débits : *PLA 4060D introduit en 1ère zone d'extrudeuse à 9 kg.h^{-1}*
  CDHP liquide préchauffé à 70 °C introduit en 4ème zone d'extrudeuse à 1 kg.h^{-1}
  PHI 002 introduit en 9ème zone d'extrudeuse à 1,1 kg.h^{-1}
- Vitesse de rotation des vis : *250 rpm*
- Temps de séjour : ≈ *6 minutes*
- Refroidissement et granulation : *air ambiant*
- Production totale : *117 kg.*

Les essais ont permis de prouver que le procédé de mélangeage par extrusion bivis du produit [90 %m (PLA 4060D + 10%m CDHP) + 10 %m PHI 002] est réalisable en une seule étape sur des machines et dans des conditions semi-industrielles. Une fois les différentes conditions opératoires définies et équilibrées, le process est très stable, davantage que l'extrusion du PLA seul. Le condensat de palme, de par son caractère lubrifiant, facilite grandement l'écoulement de la matière et les joncs sortent tous bien calibrés sans variation dans le temps.[chapitre 5] Aucune exsudation ni reflux d'additifs hors de l'extrudeuse ne sont observés et on constate que l'additif est incorporé au PLA sans difficulté. Le refroidissement des joncs par air est également réalisé aisément grâce à l'utilisation d'un tapis roulant avec circulation d'air permettant une granulation régulière (**Figure 2.22**).

2.2.4.3. Description de la ligne d'extrusion de films à plat

Ci-après sont mentionnées les caractéristiques techniques des équipements de la ligne pilote utilisée appartenant à la société prestataire Certech (Seneffe, Belgique).

- Extrudeuse monovis : *LabTech Engineering, vis diamètre 30 mm, rapport L/D = 30*
- Filière : *350 mm de large, entrefer 300 µm*
- Calandreuse : *LabTech Engineering 5 rouleaux thermorégulés*

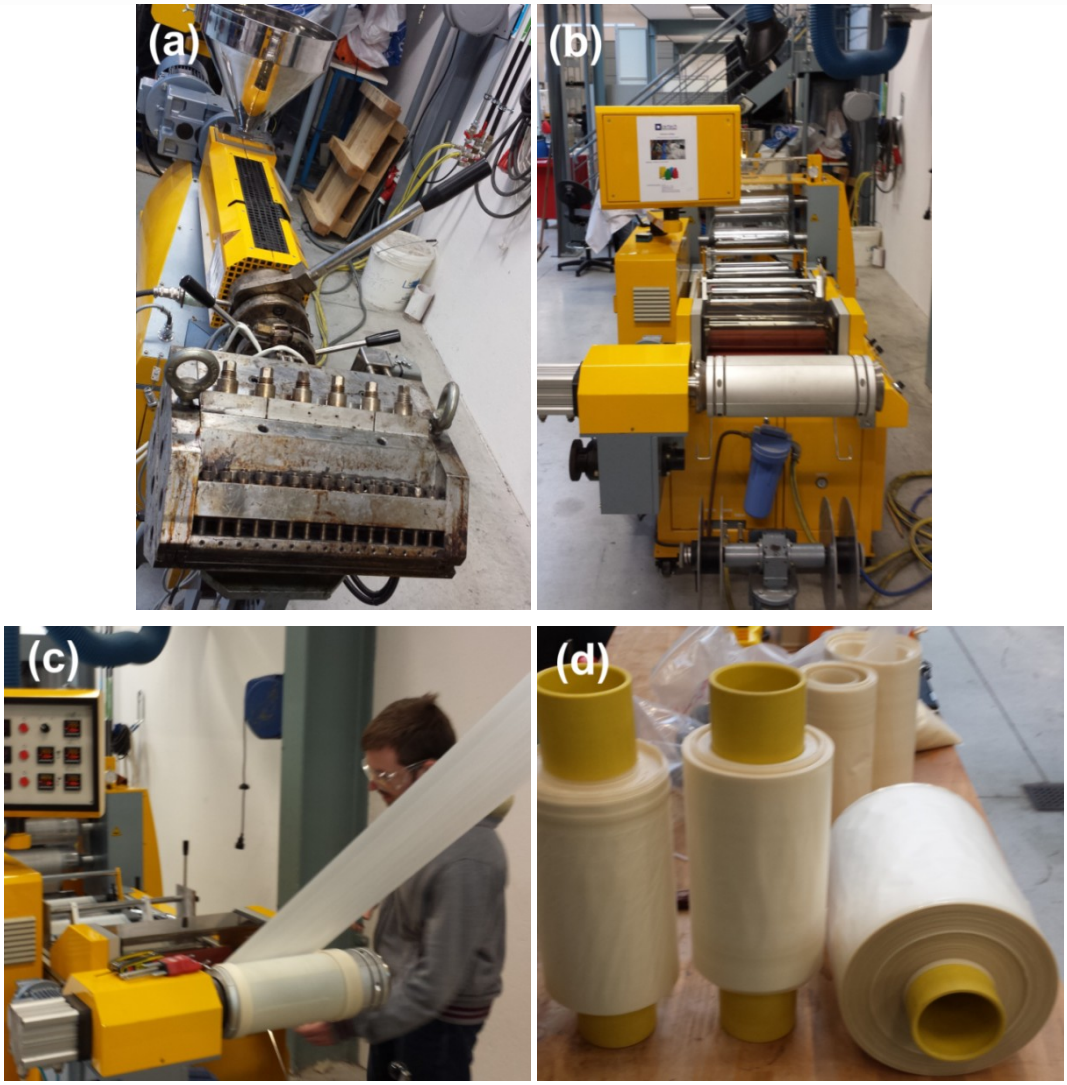

Figure 2.23 (a) Extrudeuse monovis Labtech Engineering 30 mm 30D et filière plate 350 mm, **(b)** Calandreuse, **(c)** Découpe des lisières du film et **(d)** Bobines réalisées

2.2.4.4. Protocole expérimental d'extrusion de films à plat

Les films réalisés à l'échelle pilote chez la société prestataire Certech (Seneffe, Belgique) ont été obtenus moyennant l'optimisation des conditions suivantes :

- Profil de température extrudeuse : *140/140/150/150/150 °C*
- Température filière : *155 °C*
- Vitesse de rotation de la vis : *65 rpm*
- Débit : *8 kg.h*$^{-1}$
- Temps de séjour *: ≈ 4 min*
- Vitesse de calandrage : *12,5 m.min*$^{-1}$
- Température des rouleaux de calandreuse : *14 °C*
- Largeur du film étiré sur le premier rouleau : *32 cm.*

Le procédé d'extrusion monovis à plat est stable et régulier sans phénomène de résonnance (**Figure 2.23**). Un léger phénomène de « neck-in » est observé, c'est-à-dire une variation de la largeur dans la direction de l'étirage et une variation de l'épaisseur dans les deux directions du plan de l'étirage, sans toutefois nuire de façon importante à la qualité du film. Un phénomène de surépaisseur de bord, dénommé « os de chien », nécessitant la découpe d'une bande d'environ 3 cm de large sur chaque côté du film a été constaté. Pour remédier à cela, le système de découpe longitudinal des lisières de la calandreuse a été utilisé.

2.2.5. Impression par flexographie encres à l'eau à l'échelle pilote

L'additif CDHP est un mélange naturel d'acides gras libres et autres corps gras (glycérides, stérols …) partiellement miscibles avec le PLA.[chapitres 4-6] Dès lors, une modification de l'état de surface du PLA est possible, altérant potentiellement la bonne imprimabilité du film produit. Pour cela, l'imprimabilité par flexographie encres à l'eau du film pilote a été vérifiée sur une petite ligne de production du groupe Brodart Packaging (Tilwel – Brie Comte Robert, France). Ci-après sont mentionnées les caractéristiques techniques des équipements utilisés et les conditions opératoires appliquées :

- Impression par flexographie,
- Encres à l'eau, Séries Aqua OK compost certifiées par Vinçotte, pigments minéraux 1 % poids/poids maxi de dépôt par teinte,
- Taux d'encrage en aplat : *1,46 g.m*$^{-2}$,
- Vitesse d'impression : *70 m.min*$^{-1}$,
- Température d'air pulsé : *70 °C*.

Un « test au Scotch » normalisé en sortie de tunnel d'impression a été réalisé pour contrôler l'adhésion de l'encre dépôt aplat sur le film. Le test est négatif, l'encre adhère au film. Le produit a été validé par Brodart Packaging.

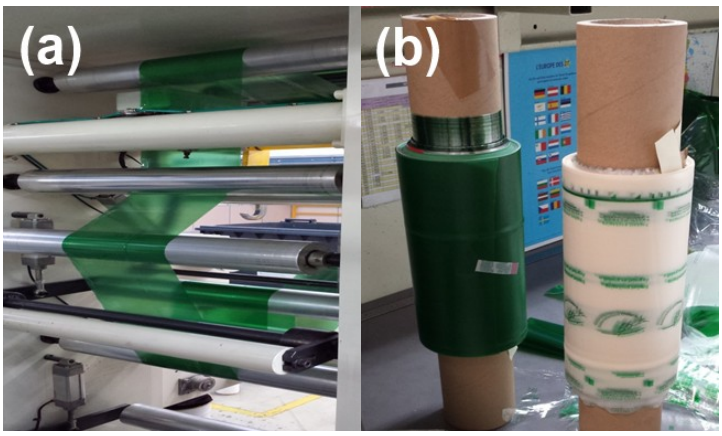

Figure 2.24 (a) Procédé d'impression flexographie et **(b)** Bobines imprimées

2.2.6. Conditionnement d'échantillons en étuve

2.2.6.1. Méthode de cristallisation du PLA 4042D

Afin d'étudier la cristallisation d'échantillons de PLA formulés avec du CDHP (chapitre 5), des plaques obtenues par thermocompression de granulés de PLA 4042D non additivé ou formulé avec 10 %m de CDHP ont été mises à cristalliser dans une étuve de marque Memmert (**Figure 2.25**) entre deux plaques rigides de métal recouvertes d'antiadhésif lisse, séparées par des cales métalliques d'1 mm d'épaisseur et surmontées d'un poids de 2 kg. Les échantillons ont été placés dans l'étuve préalablement réglée à une température de 90 °C, vérifiée par un thermocouple externe.. Les plaques ont été soumises à cette température pour une durée fixe de 24 h. Une fois ce temps écoulé, les échantillons ont été retirés de l'étuve et laissés à refroidir à température ambiante.

Figure 2.25 Etuve Memmert utilisée pour la cristallisation du PLA 4042D

2.2.6.2. Méthode de vieillissement accéléré des échantillons de PLA 4060D

Afin d'étudier les effets du vieillissement sur les échantillons (chapitre 6), des bandelettes obtenues par extrusion monovis de granulés de PLA 4060D pur ou formulé avec 10%m de CDHP et/ou PHI 002 ont été vieillies thermiquement entre 0 et 750 h dans une étuve (FisherBrand TLK 72B) à $T_a = T_g - 15$ °C sous pression réduite (0,1 bar) afin de minimiser les phénomènes de thermo-oxydation. A chaque prélèvement, les échantillons retirés ont été immédiatement découpés par emporte-pièce aux dimensions des éprouvettes (type 5A IS527-2, **Figure 2.26**), puis laissés 15 minutes à 23 °C et 50 % RH avant d'être caractérisés mécaniquement.

Figure 2.26 Etuve FisherBrand utilisée pour le vieillissement des bandelettes de PLA 4060D

Tableau synoptique des matériaux, matériels, procédés de mise en œuvre et caractérisations utilisés

Titre de l'étude	Numéro du chapitre	Polymère(s) utilisé(s)	Additifs utilisés	Procédés de mise en œuvre utilisés	Type d'échantillon obtenu	Caractérisations effectuées
Solubility Factors as Screening Tools of Biodegradable Toughening Agents of Polylactide	3	PLA 4060D	ATBC PEG 400 DOA PID 37 Squalène	Séchage de granulés *(Somos 60 L)* Extrusion bivis *(Thermo Haake 16mm 44D)* Thermocompression *(Gibitre 20 tonnes)*	Plaques *(≈ 1 mm épaisseur)*	Extraction Soxhlet Chromatographie d'exclusion stérique Analyse calorimétrique différentielle Traction uniaxiale *(25 mm/min)* Microscopie électronique à balayage Calcul solubilité Hansen-Hildebrand
Oil industry by-products increase the ductility of polylactide	4	PLA 4060D	Acide palmitique Acide oléique Huile palme hydrogéné Huile coprah hydrogéné α-tocophérol Squalène	Séchage de granulés *(Somos 60 L)* Extrusion bivis *(Thermo Haake 16mm 44D)* Extrusion monovis à plat *(Scamex 20mm 12D)*	Bandelettes *(≈ 0,8 mm épaisseur)*	Chromatographie en phase gaz Calcul solubilité Hansen-Hildebrand Analyse calorimétrique différentielle Analyse thermogravimétrique Traction uniaxiale *(25 mm/min)* Déformation sous microscope optique Microscopie électronique à balayage Analyse en Composantes Principales
			Condensat désodo huile colza Condensat désodo huile soja Condensat désodo huile olive Condensat désodo huile palme	Séchage de granulés (Somos 60 L) Extrusion bivis (Thermo Haake 16mm 44D) Thermocompression (Gibitre 20 tonnes)	Plaques *(≈ 1 mm épaisseur)*	
Biobased and biodegradable by-product of oil industry as toughening agent of polylactide	5	PLA 4060D	Condensat désodo huile palme	Séchage de granulés *(Motan 100 L)* Extrusion bivis *(Dr Collin 35mm 56D)* Extrusion monovis à plat *(Mapre 30mm 30D)* Extrusion monovis gonflage de gaine *(Mapre 30mm 30D)*	Films *(≈ 25 µm épaisseur)*	Chromatographie en phase gaz Analyse thermogravimétrique Extraction Soxhlet Chromatographie d'exclusion stérique Analyse calorimétrique différentielle Traction uniaxiale *(25 mm/min)* Analyse mécanique dynamique Perméabilité à l'oxygène Etude de biodégradation Aptitude au contact alimentaire
		PLA 4042D		Séchage de granulés *(Motan 100 L)* Extrusion bivis *(Dr Collin 35mm 56D)* Thermocompression *(Gibitre 20 tonnes)* Cristallisation en étuve *(Memmert)*	Plaques *(≈ 1 mm épaisseur)*	
Physical aging and its effect on mechanical properties of toughened PLA films	6	PLA 4060D	Condensat désodo huile palme	Séchage de granulés *(Motan 100 L)* Extrusion bivis (Thermo Haake 16mm 44D) Extrusion monovis à plat *(Scamex 20mm 12D)* Vieillissement étuve sous vide *(FisherBrand)*	Bandelettes *(≈ 1 mm épaisseur)*	Analyse thermogravimétrique Analyse calorimétrique différentielle Traction uniaxiale *(5 mm/min)* Microscopie électronique à balayage
		PLA 4060D PHI 002		Séchage de granulés *(Motan 100 L)* Extrusion bivis *(Dr Collin 35mm 56D)* Extrusion monovis à plat *(Scamex 20mm 12D)* Vieillissement étuve sous vide *(FisherBrand)*		

REFERENCES

1. Peurton, F. Nanocomposites à matrice thermoplastique et renforts plaquettaires : relations élaboration-structure-propriétés. 2008.

2. NatureWorks Crystallizing and Drying Ingeo™ Biopolymer. (accessed 13 Mars 2014).

3. Courgneau, C. Mechanisms of gas and organic compounds tranfer into Polylactide (PLA). AgroParisTech, 2011.

4. Courgneau, C.; Domenek, S.; Guinault, A.; Averous, L.; Ducruet, V., Analysis of the Structure-Properties Relationships of Different Multiphase Systems Based on Plasticized Poly(Lactic Acid). *Journal of Polymers and the Environment* 2011, 19 (2), 362-371.

CHAPITRE 3

TABLE OF CONTENTS

ABSTRACT **118**

3.1. INTRODUCTION **119**

3.2. EXPERIMENTAL **121**

3.2.1. Materials 121
3.2.2. Samples preparation 122
3.2.3. Characterization of PLA films 122
3.2.3.1. Extraction of the plasticizer from the formulated PLA *122*
3.2.3.2. Size exclusion chromatography (SEC) *123*
3.2.3.3. Differential Scanning calorimetry (DSC) *124*
3.2.3.4. Tensile Tests *124*
3.2.3.5. Scanning electron microscopy (SEM) *125*
3.2.3.6. Calculation of the solubility parameters *125*

3.3. RESULTS AND DISCUSSION **128**

3.3.1. Analysis of plasticizer content and average molecular weight of the compounded PLA 128
3.3.2. Miscibility study 129
3.3.3. Tensile properties of plasticized PLA 131

3.4. CONCLUSION **137**

ACKNOWLEDGEMENTS **137**

REFERENCES **138**

Chapitre 3 - Solubility Factors as Screening Tools of Biodegradable Toughening Agents of Polylactide

Le chapitre bibliographique a mis en évidence l'étendue de la plastification externe, qui d'une manière rapide et peu couteuse, permet de grandement améliorer les propriétés mécaniques du PLA, paramètre limitant pour de nombreuses applications. L'augmentation du volume libre, facteur prépondérant des performances développées, est cependant fonction de la solubilité des molécules plastifiantes utilisées. De ce fait, nous avons souhaité étudier l'influence de la solubilité des plastifiants sur les mécanismes physiques de déformation développés.

L'étude de la littérature montre que deux théories aisément employables, les approches de Hildebrand et de Hansen, permettent de modéliser la solubilité des molécules dans un polymère amorphe. Pour cela, l'utilisation de la méthode de contribution des groupes chimiques, afin de déterminer les paramètres thermodynamiques de chaque plastifiant étudié, a été retenue. En outre, les molécules plastifiantes ont été choisies pour leur volume molaire similaire mais leur structure chimique dissemblable (molécules branchées, linéaires, polaires, apolaires, etc.).

Le projet global ayant pour objectif le développement d'un film de PLA souple, notamment biodégradable, nous avons orienté l'étude sur la comparaison de deux additifs biosoucés et biodégradables, le Polysorbid® 37 et le squalène, par rapport à trois plastifiants pétrosourcés, l'ATBC, le PEG 400 et le DOA, dont les propriétés ont été largement commentées dans la littérature.

Cette étude est présentée sous la forme d'un article récemment proposé pour publication dans une revie scientifique internationale (J. Appl. Polym. Sci. 2015, Special Issue: Manufacturing of Advanced Biodegradable Polymeric Components).

Alexandre Ruellan[a,b,c], Alain Guinault[a,d], Cyrille Sollogoub[a,d], Violette Ducruet[e], Sandra Domenek[b]

[a.] *CNAM, Arts et Métiers ParisTech, CNRS, UMR 8006, Laboratoire PIMM, 151, Boulevard de l'Hopital, F-75013 Paris.*
[b] *AgroParisTech, Ingénierie Procédés Aliments, 1 avenue des Olympiades, F-91300 Massy.*
[c] *Brodart Packaging, Département R&D, 1 rue du Stand, F-10700 Arcis-Sur-Aube.*
[d] *CNAM, Laboratoire P2AM, 2 rue Conté, F-75003 Paris.*
[e] *INRA, Ingénierie Procédés Aliments, 1 avenue des Olympiades, F-91300 Massy.*

Abstract

Changes in thermo-mechanical properties of polylactide (PLA) plasticized by two biodegradable and biobased molecules, Polysorb® ID37 (PID37) and squalene, were compared to formulations with petroleum based plasticizers: acetyl tributyl citrate, poly(ethylene glycol) 400 and dioctyl adipate (DOA). Solubility parameters of additives were calculated and related to the plasticization behaviors. PID37 proved miscible with PLA because of its polar functions and short alkyl groups. It decreased the PLA glass transition temperature (T_g) and increased in ductility when T_g approached room temperature. Squalene had low miscibility because of the absence of polar groups. T_g was not depressed. Ductility improvements were nevertheless reached, because the immiscible inclusions efficiently induced crazing by the distribution of stress concentration points all over the material delaying failure. The maximum elongation at break was 60 % for squalene, 400 % for DOA and 500 % for PID37. Solubility factors were thus an efficient prediction tool for plasticizing behavior.

Keywords: poly(lactic acid), PLA, plasticizer, ATBC, DOA, PEG, Polysorb® ID37, squalene, solubility parameters, stress-whitening, crazing.

3.1. Introduction

Since almost two decades, new polymers are developed in the aim of lowering the environmental impact of the plastics manufacturing. Polylactide, which is a biobased and compostable polyester produced at large scale, exhibits numerous advantages in a cost effective way such as a glass transition temperature higher than room temperature, ease of processing, high transparency, printability, etc.. However, even if PLA offers satisfying mechanical properties, its low deformation at break remains a limitation for many high volume applications, such as textiles fiber production or food packaging.[1]

External plasticizing is a widely applied method for enhancing polymer ductility, because of existing know-how and the ease of implementation of such a process at the industrial scale. Many researches have been conducted to find effective PLA plasticizers, which should be high boiling point molecules, presenting miscibility with the polymer, having high associated free volume, and low glass transition temperatures. For polar polymers as polyesters, plasticizer molecules should have i) polar groups acting as strong points of attraction ensuring a good compatibility, ii) non-polar groups (as alkyl chains) masking the neighbouring polymer chain dipoles and improving free volume.[2]

As plasticizers are often used in compounds up to 30 wt%, it is interesting that they are biodegradable and biobased if such claims are envisaged to be associated to the polymer. Additives derived from biomass by-products have already been experimented to enhance the ductility of PLA. Miscibility has been observed as being a key factor. In fact, glucosemonoester and fatty acid esters,[3] glycerol,[4] liquiefied rice bran,[5] α-tocopherol and resveratrol[6] did not induce significant glass transition temperature lowering nor elongation at break improvement. In opposition, oligomeric lactic acid,[4] liquefied wood,[5] or limonene[7] both caused a large depression in the PLA glass transition temperature concomitantly with a huge

gain in the ductility. To enhance compatibility with PLA, chemically modified biomass fractions such as epoxidized soybean (ESO)[1a, 8] or palm (EPO)[9] oils were tested. Elongation at break increases were obtained,[8a, 9] while the PLA glass transition was merely decreased.

To be competitive, the performance of biobased plasticizers needs at least to approach the one of petrochemical molecules. Among petroleum based plasticizers already investigated, citrate esters[10] are the far most prominent ones. Labrecque et al.[10h] mixed triethyl citrate (TEC), tributyl citrate (TBC), acetyl triethyl citrate (ATEC) and acetyl tributyl citrate (ATBC) each at 20 wt% in PLA. In all cases, the T_g was lowered and the elongation at break raised up than 300 %. Polyethylene glycols have also attracted some interests, mainly because they are commercially available in a large range of chain lengths. It has been observed that small chain length PEG (M_w < 1,000)[10a, 10g, 11] tends to induce stronger thermo-mechanical changes than longest ones.[10a, 12] Finally, adipate esters, which own two polar functions, have been studied as PLA plasticizers.[10c, 13] Martino et al.[13b] successfully used dioctyl adipate (DOA) up to 20 % weight content increasing elongation at break close to 300 %.

In the present work we study two fully biobased and biodegradable molecules as new plasticizers in PLA. Polysorb® ID37 (PID37) is an isosorbide diester, recently developed by the Roquette Group, first intended for the lamination of PVC but potentially utilizable as a PLA plasticizer.[14] Its isosorbide core is derived from glucose and prepared from the double dehydration of sorbitol while the ester alkyl chains are issued from vegetable fats. It has recently been registered to the European Union Regulation (REACH). Furthermore, squalene is a common natural hydrocarbon compound extracted from vegetables or shark liver, mainly used in cosmetics, food supplements or as adjuvant in vaccines.

In the aim to probe the effects of those molecules and to investigate the corresponding plasticizing mechanisms, we added in amorphous PLA the novel molecules and compared to

known petrochemical plasticizers having similar molecular weight. This allowed for determination of two different mechanisms of PLA ductility increase in function of the plasticizer solubility, one linked to the lowering of the glass transition by the plasticizer and the other to the induction of crazing.

3.2. Experimental

3.2.1. Materials

PLA 4060D with a D-lactic acid content of 11 ± 1 % (according to the datasheet) was purchased from NatureWorks (U.S.A.). ATBC, PEG400, DOA and squalene were supplied by Sigma-Aldrich (France). PID37 was provided by the Roquette Group (France). Chemical structures of plasticizers are shown in **Figure 3.1**.

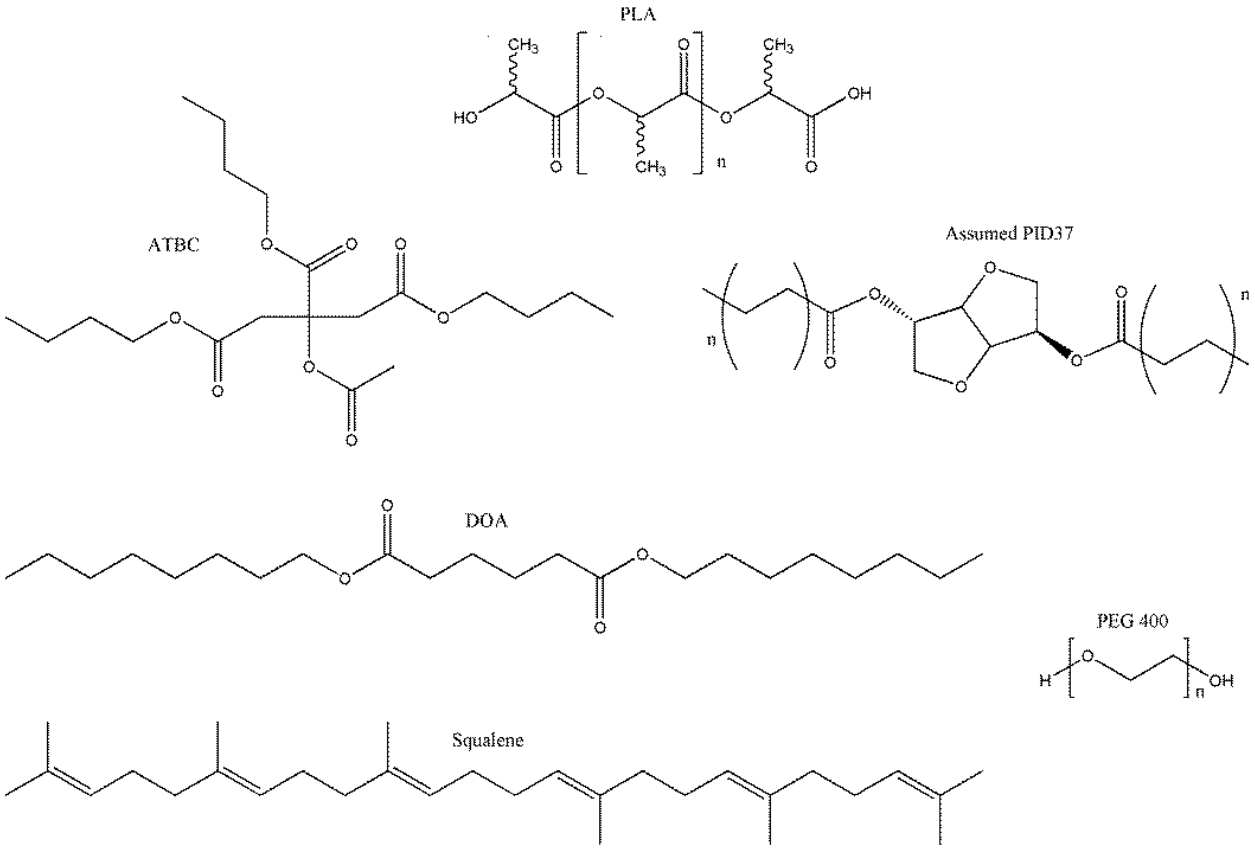

Figure 3.1 Chemical structures of PLA and plasticizers

3.2.2. Samples preparation

Prior to compounding, PLA pellets and plasticizers were dried at 60 °C for 24 h under dried air to remove water traces using a SOMOS 60 L. Relative humidity of dried pellets was controlled to being lower than 350 ppm using an Aboni FMX HydroTracer.

Neat PLA and plasticized PLA sheets were prepared in two successive steps. First, direct melt mixing of additives with PLA was carried out using a corotating twin screw extruder (Thermo Haake Ptw 16-40D) with a screw diameter of 16 mm and a length to diameter ratio (L/D) 40:1. Blends of PLA containing 5 wt%, 10 wt%, 15 wt% and 20 wt% of each plasticizer were prepared. The liquid addition of each plasticizer was performed in the third zone of seven of the extruder. Processing conditions are given in **Table 3.1**. After cooling under air, the strand was pelletized. The obtained pellets were stored in hermetic metalized sealed bags avoiding rehydration. Second, the different PLA compounds were thermo-moulded by compression at 220 bars (Laboratory Press Gibitre Instruments 20 tons). The pellets were pre-melted at 180 °C without pressure during 180 seconds and then the heated plates were closed with a progressive increase in pressure during 120 seconds to eliminate air bubbles. The obtained sheets were then cooled down to ambient temperature by air. The thickness of the sheets was about 1 mm.

3.2.3. Characterization of PLA films

3.2.3.1. Extraction of the plasticizer from the formulated PLA

In order to quantify the amount of plasticizer added in PLA, about 6 g of the formulated pellets were placed into a 125 mL Soxhlet apparatus with 200 mL of ethanol and extracted under reflux during 8 h. Then the extracted PLA pellets were dried for 2 days at 40 °C under vacuum. The weight content of the plasticizer was measured by weighting difference of the PLA pellets. Analyses were done in duplicate.

Table 3.1 Processing conditions of blend compounding by twin screw extrusion

Formulation		Temperature profile (°C)	Screw rotation speed (rpm)	PLA 4060D feeding input ($kg.h^{-1}$)	Additive feeding input ($kg.h^{-1}$)
Neat PLA		175/180/190/190/190/190/180	300	0.620	-
PLA +	5 wt% ATBC	175/180/180/180/180/180/170	300	0.600	0.031
	10 wt% ATBC	175/180/170/170/165/160/160	300	0.600	0.072
	15 wt% ATBC	175/175/170/165/160/155/155	300	0.550	0.098
	20 wt% ATBC	175/170/160/160/160/150/150	300	0.550	0.136
PLA +	5 wt% PEG 400	175/180/180/175/175/170/170	300	0.600	0.032
	10 wt% PEG 400	175/175/170/170/170/170/165	300	0.600	0.075
	15 wt% PEG 400	170/170/170/165/160/155/150	300	0.600	0.107
	20 wt% PEG 400	170/170/165/160/155/150/150	300	0.600	0.150
PLA +	5 wt% DOA	175/180/180/180/190/180/175	300	0.620	0.033
	10 wt% DOA	175/175/175/180/180/175/170	300	0.620	0.070
	15 wt% DOA	175/175/175/180/180/175/170	300	0.620	0.108
	20 wt% DOA	175/175/175/180/180/175/170	300	0.620	0.154
PLA +	5 wt% PID37	170/180/175/175/170/170/170	300	0.580	0.030
	10 wt% PID37	170/180/170/165/165/165/160	300	0.580	0.066
	15 wt% PID37	170/180/170/160/160/160/155	300	0.580	0.104
	20 wt% PID37	170/180/170/160/155/150/150	300	0.580	0.147
PLA +	5 wt% squalene	175/180/180/170/170/170/165	300	0.610	0.034
	10 wt% squalene	175/180/170/170/170/170/165	300	0.610	0.070
	15 wt% squalene	175/180/170/170/170/170/165	300	0.610	0.104
	20 wt% squalene	175/180/170/170/170/170/165	300	0.610	0.149

3.2.3.2. Size exclusion chromatography (SEC)

The average molecular weight and the dispersity of neat and formulated PLA sheets were measured by SEC using a Waters Co. apparatus equipped with an isocratic pump (GILSON 307), a column oven (Waters Control Module II), a gel column (Styragel H5E 7.8 x 300 mm) having a separation range from 2,000 to 1,000,000 $g.mol^{-1}$, an autosampler (Waters 717 plus) and a refractive Index (RI) detector (Waters 2414). Data acquisition and analysis were carried out with the help of Breeze Software. The analyses were performed at 35 °C with tehtrahydrofuran (THF) as eluent at a flow rate of 1 $mL.min^{-1}$. The calibration was done prior to the experiments, based on polystyrene standards (Shodex Standard from Showa Denko range 3,070 to 778,000 $g.mol^{-1}$). For sample preparation neat and formulated PLA pellets were dissolved in THF (20 $mg.L^{-1}$) on a shaker at 60 °C for 45 minutes. Analyses were done in triplicate.

3.2.3.3. Differential Scanning calorimetry (DSC)

The thermal analyses were performed with a Mettler Toledo DSC1 STARe System under nitrogen atmosphere (50 mL.min^{-1}). Calibration of the device was achieved using pure water and Indium standard prior to the experiments. Samples of around 7 mg were cut from the thermo-molded sheets and put into 40 µL hermetic sealed aluminum pans. For each sample, calorimetric scans were carried out at a heating/cool rate of 10 °C.min^{-1}. Thermal history was suppressed by heating from 0 °C to 70 °C (first scan), followed by an isotherm at 70 °C during 5 min. Then the samples were cooled down from 70 °C to -40 °C (second scan), then the heating scan from -40 °C to 100 °C (third scan) was performed. The glass transition temperature was taken at the midpoint from the third scan. Experiments were done in triplicate.

The plasticizer glass transition temperature was determined at the midpoint using a heating scan from -95 °C to 25 °c at a heating rate of 2 °C.min^{-1}. Experiments were carried out in duplicate.

3.2.3.4. Tensile Tests

Tensile properties were investigated at 23 °C, relative humidity (RH) regulated at 50 ± 10 % and cross-head speed of 25 mm.min^{-1}, using an universal tensile machine without extensometer (Instron model 4301). Dog bone shaped samples (ISO 527-2, type 5A) were cut from the thermo-molded sheets. Prior to tensile testing, the samples were conditioned at 23 °C and 50 ± 10 % RH for at least 72 h. The thickness of the samples varies from 0.9 to 1.1 mm. Each value is an average of 10 measurements.

3.2.3.5. Scanning electron microscopy (SEM)

The morphology of the samples before and after tensile tests was observed with SEM (Hitachi 4800 II). Observations were directly conducted on the longitudinal surface of the dog bone shaped samples without any previous preparation.

3.2.3.6. Calculation of the solubility parameters

Molar volumes and molar attraction constants of the polylactide and the plasticizers were determined according to the van Krevelen and Hoftyzer atomic group contribution method. Tables can be found in van Krevelen.[15] Because the length of the PID37 alkyl ester chains is unknown, calculations were done considering saturated alkyl chains from 6 to 10 carbons length. Because PEG 400 is an oligomer with an average molar mass between 380-420 $g.mol^{-1}$ (according to the data sheet), calculations were done with degrees of polymerization n_i=6 and n_i=7.

The average molar volume ($V_g(T)$) at 25 °C of the amorphous and glassy chains of PLA was estimated using equations **(3.1)** and **(3.2)**. According to the SEC measurements (M_n = 104,200 $g.mol^{-1}$), the average polymerization degree (n_i) is ≈ 1450. Using the amorphous molar volumes increments values at 298 °K,[15] the van der Waals volume of the repeating lactide unit is estimated being 55.72 $cm^3.mol^{-1}$.

$$V_g(T) = F\ (1.30 + 0.55\ 10^{-3}\ T_g + 0.45\ 10^{-3}\ T) \quad \textbf{(3.1)}$$

$$F = \sum n_i F_i \quad , \quad \textbf{(3.2)}$$

where Vg(T) is the molar volume of the polymer chain in $cm^3.mol^{-1}$, F the van der Waals volume of the polymer chain in $cm^3.mol^{-1}$, T_g the glass transition temperature of the polymer in K, T the room temperature in K, n_i the polymerization index of the molar chain and F_i the van der Waals volume of the polymer repetition unit in $cm^3.mol^{-1}$.[16]

The Hansen Solubility parameters (HSP) of each plasticizer were calculated using equations **(3.3)**, **(3.4)** and **(3.5)**.[17] The used molar constant values[15] are presented in **Table 3.2**. However, estimating HSP of very long chain polymers as the PLA 4060D using the group contribution method is not reliable enough, mainly because the effect of the chain length on the three-dimensional configuration is not considered, for this reason we used literature values obtained by computed calculations and published by Abbott.[18]

$$\delta_d = \frac{\sum F_{di}}{\sum V_i} \quad \textbf{(3.3)}$$

$$\delta_p = \frac{\sqrt{\sum F_{Pi}^2}}{\sum V_i} \quad \textbf{(3.4)}$$

$$\delta_h = \sqrt{\frac{\sum E_{hi}}{\sum V_i}} \quad , \quad \textbf{(3.5)}$$

where δ_d is the dispersion component of the solubility parameter in $J^{1/2}.cm^{-3/2}$, δ_p the polar component of the solubility parameter in $J^{1/2}.cm^{-3/2}$, δ_h the hydrogen bonding component of the solubility parameter in $J^{1/2}.cm^{-3/2}$, F_{di} the dispersion contribution of the molar attraction constant in $(J^{1/2}.cm^{-3/2}).mol^{-1}$, F_{pi} the polar contribution of the molar attraction constant in $(J^{1/2}.cm^{-3/2}).mol^{-1}$, E_{hi} the hydrogen bonding energy contribution of the molar attraction constant in $J.mol^{-1}$ and V the molar volume contribution of the chemical group involved in $cm^3.mol^{-1}$.

Table 3.2 Molar constant for the calculation of solubility values obtained from Ref.[15]

Group *i*	**F_d** *($(J^{1/2}.cm^{-3/2}).mol^{-1}$)*	**F_p^2** *($(J.cm^{-3}).mol^{-1}$)*	**E_h** *($J.mol^{-1}$)*	**Molar volume** *($cm^3.mol^{-1}$)*	**ATBC**	**PEG 400**	**DOA**	**PID37**	**Squalene**
>C<	-70	0	0	-19.2	1	0	0	0	0
=C<	70	0	0	-5.5	0	0	0	0	6
>CH-	80	0	0	-1.0	0	0	0	4	0
=CH-	200	0	0	13.5	0	0	0	0	6
-CH2-	270	0	0	16.1	11	16−18	18	10−18	10
-CH3	420	0	0	33.5	4	0	2	2	8
-COO-	390	240,100	7,000	18	4	0	2	2	0
-OH	210	250,000	20,000	10	0	2	0	0	0
-O-	100	160,000	3,000	3.8	0	7−8	0	2	0
Ring	190	0	0	16	0	0	0	2	0
One plane of symmetry	-	Total *0.50	-	-	0	0	1	0	1

F_d Dispersion contribution, F_p Polar contribution, E_h Hydrogen bonding energy contribution

The solubility of the five molecules in PLA is assessed using the HSP Relative Energy Difference (RED) from equations **(3.6)** and **(3.7)**:

$$distance = \sqrt{4\left(\delta d_{plast} - \delta d_{PLA}\right)^2 + \left(\delta p_{plast} - \delta p_{PLA}\right)^2 + \left(\delta h_{plast} - \delta h_{PLA}\right)^2} \quad \textbf{(3.6)}$$

$$RED = \frac{Distance}{Radius} \quad , \quad \textbf{(3.7)}$$

where δ_d, δ_p, and δ_h are the components of the solubility parameter of the plasticizer obtained from equations **(3.3)**, **(3.4)** and **(3.5)** and the ones of PLA obtained from Abbott.[18] The radius is the maximal distance obtained from Abbott,[18] beyond which the additives are not miscible anymore with the polymer. Therefore, the closer the RED to zero is, the better is the compatibility. A RED value higher than 1 means a theoretical non-miscibility of the plasticizer with the matrix.

A second method can be applied using the group contribution method with equation **(3.8)**. In this case, the Hildebrand solubility parameter δ (HiSP), which is also the outcome of HSP using equation **(3.9)**, is obtained. Cohesive energy values (E_{coh}) can be found in Ref.[15]

$$\delta = \sqrt{\frac{E_{coh}}{V}} \quad \textbf{(3.8)}$$

$$\delta = \sqrt{\delta_d^2 + \delta_p^2 + \delta_h^2} \quad , \quad \textbf{(3.9)}$$

where δ is the solubility parameter in $J^{1/2}.cm^{-3/2}$, E_{coh} the cohesive energy value of the polymer chain in $J.mol^{-1}$, V the molar volume of the polymer chain in $cm^3.mol^{-1}$, and δ_d, δ_p, δ_h the components of the solubility parameter, *i.e.* the HSP mentioned above.

The obtained value of the HiSP of PLA using equation **(3.8)** is δ = 22.1 $J^{1/2}.cm^{-3/2}$, which is close to the value δ = 21.9 $J^{1/2}.cm^{-3/2}$ determined using equation **(3.9)** and HSP of PLA found

in Ref.[18] Consequently, we consider in this study HSP of PLA found in Ref.[18] suitable to be compared with calculated HSP of plasticizers using the group contribution method.

Then, solubility of the five molecules in PLA were also assessed using the HiSP. In this case, the numerical difference between HiSP of PLA and HiSP of plasticizers was computed. The larger the value, the lower is the compatibility of the plasticizer with the matrix.

3.3. Results and Discussion

3.3.1. Analysis of plasticizer content and average molecular weight of the compounded PLA

The plasticizer incorporated in the compounds was quantified and **Table 3.3** shows the comparison of measured concentrations with the target concentration. We note that for ATBC, PEG 400, DOA and PID37, the incorporated amounts were close to the targeted value, meaning little additive loss during twin-screw extrusion. The squalene quantities were substantially smaller than the target amounts, showing loss of the plasticizer during processing. Indeed, an accumulation of liquid squalene inside the twin-screw extruder was observed.

The average molecular weight of the PLA samples is also given in **Table 3.3**. The blank PLA showed moderate thermal degradation of the macromolecular chain length due to the twin-screw extrusion process. This decrease can be linked to the high sensitivity of PLA to the hydrolysis reactions and/or the thermo-mechanical input.[1b, 10c, 10g] When adding ATBC, DOA, PID37 or squalene, the degradation is less important, likely due to the lowered extruder setpoint temperatures because of the plasticization, and/or to the internal lubrication which reduces the shearing. *A contrario*, PEG 400 induced a large decrease of both the M_n and M_w meaning main chain scissions. The decrease of the macromolecular chain length caused by

compounding with PEG was already largely described in literature and most likely explained by transesterification reactions between PLA and PEG.[10g, 19]

Table 3.3 Extracted plasticizer contents, molar weight averages and dispersitiy of PLA/plasticizer formulations

Formulation	**Targeted plasticizer content** *(wt%)*	**Extracted plasticizer content** *(wt%)*	**M_n** *($g.mol^{-1}$)*	**M_w** *($g.mol^{-1}$)*	**I**
Non-extruded PLA	-	-	104,500 ± 2,300	244,500 ± 4,100	2.34 ± 0.01
PLA + ATBC	0	-	79,300 ± 4,500	209,600 ± 5,400	2.64 ± 0.09
	5	4.2 ± 0.3	88,000 ± 2,900	211,700 ± 3,900	2,41 ± 0.04
	10	8.9 ± 0.4	88,100 ± 3,500	210,900 ± 7,000	2.39 ± 0.02
	15	13.9 ± 0.4	93,900 ± 4,300	221,800 ± 4,400	2.36 ± 0.06
	20	17.8 ± 0.6	90,600 ± 2,200	217,100 ± 2,700	2.40 ± 0.03
PLA + PEG 400	0	-	83,600 ± 1,900	214,100 ± 6,300	2.56 ± 0.02
	5	4.9 ± 0.4	76,600 ± 2,600	181,100 ± 7,500	2.36 ± 0.02
	10	10.8 ± 0.6	73,900 ± 3,400	165,900 ± 8,900	2.24 ± 0.02
	15	14.4 ± 0.2	69,100 ± 4,100	157,300 ± 5,800	2.28 ± 0.05
	20	18.3 ± 0.4	61,800 ± 2,400	128,300 ± 8,900	2.08 ± 0.07
PLA + DOA	0	-	81,200 ± 2,700	211,400 ± 4,400	2.60 ± 0.03
	5	4.7 ± 0.2	93,700 ± 2,400	209,400 ± 7,500	2.23 ± 0.02
	10	8.8 ± 0.1	94,500 ± 2,400	207,600 ± 2,100	2.20 ± 0.03
	15	12.9 ± 0.7	90,600 ± 1,200	204,100 ± 4,000	2.25 ± 0.01
	20	17.2 ± 0.5	91,900 ± 3,200	208,600 ± 8,100	2.27 ± 0.01
PLA + PID37	0	-	85,100 ± 3,600	208,400 ± 7,100	2.45 ± 0.02
	5	4.3 ± 0.4	81,400 ± 4,100	210,900 ± 3,800	2.59 ± 0.09
	10	9.8 ± 0.0	82,200 ± 2,800	207,300 ± 4,200	2.52 ± 0.04
	15	14.4 ± 0.2	80,300 ± 1,900	202,000 ± 1,900	2.52 ± 0.04
	20	18.8 ± 0.6	79,600 ± 6,500	199,900 ± 7,900	2.51 ± 0.12
PLA + squalene	0	-	85,300 ± 2,600	206,600 ± 4,900	2,42 ± 0.02
	5	3.7 ± 0.3	86,500 ± 1,900	202,400 ± 5,300	2.34 ± 0.01
	10	7.1 ± 0.2	91,300 ± 3,200	202,100 ± 2,800	2.21 ± 0.05
	15	9.9 ± 0.1	90,200 ± 2,700	205,600 ± 3,300	2.28 ± 0.03
	20	11.9 ± 0.6	87,600 ± 1,400	200,800 ± 6,300	2.29 ± 0.04

3.3.2. Miscibility study

The high D-content of the PLA grade (11 ± 1 % according to the datasheet) used in this study inhibited PLA crystallization. Generally, at D-contents higher than 6 %, PLA is amorphous under common experimental conditions.[20] Therefore, compatibility between PLA and the different plasticizers were assessed with the help of HSP and HiSP, which are prediction methods adapted to amorphous polymers.[15] Datasets are presented in **Table 3.2**. The solubility prediction by the two methods is different. The HiSP predicts highest solubility for PEG, while HSP classify PID37 to be the most soluble. This difference is caused by the contribution of the hydrogen interaction, which is only taken into account in Hansen's

method.[18] The δ_h of PEG 400 is very far from PLA (**Table 3.4**) because of the absence of hydroxyl groups able to establish H-bonding. ATBC and PID37 additives are predicted soluble with PLA according to Hansen and Hildebrand solubility parameters. PEG 400 and DOA additives have nearly the same solubility in PLA after Hansen's method. On the contrary, squalene is predicted to be faintly soluble in PLA.

Table 3.4 Physical data and computed solubility parameters of PLA and plasticizers

Substance	M_w	Molar volume	T_g	HSP			RED	HiSP	
	(g.mol^{-1})	*(cm^3.mol^{-1})*	*(°C)*	δ_d *(J$^{1/2}$.cm$^{-3/2}$)*	δ_p *(J$^{1/2}$.cm$^{-3/2}$)*	δ_h *(J$^{1/2}$.cm$^{-3/2}$)*		δ *(J$^{1/2}$.cm$^{-3/2}$)*	Difference
PLA	244,500	130,500	57	18.6[b]	9.9[b]	6.0[b]	(radius = 10.7)[b]	21.9	-
ATBC	402	364	-83.2	16.9	2.7	7.6	0.76	18.7	3.2
PEG 400	370–414	304–340	-66.2	17.9	4.2–4.0	14.2–13.7	0.94–0.91	23.2–22.9	1.3–1.0
DOA	370	393	-104[a]	16.5	0.9	6.0	0.93	17.6	4.3
PID37	342–454	300–428	-80.8	17.4–17.2	3.0–2.1	8.2–6.8	0.71–0.78	19.5–18.6	2.4–3.3
Squalene	410	477	-75.3	16.1	0	0	1.18	16.1	5.8

[a]according to Ref.[21], [b]according to Ref.[18], Hansen solubility parameters (HSP), δ_d dispersion component, δ_p polar component, δ_h hydrogen bonding component, δ Hildebrand solubility parameter (HiSP)

The prediction of solubility was completed by studying miscibility and miscibility limits of the plasticizer by monitoring the T_g decrease of a polymer compound and modeling with Fox's equation, **(3.10)**:

$$\frac{1}{T_g} = \frac{\omega_{PLA}}{T_{g_{PLA}}} + \frac{\omega_{Plast}}{T_{g_{Plast}}} \quad , \qquad \textbf{(3.10)}$$

where T_g is the glass transition temperature of the compound, T_{gPLA} and T_{gPlast}, respectively these of the neat PLA and the pure plasticizer and ω_{PLA} and ω_{Plast} the weight fraction of the neat PLA and pure plasticizer.

Results are presented in **Figure 3.2**. PID37 shows similar behavior to ATBC. Both are miscible with PLA over the whole experimental concentration range, shown by the good concordance between the experimental and predicted T_g. Regarding the PEG 400, the experimental values are slightly lower than the calculated ones, maybe due to a supplementary decrease of T_g caused by the PLA chain scission during processing, which was shown in **Table 3.3**. A

deviation of the T_g decrease from Fox's equation indicating reaching of the miscibility limit was observed after 15 wt% of PEG 400. This concentration was smaller than the miscibility limit of PEGs smaller than M_w = 34,000 g.mol^{-1} established at 20 wt%,[10a, 22] and higher than the limit at 10 wt% observed by Ref[10g]. Squalene and DOA showed a levelling off of the T_g at 48 °C and 41 °C respectively, despite the increase in plasticizer content. The miscibility limit of DOA in PLA was reached at 5 wt%, which is in accordance with Murariu et al.,[10c] and the one of squalene at 3 wt%. These observations are pursuant to the prediction of lower solubility by the Hansen and Hildebrand solubility parameters. Solubility theories are thus a valuable tool for screening biobased plasticizers.

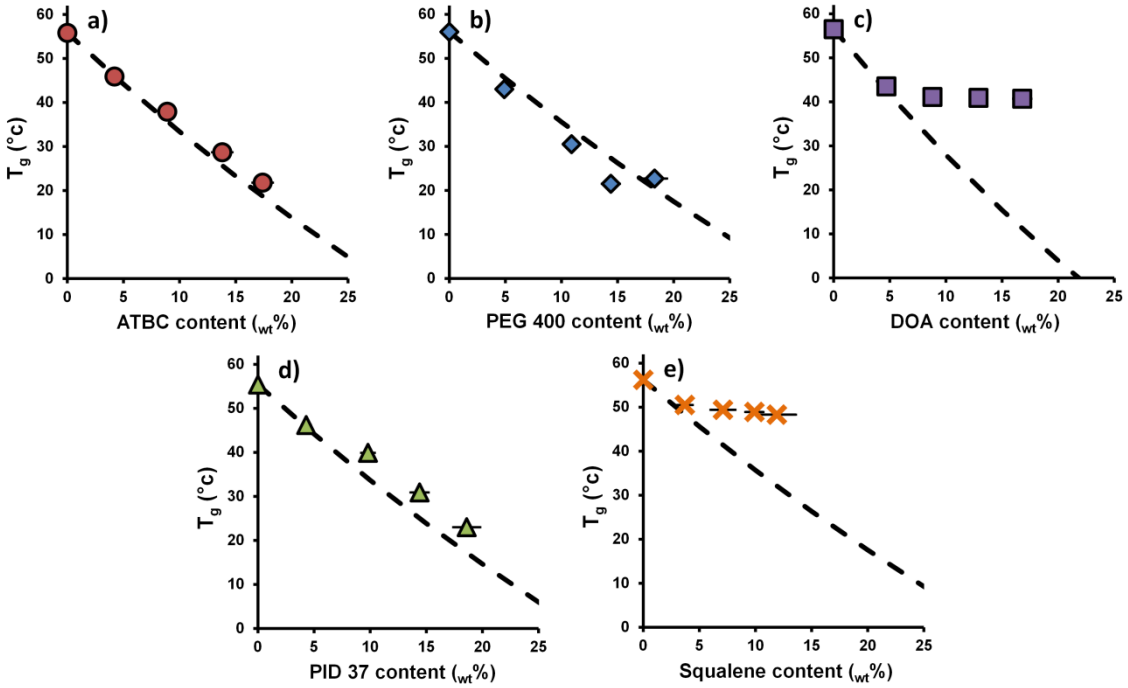

Figure 3.2 Experimental T_g values of PLA/plasticizer formulations plotted with corresponding Fox equation (○) ATBC ; (◊) PEG 400 ; (□) DOA ; (Δ) PID37 ; (X) Squalene ; (- -) Fox Equation

3.3.3. Tensile properties of plasticized PLA

Figure 3.3 shows typical results of tensile testing of the PLA samples containing the different plasticizers. The numerical data are given in **Table 3.5**.

Neat PLA shows brittle fracture at ε ≈ 5 %, behavior largely described in literature.[10c, 11b, 13b] The fracture mechanism of PLA glasses is related to crazing, linked to the low entanglement density.[23] The inclusion of the different plasticizers induces the brittle to ductile transition, where two behavior groups can be distinguished, which is coherent with the prediction of the solubility parameters.

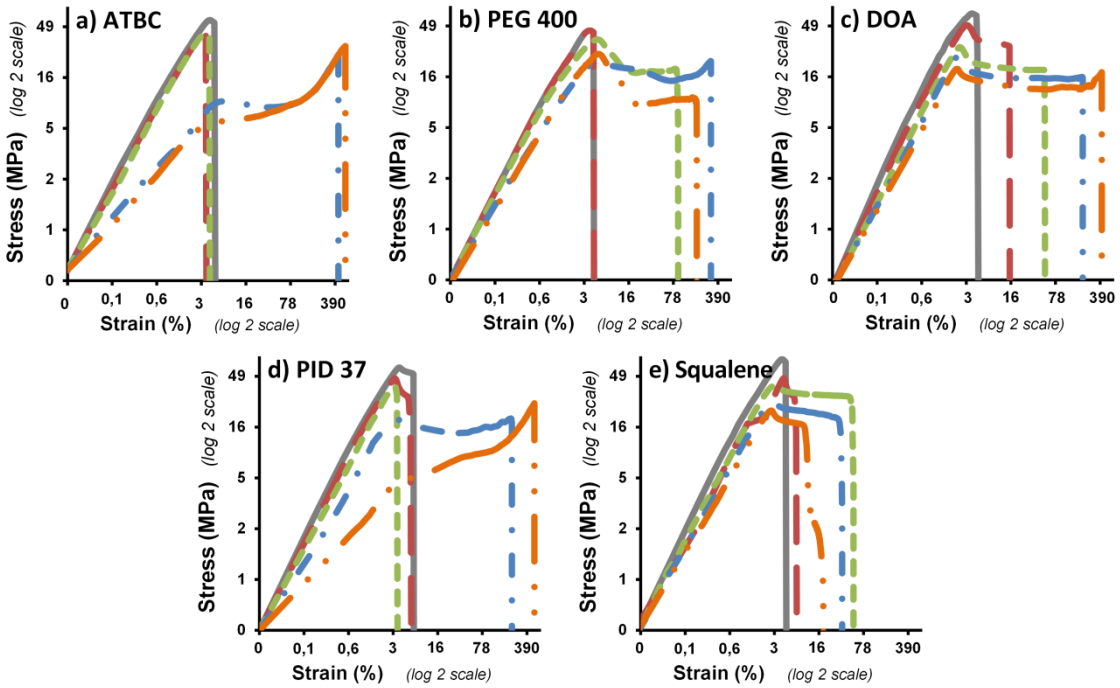

Figure 3.3 Typical stress/strain curves of PLA/plasticizer formulations
(—) PLA; (— —) PLA + 5 wt% additive; (- -) PLA + 10 wt% additive; (—•—) PLA + 15 wt% additive; (—••—) PLA + 20 wt% additive

PID37 can be classified with ATBC and PEG 400 in the first behavior group. In that case the brittle to ductile transition occurs when the plasticizer content was high enough to depress T_g to tensile testing temperature, more precisely when the onset of the glass transition region was at 23 °C. PLA/ATBC mixtures show no decrease in stress at yield up to 10 wt% of plasticizer, while beyond this value plasticizing is very efficient. The curves loose the yield peak, show plastic flow and hardening at high elongations due to necking. This sudden change between 10 and 15 wt% ATBC was already shown.[10g] ATBC brings most probably only starting from this amount enough free volume to the polymer for allowing chain rearrangement. Molecules

with branched non polar groups, such as ATBC, have faculty to shield polymer dipoles, which might lower the induced softening effect. This effect is then mainly brought be the added free volume of the branched molecue.[24] Interestingly, PID37, which has a higher dispersive component (**Table 3.4**) but in sum almost equal solubility parameters and molecular volume, showed a more gradual behavior. Gain in ε was observed at 15 wt%. The highest value of elongation at break observed was equal to ATBC plasticizing, which makes PID37 an interesting biobased and biodegradable alternative to ATBC. Probably the long aliphatic chains of PID37 help to reduce polar interactions of PLA chains and provide chain mobility at lower contents. The more gradual plasticizing behavior was also measured with PEG, which is a linear molecule. However, at high PEG contents, ε decreased again, likely due to phase separation as the miscibility limit was reached.[11a, 25] This is consistent with the miscibility prediction by the analysis of the T_g, shown in **Figure 3.2**. The PEG phase separation induces flaws in the materials from which cracks start and yield in consequence failure at lower elongation.[11a, 25]

A contrario, DOA and squalene formulations can be classified in the second behavior group. They reached high ε values, while PLA glass transition temperature remained higher than room temperature (**Table 3.5**). Stress crazing is typical of brittle materials whereas stress shearing enables high plasticity and ductile behavior.[26] Transition between these two mechanisms is related, on the one side to the molecular entanglement density. Low entanglement density promotes crazing while high one being causes shearing.[27] The plasticizers DOA and squalene did apparently not bring enough free volume to the polymer to allow chain rearrangement under stretching due to their low miscibility. The T_g of the DOA and squalene formulations are significantly higher than experimental temperature. The ductility was therefore linked to the cavitation and crazing. The crazes in the material appeared most likely from the matrix discontinuities created by the inclusion of additive

droplets. The soluble quantity of the plasticizers could have enhanced chain slippage into the craze, which is needed for rapid fibril formation.[27c, 28] The stress at yield level of the shear flow plateau decreased in function of the plasticizer quantity. The occurrence of cavitation and fibril formation could be observed by extensive stress whitening of both samples, phenomenon which was not observed in the case of miscible molecules (**Figure 3.4**).

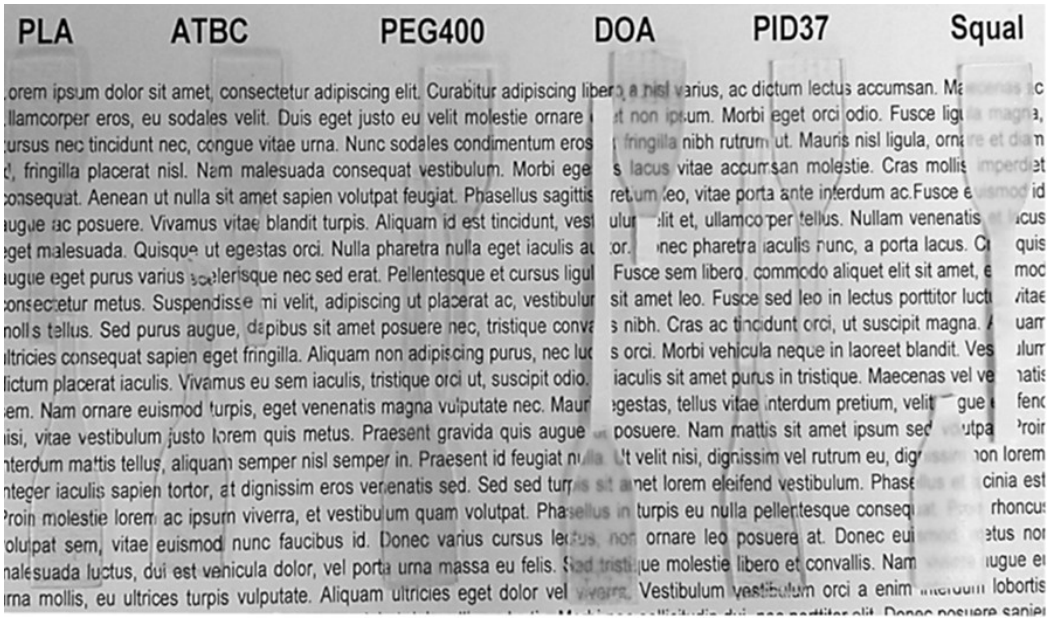

Figure 3.4 Picture of PLA + 15 wt% plasticizer samples after failure

For illustrating the cavitation mechanism, SEM pictures of the surface of stretched samples of PLA + 15 wt% plasticizer until breakage were taken (**Figure 3.5**). For highly miscible molecules, *i.e.* ATBC and PID37, no significant presence of dispersed phase was observed. Some few narrow cracks perpendicularly to the stretching direction appeared. Based on the corresponding tensile curves, strain hardening before ultimate rupture locally could have been caused by disentangled portions of polymer. For PEG 400, which is less soluble than ATBC or PID37 when averaging results of the two solubility theories, some dispersed domains which likely are not dissolved droplets of additives are seen. Although cavitation gave rise to a few micro crazes, no stress whitening was observed. For DOA and squalene samples, an

important dispersed phase was seen and cavitation phenomenon evolved into bigger cracks, especially for the least soluble squalene.

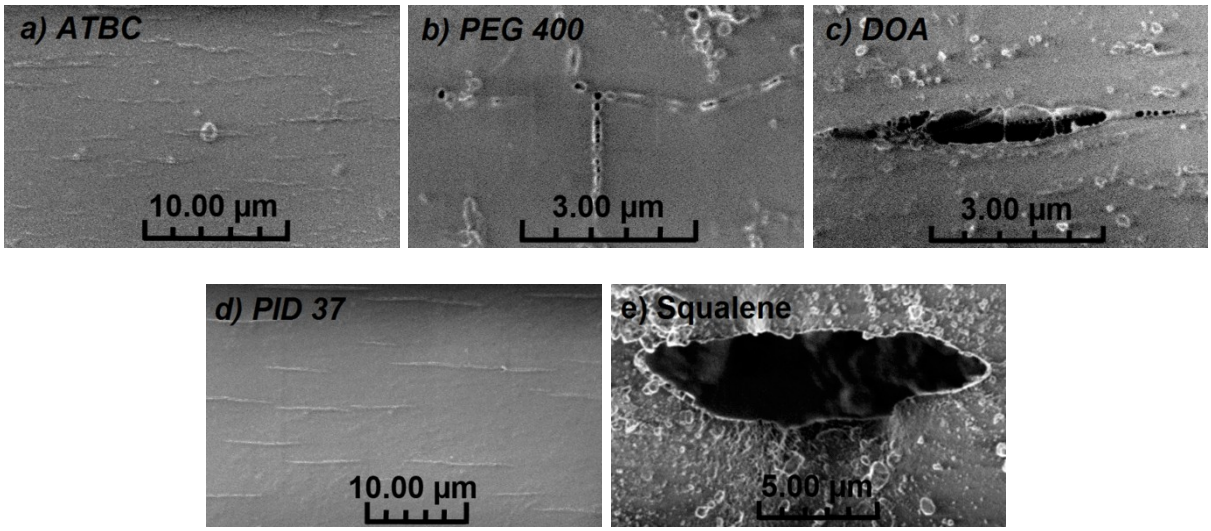

Figure 3.5 SEM micrographs taken on the longitudinal surface of PLA + 15wt% plasticizer samples near the breaking zone after failure

Table 3.5 Tensile testing results and T_g data of PLA/plasticizer formulations

Formulation	**Plasticizer content** *($_{wt}$%)*	**Elongation at break** *(%)*	**Young modulus** *(MPa)*	**Elongation at yield** *(%)*	**Stress at yield** *(MPa)*	**T_g** *(°C)*
PLA + ATBC	0	4.8 ± 0.8	1,660 ± 105	4.3 ± 0.8	65 ± 5	56.1 ± 0.2
	4.2 ± 0.3	4.3 ± 0.3	1,540 ± 90	3.9 ± 0.1	57 ± 5	45.9 ± 0.5
	8.9 ± 0.4	4.4 ± 0.4	1,405 ± 125	4.0 ± 0.4	53 ± 5	37.9 ± 0.3
	13.9 ± 0.4	455 ± 125	270 ± 120	4.3 ± 0.8	7 ± 3	28.0 ± 0.8
	17.8 ± 0.6	505 ± 70	70 ± 20	4.5 ± 0.3	4 ± 1	21.6 ± 0.8
PLA + PEG 400	0	5.0 ± 0.3	1,755 ± 170	4.4 ± 0.3	64 ± 2	56.0 ± 0.7
	4.9 ± 0.4	4.9 ± 0.7	1,580 ± 135	4.2 ± 0.6	47 ± 6	41.8± 0.7
	10.8 ± 0.6	110± 80	1,040 ± 80	4.8 ± 0.1	29 ± 4	30.5 ± 0.2
	14.4 ± 0.2	275 ± 35	740 ± 45	4.8 ± 0.2	16 ± 6	21.7 ± 0.4
	18.3 ± 0.4	135 ± 120	710 ± 65	4.6 ± 0.4	21 ± 4	22.2 ± 0.8
PLA + DOA	0	4.9 ± 0.9	1,750 ± 100	4.0 ± 0.2	69 ± 3	57.4 ± 0.4
	4.7 ± 0.2	23 ± 7	1,495 ± 60	2.9 ± 0.2	52 ± 5	42.5 ± 0.2
	8.8 ± 0.1	54 ± 13	1,385 ± 15	2.6 ± 0.1	34 ± 1	41.1 ± 0.4
	12.9 ± 0.7	175 ± 40	1,340 ± 40	2.4 ± 0.1	25 ± 3	40.9 ± 0.3
	17.2 ± 0.5	410 ± 10	1,095 ± 60	2.3 ± 0.2	21 ± 1	40.7 ± 0.8
PLA + PID37	0	4.9 ± 0.9	1,770 ± 60	3.9 ± 0.2	69 ± 3	56.2 ± 0.6
	4.3 ± 0.4	4.7 ± 0.5	1,730 ± 40	3.6 ± 0.4	65 ± 3	46.2 ± 0.3
	9.8 ± 0.0	4.5 ± 0.9	1,670 ± 45	3.2 ± 0.2	57 ± 3	40.4 ± 1.0
	14.4 ± 0.2	200 ± 25	915 ± 110	3.8 ± 0.2	20 ± 4	31.9 ± 0.5
	18.8 ± 0.6	530 ± 15	30 ± 20	3.5 ± 0.5	6 ± 4	22.4 ± 0.5
PLA + squalene	0	5.2 ± 0.4	1,685 ± 85	4.3 ± 0.3	67 ± 4	56.2 ± 0.5
	3.7 ± 0.3	40 ± 5	1,285 ± 70	3.2 ± 0.6	54 ± 5	50.9 ± 0.7
	7.1 ± 0.2	60 ± 10	1,150 ± 20	3.1 ± 0.4	42 ± 5	49.4 ± 0.3
	9.9 ± 0.1	30 ± 10	1,045 ± 55	2.8 ± 0.2	29 ± 6	48.9 ± 0.8
	11.9 ± 0.6	20 ± 10	1,000 ± 110	2.5 ± 02	26 ± 4	48.0 ± 1.2

Even with non-miscible plasticizers, the ductility of PLA could thus be improved. In a number of applications the improvement in elongation at break could be sufficient with the advantage that the Young modulus remains high, on condition that whitened appearance is not prohibitive. For example, the maximum elongation at break of PLA/DOA mixtures reached to 410 %, which was higher than the one obtained with PEG 400 (**Table 3.5**). Modifying the crack-propagation behavior and reducing the brittleness while maintaining the stiffness are typical effects of impact modifiers on PLA.[29] According to NatureWorks, effective impact modifiers are rubbery compounds with a low T_g and no or low crystallinity degree. Moreover they are immiscible and dispersed in small domains into a glassy matrix and present a good interfacial adhesion to PLA.[30] Both DOA and squalene showed these characteristics. However, below 10 wt% DOA, Murariu et al. observed a decrease in the impact strength explained by the antiplasticization effect.[10c]

The difference between DOA and squalene could be anticipated with the help of the solubility factors, which show that squalene is clearly outside of the solubility sphere of PLA, while DOA was just at the limit. The small part of miscible DOA molecules which lowers T_g could bring enough mobility to enhance chain slippage at the edges of the crazes as proposed by Piorkowska et al.[25] Moreover, the slightly better miscibility of DOA likely allows a more homogeneous distribution of the additive droplets in PLA. These differences are likely responsible for the higher elongation at break obtained with DOA rather than with squalene. Indeed, a larger number of stress concentration points ensures a better sharing of the mechanical energy during the stretching process, delaying the effective failure of the sample.[25]

3.4. Conclusion

The plasticizing behaviour of the biobased molecules PID37 and squalene in PLA was discriminated with the help of their solubility factors. They can provide a sound prediction on the possibility of a given molecule to lower T_g. If the additive miscibility in PLA is important, the ductility increases only when the PLA becomes rubbery at testing temperature. In consequence, a minimal amount of plasticizer is required and the rigidity of the material is strongly depressed. In this case, PID37 is found to be an effective biobased and biodegradable plasticizer. If the plasticizer is merely miscible as in the case of squalene, the ductility can be nevertheless enhanced while the PLA remains at the glassy state by cavitational deformation. Furthermore, efficient dispersion of non-miscible inclusions allows maintaining stiffness. Providing that no wide ductility is required, squalene could constitute an interesting eco-friendly additive.

Acknowledgements

This work was financially supported by Brodart Packaging and the ANRT and is part of the French project BIP-ADEME CREABioM supported by the ADEME. The authors gracefully acknowledge The Roquette Group for PID37 free supply and especially Dr. Vincent Berthe for his valuable help. We also very much thank Anne Grandmontagne and Cedric Plessis for their valuable technical support.

REFERENCES

1. **(a)** Anderson, K. S.; Schreck, K. M.; Hillmyer, M. A., Toughening Polylactide. Polymer Reviews 2008, 48 (1), 85-108.
(b) Lim, L. T.; Auras, R.; Rubino, M., Processing technologies for poly(lactic acid). Prog. Polym. Sci. 2008, 33 (8), 820-852.

2. Ruellan, A.; Ducruet, V.; Domenek, S., Plasticization of Poly(lactide). In *Poly(lactic acid) Science and Technology: Processing, Properties, Additives and Applications*, The Royal Society of Chemistry: 2015; pp 124-170.

3. Jacobsen, S.; Fritz, H. G., Plasticizing polylactide - The effect of different plasticizers on the mechanical properties. *Polymer Engineering & Science* 1999, *39* (7), 1303-1310.

4. Martin, O.; Averous, L., Poly(lactic acid): plasticization and properties of biodegradable multiphase systems. *Polymer* 2001, *42* (14), 6209-6219.

5. Azwar, E.; Yin, B.; Hakkarainen, M., Liquefied biomass derived plasticizer for polylactide. *Journal of Chemical Technology & Biotechnology* 2012, *88* (5), 897-903.

6. Hwang, S. W.; Shim, J. K.; Selke, S. E. M.; Soto-Valdez, H.; Matuana, L.; Rubino, M.; Auras, R., Poly(L-lactic acid) with added α-tocopherol and resveratrol: optical, physical, thermal and mechanical properties. *Polymer International* 2012, *61* (3), 418-425.

7. Arrieta, M. P.; Lopez, J.; Ferrandiz, S.; Peltzer, M. A., Characterization of PLA-limonene blends for food packaging applications. *Polymer Testing* 2013, *32* (4), 760-768.

8. **(a)** Al-Mulla, E. A. J.; Suhail, A. H.; Aowda, S. A., New biopolymer nanocomposites based on epoxidized soybean oil plasticized poly(lactic acid)/fatty nitrogen compounds modified clay: Preparation and characterization. Industrial Crops and Products 2010, 33 (1), 23-29.
(b) Xiong, Z.; Yang, Y.; Feng, J.; Zhang, X.; Zhang, C.; Tang, Z.; Zhu, J., Preparation and characterization of poly(lactic acid)/starch composites toughened with epoxidized soybean oil. Carbohydr. Polym. 2012, 92 (1), 810-816.

9. **(a)** Al-Mulla, E. A. J.; Yunus, W.; Ibrahim, N. A. B.; Ab Rahman, M. Z., Properties of epoxidized palm oil plasticized polytlactic acid. Journal of Materials Science 2010, 45 (7), 1942-1946.
(b) Silverajah, V. S. G.; Ibrahim, N. A.; Yunus, W.; Abu Hassan, H.; Woei, C. B., A Comparative Study on the Mechanical, Thermal and Morphological Characterization of Poly(lactic acid)/Epoxidized Palm Oil Blend. Int. J. Mol. Sci. 2012, 13 (5), 5878-5898.
(c) Silverajah, V. S. G.; Ibrahim, N. A.; Zainuddin, N.; Yunus, W.; Abu Hassan, H., Mechanical, Thermal and Morphological Properties of Poly(lactic acid)/Epoxidized Palm Olein Blend. Molecules 2012, 17 (10), 11729-11747.
(d) Ali, F.; Chang, Y.-W.; Kang, S. C.; Yoon, J. Y., Thermal, mechanical and rheological properties of poly (lactic acid)/epoxidized soybean oil blends. Polymer Bulletin 2009, 62 (1), 91-98.

10. **(a)** Baiardo, M.; Frisoni, G.; Scandola, M.; Rimelen, M.; Lips, D.; Ruffieux, K.; Wintermantel, E., Thermal and mechanical properties of plasticized poly(L-lactic acid). Journal of Applied Polymer Science 2003, 90 (7), 1731-1738.
(b) Ljungberg, N.; Andersson, T.; Wesslen, B., Film extrusion and film weldability of poly(lactic acid) plasticized with triacetine and tributyl citrate. Journal of Applied Polymer Science 2003, 88 (14), 3239-3247.
(c) Murariu, M.; Da Silva Ferreira, A.; Alexandre, M.; Dubois, P., Polylactide (PLA) designed with desired end-use properties: 1. PLA compositions with low molecular weight ester-like plasticizers and related performances. Polymers for Advanced Technologies 2008, 19 (6), 636-646.

(d) Lemmouchi, Y.; Murariu, M.; Dos Santos, A. M.; Amass, A. J.; Schacht, E.; Dubois, P., Plasticization of poly(lactide) with blends of tributyl citrate and low molecular weight poly(D,L-lactide)-b-poly(ethylene glycol) copolymers. European Polymer Journal 2009, 45 (10), 2839-2848.
(e) Wang, R. Y.; Wan, C. Y.; Wang, S. F.; Zhang, Y., Morphology, Mechanical Properties, and Durability of Poly(Lactic Acid) Plasticized With Di(Isononyl) Cyclohexane-1,2-Dicarboxylate. Polymer Engineering and Science 2009, 49 (12), 2414-2420.
(f) Sierra, J.; Noriega, M.; Cardona, E.; Ospina, S., Relationship between properties, citrate content and postproduction time for a plasticized polylactic acid. ANTEC 2010 [Proceedings] 2010.
(g) Courgneau, C.; Domenek, S.; Guinault, A.; Averous, L.; Ducruet, V., Analysis of the Structure-Properties Relationships of Different Multiphase Systems Based on Plasticized Poly(Lactic Acid). J. Polym. Environ. 2011, 19 (2), 362-371.
(h) Labrecque, L. V.; Kumar, R. A.; Davé, V.; Gross, R. A.; McCarthy, S. P., Citrate esters as plasticizers for poly(lactic acid). J. Appl. Polym. Sci. 1997, 66 (8), 1507-1513.

11. **(a)** Kulinski, Z.; Piorkowska, E.; Gadzinowska, K.; Stasiak, M., Plasticization of poly(L-lactide) with poly(propylene glycol). Biomacromolecules 2006, 7 (7), 2128-2135.
(b) Kulinski, Z.; Piorkowska, E., Crystallization, structure and properties of plasticized poly(l-lactide). Polymer 2005, 46 (23), 10290-10300.

12. **(a)** Hu, Y.; Rogunova, M.; Topolkaraev, V.; Hiltner, A.; Baer, E., Aging of poly(lactide)/poly(ethylene glycol) blends. Part 1. Poly(lactide) with low stereoregularity. Polymer 2003, 44, 5701-5710.
(b) Hu, Y.; Hu, Y. S.; Topolkaraev, V.; Hiltner, A.; Baer, E., Aging of poly(lactide)/poly(ethylene glycol) blends. Part 2. Poly(lactide) with high stereoregularity. Polymer 2003, 44 (19), 5711-5720; **(c)** Li, H.; Huneault, M. A., Effect of Nucleation and Plasticization on the Crystallization of Poly(Lactic Acid). Polymer 2007, 48, 6855-6866.

13. **(a)** Martino, V.; Ruseckaite, R.; Jiménez, A., Thermal and mechanical characterization of plasticized poly (L-lactide-co-D,L-lactide) films for food packaging. Journal of Thermal Analysis and Calorimetry 2006, 86 (3), 707-712.
(b) Martino, V. P.; Jimenez, A.; Ruseckaite, R. A., Processing and Characterization of Poly(lactic acid) Films Plasticized with Commercial Adipates. J. Appl. Polym. Sci. 2009, 112 (4), 2010-2018.

14. **(a)** Hamann, C. P.; Plamthottam, S. S. Polylactide hydrosol and articles made therefrom. 2011.
(b) Hamann, C. P.; Plamthottam, S. S. Polylactic acid gloves and methods of manufacturing same. 2011.

15. van Krevelen, D. W.; Nijenhuis, K., Cohesive Properties and Solubility. In *Properties of Polymers. Their Correlation with Chemical Structure; Their Numerical Estimation and Prediction from Additive Group Contributions*, 4th. ed.; Elsevier, Ed. Amsterdam, 2009; p 189.

16. Bondi, A. A., *Physical Properties of Molecular Crystals, Liquids and Glasses*. John Wiley & Sons: New York, 1968.

17. **(a)** van Krevelen, D. W., Chemical Structure and Properties of Coal. XXVIII. Coal Constitution and Solvent Extraction. *Fuel* 1965, *44* (44).
(b) van Krevelen, D. W.; Hoftyzer, P. J., Practical evaluation of the [η]–M relationship. III. Estimation of the exponent a. *Journal of Applied Polymer Science* 1967, *11* (11), 2189-2200.

18. Abbott, S. J., Chemical Compatibility of Poly (Lactic Acid) : A practical Framework using Hansen Solubility parameters. In *Poly(lactic acid): Synthesis, Structures, Properties, Processing, and Applications*, Wiley: 2010; pp 83-93.

19. Hyon, S. H.; Jamshidi, K.; Ikada, Y., Effects of residual monomer on the degradation of DL-lactide polymer. *Polymer International* 1998, *46* (3), 196-202.

20. **(a)** Auras, R.; Harte, B.; Selke, S., An Overview of Polylactides as Packaging Materials. Macromolecular Bioscience 2004, 4 (9), 835-864.
(b) Saeidlou, S.; Huneault, M. A.; Li, H.; Park, C. B., Poly(lactic acid) crystallization. Progress in Polymer Science 2012, 37 (12), 1657-1677.

21. Wypych, G., *Handbook of plasticizers*. ChemTech Publishing: Toronto-Scarborough, 2004.

22. Pillin, I.; Montrelay, N.; Grohens, Y., Thermo-mechanical characterization of plasticized PLA: Is the miscibility the only significant factor? *Polymer* 2006, *47* (13), 4676-4682.

23. Stoclet, G.; Lefebvre, J. M.; Séguéla, R.; Vanmansart, C., In-situ SAXS study of the plastic deformation behavior of polylactide upon cold-drawing. *Polymer* 2014, *55* (7), 1817-1828.

24. Moorshead, T. C., Advances in PVC Compounding and Processing. Sons, M. K., Ed. London, 1962.

25. Piorkowska, E.; Kulinski, Z.; Galeski, A.; Masirek, R., Plasticization of semicrystalline poly(l-lactide) with poly(propylene glycol). *Polymer* 2006, *47* (20), 7178-7188.

26. Ishikawa, M.; Ogawa, H.; Narisawa, I., Brittle fracture in glassy polymers. *Journal of Macromolecular Science, Part B* 1981, *19* (3), 421-443.

27. **(a)** Donald, A. M.; Kramer, E. J., Deformation zones and entanglements in glassy polymers. *Polymer* 1982, *23* (8), 1183-1188.
(b) Donald, A. M.; Kramer, E. J., Effect of molecular entanglements on craze microstructure in glassy polymers. *Journal of Polymer Science: Polymer Physics Edition* 1982, *20* (5), 899-909; **(c)** Dettenmaier, M.; Kausch, H., Intrinsic crazes in polycarbonate: Phenomenology and molecular interpretation of a new phenomenon. *In Crazing in Polymers*. Springer Berlin / Heidelberg: 1983; Vol. 52-53, pp 57-104.

28. Kramer, E.; Berger, L., Fundamental processes of craze growth and fracture. In *Crazing in Polymers Vol. 2*, Kausch, H. H., Ed. Springer Berlin Heidelberg: 1990; Vol. 91/92, pp 1-68.

29. **(a)** Wang, L.; Ma, W.; Gross, R. A.; McCarthy, S. P., Reactive compatibilization of biodegradable blends of poly(lactic acid) and poly(epsilon-caprolactone). *Polym. Degrad. Stab.* 1998, *59*, 161-168.
(b) Broz, M. E.; VanderHart, D. L.; Washburn, N. R., Structure and mechanical properties of poly(D,L-lactic acid)/poly(epsilon-caprolactone) blends. *Biomaterials* 2003, *24* (23), 4181-4190.
(c) Ma, X.; Yu, J.; Wang, N., Compatibility characterization of poly(lactic acid)/poly(propylene carbonate) blends. *J. Polym. Sci., Part B: Polym. Phys.* 2006, *44* (1), 94-101.
(d) Jiang, L.; Wolcott, M. P.; Zhang, J., Study of biodegradable polylactide/poly(butylene adipate-co-terephthalate) blends. *Biomacromolecules* 2005, *7* (1), 199-207.
(e) Shibata, M.; Inoue, Y.; Miyoshi, M., Mechanical properties, morphology, and crystallization behavior of blends of poly(L-lactide) with poly(butylene succinate-co-L-lactate) and poly(butylene succinate). *Polymer* 2006, *47* (10), 3557-3564.
(f) Odent, J.; Raquez, J. M.; Duquesne, E.; Dubois, P., Random aliphatic copolyesters as new biodegradable impact modifiers for polylactide materials. *European Polymer Journal* 2012, *48* (331-340).

30. NatureWorks Technology Focus Report: Toughened PLA. Ver.3/1/2007. (accessed 17.04.2014).

CHAPITRE 4

TABLE OF CONTENTS

ABSTRACT **144**

4.1. INTRODUCTION **145**

4.2. EXPERIMENTAL **147**

4.2.1. Materials 147
4.2.2. Film fabrication 148
4.2.3. Characterization 150
4.2.3.1. Composition of HPO, HCO, RODC, SODC, OODC and PODC *150*
4.2.3.2. Calculation of molar volume and solubility parameters in PLA *153*
4.2.3.3. Differential Scanning Calorimetry (DSC) *154*
4.2.3.4. Tensile tests *155*
4.2.3.5. Uniaxial deformation under optical microscopy *155*
4.2.3.6. Scanning Electron Microscopy (SEM) *155*
4.2.3.7. Principal Component Analysis (PCA) *156*

4.3. RESULTS AND DISCUSSION **156**

4.3.1. Effects of free fatty acids, glycerides, α-tocopherol and squalene on PLA ductility 156
4.3.2. Properties of PLA blends with vegetable oil deodorization condensates 162
4.3.3. Study of the deformation mechanisms involved in PLA/oil deodorization condensates blends 163
4.3.4. Role of the chemical composition of deodorization condensates in ductility improvement 166

4.4. CONCLUSIONS **169**

ACKNOWLEDGEMENTS **169**

REFERENCES **170**

Chapitre 4 - Industrial vegetable oil by-products increase the ductility of polylactide

La précédente étude a montré l'importance de la solubilité du plastifiant sur les propriétés thermomécaniques dévellopées. Une solubilité élevée autorise une importante augmentation du volume libre du PLA qui, à taux d'additivation suffisant, devient caoutchoutique et acquiert une ductilité considérable mais hérite d'une piètre rigidité. A l'opposé, une faible solubilité du plastifiant ne permet pas de rendre le PLA caoutchoutique mais peut parfois entrainer, si saturation, la création d'une phase dispersée capable de favoriser la cavitation, retardant ainsi la rupture finale du PLA qui a conservé sa rigidité. La littérature montre notamment le rôle de la solubilité de l'additif sur l'efficacité de ce second mécanisme : il est nécessaire que l'adhesion interfaciale de la phase dispersée avec la matrice soit élevée pour permettre le dévellopement homogène du mécanisme de cavitation/craquelage et obtenir de bonnes propriétés mécaniques.

Après avoir identifié au cours d'études préliminaires les condensats de désodorisation d'huiles végétales comme additifs permettant d'améliorer significativement la ductilité du PLA, nous avons réalisé une investigation du rôle de leurs molécules constitutives et sélectionné la source végétale la plus prometteuse. Ce chapitre présente les résultats des recherches menées sur 32 formulations, dont les propriétés thermomécaniques ont été statistiquement traitées par Analyse en Composantes Principales (ACP) en correlation avec les caractéristiques physico-chimiques des molécules présentes dans les condensats. Les mécanismes de déformation autorisés par l'ajout de ces corps gras ont également été étudiés par observations en microscopies optique et électronique. Ce chapitre contient la publication "Industrial vegetable oil by-products increase the ductility of polylactide" soumise pour publication au mois de mars 2015 à la revue scientifique internationale Express Polymer Letters.

Alexandre Ruellan[a,b,c], Alain Guinault[a,d], Cyrille Sollogoub[a,d], Guillaume Chollet[e], Aziza Ait-Mada[b], Violette Ducruet[g], Sandra Domenek[b]

[a]*CNAM, Arts et Métiers ParisTech, CNRS, UMR 8006, Laboratoire PIMM, 151, Boulevard de l'Hopital, F-75013 Paris.*
[b]*AgroParisTech, Ingénierie Procédés Aliments, 1 avenue des Olympiades, F-91300 Massy.*
[c]*Brodart Packaging, Département R&D, 1 rue du Stand, F-10700 Arcis-Sur-Aube.*
[d]*CNAM, Laboratoire P2AM, 2 rue Conté, F-75003 Paris.*
[e]*ITERG, Lipochimie Hall Industriel, 11 rue Monge, F-33600 Pessac.*
[f]*INRA, Ingénierie Procédés Aliments, 1 avenue des Olympiades, F-91300 Massy.*

Abstract

The use of industrial by-products of the vegetable oil industry as ductility agents of polylactide (PLA) was investigated. Vegetable oil deodorization condensates were melt-blended by twin-screw extrusion up to a maximum inclusion quantity of 20 wt% without preliminary purification. Sample films were obtained by single screw cast extrusion. Compounded PLA films featured largely improved ductility in tensile testing with an elongation at break up to 180 %. The glass transition temperature remained higher than room temperature. The native mixture of molecules contained in the deodorization condensates had superior performance compared to a synthetic mixture of main compounds. The investigation of the correlation between composition of the additives and the ductility of the PLA blends by Principal Component Analysis showed a synergistic effect between fatty acids having a melting point below and beyond the room temperature. Furthermore, a compatibilizing effect of molecules present in the native mixture was evidenced. Oil deodorization condensates, which are a low-priced by-product of the vegetable oil industry, are therefore a very promising biobased and biodegradable additive for improving PLA ductility.

Keywords: Poly(lactic acid), PLA, ductility, vegetable oil mill industry, deodorization condensate, crazing, tensile properties, melt blending, extrusion.

4.1. Introduction

Biodegradable and/or biobased polymers are widely studied to replace petroleum-based materials in the aim of contributing to higher sustainability of plastics. However, in many cases these new products still do not meet economical or functional requirements to be competitive in commodity applications. Polylactide (PLA) is one of the polymers which can potentially enter those high volume markets, mostly in the food packaging[1] or textile[2] sector. Polylactide is a compostable polymer[3] issued from polymerization of lactic acid produced by fermentation of starch, potatoes or beets.[3c, 4] Although this biobased thermoplastic has been known for decades,[5] production cost reduction thanks to breakthroughs in the polymerization technology,[6] made it economically competitive with petroleum-based materials. PLA offers many interests[1a, 7] such as a glass transition higher than room temperature, ease of processing, high transparency, printability, glossy aspect… However, its mechanical properties still remain an obstacle for many applications. In fact, PLA features high tensile strength and modulus but also high brittleness.[8]

In order to enhance the PLA ductility, melt-blending with rubbery materials as poly(ether)urethane,[9] polyamide elastomer,[10] acrylonitrile-butadiene-styrene copolymer, or various impact modifiers[11] is effective. Plasticizers such as citrate esters,[12] polyethylene glycols[12a, 12g, 13] or manifold other molecules[12c, 13f, 14] can be used. Unfortunately, those additives are generally not biodegradable nor biobased, degrading one important environmental advantage of employing PLA. Therefore biobased and biodegradable additives have been investigated for toughening PLA. Chemically modified vegetable oils have received important research interest, because ester or epoxy groups can be degraded by micro-organisms,[15] maintaining the biodegradability of blends with PLA. Polymerized soybean oil derivatives prepared by crosslinking double bonds of alkyl chains were able to increase ductility after melt-blending with PLA and using a compatibilizer.[16] Improvements were also

obtained with conjugated soybean oil which was reactively compatibilized with PLA by unsaturated triglycerides.[17] Epoxidized soybean oil[18] and epoxidized palm oil[19] also showed some positive effects on PLA toughness. Another approach consists in using rigid particles, which usually increased stiffness but is ineffective, or even detrimental for the ductility. Nonetheless, NatureWorks[20] reported the use of EMforce®, a bio additive mineral, able to change the polymer failure mode from brittle to ductile state. In fact, the efficient crack initiation in glassy PLA, which was provided by the well-dispersed additive with good interfacial adhesion to the matrix, enhanced the PLA elongation at break.

Expertise from plasticizing polyvinylchloride teaches that mixtures of different plasticizers are efficient for increasing toughness, because they make use of the different mechanisms available for ductility improvement. For example, a mixture of tributyl citrate (TBC) and a block copolymer PLA-g-polyethyleneglycol yielded a material with high elongation at break and satisfying stress at yield.[12d] Al-Mulla et al. successfully used modified nanoclays in combination with epoxidized soybean oil[18d] to increase stiffness and ductility. The combination of PLA with rubber and compatibilizers has also been investigated by several authors, showing important gains in ductility, with an elongation at break of up to 160 % for high rubber concentrations[21] or bicontinous phases,[22] and up to 200 % when using compatibilizers.[23] However, these solutions often require the inclusion of several additives, chemically modified components, often costly, which increases the price of the final formulation and is inappropriate for a large volume production. Finding a low cost biobased and biodegradable toughening agent would therefore help PLA to conquer new markets.

Vegetable oils contain a number of potentially interesting molecules for PLA toughening and the refinery of vegetable oils gives rise to several by-products. Among those, oil deodorization condensates represent a high-volume by-product, which is chemically close to the vegetable oil. They are obtained by distillation in the aim of purifying the raw oil from

odorous compounds, which are negative for the sensorial properties of vegetable oils. Deodorization condensates contain free fatty acids, glycerides and unsaponifiable molecules. The objective of this study was to use vegetable oils and the by-product deodorization condensate without separation of the contained chemical compounds for toughening PLA. In the aim of understanding the effects of the different molecular classes, which compose oils and deodorization condensates, on the mechanical properties of the polymer, the properties of the major molecules and several vegetable oils were screened.

4.2. Experimental

4.2.1. Materials

PLA 4060D was supplied by NatureWorks (U.S.A.) and consists of 89 ± 1% L-lactic acid and 11±1% D-lactic acid units, making it unable to crystallize under common conditions.[1a, 24] The glass transition temperature (T_g) obtained from differential scanning calorimetry (DSC) measurements was 56 °C. Average molecular weights obtained from size exclusion chromatography (SEC) measurements were M_w = 236,800 g.mol^{-1}, M_n = 103,700 g.mol^{-1} and dispersity M_w/M_n = 2.28.

Hydrogenated palm oil (HPO), Hydrogenated Copra Oil (HCO), Rapeseed Oil Deodorization Condensate (RODC), Soybean Oil Deodorization Condensate (SODC), Olive Oil Deodorization Condensate (OODC) and Palm Oil Deodorization Condensate (PODC) were supplied by ITERG (Bordeaux, France).

Palmitic acid (purity > 98 %) *i.e.* hexadecanoic acid (C16:0), oleic acid (purity > 96 %) *i.e.* 9-octadecenoic acid (C18:1), squalene (purity > 98 %) *i.e.* (6E,10E,14E,18E)-2,6,10,15,19,23-Hexamethyltetracosa-2,6,10,14,18,22-hexaene, and alpha-tocopherol (purity > 96 %) *i.e.* (2R)-2,5,7,8-Tetramethyl-2-[(4R,8R)-(4,8,12-trimethyltridecyl)]-6-chromanol, were supplied by Sigma-Aldrich (France).

4.2.2. Film fabrication

Prior to melt-blending, PLA pellets were dried at 60 °C for 24 h under dried air using a SOMOS 60L. Relative humidity of dried pellets was controlled to be lower than 350 ppm using an Aboni FMX Hydrotracer. Melt-mixing of PLA with or without additives was carried out using a twin screw extruder (Thermo Haake Ptw 16-40D), having a screw diameter of 16 mm and a length to diameter ratio (L/D) 40:1. A temperature of 180 °C was used to process by twin-screw extrusion the PLA pellets as reference material, while the temperature profile of the 7 heating zones decreased from 180 to about 150/130 °C along the extrusion flow, depending on the nature and the amount of additive. The exact temperature profile for each formulation is given in the supporting information **S4.1**. To properly control the feed rate of additives, which are solid at room temperature, a home-made apparatus consisting in a heated syringe was used. Obtained pellets were stored into hermetic sealed metalized bags to avoid PLA rehydration.

Films of about 0.8 mm thickness containing palmitic acid, oleic acid, hydrogenated palm oil, (HPO), hydrogenated copra oil (HCO), squalene, α-tocopherol and some combinations of these products were obtained using a single screw extruder (Scamex Rheoscam), mounted with a screw of 20 mm diameter and a length to diameter ratio (L/D) 12:1 and a flat die of 40 mm width and 1 mm thickness. Films were stretched and cooled with chill rolls. Due to the short length of the screw, an increasing temperature profile from 180 to 195 °C over the 3 heating zones was used for PLA, while it was decreasing from 180 to about 170 °C for blends. The specific temperatures depending on the nature and the amount of additive are given in the supporting information **S4.2**.

Supporting information S4.1 Processing conditions of melt-mixing twin screw extrusion

Formulation	Temperature profile *(°C)*	Screw rotation speed (rpm)	PLA 4060D feeding input *($kg.h^{-1}$)*	Additive feeding input *($kg.h^{-1}$)*
Neat PLA	175/180/190/190/190/190/180	300	0.600	-
PLA + 10 wt% C16:0	175/180/180/170/170/170/170	300	0.550	0.062
PLA + 10 wt% C18:1	175/180/180/170/170/170/170	300	0.550	0.061
PLA + 10 wt% [50 wt% C16:0 + 50 wt% C18:1]	175/180/180/170/170/170/170	300	0.550	0.062
PLA + 10 wt% [95 wt% (50 wt% C16:0 + 50 wt% C18:1) + 5 wt% HPO]	175/180/180/170/170/170/170	300	0.550	0.059
PLA + 5 wt% HCO	175/180/180/180/180/170/170	300	0.520	0.027
PLA + 10 wt% HCO	175/180/180/180/180/170/170	300	0.520	0.059
PLA + 15 wt% HCO	175/180/180/180/170/170/160	300	0.520	0.093
PLA + 5 wt% HPO	175/180/180/180/180/170/170	300	0.520	0.029
PLA + 10 wt% HPO	175/180/180/180/180/170/170	300	0.520	0.058
PLA + 15 wt% HPO	175/180/180/180/180/170/170	300	0.520	0.091
PLA + 5 wt% α-tocopherol	175/180/180/180/180/180/180	300	0.500	0.026
PLA + 10 wt% α-tocopherol	175/180/180/180/180/180/170	300	0.500	0.056
PLA + 15 wt% α-tocopherol	175/180/180/180/180/170/170	300	0.500	0.088
PLA + 5 wt% squalene	175/180/180/180/180/180/180	300	0.560	0.030
PLA + 10 wt% squalene	175/180/180/180/180/170/170	300	0.560	0.062
PLA + 15 wt% squalene	175/180/180/180/180/170/170	300	0.560	0.100
PLA + 5 wt% RODC	175/180/180/180/180/175/170	300	0.620	0.034
PLA + 10 wt% RODC	175/180/180/180/180/170/160	300	0.620	0.069
PLA + 15 wt% RODC	175/180/180/180/180/170/160	300	0.620	0.108
PLA + 20 wt% RODC	175/180/180/180/170/160/150	300	0.620	0.154
PLA + 5 wt% SODC	175/180/180/180/180/175/170	300	0.590	0.031
PLA + 10 wt% SODC	175/180/180/180/180/170/160	300	0.610	0.068
PLA + 15 wt% SODC	175/180/180/180/180/170/160	300	0.610	0.107
PLA + 20 wt% SODC	175/180/180/180/170/160/150	300	0.610	0.149
PLA + 5 wt% OODC	175/180/180/170/170/170/170	300	0.540	0.029
PLA + 10 wt% OODC	175/180/180/170/170/170/170	300	0.620	0.070
PLA + 15 wt% OODC	175/180/180/170/170/160/160	300	0.620	0.109
PLA + 20 wt% OODC	175/180/180/170/160/150/150	300	0.620	0.152
PLA + 5 wt% PODC	175/180/180/180/180/175/170	300	0.600	0.033
PLA + 10 wt% PODC	175/180/180/180/170/160/155	300	0.620	0.068
PLA + 15 wt% PODC	175/180/180/180/170/160/150	300	0.620	0.110
PLA + 20 wt% PODC	175/180/180/170/160/150/135	300	0.620	0.152

Supporting information S4.2 Processing conditions of cast films extrusion

Formulation	Temperature profile *(°C)*	Die temperature *(°C)*	Screw rotation speed (rpm)
Neat PLA	180/190/195	185	65
PLA + 10 wt% C16:0	180/180/175	170	65
PLA + 10 wt% C18:1	180/180/175	170	65
PLA + 10 wt% [50 wt% C16:0 + 50 wt% C18:1]	180/180/175	170	65
PLA + 10 wt% [95 wt% (50 wt% C16:0 + 50 wt% C18:1) + 5 wt% HPO]	180/180/175	170	65
PLA + 5 wt% HCO	180/180/180	180	80
PLA + 10 wt% HCO	180/170/170	170	80
PLA + 15 wt% HCO	180/170/170	170	90
PLA + 5 wt% HPO	180/180/180	170	70
PLA + 10 wt% HPO	180/170/170	170	80
PLA + 15 wt% HPO	180/170/170	170	80
PLA + 5 wt% α-tocopherol	180/180/180	180	80
PLA + 10 wt% α-tocopherol	180/180/180	180	80
PLA + 15 wt% α-tocopherol	180/175/170	170	80
PLA + 5 wt% squalene	180/180/180	180	70
PLA + 10 wt% squalene	180/180/175	170	90
PLA + 15 wt% squalene	180/180/170	170	90

In the case of the deodorization condensates of the vegetable oils (RODC, SODC, OODC, PODC), the available quantity was insufficient for carrying out a single screw extrusion in the aim to obtain films. In that case PLA sheets of 1 mm thickness were thermo-moulded by compression at 220 bar (Laboratory Press Gibitre Instruments 20 tons). For this, pellets were pre-melted at 180 °C without pressure during 180 seconds then heating plates were closed with progressive increase in pressure during 120 seconds to eliminate air bubbles.

4.2.3. Characterization

4.2.3.1. Composition of HPO, HCO, RODC, SODC, OODC and PODC

Glyceride composition of fats was determined according to the IUPAC 6.002 and EN 14105 standards using a Shimadzu GC-2010 Plus gas chromatograph equipped with a Zebron ZB 5 HT Inferno (15 m, 0.25 mm, 0.1 μm) column and a flame ionization detector set at 380 °C. The vector gas was H_2 at a flow rate of 1.17 $mL.min^{-1}$. Both the injector and the oven temperature were set at 60 °C for 3 min, raised to 370 °C at 10 $°C.min^{-1}$ and held at 370 °C for 12 min. Direct on-column injection was performed.

Fatty acid composition was determined according to the ISO 12966-2 standard using a Shimadzu GC-2010 Plus gas chromatograph equipped with a BPX70 (50 m, 0.22 mm, 0.25 μm) column, and a flame ionization detector set at 250 °C. The vector gas was H_2 at a flow rate of 0.32 $mL.min^{-1}$.The oven temperature was set at 60 °C for 2 min, raised to 170 °C at 20 $°C.min^{-1}$, held at 170 °C for 25 min, raised to 230 °C at 4 $°C.min^{-1}$ and held at 230 °C for 10 min. The injector temperature was set at 250 °C and a split ratio of 200 was used.

Acid value was determined according to the ISO 660 standard using a mixture of ethanol 95 % and diethylic ether as solvent, potassium hydroxide 0.5 $mol.L^{-1}$ in ethanol 95 % as titrant and alkali blue 6B as indicator.

Saponification value was determined according to the ISO 3657 standard. Samples were saponified with potassium hydroxide 0.5 mol.L^{-1} in ethanol 95 % boiled under reflux during 2 h. Hydrochloric acid 0.5 mol.L^{-1} was used as titrant and alkali blue 6B as indicator.

Water content was measured using a Mettler Toledo HB43 S Halogen Moisture Analyzer set at 103 °C.

Melting point of free fatty acids was determined from literature.[25] Estimation of mono, di and triglycerides average chemical structure of oil deodorization condensates was based on the averages unsaturation number and the alkyl chains length of the corresponding free fatty acids composition profile (**Table 4.1**). Average glycerides melting point was estimated calculating a weighted average of the specific melting points of the contained molecules taken from references.[25-26] Physical properties of molecules are given in **Table 4.2**.

Table 4.1 Composition of hydrogenated vegetable oils and vegetable oil deodorization condensates

Type			HPO	HCO	RODC	SODC	OODC	PODC
Glyceride composition *(%)*	Free fatty acids		0.0	39.0	43.1	39.2	95.4	0.0
	Monoglycerides		0.2	11.2	2.9	2.0	1.7	0.0
	Diglycerides		10.6	2.7	9.0	8.4	2.2	0.0
	Triglycerides		88.9	12.2	16.8	33.5	0.7	100.0
	Sterols (α-tocopherol)		0.0	25.7	9.8	1.6	0.0	0.0
	Hydrocarbons (Squalene)		0.0	0.0	13.8	13.0	0.0	0.0
	Unidentified		0.3	9.2	4.6	2.3	0.0	0.0
Acid value *(mg KOH.g^{-1})*			0.1	0.1	65.3	68.4	47.7	201.0
Saponification value *(mg KOH.g^{-1})*			198.6	255.2	125.1	157.9	162.2	205.7
Water content *(%)*			0.11	0.10	0.55	0.34	0.37	0.16
Fatty acid composition *(%)*	Caproic acid	C6:0	0.0	0.0	0.0	0.0	0.0	0.5
	Caprylic acid	C8:0	0.0	0.0	0.0	0.0	0.0	6.8
	Capric acid	C10:0	0.0	0.0	0.1	0.0	0.0	5.7
	Lauric acid	C12:0	0.0	0.8	0.0	0.4	0.5	47.5
	Myristic acid	C14:0	0.0	0.4	0.0	1.3	1.2	18.1
	Palmitic acid	C16:0	7.4	12.3	11.3	49.8	43.6	9.4
	Palmitoleic acid	C16:1	0.0	0.0	0.0	0.2	0.0	0.0
	Stearic acid	C18:0	3.4	4.1	2.5	4.1	53.8	10.8
	Oleic acid	C18:1	27.3	21.7	69.5	35.2	0.0	1.0
	Linoleic acid	C18:2	42.4	49.7	10.9	7.8	0.0	0.0
	Linolenic acid	C18:3	1.5	6.4	0.6	0.3	0.0	0.0
	Arachidic acid	C20:0	0.5	0.3	0.4	0.3	0.5	0.1
	Eicosenoic acid	C20:1	0.3	0.2	0.4	0.1	0.0	0.0
	Behenic acid	C22:0	1.0	0.5	0.0	0.0	0.1	0.0
	Lignoceric acid	C24:0	0.5	0.2	0.1	0.0	0.1	0.0
	Unidentified		0.2	15.7	3.4	4.2	0.5	0.1
Average alkyl chain carbon quantity			17.1	13.0	17.9	17.7	17.8	16.9
Average alkyl chain unsaturation quantity			0.0	0.0	1.4	1.5	1.0	0.5

Table 4.2 Physical properties and solubility parameters of fatty acids, mono-, di-, and tri-glycerides contained in the hydrogenated vegetable oils and oil deodorization condensates

			Molar weight	**Molar volume**	**Melting point**	**Hansen Solubility Parameters (HSP)**				
			(g.mol-1)	*($cm^3.mol^{-1}$)*	*(°C)*	**δ_d** ($J^{1/2}.cm^{-3/2}$)	**δ_p** ($J^{1/2}.cm^{-3/2}$)	**δ_h** ($J^{1/2}.cm^{-3/2}$)	**Distance** *with PLA*	**RED** *with PLA*
PLA 4060D			242.800	-	-	18.6	9.9	6.0	(radius: 10.7)	-
Free fatty acids	Caproic acid	C6:0	116	126	-3[a]	16.06	3.32	8.89	8.80	0.82
	Caprylic acid	C8:0	144	159	16[a]	16.20	2.65	7.94	8.91	0.83
	Capric acid	C10:0	172	191	31[a]	16.30	2.20	7.24	9.05	0.85
	Lauric acid	C12:0	200	223	44[a]	16.37	1.88	6.70	9.20	0.86
	Myristic acid	C14:0	228	255	55[a]	16.42	1.65	6.26	9.34	0.87
	Palmitic acid	C16:0	256	287	63[a]	16.46	1.46	5.90	9.46	0.88
	Palmitoleic acid	C16:1	254	282	1[a]	16.27	1.49	5.95	9.62	0.90
	Stearic acid	C18:0	285	320	70[a]	16.49	1.31	5.59	9.58	0.89
	Oleic acid	C18:1	283	314	13[a]	16.32	1.34	5.64	9.71	0.91
	Linoleic acid	C18:2	280	309	-9[a]	16.14	1.36	5.69	9.86	0.92
	Linolenic acid	C18:3	278	304	-14[a]	15.95	1.38	5.74	10.03	0.94
	Arachidic acid	C20:0	313	352	75[a]	16.52	1.19	5.33	9.68	0.90
	Eicosenoic acid	C20:1	311	347	23[a]	16.36	1.21	5.37	9.80	0.92
	Behenic acid	C22:0	341	384	80[a]	16.54	1.09	5.10	9.77	0.91
	Lignoceric acid	C24:0	369	416	84[a]	16.55	1.01	4.90	9.85	0.92
Monoglycerides	HPO	$_2$(HO)-Gly-(C17.1:0)	346	346	68 – 76[b]	17.14	2.49	11.66	9.77	0.91
	RODC	$_2$(HO)-Gly-(C17.9:1.4)	354	351	10 – 22[b]	16.92	2.45	11.56	9.89	0.92
	SODC	$_2$(HO)-Gly-(C17.5:1.5)	351	348	8 – 18[b]	16.56	2.47	11.63	10.17	0.95
	OODC	$_2$(HO)-Gly-(C17.8:1.0)	354	352	25 – 32[b]	16.98	2.44	11.56	9.84	0.92
	PODC	$_2$(HO)-Gly-(C16.9:0.5)	342	340	45 – 55[a, c]	17.07	2.53	10.00	8.93	0.83
Diglyceriedes	HPO	HO-Gly-$(C17.1:0)_2$	600	630	65 – 72[b]	16.82	1.36	7.34	9.35	0.87
	RODC	(HO)-Gly-$(C17.9:1.4)_2$	617	642	2 – 12[b]	16.59	1.33	6.49	9.48	0.89
	SODC	(HO)-Gly-$(C17.7:1.5)_2$	611	634	-4 – 8[b]	16.57	1.35	7.32	9.56	0.89
	OODC	(HO)-Gly-$(C17.8:1.0)_2$	615	643	10 – 20[b]	16.66	1.33	7.27	9.50	0.89
	PODC	(HO)-Gly-$(C16.9:0.5)_2$	592	619	42 – 48[b]	16.74	1.38	7.41	9.41	0.88
Triglycerides	HCO	Gly-$(C13:0)_3$	681	717	8 – 42	16.68	1.18	5.41	9.54	0.89
	HPO	Gly-$(C17.1:0)_3$	854	915	62 – 66[c]	16.70	0.93	4.79	9.82	0.92
	RODC	Gly-$(C17.9:1.4)_3$	879	932	-30 – -26[c]	16.46	0.91	4.75	10.03	0.94
	SODC	Gly-$(C17.7:1.5)_3$	870	921	-32 – -28[c]	16.44	0.92	4.78	10.04	0.94
	OODC	Gly-$(C17.8:1.0)_3$	877	933	-14 – -10[c]	16.53	0.91	4.74	9.98	0.93
	PODC	Gly-$(C16.9:0.5)_3$	842	898	15 – 25[c]	16.61	0.95	4.84	9.87	0.92
Others	α-tocopherol	-	431	436	2[a]	17.63	1.47	7.27	8.74	0.82
	Squalene		411	477	-7[a]	16.10	0.00	0.00	12.61	1.18

[a] from Ref[25], [b] from Ref[26a], [c] from Ref[26b]

4.2.3.2. Calculation of molar volume and solubility parameters in PLA

Molar volumes and molar attraction constants of polylactide and additives were determined according to the van Krevelen and Hoftyzer atomic group contribution method.[27] Average molar volumes and average molar attraction constants of mono, di and triglycerides of oil deodorization condensates were estimated based on average chemical structures previously determined.

Hansen Solubility parameters were calculated using equations **(4.1)**, **(4.2)** and **(4.3)**.[28] Used molar constant values[27] are presented in the supporting information **S4.3**.

$$\delta_d = \frac{\sum F_{dt}}{\sum V_i} \quad \textbf{(4.1)}$$

$$\delta_p = \frac{\sqrt{\sum F_{Pi}^2}}{\sum V_i} \quad \textbf{(4.2)}$$

$$\delta_h = \sqrt{\frac{\sum E_{hi}}{\sum V_i}} \quad \textbf{(4.3)}$$

where δ_d is the dispersion component of the solubility parameter in $J^{1/2}.cm^{-3/2}$, δ_p the polar component of the solubility parameter in $J^{1/2}.cm^{-3/2}$, δ_h the hydrogen bonding component of the solubility parameter in $J^{1/2}.cm^{-3/2}$, F_d the dispersion contribution of the molar attraction constant in $(J^{1/2}.cm^{-3/2}).mol^{-1}$, F_p the polar contribution of the molar attraction constant in $(J^{1/2}.cm^{-3/2}).mol^{-1}$, E_h the hydrogen bonding energy contribution of the molar attraction constant in $J.mol^{-1}$and V the molar volume contribution of the chemical group involved in $cm^3.mol^{-1}$.

Supporting information S4.3 Used group contribution molar constants

Group	F_d $((J^{1/2}.cm^{-3/2}).mol^{-1})$	F_p^2 $((J.cm^{-3}).mol^{-1})$	E_h $(J\ mol^{-1})$	Molar volume $(cm^3\ mol^{-1})$
$-CH_3$	420	0	0	33.5
$-CH_2-$	270	0	0	16.1
=CH-	200	0	0	13.5
>CH-	80	0	0	-1.0
>C<	-70	0	0	-1
=C<	70	0	0	-5.5
-COO-	390	240,100	7,000	18
-COOH	530	176,400	10,000	28.5
-OH	210	250,000	20,000	10
Ring	190	0	0	16

The solubility of the molecules in PLA (**Table 4.2**) was assessed using the HSP Relative Energy Difference (RED) from equations **(4.4)** and **(4.5)**:

$$distance = \sqrt{4(\delta d_{molec} - \delta d_{PLA})^2 + (\delta p_{molec} - \delta p_{PLA})^2 + (\delta h_{molec} - \delta h_{PLA})^2} \quad \textbf{(4.4)}$$

$$RED = \frac{Distance}{Radius} \quad \textbf{(4.5)}$$

where δ_d, δ_p, and δ_h are the components of the solubility parameter of the molecules and the PLA obtained from equations **(4.3)**, **(4.4)** and **(4.5)**. Where the radius value is the maximal distance obtained from Ref[29] beyond which the molecules are not miscible anymore with the polymer. Therefore, the closer the RED value from zero, the better the compatibility. A RED value upper than 1 means a theoretical non-miscibility of the additivie within the PLA.

4.2.3.3. Differential Scanning Calorimetry (DSC)

Differential Scanning Calorimetry (DSC) analyses were performed using a Mettler Toledo DSC1 STARe System under nitrogen atmosphere (50 mL.min^{-1}) in 40 µL standard Aluminum pans (Mettler). Calibration of the device was done using Indium and Zinc standards. Calorimetric scans of additives were performed from -80 to 220 °C at a heating rate of 2 °C.min^{-1}. Experiments were carried out in duplicate. Calorimetric scans of blended PLA samples were done at a heating/cooling rate of 10 °C.min^{-1}. The first heating scan in which thermal history is suppressed was performed from 25 to 75 °C with an isotherm at 75 °C during 2 min. Then, the cooling scan was from 75 to -20 °C and the second heating scan from

-20 to 100 °C. The glass transition temperature (T_g) was taken at the midpoint of the second heating scan. Experiments were done in triplicate.

4.2.3.4. Tensile tests

Tensile properties were investigated at 23 °C, relative humidity (RH) 50 ± 10 % and cross-head speed of 25 $mm.min^{-1}$, using an universal tensile machine (Instron model 4301) equipped with a load cell 1,000 ± 1 N and without extensometer. The dog bone shaped samples (ISO 527-2, type 5A) were directly cut from the materials. Prior to tensile testing, samples were conditioned at 23 °C and 50 ± 10 % RH for at least 72 h. Each mechanical characteristic value is an average of 8 measurements.

4.2.3.5. Uniaxial deformation under optical microscopy

Uniaxial deformation under an optical microscope was done in cutting rectangular samples of 20 mm length, 4 mm width, and 0.8 mm thickness from blank PLA, PLA + 10 wt% C16:0, PLA + 10 wt% C18:1 and PLA + 10 wt% PODC films. They were stretched at 5 $mm.min^{-1}$ using a homemade tensile machine placed under an Olympus Japan optical microscope mounted with WHK 10x/20 L ocular lens and MD Plan 10 0.25 objective lens. Observations were performed in optical transmission light mode using a Sony CCD-IRIS Model DXC-107P camera.

4.2.3.6. Scanning Electron Microscopy (SEM)

The morphology of the dispersed phase of PLA + 10 wt% C16:0, PLA + 10 wt% C18:1 and PLA + 10 wt% PODC materials before and after being stretched was observed with Scanning Electron Microscopy (SEM) (Hitachi 4800 II). Observations were directly conducted on the longitudinal surface of the dog bone shaped samples without any previous preparation.

4.2.3.7. Principal Component Analysis (PCA)

PCA was carried out considering contents of each free fatty acid, mono, di and triglyceride types, hydrocarbons, sterols and water, the additive acid and saponification values and the measured elongation at break, Young modulus and T_g values of the formulations tested. PCA was done with XLstat software.

4.3. Results and discussion

4.3.1. Effects of free fatty acids, glycerides, α-tocopherol and squalene on PLA ductility

To investigate components present in vegetable oils, which could feature toughening ability for PLA oils effects of ubiquitous free fatty acids, glycerides and the unsaponifiable components as α-tocopherol and squalene were tested. In order to denote the most efficient formulation, the solubility of a molecule in the polymer matrix is one determinant for its plasticizing power.[12j] Therefore the Hansen Solubility Parameters (HSP) of each compound were calculated. HSP (**Table 4.2**) show low solubility of the different compounds in the PLA matrix. All the obtained values are close to one, which marks the solubility limit. The highest solubility (although still modest) was displayed by small fatty acids and α-tocopherol. The mechanical and thermal properties of the corresponding compounds are given in **Table 4.3**. The supporting information presents the raw data of typical stress/strain curves of blends (**S4.4**) and the DSC thermograms of neat additives (**S4.5**) and blends (**S4.6**) for further information.

Not surprisingly, the impact of the tested fatty acids (C16:0, C18:1), vegetable oils (HPO and HCO) and unsaponifiable compounds on T_g was negligible due to their low solubility in PLA.

Most interestingly, despite the low solubility of the compounds, PLA ductility was increased in some cases. In particular, HCO, which contains mainly triglycerides with short chain length

improved the PLA ductility and lowered the apparent Young modulus, stress and elongation at yield. HPO, which mostly contains triglycerides and some diglycerides, but with higher chain length did not bring significant ductility enhancement nor T_g decrease. HSP of di-and tri-glycerides from HPO and triglycerides from HCO are close. The average molar volume and molecular weight of triglycerides from HCO are smaller than the ones from HPO (**Table 4.2**). Testing of single fatty acids with longer chain length (C16:0, C18:1) showed that they were not able to increase PLA ductility. This is coherent with existing literature.[30] Blended PLA with fatty acid esters did not show any significant ductility improvement. To obtain positive effects on the PLA ductility, vegetable oils had to be chemically modified[16, 18a-c, 19, 31] to improve their compatibility with PLA. The blend with the unsaponifiable compound α-tocopherol showed small gains in elongation at break, which extends already existing knowledge. Its use as a natural antioxidant in PLA at small quantities (< 4 wt%) induced a slightly T_g decrease[32] but no increase in elongation at break.[33] Here, no elongation at break improvement upon was found using greater α-tocopherol amounts, despite solubility was assessed to be higher than other molecules (such as HPO and HCO, **Table 4.2**) and T_g decrease was observed (**Table 4.3**). Squalene, which is a natural tri-terpene found in vegetable oils, showed some toughening abilities (**Table 4.3**) despite its low solubility in PLA (**Table 4.2**). In fact, the creation of a dispersed phase promoting crazing was most probably responsible for this effect.[12j]

The most interesting result was obtained upon mixing different compounds. A mix of C18:1 and C16:0 fatty acids increased the PLA ductility much more than using them separately. The Young modulus and the T_g remained higher than using only C18:1 likely because of its lower content involved, while the stress and elongation at yield were lessened as much as adding only C18:1. Mixture made of [95 wt% (50 wt% C16:0 + 50 wt% C18:1) + 5 wt% HPO] at a

total content of 10 wt% in PLA, further enhanced the ductility. There was apparently a synergistic effect between compounds, which can be possibly exploited.

Table 4.3 Mechanical and thermal properties of formulations

Formulation		**Elongation at break** *(%)*	**Young modulus** *(MPa)*	**Elongation at yield** *(%)*	**Stress at yield** *(MPa)*	**T_g** *(°C)*
PLA (twin screw pellets)		6 ± 1	1,760 ± 90	4.2 ± 0.4	64 ± 5	56.3 ± 0.2
PLA + 10 wt% C16:0		4 ± 1	1,720 ± 60	3.2 ± 0.1	50 ± 3	49.3 ± 0.1
PLA + 10 wt% C18:1		16 ± 5	1,440 ± 50	2.2 ± 0.1	28 ± 2	45.2 ± 0.2
PLA + 10 wt% [50 wt% C16:0 + 50 wt% C18:1]		45 ± 12	1,590 ± 80	2.2 ± 0.1	31 ± 2	40.7 ± 0.3
PLA + 10 wt% [95 wt% (50 wt% C16:0 + 50 wt% C18:1) + 5 wt% HPO]		74 ± 15	1,550 ± 120	2.2 ± 0.2	25 ± 4	39.8 ± 0.4
PLA +	5 wt% HCO	9 ± 3	1,680 ± 70	3.6 ± 0.2	51 ± 1	54.1 ± 0.2
	10 wt% HCO	9 ± 6	1,540 ± 80	3.6 ± 0.2	42 ± 2	54.1 ± 0.1
	15 wt% HCO	11 ± 5	1,460 ± 70	3.8 ± 0.2	38 ± 2	54.8 ± 0.3
PLA +	5 wt% HPO	55 ± 20	1,610 ± 50	2.7 ± 0.1	38 ± 1	52.6 ± 0.2
	10 wt% HPO	85 ± 15	1,420 ± 70	2.6 ± 0.2	26 ± 2	54.4 ± 0.4
	15 wt% HPO	91 ± 14	1,300 ± 80	2.4 ± 0.1	26 ± 1	53.9 ± 0.3
PLA +	5 wt% α-tocopherol	6 ± 2	1,150 ± 90	3.8 ± 0.2	41 ± 4	51.3 ± 0.2
	10 wt% α-tocopherol	5 ± 2	1,070 ± 60	4.0 ± 0.4	31 ± 3	49.8 ± 0.2
	15 wt% α-tocopherol	8 ± 3	990 ± 70	3.9 ± 0.3	29 ± 4	47.1 ± 0.2
PLA +	5 wt% squalene	38 ± 7	1,180 ± 90	3.3 ± 0.4	36 ± 7	51.4 ± 0.2
	10 wt% squalene	51 ± 9	990 ± 60	3.1 ± 0.9	28 ± 3	49.5 ± 0.2
	15 wt% squalene	29 ± 7	890 ± 80	2.9 ± 0.7	19 ± 2	49.4 ± 0.1
PLA +	5 wt% RODC	22 ± 3	1,530 ± 80	3.2 ± 0.2	40 ± 3	52.6 ± 0.2
	10 wt% RODC	55 ± 7	1,490 ± 140	2.4 ± 0.2	28 ± 4	49.1 ± 0.1
	15 wt% RODC	65 ± 15	1,380 ± 155	2.3 ± 0.3	23 ± 4	48.8 ± 0.1
	20 wt% RODC	73 ± 20	1,270 ± 150	2.2 ±0.3	20 ± 4	48.5 ± 0.3
PLA +	5 wt% SODC	29 ± 8	1,550 ± 110	3.3 ± 0.3	41 ± 7	50.6 ± 0.1
	10 wt% SODC	73 ± 18	1,510 ± 90	2.3 ± 0.2	25 ± 5	49.4 ± 0.3
	15 wt% SODC	80 ± 13	1,340 ± 80	2.2 ± 0.3	23 ± 3	48.7 ± 0.1
	20 wt% SODC	52 ± 15	1,220 ± 100	2.1 ± 0.4	16 ± 4	47.5 ± 0.1
PLA +	5 wt% OODC	49 ± 6	1,430 ± 90	3.1 ± 0.3	34 ± 4	49.5 ± 0.2
	10 wt% OODC	85 ± 17	1,490 ± 90	2.6 ± 0.2	31 ± 2	49.0 ± 0.1
	15 wt% OODC	88 ± 16	1,360 ± 70	2.1 ± 0.2	20 ± 3	48.5 ± 0.1
	20 wt% OODC	67 ± 16	1,370 ± 110	2.2 ± 0.2	21 ± 3	48.7 ± 0.1
PLA +	5 wt% PODC	51 ± 17	1,680 ± 110	2.5 ± 0.2	36 ± 2	45.3 ± 0.1
	10 wt% PODC	132 ± 18	1,460 ± 40	2.1 ± 0.2	24 ± 1	39.2 ± 0.2
	15 wt% PODC	179 ± 15	1,180 ± 130	2.3 ± 0.3	18 ± 2	35.1 ± 0.2
	20 wt% PODC	84 ± 31	1,130 ± 60	2.0 ± 0.4	14 ± 3	33.8 ± 0.2

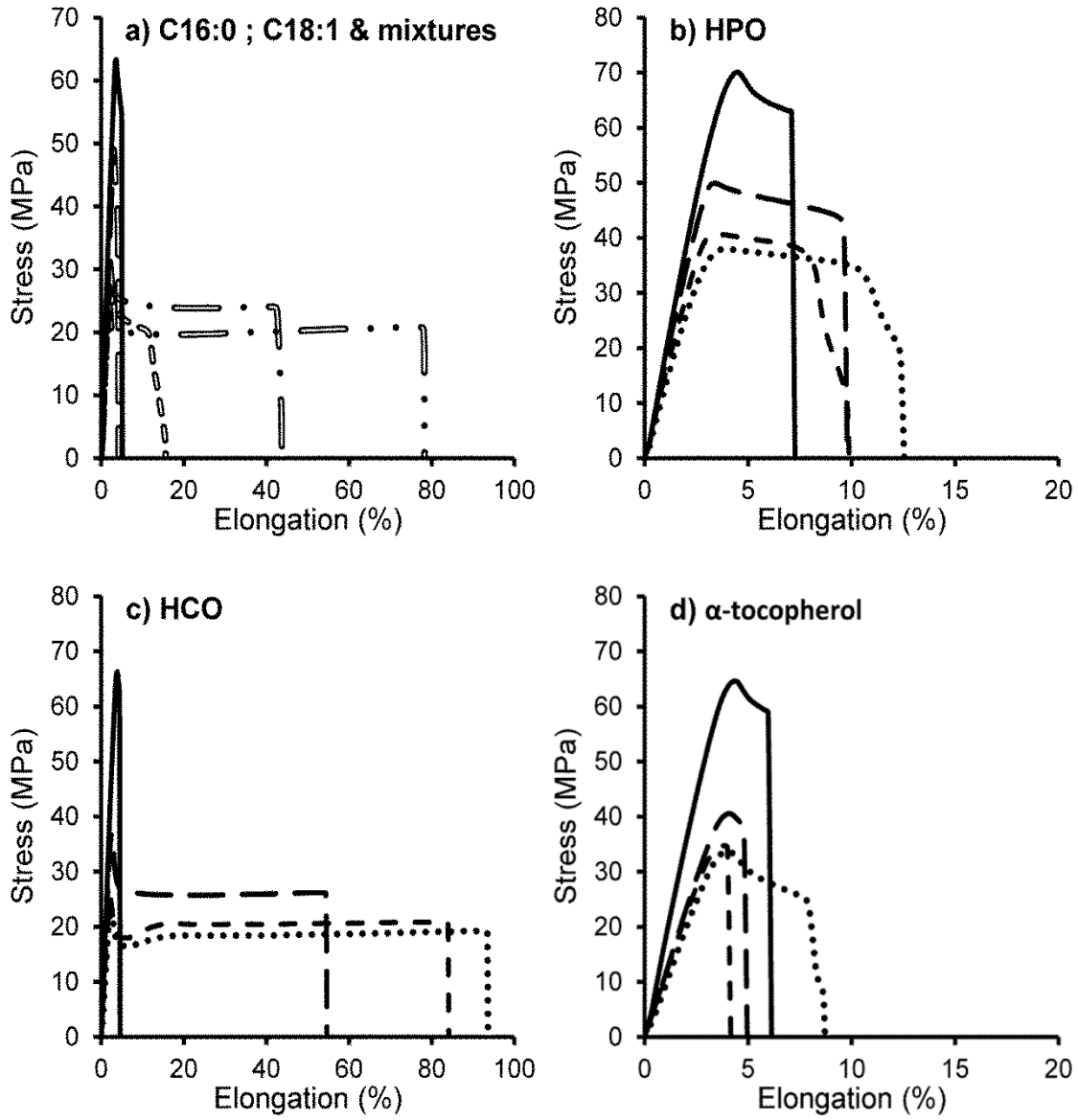

Supporting information S4.4 Stress/strain curves of PLA blends with free fatty acids, hydrogenated vegetable oils (HPO and HCO), unsaponifiable compounds (squalene, α-tocopherol), and vegetable oil deodorization condensates (palm oil PODC, olive oil OODC, soybean oil SODC and rapeseed oil RODC);
(—) neat PLA ; (== ==) PLA + 10 wt% C16:0 ; (= =) PLA + 10 wt% C18:1 ; (== •) PLA + 10 wt% [50 wt% C16:0 + 50 wt% C18:1] ; (== • •) PLA + 10 wt% [95 wt% (50 wt% C16:0 + 50 wt% C18:1) + 5 wt% HPO] ; (— —) PLA + 5 wt% additive ; (- - -) PLA + 10 wt% additive ; (• •) PLA + 15 wt% additive ; (— • •) PLA + 20 wt% additive

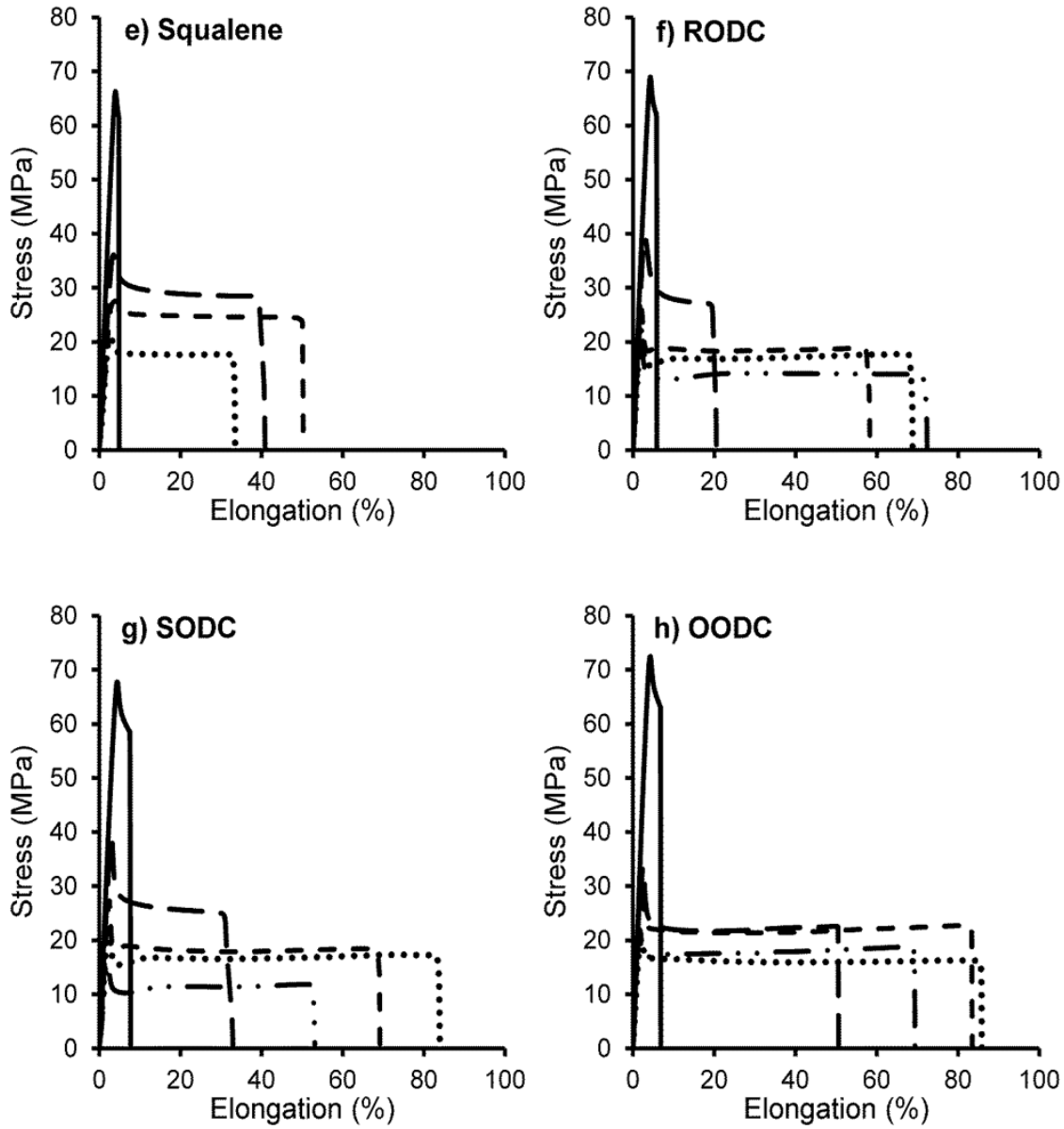

Supporting information S4.4 (Continued) Stress/strain curves of PLA blends with free fatty acids, hydrogenated vegetable oils (HPO and HCO), unsaponifiable compounds (squalene, α-tocopherol), and vegetable oil deodorization condensates (palm oil PODC, olive oil OODC, soybean oil SODC and rapeseed oil RODC); (—) neat PLA ; (== ==) PLA + 10 wt% C16:0 ; (= =) PLA + 10 wt% C18:1 ; (== •) PLA + 10 wt% [50 wt% C16:0 + 50 wt% C18:1] ; (== • •) PLA + 10 wt% [95 wt% (50 wt% C16:0 + 50 wt% C18:1) + 5 wt% HPO] ; (— —) PLA + 5 wt% additive ; (- - -) PLA + 10 wt% additive ; (• •) PLA + 15 wt% additive ; (— • •) PLA + 20 wt% additive

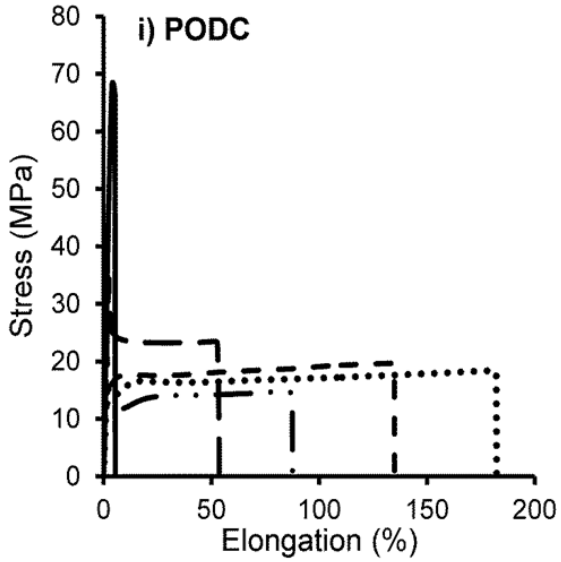

Supporting information S4.4 (Continued) Stress/strain curves of PLA blends with free fatty acids, hydrogenated vegetable oils (HPO and HCO), unsaponifiable compounds (squalene, α-tocopherol), and vegetable oil deodorization condensates (palm oil PODC, olive oil OODC, soybean oil SODC and rapeseed oil RODC); (—) neat PLA ; (== ==) PLA + 10 wt% C16:0 ; (= =) PLA + 10 wt% C18:1 ; (== •) PLA + 10 wt% [50 wt% C16:0 + 50 wt% C18:1] ; (== • •) PLA + 10 wt% [95 wt% (50 wt% C16:0 + 50 wt% C18:1) + 5 wt% HPO] ; (— —) PLA + 5 wt% additive ; (- - -) PLA + 10 wt% additive ; (• •) PLA + 15 wt% additive ; (— • •) PLA + 20 wt% additive

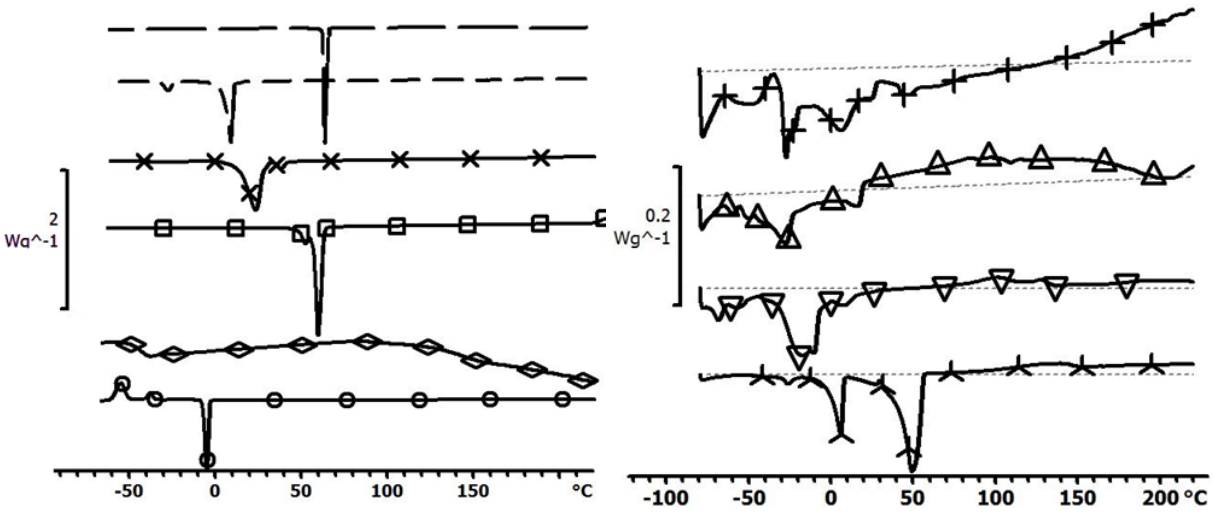

Supporting information S4.5 Thermograms of free fatty acids, hydrogenated vegetable oils (HPO and HCO), unsaponifiable compounds (squalene, α-tocopherol), and vegetable oil deodorization condensates (palm oil PODC, olive oil OODC, soybean oil SODC and rapeseed oil RODC)

(— —) C16:0 ; (– –) C18:1 ; (X) HCO ; (▭) HPO ; (◊) α-tocopherol ; (○) squalene ; (=) RODC ; (△) SODC ; (▽) OODC ; (⅄) PODC

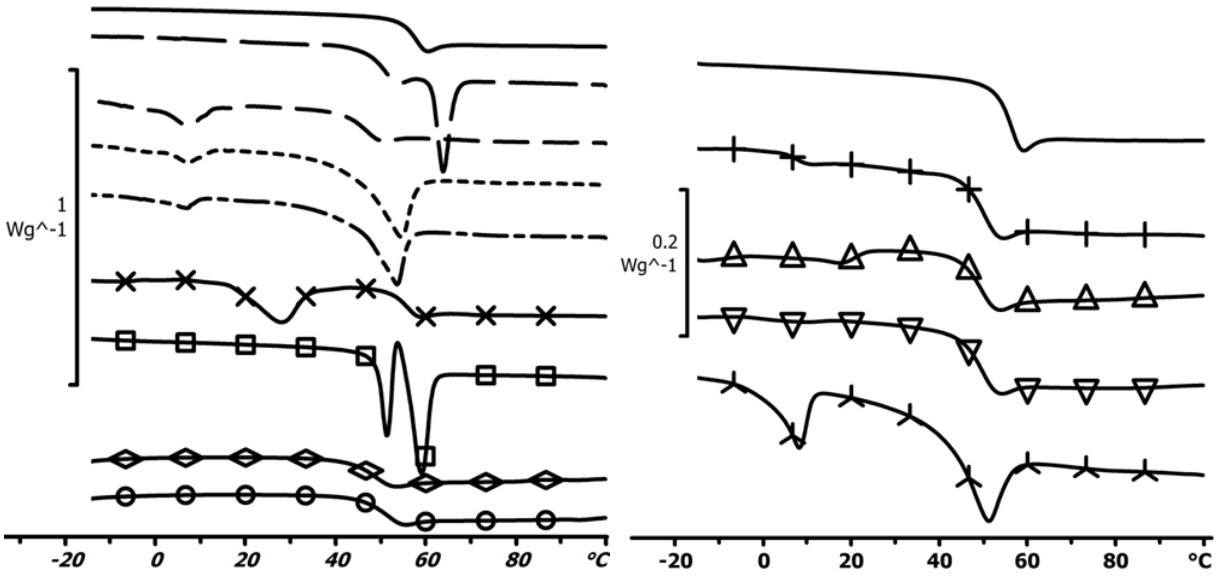

Supporting information S4.6 Thermograms of PLA blends with free fatty acids, hydrogenated vegetable oils (HPO and HCO), unsaponifiable compounds (squalene, α-tocopherol), and vegetable oil deodorization condensates (palm oil PODC, olive oil OODC, soybean oil SODC and rapeseed oil RODC)
(—) neat PLA ; (— —) PLA + 10 wt% C16:0 ; (– –) PLA + 10 wt% C18:1 ; (- - -) PLA + 10 wt% [50 wt% C16:0 + 50 wt% C18:1] ; (— -) PLA + 10 wt% [95 wt% (50 wt% C16:0 + 50 wt% C18:1) + 5 wt% HPO]
(Ⓧ) PLA + 10 wt% HCO ; (⊟) PLA + 10 wt% HPO ; (⟠) PLA + 10 wt% α-tocopherol ;
(⊖) PLA + 10 wt% squalene ; (⊹)PLA + 10 wt% RODC ; (⍋)PLA + 10 wt% SODC ; (⍒)PLA + 10 wt% OODC ;
(⍲) PLA + 10 wt% PODC

4.3.2. Properties of PLA blends with vegetable oil deodorization condensates

Deodorization oil condensates are mixtures of different molecules contained in vegetable oils, the composition of which depends on the botanic source and oil refinery process. Four kinds of oil deodorization condensates (RODC, SODC, OODC and PODC) were blended with PLA, each at four concentrations (5, 10, 15 and 20 wt%). As shown in **Table 4.1**, content in free fatty acids, mono di or triglycerides, sterols (mainly α-tocopherol) and hydrocarbons (mainly squalene) was highly variable, as well as unsaturation degree of fatty acids. From the composition, an average HSP was calculated and is given in **Table 4.2**. As observed in **Table 4.2**, the longer and/or unsaturated the alkyl chain is, the lower the solubility in PLA. However, except for very short fats alkyl chains and organic compounds as α-tocopherol or squalene, HSP of involved molecules appear to be rather similar. Mechanical and thermal properties of

PLA/oil deodorization condensates blends are given in **Table 4.3** and typical curves of raw data are shown in the supporting information **S4.4**. Significant increases in elongation at break were obtained, especially with the PODC. Addition of too much additive, *i.e.* about 20 wt%, induced a stagnation or decrease in the elongation at break. All the deodorization condensates led to a lowering in the stress and elongation at yield. Interestingly, the apparent Young modulus of materials remained high. The stress/strain curves (supporting information **S4.4**) showed that the yielding peak was shrunk and flattened with the increase in additive content, as if the yield critical stress would tend to meet the plateau value where the stress remains constant with the strain. There is thus an important gain of using native mixtures of fatty acids present in deodorisation condensates for PLA ductility increase.

4.3.3. Study of the deformation mechanisms involved in PLA/ oil deodorization condensates blends

In all samples the T_g remained higher than the measurement temperature, the main deformation mechanism was thus crazing of the glassy polymer.[12j] The yield process in glassy amorphous polymers can be described as a stress induced glass-transition. In fact, because PLA Poisson's ratio is less than 0.5 (νPLA = 0.36),[34] the volume of PLA increases when subjected to tensile stress. Correspondingly, samples experienced important stress whitening (supporting information **S4.7**), which appeared simultaneously with yielding. Stress whitening is caused by the formation of sizeable microvoids in the polymer matrix due to cavitation and crazes.[35] Crazes can also be initiated inside non-miscible inclusions in the polymer matrix or on the interface between inclusion and polymer in the case of low compatibility. The addition of oil deodorization condensates initiated crazes at stress levels substantially below those of the brittle failure of neat PLA, which propagated perpendicularly to the stretching direction. When 100 % elongation was reached, cracks were highly expanded reaching more than 1 mm width (supporting information **S4.7**). Morphological analysis of the form and size of inclusions

of PODC, C16:0 and C18:1 was done to help interpretation. The **Figure 4.1** shows SEM micrographs of [PLA/C16:0], [PLA/C18:1] and [PLA/PODC] 90 wt% / 10 wt% blends. [PLA/C16:0] blends exhibit rods of about 5 to 10 µm length and 1 to 2 µm width, corresponding to fatty acid crystals. [PLA/C18:1] showed small spherical domains of fatty acids of about 0.5 µm diameters and some aggregates of about 3 to 5 µm diameters. The [PLA/PODC] blend micrograph showed both rods and aggregates of droplets, where the droplets appear to be distributed all around the crystals.

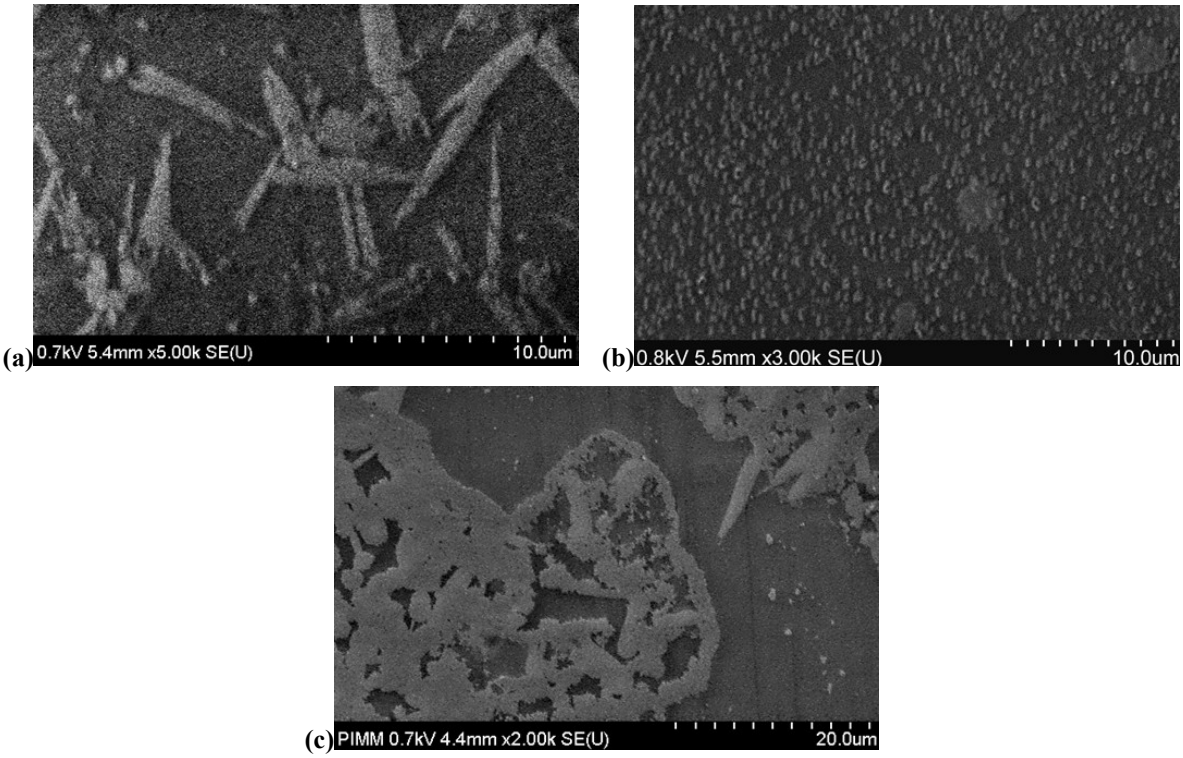

Figure 4.1 SEM micrographs of **(a)** C16:0, **(b)** C18:1 and **(c)** PODC blends with PLA at 10 wt%

Figure 4.2 shows optical micrographs in transmission mode of stretched samples under the microscope taken at different percentages of elongation. Many small cracks started appear in neat PLA when approaching the yield peak, which is common for glassy amorphous polymers. Addition of C16:0, *i.e.* rod like crystals, increased both the occurrence and the length of cracks. Cracks quantity upon stretching caused the material to become opaque.

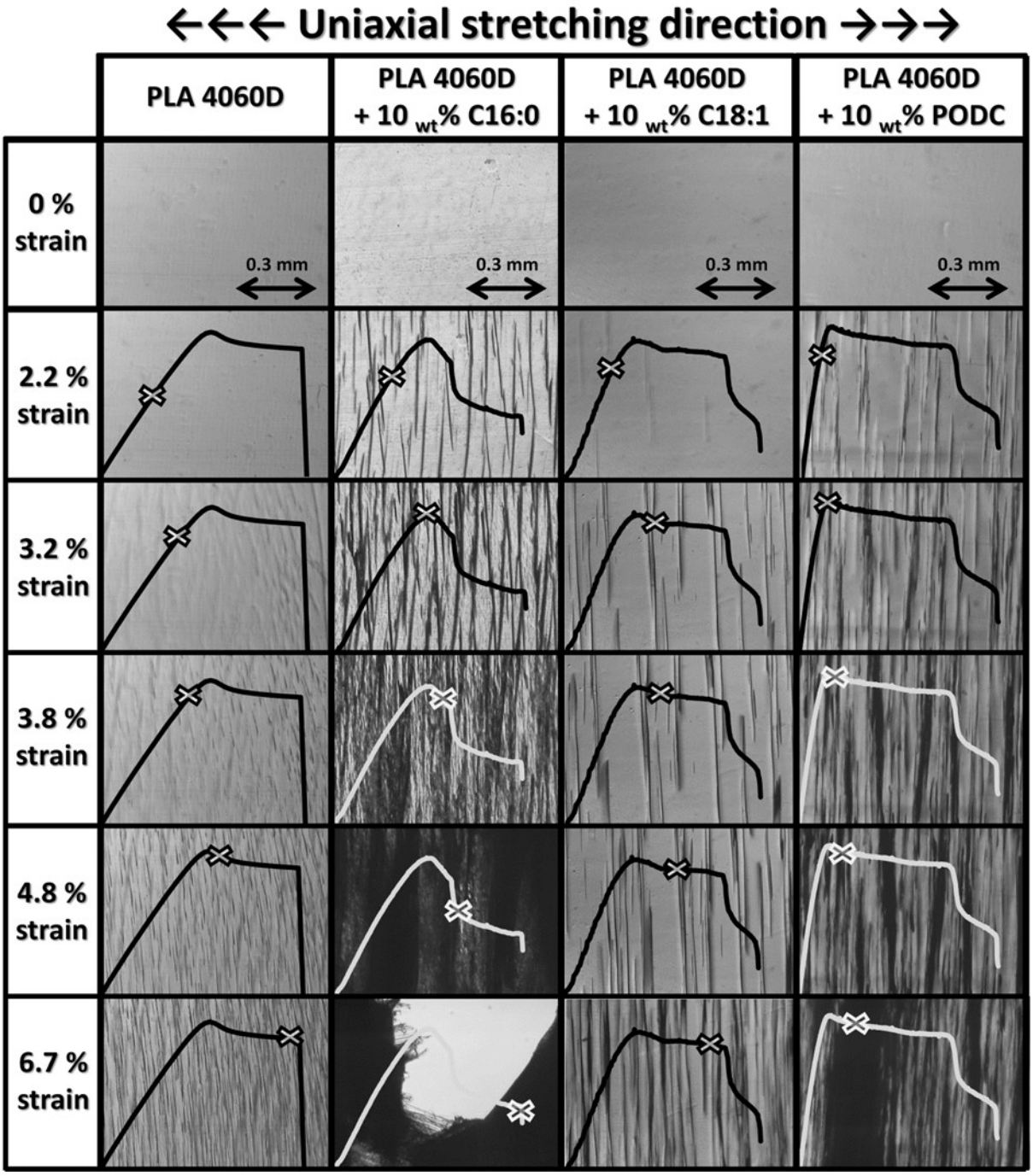

Figure 4.2 Optical micrographs of uniaxially stretched PLA and PLA blends with free fatty acids (C16:0, C18:1) and palm oil deodorization condensate (PODC) at different strain

Failure of the blend revealed PLA fibrils. C18:1, *i.e.* small spherical liquid domains, induced fewer but much larger cracks as if their extensibility was eased. PODC, *i.e.* mostly a combination of C16:0 and C18:1 and some minor constituents, showed a high number of cracks but with smaller width as if using only C18:1. The mixture of palmitic acid crystals and liquid inclusions of oleic acid had thus a synergistic effect allowing for efficient craze

initiation by the crystals and by cavitation inside the liquid inclusions. The superior performance of the PODC blends seems thus to be linked to the chemical composition in fatty acids and the presence of the minor constituents.

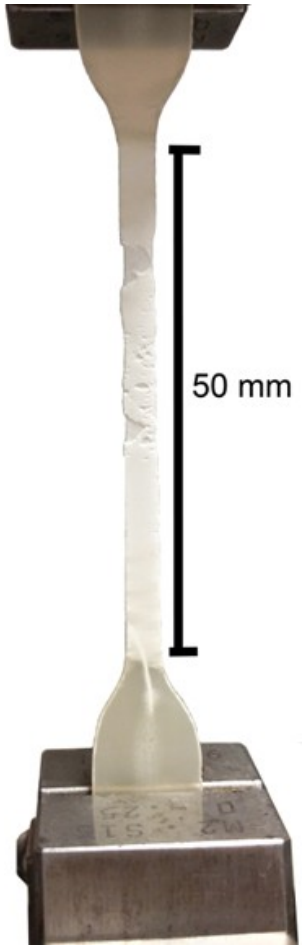

Supporting information S4.7 PLA + 10 wt% PODC blend stretched at 100 % strain

4.3.4. Role of the chemical composition of deodorization condensates in ductility improvement

In the aim of discriminating the effect of the different compounds contained in the deodorization condensates on PLA ductility improvement, a Principal Components Analysis (PCA) was carried out including composition data and physico-chemical characteristics of the concerned molecules. **Figure 4.3** shows the principal components projection plot of F1 and F2 of the data set. Only 50 % of the total variance in these PLA samples is extracted according to

F1 and F2 axes. In fact, scores of formulations containing squalene, α-tocopherol, HPO, HCO and mixtures of C16:0, C18:1 and HPO are not discriminated. However discrimination of PLA samples containing deodorization condensates of each kind of vegetable oils and according to their respective amount is obtained. Corresponding loadings are plotted in **Figure 4.4**.

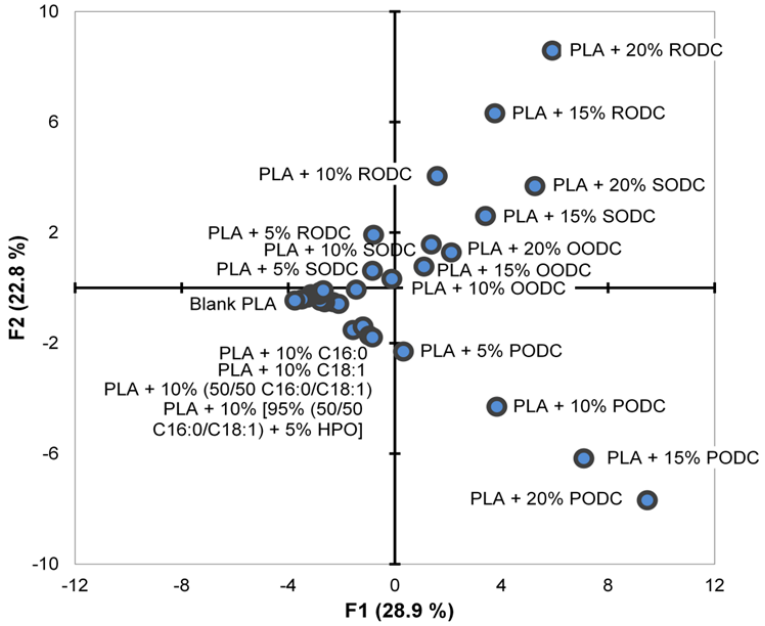

Figure 4.3 Principal components projection plot of F1 and F2 of the data set

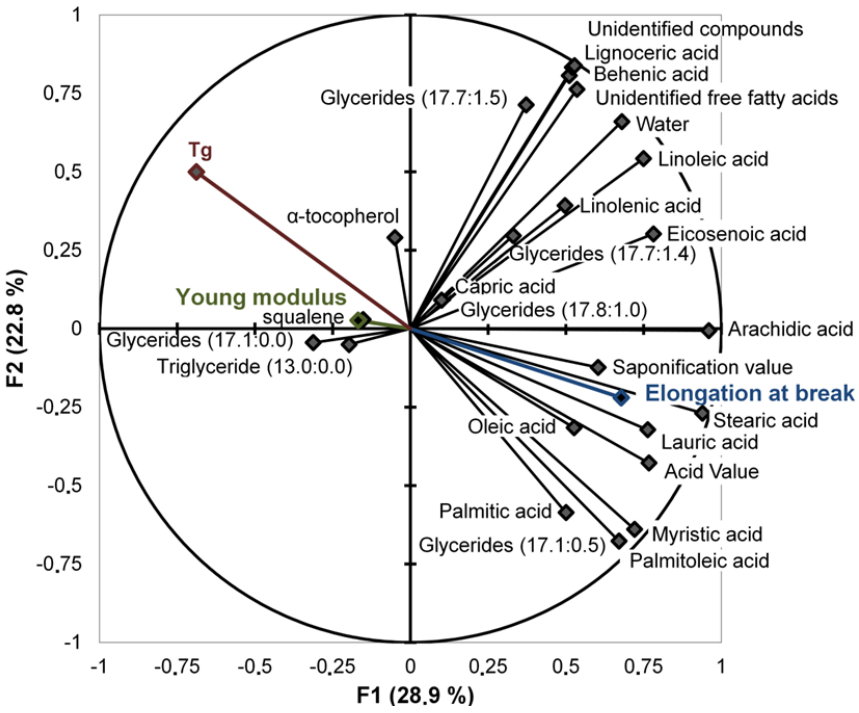

Figure 4.4 Loadings plot of the Principal Components Analysis of the dataset

The positive part of F1 axis appears to be mainly governed by the elongation at break and as opposed to its negative part with the T_g. The F2 axis mostly separates fats in function of the unsaturation and length of their alkyl chains. Looking at the elongation at break improvement, unsaturation of alkyl chains appears to be required, but the lower the ratio, the larger the enhancement was. Medium alkyl chain length, *i.e.* from lauric (C12) to stearic (C18) acid, also tends to be preferable than the long ones as behenic (C22) or lignoceric (C24) acids. Both the unsaturation and the length of alkyl chains are main physical factors governing the melting point of fats. One common point is that unsaturation decreases melting points while length increases it. Therefore, efficiency of fats in toughening PLA appeared to be linked to medium melting point properties. A mixture of crystalline and liquid fatty acids at room temperature seemed favorable. This could explain the ability of HCO triglycerides to increase the PLA ductility while HPO did not, although their HSP were similar, as their ability to depress the T_g of PLA. In fact, due to short alkyl chains, HCO triglycerides are waxy at room temperature. The DSC thermogram (supporting information **S4.5**) shows a broad melting peak going from 8 to 42 °C of HCO while it is beyond 55 °C for HPO. Literature shows that combining liquid and solid additives can sometimes be effective.[36] Acid and saponification values are related to the elongation at break improvement (**Figure 4.4**). Therefore, the higher the esterified fats and/or the free fatty acid contents, the better the efficiency of the additive. In opposite, unidentified compounds, *i.e.* mostly unsaponifiable compounds, are not favorable to the ductility increase. Therefore, the superiority in toughening abilities of the PODC compared to the alike mixture made of [95 wt% (50 wt% C16:0 + 50 wt% C18:1) + 5 wt% HPO] can be attributed to the complex and favorable mixture of fatty acids having different chain length.

4.4. Conclusions

The use of by-products of the vegetable oils industry, namely deodorization condensates, as biobased additives for ductility improvement of PLA was investigated. The deodorization condensates improve substantially the elongation at break of PLA up to 160 %. The glass transition is merely decreased which brings ductility to the still glassy polymer. The deformation mechanism was efficient craze initiation delaying failure. Most importantly, it was shown that the industrial by-product of the palm oil refinery had superior properties compared to mixtures of fatty acids and vegetable oils because it contained a mixture of fatty acids with melting points below and beyond room temperature. This makes deodorization condensates efficient and low price additives for PLA able to be used in commodity applications such as food packaging.

Acknowledgements

This work was financially supported by Brodart Packaging and the BIP-ADEME French project CREABioM. The authors greatly thank the laboratory Institut des Corps Gras (ITERG – Bordeaux, France) for its technical support.

REFERENCES

1. **(a)** Auras, R.; Harte, B.; Selke, S., An Overview of Polylactides as Packaging Materials. *Macromolecular Bioscience* 2004, *4* (9), 835-864.
(b) Auras, R. A.; Singh, S. P.; Singh, J. J., Evaluation of oriented poly(lactide) polymers vs. existing PET and oriented PS for fresh food service containers. *Packaging Technology and Science* 2005, *18* (4), 207-216.
(c) Petersen, K., Vaeggemose Nielsen, P., Bertelsen, G., Lawther, M., Olsen, M., Nilsson, N., Mortensen, G., Potential of biobased materials for food packaging. *Trends in Food Science & Technology* 1999, *10*, 52-68.

2. Solarski, S. Développement de nouveaux filaments de polylactide nanocomposites. Lille 1, 2006.

3. **(a)** Zhang, J.-F.; Sun, X., Mechanical and thermal properties of poly(lactic acid)/starch blends with dioctyl maleate. *Journal of Applied Polymer Science* 2004, *94* (4), 1697-1704.
(b) Södergard, A., Stolt, M., Properties of lactic acid based polymers and their correlation with composition. *Progress in Polymer Science* 2002, *27* (6), 1123-1163.
(c) Amass, W.; Amass, A.; Tighe, B., A review of biodegradable polymers: uses, current developments in the synthesis and characterization of biodegradable polyesters, blends of biodegradable polymers and recent advances in biodegradation studies. *Polymer International* 1998, *47* (2), 89-144.

4. Kaplan, D. L., Biopolymers from renewable resources. *Springer Verlag* 1998, 367-411.

5. Lowe, C. E., In U.S. Patent US2668162 A: Du Pont De Nemous And Company. 1954.

6. **(a)** Gruber, P. R.; E. S. Hall; J. J. Kolstad; M. L. Iwen; R. D. Benson; Borchardt, R. L., U.S. Patent 6,326,458. 2001.
(b) Gruber, P. R.; E. S. Hall; J. J. Kolstad; M. L. Iwen; R. D. Benson; Borchardt, R. L., U.S. Patent 5,357,035. 1994.

7. **(a)** Avérous, L., Monomers, Polymers and Composites from Renewable Resources. *Polylactic acid: synthesis, properties and applications* 2008, (21), 433-450.
(b) Siracusa, V.; Rocculi, P.; Romani, S.; Rosa, M. D., Biodegradable polymers for food packaging: a review. *Trends in Food Science & Technology* 2008, *19* (12), 634-643.

8. Liu, H. Z.; Zhang, J. W., Research Progress in Toughening Modification of Poly(lactic acid). *J. Polym. Sci. Pt. B-Polym. Phys.* 2011, *49* (15), 1051-1083.

9. **(a)** Li, Y.; Shimizu, H., Toughening of Polylactide by Melt Blending with a Biodegradable Poly(ether)urethane Elastomer. *Macromolecular Bioscience* 2007, *7* (7), 921-928.
(b) NatureWorks Technology Focus Report: Toughened PLA. (accessed 2014-10-14).

10. Zhang, W.; Chen, L.; Zhang, Y., Surprising shape-memory effect of polylactide resulted from toughening by polyamide elastomer. *Polymer* 2009, *50* (5), 1311-1315.

11. **(a)** Byrne, F.; Ward, P.; Kennedy, J.; Imaz, N.; Hughes, D.; Dowling, D., The Effect of Masterbatch Addition on the Mechanical, Thermal, Optical and Surface Properties of Poly(lactic acid). *Journal of Polymers and the Environment* 2009, *17* (1), 28-33.
(b) Murariu, M.; Da Silva Ferreira, A. l.; Degée, P.; Alexandre, M.; Dubois, P., Polylactide compositions. Part 1: Effect of filler content and size on mechanical properties of PLA/calcium sulfate composites. *Polymer* 2007, *48* (9), 2613-2618.
(c) Murariu, M.; Ferreira, A. D. S.; Duquesne, E.; Bonnaud, L.; Dubois, P., Polylactide (PLA) and Highly Filled PLA - Calcium Sulfate Composites with Improved Impact Properties. *Macromolecular Symposia* 2008, *272* (1), 1-12.
(d) Hughes, P. A.; Becraft, M. L.; Opusko, S. US Patent US20070255013 A1. Polymeric blend comprising polylactic acid. 2007.
(e) Brulé, B.; Fine, T.; Flat, J.J.; Yasuda, M., Composite based on polylactic acid and polyamide, having improved impact resistance, its manufacturing process and use. WO2007144543, 2007.

(f) Markarian, J., Biopolymers present new market opportunities for additives in packaging. *Plastics, Additives and Compounding* 2008, *10* (3), 22-25.
(g) Jin, H.-J.; Chin, I.-J.; Kim, M.-N.; Kim, S.-H.; Yoon, J.-S., Blending of poly(L-lactic acid) with poly(cis-1,4-isoprene). *European Polymer Journal* 2000, *36* (1), 165-169.
(h) Li, Y.; Shimizu, H., Improvement in toughness of poly(l-lactide) (PLLA) through reactive blending with acrylonitrile - butadiene - styrene copolymer (ABS): Morphology and properties. *European Polymer Journal* 2009, *45* (3), 738-746.
(i) McCarthy, S. P.; Gross, R. A.; Ma, W. US Patent US5883199 A. Polylactic Acid Based Blends. 1999.

12. **(a)** Baiardo, M.; Frisoni, G.; Scandola, M.; Rimelen, M.; Lips, D.; Ruffieux, K.; Wintermantel, E., Thermal and mechanical properties of plasticized poly(L-lactic acid). *J. Appl. Polym. Sci.* 2003, *90* (7), 1731-1738.
(b) Ljungberg, N.; Andersson, T.; Wesslen, B., Film extrusion and film weldability of poly(lactic acid) plasticized with triacetine and tributyl citrate. *J. Appl. Polym. Sci.* 2003, *88* (14), 3239-3247.
(c) Murariu, M.; Da Silva Ferreira, A.; Alexandre, M.; Dubois, P., Polylactide (PLA) designed with desired end-use properties: 1. PLA compositions with low molecular weight ester-like plasticizers and related performances. *Polymers for Advanced Technologies* 2008, *19* (6), 636-646.
(d) Lemmouchi, Y.; Murariu, M.; Dos Santos, A. M.; Amass, A. J.; Schacht, E.; Dubois, P., Plasticization of poly(lactide) with blends of tributyl citrate and low molecular weight poly(D,L-lactide)-b-poly(ethylene glycol) copolymers. *Eur. Polym. J.* 2009, *45* (10), 2839-2848.
(e) Wang, R. Y.; Wan, C. Y.; Wang, S. F.; Zhang, Y., Morphology, Mechanical Properties, and Durability of Poly(Lactic Acid) Plasticized With Di(Isononyl) Cyclohexane-1,2-Dicarboxylate. *Polym. Eng. Sci.* 2009, *49* (12), 2414-2420.
(f) Sierra, J.; Noriega, M.; Cardona, E.; Ospina, S., Relationship between properties, citrate content and postproduction time for a plasticized polylactic acid. *ANTEC 2010 [Proceedings]* 2010.
(g) Courgneau, C.; Domenek, S.; Guinault, A.; Averous, L.; Ducruet, V., Analysis of the Structure-Properties Relationships of Different Multiphase Systems Based on Plasticized Poly(Lactic Acid). *J. Polym. Environ.* 2011, *19* (2), 362-371.
(h) Labrecque, L. V.; Kumar, R. A.; Davé, V.; Gross, R. A.; McCarthy, S. P., Citrate esters as plasticizers for poly(lactic acid). *J. Appl. Polym. Sci.* 1997, *66* (8), 1507-1513.
(i) Yu, J.; Wang, N.; Ma, X., Fabrication and Characterization of Poly(lactic acid)/Acetyl Tributyl Citrate/Carbon Black as Conductive Polymer Composites. *Biomacromolecules* 2008, *9* (3), 1050-1057.
(j) Ruellan, A.; Guinault, A.; Sollogoub, C.; Ducruet, V.; Domenek, S., Solubility Factors as Screening Tools of Biodegradable Toughening Agents of Polylactide. *J. Appl. Polym. Sci.* 2015, *Special Issue: Manufacturing of Advanced Biodegradable Polymeric Components*.

13. **(a)** Kulinski, Z.; Piorkowska, E.; Gadzinowska, K.; Stasiak, M., Plasticization of poly(L-lactide) with poly(propylene glycol). *Biomacromolecules* 2006, *7* (7), 2128-2135.
(b) Kulinski, Z.; Piorkowska, E., Crystallization, structure and properties of plasticized poly(l-lactide). *Polymer* 2005, *46* (23), 10290-10300.
(c) Hu, Y., Hu, Y. S., Topolkaraev, V., Hiltner, A., Baer, E., Crystallization and phase separation in blends of high stereoregular poly(lactide) with poly(ethylene glycol). *Polymer* 2003, *44*, 5681-5689.
(d) Jacobsen, S.; Fritz, H. G., Plasticizing polylactide—the effect of different plasticizers on the mechanical properties. *Polymer Engineering & Science* 1999, *39* (7), 1303-1310.
(e) Martin, O.; Averous, L., Poly(lactic acid): plasticization and properties of biodegradable multiphase systems. *Polymer* 2001, *42* (14), 6209-6219.
(f) Pillin, I.; Montrelay, N.; Grohens, Y., Thermo-mechanical characterization of plasticized PLA: Is the miscibility the only significant factor? *Polymer* 2006, *47* (13), 4676-4682.
(g) Sheth, M.; Kumar, R. A.; Davé, V.; Gross, R. A.; McCarthy, S. P., Biodegradable polymer blends of poly(lactic acid) and poly(ethylene glycol). *Journal of Applied Polymer Science* 1997, *66* (8), 1495-1505.

14. **(a)** Martino, V.; Ruseckaite, R.; Jiménez, A., Thermal and mechanical characterization of plasticized poly (L-lactide-co-D,L-lactide) films for food packaging. *Journal of Thermal Analysis and Calorimetry* 2006, *86* (3), 707-712.
(b) Martino, V. P.; Jimenez, A.; Ruseckaite, R. A., Processing and Characterization of Poly(lactic acid) Films Plasticized with Commercial Adipates. *J. Appl. Polym. Sci.* 2009, *112* (4), 2010-2018.
(c) Ljungberg, N.; Wesslén, B., Thermomechanical film properties and aging of blends of poly(lactic acid) and malonate oligomers. *J. Appl. Polym. Sci.* 2004, *94* (5), 2140-2149.

(d) Ren, Z.; Dong, L.; Yang, Y., Dynamic mechanical and thermal properties of plasticized poly(lactic acid). *Journal of Applied Polymer Science* 2006, *101* (3), 1583-1590.

15. Rahman, M.; Brazel, C. S., The plasticizer market: an assessment of traditional plasticizers and research trends to meet new challenges. *Progress in Polymer Science* 2004, *29* (12), 1223-1248.

16. Robertson, M. L.; Chang, K.; Gramlich, W. M.; Hillmyer, M. A., Toughening of Polylactide with Polymerized Soybean Oil. *Macromolecules* 2010, *43* (4), 1807-1814.

17. Gramlich, W. M.; Robertson, M. L.; Hillmyer, M. A., Reactive Compatibilization of Poly(l-lactide) and Conjugated Soybean Oil. *Macromolecules* 2010, *43* (5), 2313-2321.

18. **(a)** Ali, F.; Chang, Y.-W.; Kang, S. C.; Yoon, J. Y., Thermal, mechanical and rheological properties of poly (lactic acid)/epoxidized soybean oil blends. *Polym. Bull.* 2009, *62* (1), 91-98.
(b) Xu, Y. Q.; Qu, J. P., Mechanical and Rheological Properties of Epoxidized Soybean Oil Plasticized Poly(lactic acid). *J. Appl. Polym. Sci.* 2009, *112* (6), 3185-3191.
(c) Xiong, Z.; Yang, Y.; Feng, J.; Zhang, X.; Zhang, C.; Tang, Z.; Zhu, J., Preparation and characterization of poly(lactic acid)/starch composites toughened with epoxidized soybean oil. *Carbohydrate Polymers* 2012, *92* (1), 810-816.
(d) Al-Mulla, E. A. J.; Suhail, A. H.; Aowda, S. A., New biopolymer nanocomposites based on epoxidized soybean oil plasticized poly(lactic acid)/fatty nitrogen compounds modified clay: Preparation and characterization. *Industrial Crops and Products* 2010, *33* (1), 23-29.

19. **(a)** Silverajah, V. S. G.; Ibrahim, N. A.; Zainuddin, N.; Yunus, W.; Abu Hassan, H., Mechanical, Thermal and Morphological Properties of Poly(lactic acid)/Epoxidized Palm Olein Blend. *Molecules* 2012, *17* (10), 11729-11747.
(b) Silverajah, V. S. G.; Ibrahim, N. A.; Yunus, W.; Abu Hassan, H.; Woei, C. B., A Comparative Study on the Mechanical, Thermal and Morphological Characterization of Poly(lactic acid)/Epoxidized Palm Oil Blend. *Int. J. Mol. Sci.* 2012, *13* (5), 5878-5898.
(c) Al-Mulla, E. A. J.; Yunus, W.; Ibrahim, N. A. B.; Ab Rahman, M. Z., Properties of epoxidized palm oil plasticized polytlactic acid. *Journal of Materials Science* 2010, *45* (7), 1942-1946.

20. NatureWorks Technology Focus Report: Polylactic Acid Containing Fillers and Fibers. (accessed 2014-10-15).

21. Bitinis, N.; Fortunati, E.; Verdejo, R.; Bras, J.; Kenny, J. M.; Torre, L.; Lopez-Manchado, M. A., Poly(lactic acid)/natural rubber/cellulose nanocrystal bionanocomposites. Part II: Properties evaluation. *Carbohydrate Polymers* 2013, *96* (2), 621-627.

22. Yuan, D. S.; Chen, K. L.; Xu, C. H.; Chen, Z. H.; Chen, Y. K., Crosslinked bicontinuous biobased PLA/NR blends via dynamic vulcanization using different curing systems. *Carbohydrate Polymers* 2014, *113*, 438-445.

23. **(a)** Thepthawat, A.; Srikulkit, K., Improving the Properties of Polylactic Acid by Blending With Low Molecular Weight Polylactic Acid-g-Natural Rubber. *Polym. Eng. Sci.* 2014, *54* (12), 2770-2776.
(b) Ayutthaya, W. D. N.; Poompradub, S., Thermal and mechanical properties of poly(lactic acid)/natural rubber blend using epoxidized natural rubber and poly(methyl methacrylate) as co-compatibilizers. *Macromol. Res.* 2014, *22* (7), 686-692.

24. Hughes, J.; Thomas, R.; Byun, Y.; Whiteside, S., Improved flexibility of thermally stable poly-lactic acid (PLA). *Carbohydr. Polym.* 2012, *88* (1), 165-172.

25. Bradley, J.-C.; Williams, A.; Lang, A., Jean-Claude Bradley Open Melting Point Dataset. figshare, 2014.

26. **(a)** Vereeckeen, J.; Foubert, I.; Meeussen, W.; Lesaffer, A.; Dewettinck, K., Fat structuring with partial glycerides: Effect on solid fat particles. In *SCI Forum*, Ghent, Belgium, 2008.

(b) Sato, K., Kinetic aspects in Polymorphic Crystallization and Transformation of Fats Mixed and Dispersed Systems. In *Physical Properties of Fats, Oils, and Emulsifiers*, Widlak, N., Ed. The American Oil Chemists Society: United States of America, 1999

27. van Krevelen, D. W.; Nijenhuis, K., Cohesive Properties and Solubility. In *Properties of Polymers. Their Correlation with Chemical Structure; Their Numerical Estimation and Prediction from Additive Group Contributions*, 4th. ed.; Elsevier, Ed. Amsterdam, 2009; p 189.

28. **(a)** van Krevelen, D. W., Chemical Structure and Properties of Coal. XXVIII. Coal Constitution and Solvent Extraction. *Fuel* 1965, *44* (44).
(b) van Krevelen, D. W.; Hoftyzer, P. J., Practical evaluation of the [η]–M relationship. III. Estimation of the exponent a. *J. Appl. Polym. Sci.* 1967, *11* (11), 2189-2200.

29. Abbott, S. J., Chemical Compatibility of Poly (Lactic Acid) : A practical Framework using Hansen Solubility parameters. In *Poly(lactic acid): Synthesis, Structures, Properties, Processing, and Applications*, Wiley: 2010; pp 83-93.

30. Jacobsen, S.; Fritz, H. G., Plasticizing polylactide - The effect of different plasticizers on the mechanical properties. *Polymer Engineering & Science* 1999, *39* (7), 1303-1310.

31. Robertson, M. L.; Paxton, J. M.; Hillmyer, M. A., Tough Blends of Polylactide and Castor Oil. *ACS Applied Materials & Interfaces* 2011, *3* (9), 3402-3410.

32. Manzanarez-Lopez, F.; Soto-Valdez, H.; Auras, R.; Peralta, E., Release of alpha-Tocopherol from Poly(lactic acid) films, and its effect on the oxidative stability of soybean oil. *J. Food Eng.* 2011, *104* (4), 508-517.

33. Hwang, S. W.; Shim, J. K.; Selke, S. E. M.; Soto-Valdez, H.; Matuana, L.; Rubino, M.; Auras, R., Poly(L-lactic acid) with added α-tocopherol and resveratrol: optical, physical, thermal and mechanical properties. *Polymer International* 2012, *61* (3), 418-425.

34. Jamshidian, M.; Tehrany, E. A.; Imran, M.; Jacquot, M.; Desobry, S., Poly-Lactic Acid: Production, Applications, Nanocomposites, and Release Studies. *Comprehensive Reviews in Food Science and Food Safety* 2010, *9*, 552-571.

35. Lampman, S., Fracture and Fractography. In *Characterization and Failure Analysis of Plastics*, First ed.; Handbooks, A. I., Ed. ASM International: U.S.A, 2003; pp 404-416.

36. Notta-Cuvier, D.; Odent, J.; Delille, R.; Murariu, M.; Lauro, F.; Raquez, J. M.; Bennani, B.; Dubois, P., Tailoring polylactide (PLA) properties for automotive applications: Effect of addition of designed additives on main mechanical properties. *Polymer Testing* 2014, *36* (0), 1-9.

CHAPITRE 5

TABLE OF CONTENTS

ABSTRACT **178**

5.1. INTRODUCTION **179**

5.2. EXPERIMENTAL **181**

5.2.1. Materials 181
5.2.2. Polymer processing 181
5.2.3. Characterization 183
5.2.3.1. Composition of the PODC *183*
5.2.3.2. Weighting of PODC content from the formulated PLA materials *183*
5.2.3.3. Size Exclusion Chromatography *184*
5.2.3.4. Differential Scanning Calorimetry (DSC and MDSC) *185*
5.2.3.5. Tensile tests *186*
5.2.3.6. Dynamic Mechanical Analysis (DMA) *186*
5.2.3.7. Oxygen permeability *186*
5.2.3.8. Biodegradation *186*
5.2.3.9. Migration of PODC in food simulants *187*
5.2.3.10. Sensorial testing *188*

5.3. RESULTS AND DISCUSSION **189**

5.3.1. Processability of PLA/PODC blends and effects of the process on molecular weight of PLA and PODC contents 190
5.3.2. Thermal and mechanical properties of amorphous PLA 4060D/PODC blends 192
5.3.3. Oxygen barrier properties of amorphous PLA 4060D/PODC films 195
5.3.4. Aging of amorphous PLA 4060D/PODC films at ambient conditions 195
5.3.5. Effect of crystallization of PLA 4042D/PODC blends on thermal and mechanical properties 196
5.3.6. Compliance of PLA 4060D/PODC film with requirements of Food Contact Material regulation 200
5.3.7. Biodegradation of the PLA 4060D/PODC cast extruded film 202

5.4. CONCLUSION **203**

ACKNOLEWDGEMENTS **203**

REFERENCES **204**

Chapitre 5 - Biobased and biodegradable by-product of oil industry as toughening agent of polylactide

Les condensats de désorodorisation d'huile de palme, de part leur composition riche en acides gras libres ayant notamment une intéressante parité entre chaînes alkyles saturées et insaturées, permettent d'augmenter très significativement l'élongation à la rupture du polylactide, en conservanant toutefois sa rigidité élevée et sa température de transition vitreuse supérieure aux températures ambiantes usuelles. Les mécanismes de plastification/lubrification (au sens de la théorie du Gel) en synergie avec ceux de déformation par endommagement (cavitation/craquelage) ont été pointés comme certainement responsables des propriétés mécaniques accrues.

Compte-tenu de l'importante ductilité déjà obtenue en incorporant 10 %m de condensat de désodorisation d'huile de palme (chapitre 4) et de la stabilité observée à l'échelle laboratoire du procédé de mise en œuvre (chapitre 2), nous avons retenu cette formulation pour la suite du projet. Afin de mener à bien son dévellopement industriel, nous avons réalisé des essais d'accroissement d'échelle de production de granulés formulés sur une extrudeuse bivis de taille semi-industrielle (øvis = 35 mm) et ensuite travaillé à la réalisation de films par extrusion à plat et extrusion gonflage à l'échelle semi-pilote.

L'influence du procédé de mise en œuvre sur les propriétés physico-chimiques des films obtenus a été étudiée et leurs propriétés d'usage comme l'aptitude au contact alimentaire et la biodégradabilité vérifiées. Les effets du vieillissement et ceux de de la cristallisation du PLA sur les propriétés tehrmiques, mécaniques et barrière ont également été caractérisés afin de proposer un matériau répondant aux exigences d'une mise sur le marché de grande consommation.

Alexandre Ruellan[a,b,c], Audrey Gratia[d], Alain Guinault[a,e], Cyrille Sollogoub[a,e], Guillaume Chollet[f], Violette Ducruet[g], Sandra Domenek[b]

[a]*CNAM, Arts et Métiers ParisTech, CNRS, UMR 8006, Laboratoire PIMM, 151, Boulevard de l'Hopital, F-75013 Paris.*
[b]*AgroParisTech, Ingénierie Procédés Aliments, 1 avenue des Olympiades, F-91300 Massy.*
[c]*Brodart Packaging, Département R&D, 1 rue du Stand, F-10700 Arcis-Sur-Aube.*
[d]*LNE, Département Chimie et Physico-Chimie des Matériaux, 78197 Trappes*
[e]*CNAM, Laboratoire P2AM, 2 rue Conté, F-75003 Paris.*
[f]*ITERG, Lipochimie Hall Industriel, 11 rue Monge, F-33600 Pessac.*
[g]*INRA, Ingénierie Procédés Aliments, 1 avenue des Olympiades, F-91300 Massy.*

Abstract

Stable sourced natural by-product, namely palm oil deodorization condensate (PODC), was used to enhance the elongation at break of an amorphous polylactide (PLA) film up to 130 %, while maintaining its stiffness and ecological advantages. Due to its processing aid abilities, the processing temperatures were significantly lowered allowing to perform blown extrusion film as well as the cast one. Films specifications including barrier properties, aging behaviour, biodegradability, overall migration in food simulants and sensorial testing were assessed, defining the product about prospective applications as food packaging. Effects on the crystallization behavior of a semi-crystalline PLA and induced thermomechanical properties were also studied. An increase in the maximum crystallinity was observed improving the rigidity while the ductility remained satisfying (55 %).

Keywords: poly(lactic acid), PLA, ductility, food packaging, toughening agent, processing aid, biodegradation, oil refinery by-product

5.1. Introduction

Nowadays, the growing environmental concerns generate a significant interest for biodegradable plastics.[1] Meanwhile, because of the price increase of the fossil resources, the development of alternative biobased polymers also becomes economically opportune. There is thus a demand for eco-friendly products provided they have equal or better performances than petrochemical materials commonly used. Among the biobased and biodegradable matrices, polyesters and especially polylactide (PLA)[2] which is already available in large commercial quantities,[3] shows a good potential.[4] Although PLA reaches many of the requirements needed to manufacture efficient thermoplastic films for food packaging, [4a, 5] its poor melt strength compared to polyolefins makes difficult to get a stable bubble during extrusion blowing[4c, 6] and its low ductility[4b, 4d, 7] narrow its usage potential.

Presently, external plasticization is the main solution employed trying to enhance the elongation at break of PLA.[4d, 8] Because of the plasticization physical principle, *i.e.* the free volume increase,[9] improving the drawability, generally means turning the material into the rubbery state leading to a large decrease in the polymer stiffness.[8a, 8c, 8h, 8k, 8m-v, 8x]. In addition, efficient plasticizers usually have a petrochemical origin and are generally added at weight contents from 10 to 30 %.[8a, 8c-f, 8h-w] This reduces the biobased carbon content of the formulated material and may be the cause of failing of the product to comply with biodegradability norms. Besides, many plasticizers contain in their structure chemical moieties having toxicological alerts, so their employment in food contact materials is strictly regulated by legislators, with two types of regulations elaborated by the European and the North American agencies.[10]

Impact modifiers can be an alternative in order to reduce the brittleness while preserving the PLA stiffness and thermal characteristics.[11] However, because of their specific requirements, *i.e.* small immiscible particles of rubber phase with no or low crystallinity, low glass

transition temperature and good interfacial adhesion with PLA,[12] combined with the fact that chemical engineering is predominantly based on petrochemical knowledge, they usually are non-biodegradable copolymers issued from petroleum based materials.[13] Therefore, as for plasticizers, ecological benefits of PLA are generally not retained.

Biodegradable polymers have also been successfully used as toughening agents, like poly(ε-caprolactone),[14] poly(butylene adipate-co-terephthalate),[15] or poly(-R-3-hydroxybutyrate),[16] a highly crystalline and very brittle polyester. Many of those biodegradable polymers are however not readily available in large quantities yet.

Consequently, developing a biobased and biodegradable additive suitable for food contact material, with a low cost and a stable sourcing, could constitute a very attractive product for the industrial development of PLA as a food packaging. Based on these requirements, we identified the oil mill industry as generating natural by-products with an important diversity of relevant organic molecules at various stages: in particular during the refinery process, the deodorization step which consists in blowing steam through heated fat held under high vacuum, sweeps away small volatile components.[17] This classical industrial deodorization process of edible palm oil produces a by-product named the palm oil deodorization condensate (PODC). Presently, oil deodorization condensates are common by-products having a stable sourcing but receiving low value. The goal of our study is to assess the use of this by-product as a biobased and biodegradable additive in order to improve the toughening of PLA.

5.2. Experimental

5.2.1. Materials

Polylactides used in this study were purchased from NatureWorks (U.S.A.). Amorphous PLA 4060D contains 89 ± 1 % L-lactide and 11 ± 1 % D-lactide units (according to the datasheet), making it unable to crystallize under common processing conditions.[4b, 18] Semi-crystalline PLA 4042D contains 96 ± 0.5 % L-lactide and 4 ± 0.5 % D-lactide (according to the datasheet). The glass transition temperatures (T_g) obtained from DSC measurements are respectively about 57 °C and 59 °C (midpoint). PLA 4060D and PLA 4042D average molecular weights obtained from SEC measurements are respectively M_w = 242,800 g.mol^{-1}, M_n = 108,700 g.mol^{-1}, dispersity M_w/M_n = 2,23 ; and M_w = 198,300 g.mol^{-1}, Mn = 111,900 g.mol^{-1}, dispersity M_w/M_n = 1,77.

The palm oil deodorization condensate (PODC), used in this study as a toughening agent in PLA, was supplied by ITERG (Bordeaux, France). Specifications of the palm oil condensate employed are given in **Table 5.2**.

5.2.2. Polymer processing

In order to remove water traces prior to the melt blending process, PLA 4060D and PLA 4042D were respectively dried at 60 °C and 80 °C for 24 hours under dried air using a Motan 100 L Dryer. Melt blending of PODC with PLA 4060D or PLA 4042D was realized using a corotating twin-screw extruder (Dr. Collin) with a screw diameter of 35 mm and a length to diameter ratio (L:D) 56:1. Liquid addition of the PODC was carried out to reach 10 % in PLA weight using a Robatech PuMelt D280 pump heated at 70 °C. The twin-screw extruder temperatures were 180 °C for all zones of the extruder processing neat PLA (introduction in the 1st zone of the extruder) and 60/180/180/180/180/180/180/170/170/160/160/150/140/140/ 140 °C along the extrusion flow when adding PODC (introduction in the 9th zone of the

extruder). Feeding rates were 9 $kg.h^{-1}$ for PLA and 1 $kg.h^{-1}$ for PODC. The twin-screw rotation speed was 250 rpm. Cooling of the strands was done under air. The obtained pellets were stored in hermetic metalized sealed bags to avoid water recapture.

Two film extrusion processes were tested on PLA 4060D/PODC blends. Single screw cast extrusions of neat PLA 4060D and PLA 4060D/PODC films were done using Mapre E1 30 33D single-screw extruder, respectively using temperature profiles 180/180/180/180/180/170/ 170 °C for neat PLA and 160/160/155/150/150/150/145 °C along the extrusion flow, through a flat die of 550 µm thickness and 200 mm width, respectively heated at 170 °C and 140 °C. Films were stretched and cooled with chill rolls rotating at a chosen speed, adjusting the final film thickness to about 30 µm. Blown film of PLA 4060D/PODC was done with Mapre E1 30 33D single-screw extruder using a temperature profile 140/145/150/150/150/150/155 °C along the extrusion flow, mounted with a film blowing device (Dr. Collin) equipped with a spiral die ending in an annular ring of 800 µm thickness and 50 mm diameter heated at 145°C. A blowing ratio of about 2.5 was applied and the rolls speed was adjusted to get a final film thickness of about 25 µm.

Crystallization of neat and formulated PLA 4042D samples was carried out on 1 mm thickness sheets obtained by thermo-molding at 190 °C and 220 bars (Laboratory Press Gibitre Instruments 20 tons). In fact pellets were pre-melted at 190°C without pressure during 180 seconds and then the heated plates were closed with a progressive increase in pressure during 120 seconds to eliminate air bubbles. Obtained sheets were quenched in cold water and some subsequently annealed in an oven at 90 °C for 24 h.

5.2.3. Characterization

5.2.3.1. Composition of the PODC

Glyceride composition of the PODC was determined according both to the IUPAC 6.002 and EN 14105 standards using a Shimadzu GC-2010 Plus gas chromatograph equipped with a Zebron ZB 5 HT Inferno (15 m, 0.25 mm, 0.1 μm) column, and a flame ionization detector set at 380 °C. The vector gas was H_2 at a flow rate of 1.17 $mL.min^{-1}$. The oven temperature was set to 60 °C for 3 min, then raised at 10 $°C.min^{-1}$ to 370 °C and held at 370 °C for 12 min. Samples were injected on-column.

Fatty acid composition of the PODC was determined according to the ISO 12966-2 standard using a Shimadzu GC-2010 Plus gas chromatograph equipped with a BPX70 (50 m, 0.22 mm, 0.25 μm) column and a flame ionization detector set at 250 °C. The vector gas was H_2 at a flow rate of 0.32 $mL.min^{-1}$. The temperature program consisted in an initial isotherm of 2 min at 60 °C, a heating ramp at 20 $°C.min^{-1}$ to 170 °C and isotherm at 170 °C for 25 min, a second ramp at 4 $°C.min^{-1}$ to 230 °C and finally an isotherm at 230 °C for 10 min. The injector temperature was set at 250 °C and a split ratio of 200 was applied.

Water content of the PODC was measured using a Mettler Toledo HB43 S Halogen Moisture Analyzer set at 103 °C.

5.2.3.2. Weighting of PODC content from the formulated PLA materials

Thermogravimetric measurements were conducted using a TGA Q500 thermobalance (TA Instruments). Prior to experiments, weight calibration of the device was performed using calibration weights and temperature calibration by an external thermometer and the Curie point of Nickel. Samples of about 3 mg were heated under N_2 atmosphere (40 $mL.min^{-1}$) between 25 and 500 °C at a heating rate of 10 $°C.min^{-1}$. The chosen comparison temperature at which the PODC amount was estimated into formulated samples was 250 °C because

measurements showed that a large amount of neat PODC was volatilized while only a very low weight loss for neat PLA was observed. Thus, the following calculation was applied to estimate the PODC content in samples. Experiments were carried out in triplicate.

$$\text{PODC wt\%} = \frac{\left(\text{PLA/PODC}_{\text{weight loss}}\right)_{(t)} - 0{,}9*\left(\text{PLA}_{\text{weight loss}}\right)_{(t)}}{\left(\text{PODC}_{\text{weight loss}}\right)_{(t)}} * 100 \quad \textbf{(5.1)}$$

where PODC wt% is the PODC weight content in the formulation and $PLA/PODC_{weight\ loss}$, $PLA_{weight\ loss}$ and $PODC_{weight\ loss}$ are the relative weight loss of the blend, the neat PLA and the neat PODC at 250 °C, respectively.

In order to validate the weighted amount of PODC using the TGA method, about 6 grams of the materials were cut in 0.5 cm^2 pieces and placed into a 125 mL Soxhlet apparatus with 200 mL of ethanol boiled under reflux during 8 h. The extracted PLA samples were dried in an oven for 2 days at 40 °C under vacuum. Then, materials were weighted to determine the weight content of PODC. Analyses were done in triplicate.

5.2.3.3. Size Exclusion Chromatography

The average molecular weight and the dispersity of neat and formulated PLA samples were measured by SEC using a Waters Co. apparatus equipped with an isocratic pump (GILSON 307), a column oven (Waters Control Module II), a gel column (Styragel H5E 7.8 x 300 mm) having a separation range from 2,000 to 1,000,000 $g.mol^{-1}$, an autosampler (Waters 717 plus) and a refractive Index (RI) detector (Waters 2414). Data acquisition and analysis were carried out with the help of Breeze Software. The analyses were performed at 35 °C with tehtrahydrofuran (THF) as eluent at a flow rate of 1 $mL.min^{-1}$. The calibration was done prior to the experiments, based on polystyrene standards (Shodex Standard from Showa Denko range 3,070 to 778,000 $g.mol^{-1}$). For sample preparation neat and formulated PLA pellets

were dissolved in THF (20 mg.L^{-1}) on a shaker at 60 °C for 45 minutes. Analyses were done in triplicate.

5.2.3.4. Differential Scanning Calorimetry (DSC and MDSC)

Standard DSC analyses of neat PODC and PLA 4042D formulations were performed with a Mettler Toledo DSC1 STARe System under nitrogen atmosphere (50 mL.min^{-1}). Calibration of the device was done using Indium and Zinc standards. Samples of around 8 mg were sealed in a 40 µL hermetic aluminum pan. The calorimetric analysis of PODC was carried out with a heating scan at a rate of 10 °C.min^{-1} from -60 to 250 °C. Experiments were done in duplicate. The PLA 4042D crystallinity degree was determined from scan performed at 10°C.min^{-1} from 25 to 200 °C, considering an enthalpy of fusion of 93.1 J.g^{-1} for a 100 % crystalline PLA homopolymer having infinite crystal thickness,[19] using equation (**5.2**). Experiments were performed in duplicate.

$$\chi_c(\%) = \frac{\Delta H_m - \Delta H_c}{\Delta H_{m0} * (1 - W_{PODC})} * 100 \quad \textbf{(5.2)}$$

where χ_c is the PLA crystallinity degree, ΔH_m is the measured heat of fusion, ΔH_c is the heat of cold crystallization, ΔH_{m0} is the enthalpy of fusion of 100 % crystalline PLA homopolymer having infinite crystal thickness and W_{PODC} is the averaged weight fraction of PODC obtained from solvent extraction and TGA measurements.

The glass transition temperature (T_g) of neat and formulated films was investigated using temperature modulated DSC (MDSC) Q100 (TA Instruments). Instrument calibration was done with sapphire standards for calibration of the heat capacity, Indium and Zinc standards for temperature and heat flow calibration. Analyses were carried out under nitrogen flow (50 mL.min^{-1}). Samples of around 4 mg were put into hermetic aluminium pans (TZero, TA Instruments). Heating scans were performed under sinusoidal temperature modulation in “heat

only" mode at a heating rate of 2 °C.min^{-1}, a period of 60 s and a modulation of 0.318 °C from 0 to 85 °C. The T_g was taken from the reversing signal at the midpoint of the heat capacity change. Experiments were carried out in triplicate.

5.2.3.5. Tensile tests

Tensile properties were investigated at 23 °C, a relative humidity (RH) regulated at 50 ± 10 % and a cross-head speed of 25 mm.min^{-1}, using an universal tensile machine (Instron model 4301) equipped with a load cell 100 ± 0.1 N for films and a 1,000 ± 1 N for sheets, both without using an extensometer. The dog bone shaped samples (ISO 527-2, type 5A) were directly cut from the materials. Prior to tensile testing, the samples were conditioned at 23 °C and 50 ± 10 % RH for at least 72 h. Each mechanical value is an average of 8 measurements.

5.2.3.6. Dynamic Mechanical Analysis (DMA)

Measurements were carried out with a DMA Q800 (TA Instruments) at a frequency of 1 Hz and at 0.05 % deformation. Prior to the experiments, calibration of the device was performed using a steel plate with known mechanical properties. Samples were heated from -90 to 160 °C at 2 °C.min^{-1}. Experiments were done in duplicate.

5.2.3.7. Oxygen permeability

Oxygen transmission rate (OTR) was measured with a Mocon Ox-Tran Model 2/21 apparatus at 23 °C and 0 % RH. Oxygen permeability was calculated dividing OTR by the film thickness. Analyses were done in triplicate.

5.2.3.8. Biodegradation

The biodegradation study of the film samples was done according to the EN 14855 standard. Microcrystalline cellulose (44 % carbon content), purchased from Aldrich (France), was used as reference material. Biodegradation was carried out at 58 °C. The testing series consisting of

the film samples, the cellulose reference and a blank, were inoculated by a mature compost (pH = 7.2 ± 0.3 %, C/N = 13.7 ± 0.5 % and organic carbon content = 26.9 ± 0.2 %) supplied by Compomar Company (France). Purified air (without CO_2) was bubbled in each reaction vessel, and air output flow rate was determined with Aalborg AIR 0-10 L/MIN mass flowmeter. Quantification of carbon mineralization was done based on the respirometry principle. The quantity of carbon dioxide generated during fermentation was measured with a Vaisala IR GMP343 sensor calibrated from 200 ppm to 2 %. A weight ratio sample/compost of 1/20 was used both for the reference material and the formulated PLA film. Experiments were done in duplicate.

5.2.3.9. Migration of PODC in food simulants

Quantification of the PODC migration from the PLA 4060D/PODC cast extruded film into food simulants was conducted according to the EN 1186 standard and the Regulation (EU) No 10/2011 on plastic materials and articles intended to come into contact with food (the "Plastics Regulation"). Sunflower oil, ethanol 50 % and acetic acid 3 %, which are simulants of fatty foods, acid foods and milk and dairy products, respectively, were used. Film was cut into 1 dm^2 pieces and placed in contact with food simulants for 10 days at 5 °C or 40 °C using a migration cell. Analyses were done in duplicate.

After the contact time, samples conditioned in sunflower oil food simulant were wiped and placed in a conditioned chamber at 23 ± 2 °C and 50 ± 5 % RH for 16 hours. For analysis of sunflower oil sorbed in the films, samples were extracted using a Soxhlet apparatus for 7 hours with 240 mL pentane plus 10 mL of methyl 7-phenylheptanoate at 0.5 $g.L^{-1}$ in pentane as internal standard. The extract was then reduced to 10 mL with a rotary evaporator (Buchi Rotavapor® R-3000) then dried using a heating plate. The dried extract was dissolved with 10 mL of heptane. Saponification of triglycerides was carried out by addition of 10 mL of KOH at 11 $g.L^{-1}$. For analysis by gas chromatography, methylation of free fatty acids was done

under reflux for 2 min upon addition of 5 mL of BF_3. The solution was dried using sulphate sodium and decanted. The organic phase was analysed by gas chromatography using a Perkin Elmer Clarus 500 apparatus equipped with a SEG Analytical Science BPX70 column (130 m, 0.32 mm, 0.25 µm) and a Flame Ionization detector (FID) set at 250 °C. The oven temperature was programmed to increase from 165 °C to 177 °C at 2 °C.min^{-1} then from 177 °C to 200 °C at 30 °C.min^{-1}. The sample was injected in split mode and the injector port was heated to 250 °C.

For samples tested in aqueous simulants, *i.e.* acetic acid 3 % and ethanol 50 %, the simulants were evaporated to dryness using a heating plate and then a oven set at 107 °C for 1 hour. Dried residues were conditioned at 23 ± 2 °C and 50 ± 5 % RH for 16 hours. The migration was determined by weighting. Experiments were done in triplicate.

5.2.3.10. Sensorial testing

Changes in the flavor and taste of packaged foods were assessed by the Robinson test according to "Analytical Methods of the Office International du Cacao et du Chocolate (OICC)", *Analytical methods page 12 – E/1964:a. Transfer of packaging odours to cacao and chocolate products*. Samples were placed close to pieces of chocolate at 23 °C and 50 % RH into a glass recipient for 48 hours in a dark room. Then panel of 10 trained judges tasted standards and chocolates conditioned with the PLA samples. Flavor and taste changes were evaluated on a scale from 0 to 4. A comparison between neat PLA and formulated film was done after performing Grubbs statistical test, then averaging the marks. In fact, to characterize a packaging, calculations are based on the difference between attributed marks to a "chocolate reference" and a "chocolate sample". The maximum statistical difference (D) authorized was 1, meaning that if the average mark is lower than (D), no modification of the flavor nor the taste was observed.

5.3. Results and Discussion

5.3.1. Processability of PLA/PODC blends and effects of the process on molecular weight of PLA and PODC contents

Both the twin-screw extrusions of the neat PLA 4060D and the neat PLA 4042D were realized at 180 °C with a screw rotation speed of 250 rpm. The residence time was measured by coloured pellets to be about 6 min. This temperature was high enough to plasticize/melt PLA pellets without exceeding the maximum admissible torque of the device, determined from the amount of the electric charge (A) provided to the motor.

When 10 wt% PODC was introduced in the extruder in its mid length (9^{th} zone on 15), an important lowering in the torque, was observed. In fact, at 180 °C and 250 rpm, the torque diminished by a factor 2, *i.e.* from about 14 to 7 A. Temperatures of the 9^{th} to 15^{th} zones were then decreasingly set from 170 °C to 140 °C along the extrusion flow, raising the melt viscosity of the blend to get towable strands. The temperatures of the 1^{st} to 8^{th} zones remained at 180 °C. Using these conditions, the torque raised (electric charge ≈ 12 A), with a significantly lowered deviation than that observed when processing neat PLA. The residence time was measured to be about 5 min, which is quite briefer than for neat PLA. Actually, PODC acted in both cases as a processing aid stabilizing the extrusion flow and lowering the extrusion temperatures.

Single screw cast extrusion of neat PLA 4060D and PLA 4060D/PODC films showed similar behavior as observed during the melt-blending step. The required temperatures profile to extrude the neat PLA 4060D film was 170/180/180/180/180/170 °C with a screw rotation speed of 30 rpm and a flat die heated at 170 °C, giving an output flow rate of about 2.4 $kg.h^{-1}$. Using the same conditions, the PLA/PODC blend was not filmable because of its too low melt-strength. When maintaining the same screw rotation speed, the temperatures profile of

the extruder had to be 170/165/160/155/150/145 °C along the extrusion flow, and the flat die heated at 140 °C to get a semi-solid sheet able to be cast with chill rolls. The obtained ouput film rate flow of PLA/PODC mixture was about 3.1 $kg.h^{-1}$, which is higher than for neat PLA while temperatures were lower.

Blown film of neat PLA 4060D was impossible to obtain because of the too high temperature needed (≈ 180 °C) to extrude the PLA. In fact, at this temperature the melt strength of PLA is insufficient to yield the weak semi-solid tube. In contrast, by using PODC as a processing aid capable of lowering the required extrusion temperatures, blown film of PLA/PODC mixture was obtained. The extruder temperatures profile was 140/145/150/155/155/155 °C along the extrusion flow. The blowing die had however to be heated warmer (155 °C) than the flat die (140 °C) in order to get the adequate melt strength of the material. The blown film output of PLA/PODC mixture was about 3.0 $kg.h^{-1}$, which is similar to the output by cast extrusion process.

Molecular weights of neat PLA and PLA/PODC pellets, films and sheets are given in Table 5.1. A reduction of both the molecular weights in number (Mn) and weight (Mw), with an increase in the dispersity (I) is observed after processing. Despite the vigorous drying of PLA pellets before processing, the polymer most probably suffered thermo-hydrolysis being the main degradation mechanism of PLA.20 PODC introduction brings about additional reduction in chain length. One reason might be additional water brought into the melt, as water is contained in PODC (0.16 wt%). Furthermore, the acid groups of fatty acids might cause chain scission by transesterification (acidolysis), a process described for other additives holding reactive hydroxyl or carboxylic groups.[8n, 21]

Table 5.1 PODC content and molar weight averages and dispersitiy of PLA and PLA/PODC formulations

Sample	PODC Content		Molecular Weights		
	(Soxhlet extraction method)	*(Thermogravimetric method)*	*(Size exclusion Chromatography)*		
	Content *(wt %)*	**Content** *(wt %)*	**Mw** *(g/mol)*	**Mn** *(g/mol)*	**I**
PLA 4060D (neat pellets)	-	-	242,800 ± 2,100	108,700 ± 2,200	2.2 ± 0.1
PLA 4060D (twin-screw extruded pellets)	-	-	221,000 ± 3,600	90,200 ± 1,100	2.5 ± 0.1
PLA 4060D (cast extruded film)	-	-	209,600 ± 4,200	83,600 ± 1,800	2,5 ± 0,1
PLA 4060D/PODC (twin-screw pellets)	8.4 ± 0.5	9.0 ± 0.2	194,300 ± 3,700	84,100 ± 3,000	2.3± 0.1
PLA 4060D/PODC (cast extruded film)	8.1 ± 0.3	8.7 ± 0.1	164,100 ± 4,800	77,400 ± 3,600	2.1 ± 0.2
PLA 4060D/PODC (blown extruded film)	7.7 ± 0.6	8.4 ± 0.2	152,600 ± 4,200	73,200 ± 2,900	2.1 ± 0.1
PLA 4042D (neat pellets)	-	-	198,300 ± 2,200	111,900 ± 3,200	1.8 ± 0.1
PLA 4042D (twin-screw pellets)	-	-	182,300 ± 2,900	92,100 ± 900	2.0 ± 0.1
PLA 4042D (thermo-molded sheet)	-	-	173,300 ± 3,000	83,700 ± 4,100	2.1 ± 0.1
PLA 4042D (thermo-molded sheet + annealed 24 h at 90°C)	-	-	160,100 ± 1,900	70,600 ± 4,400	2.3 ± 0.2
PLA 4042D/PODC (twin-screw pellets)	8.3 ± 0.4	8.1 ± 0.3	156,600 ± 4,300	87,400 ± 4,000	1.8 ± 0.1
PLA 4042D/PODC (thermo-molded sheet)	7.6 ± 0.3	7.9 ± 0.1	144,100 ± 2,000	83,400 ± 2,400	1.7 ± 0.1
PLA 4042D/PODC (thermo-molded sheet + annealed 24 h at 90°C)	6.1 ± 0.4	6.4 ± 0.3	121,000 ± 4,100	66,600 ± 1,900	1.8 ± 0.1

The amount of PODC in the pellets and films was characterized by a thermogravimetric method (**Table 5.1**). Thermogravimetric curves of neat PLA 4060D pellets, neat PODC and blended PLA 4060D/PODC pellets are shown in **Figure 5.1**. The amounts of PODC determined by TGA agree with the results by Soxhlet extraction. However, the PODC contents by both methods are lower than the expected value of 10 % of PLA weight. Thus, the PODC provided during the melt-blending process was not totally incorporated into PLA. More, the materials made from the formulated pellets through a second process, *i.e.* a film extrusion or thermo-molding, show even lower PODC contents. The thermogravimetric curve of neat PODC shown in **Figure 5.1** indicates a weight loss starting around 140 °C with a maximal loss speed reached at 195 °C. Because the different samples processes require setpoint temperatures upper than 140 °C, a part of PODC was volatilized. Furthermore, the PODC content in the blown film is lower than in the cast extruded film. In fact, the blowing die was set at 155 °C while the flat die was heated at 140 °C, likely boosting the volatilization. In addition, the blowing die system is quite longer than the flat die one, possibly extending this phenomenon.

Same observations are conducted on sheets made of PLA 4042D and PODC. Each thermal process (thermos-molding and annealing in oven) induced an additional decrease in the PODC content.

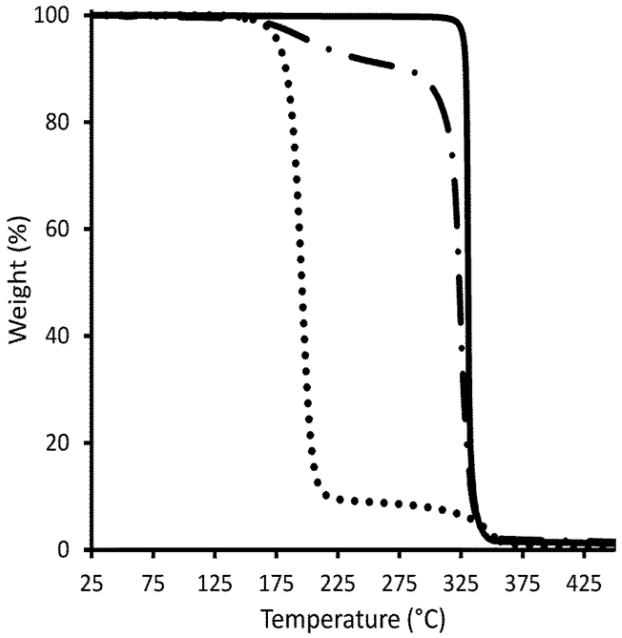

Figure 5.1 Thermogravimetric curves of neat PLA 4060D pellets, neat PODC and PLA 4060D/PODC blend pellets (—) neat PLA 4060D ; (• •) neat PODC ; (— •) PLA 4060D/PODC pellets

5.3.2. Thermal and mechanical properties of amorphous PLA 4060D/PODC blends

Table 5.2 shows the determined fats composition of the palm oil deodorization condensate. The free fatty acids amount is huge compared to the glycerides one.

Table 5.2 Composition of the PODC

	Type	**Content** *(%)*
Glyceride Composition	Free Fatty Acids	95.4
	Mono Glycerides	1.7
	Di Glycerides	2.2
	Tri Glycerides	0.7
Water		0.16

	Usual Name	**Formula**	**Content** *(%)*
Fatty Acid Composition	Lauric Acid	C12:0	0.4
	Myristic Acid	C14:0	1.3
	Palmitic Acid	C16:0	49.8
	Palmitoleic Acid	C16:1 cis	0.2
	Stearic Acid	C18:0	4.1
	Oleic Acid	C18:1 cis	35.0
		C18:1 trans	0.2
	Linoleic Acid	C18:2 cis	7.7
		C18:2 trans	0.1
	Linolenic Acid	C18:3 cis	0.3
	Arachidic Acid	C20:0	0.3
	Eicosenoic Acid	C20:1 cis	0.1
	Unidentified	-	0.7

Table 5.3 gives thermal properties of the films measured by MDSC. This methodology was chosen for analysis of T_g, because PODC contains a mixture of saturated and unsaturated fatty acids which can crystallize. In fact, the melting of palmitic acid crystals contained in PODC happens in the same temperature range as the PLA glass transition. Unsaturated fatty acid molecules such as linoleic acid ($T°_{melt}$ = -14 and -7 °C)[22] or oleic acid ($T°_{melt}$ = 13 °C)[22] are liquid at room temperature, while saturated ones such as palmitic ($T°_{melt}$ = 63 °C)[22] acid are crystallized.[22] Blending of PLA with about 8 wt% PODC decreased T_g only by 14 °C, which is caused by the low miscibility of both compounds.[23] The width of the glass transition (midpoint – onset) of PLA 4060D/PODC films is larger than that of neat PLA 4060D. This indicates higher material heterogeneity, probably due to the poor miscibility of PODC in PLA.

Table 5.3 Physical properties of PLA 4060D and PLA 4060D /PODC films

	Aging	**Glass transition** *(MDSC)*		**Tensile properties**					**Barrier properties**
	(Ambient Conditions)	**Onset** *(°C)*	**Tg** *(°C)*	**Elongation at break** (%)	**Young Modulus** (MPa)	**Stress at yield** *(MPa)*	**Elongation at yield** *(%)*	**Stress at break** (MPa)	**O2 permeability** *(*10^{18}*.*m^3*.*m*.*m^{-2}*.*s^{-1}*.*Pa^{-1}*)*
PLA 4060D (Cast extruded film)	T_0-	57 ± 0.2	57.7 ± 0.1	6 ± 1	1,520 ± 85	56 ± 3	4.3 ± 0.2	55 ± 3	3.26 ± 0.05
	6 months	55.8 ± 0.4	56.0 ± 0.3	5 ± 2	1,670 ± 90	64 ± 5	3.9 ± 0.1	62 ± 2	3.02 ± 0.09
PLA 4060D/ PODC (Cast extruded film)	T_0-	39.2 ± 0.3	43.1 ± 0.6	135 ± 25	1,330 ± 50	29 ± 2	2.3 ± 0.1	22 ± 2	3.31 ± 0.08
	6 months	48.0 ± 0.2	48.6 ± 0.3	90 ± 25	1,420 ± 55	35 ± 3	2.3 ± 0.2	24 ± 1	3.20 ± 0.11
PLA 4060D/ PODC (Blown extruded film)	T_0-	40.2 ± 0.6	44.0 ± 0.4	100 ± 15	1,260 ± 70	24 ± 1	2.5 ± 0.1	22 ± 2	3.17 ± 0.07
	6 months -	46.0 ± 0.2	47.4 ± 0.2	65 ± 20	1,340 ± 35	27 ± 2	2.2 ± 0.2	25 ± 1	2.96 ± 0.08

Figure 5.2 exhibits the stress/strain curves of PLA 4060D and PLA 4060D/PODC films. Quantified properties are listed in **Table 5.3**. The addition of PODC in PLA 4060D increased considerably the elongation at break of PLA 4060D without much decreasing the Young modulus. Stress at yield and elongation at yield were nearly halved. In fact, the poor miscibility of PODC in PLA led to the inclusion of a dispersed phase into the glassy matrix, promoting the cavitation mechanism and appearance of crazes observed through an extensive stress whitening of the films.[23] Each inclusion acts as a stress concentration point enabling the drawability mainly through the debonding of interfaces between the dispersed phase and the

matrix. Such mechanism allows ensuring a better sharing of the mechanical energy during the stretching process[8t] and retaining an acceptable stiffness due to the remaining glassy state of the polymer. The blown film showed shorter elongation at break and lower stress at yield than the cast film, although PODC concentrations were close. The blowing method consists in inflating a semi-solid tube of PLA, which may induce some additional mechanical stress and likely may lower the elastic capacity of the material. In both cases, obtained mechanical properties could be of interest for food packaging films requiring high stiffness and drawability.

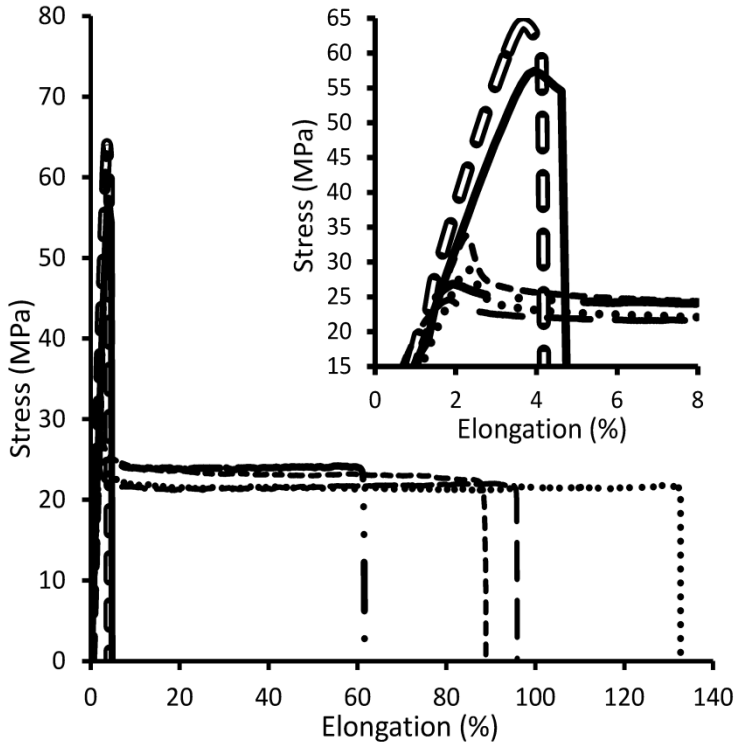

Figure 5.2 Stress-strain curves of PLA 4060D and PLA 4060D/PODC films

(—) PLA 4060D cast extruded film ; (= =) PLA 4060D cast extruded film aged 6 months ;

(• •) PLA 4060D/PODC cast extruded film ; (- -) PLA 4060D/PODC cast extruded film aged 6 months ;

(— —) PLA 4060D/PODC blown extruded film ; (— • •) PLA 4060D/PODC blown extruded film aged 6 months

5.3.3. Oxygen barrier properties of amorphous PLA 4060D/PODC films

Oxygen barrier is an important use property of food packaging. Therefore the PLA 4060D/PODC films were tested and results are presented in **Table 5.3**. The measured oxygen permeability of the neat PLA films was consistent with the literature values ranging from 1.2 to 4.3 $*10^{18}.m^3.m.m^{-2}.s^{-1}.Pa^{-1}$.[8n, 24] The value is in the higher permeability range likely because of the high D-lactide content in PLA 4060D, which induces higher irregularity in the chain packing. Interestingly, despite a decrease in T_g of the PLA 4060D/PODC films, the oxygen permeability was maintained. So in opposite to conventional plasticizers of PLA which are largely soluble into the matrix but lead to an important decrease of the oxygen barrier,[8n, 8o] PODC present as inclusion of insoluble particles maintains the barrier properties of neat PLA. PODC may therefore be suitable for applications where the demand of oxygen barrier of PLA is sufficient.

5.3.4. Aging of amorphous PLA 4060D/PODC films at ambient conditions

The stability of PLA 4060D/PODC films at ambient conditions (25 ± 5 °C) was tested after storage of the films for 6 months. The glass transition values of aged films are given in **Table 5.3**. Stress-strain typical curves are shown in **Figure 5.2** in comparison to the initial samples and mechanical properties quantification is given in **Table 5.3**. We observe that the width of the glass transition decreased and the T_g of blends increased. This change may be explained by some exudation or phase separation of PODC. It is however important to note that films surfaces did not become greasy or sticky with time.

Studying the heat flow of MDSC analyses (**Figure 5.3**) a growth of the enthalpy relaxation peak is observed with aging time. Increased aging rate of plasticized PLA was recently shown.[25] Oxygen permeability (**Table 5.3**) was used as a structure probe for densification phenomena during physical aging.[8v, 8x, 26] In the present case, no change is observed, even for the neat PLA 4060D. No significant densification due to physical aging occurred over the

tested time period. The aging behavior of the present additive with low solubility is thus very different from the one of miscible plasticizers where barrier properties increased with aging.[8v, 8x, 26] Embrittlement of samples is observed (**Table 5.3**). Even if no densification was shown by oxygen permeability, mobility of polymers is reduced during physical aging, but at a lesser degree compared to commonly used petrochemical plasticizers of PLA.[8v, 8x, 27]

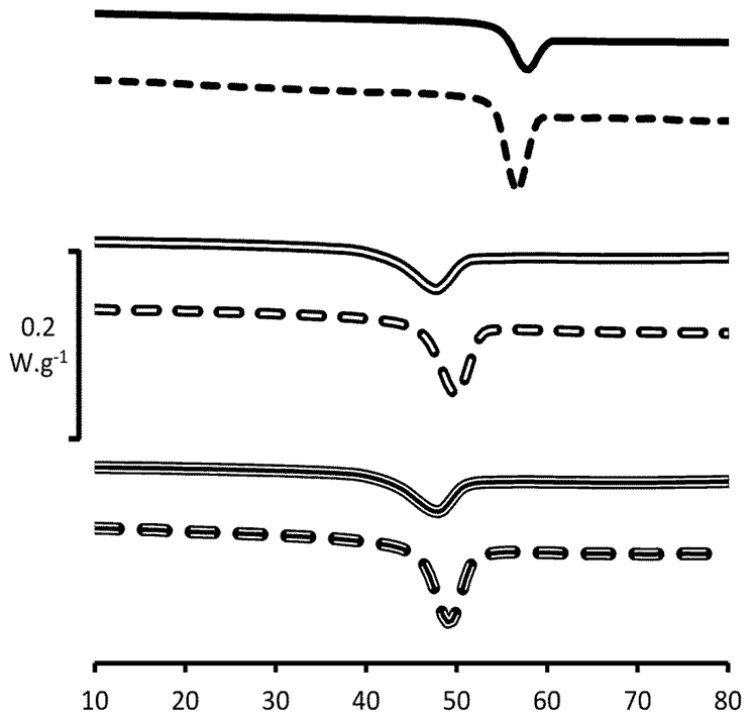

Figure 5.3 Heatflow (exo-up) of PLA 4060D and PLA4060D/PODC films measured by MDSC
(—) PLA4060D film ; (– –) PLA 4060D film aged 6 months ; (=) PLA 4060D/PODC cast extruded film ;
(= =) PLA 4060D/PODC cast extruded film aged 6 months ; (≡) PLA 4060D/PODC blown extruded film ;
(≡ ≡) PLA 4060D/PODC blown extruded film aged 6 months

5.3.5. Effect of crystallization of PLA 4042D/PODC blends on thermal and mechanical properties

Most PLA grades are semi-crystalline. In the case of food packaging, crystallization of the polymer is favorable for most applications. Therefore we investigated crystallization on PLA 4042D/PODC blends on thermo-molded sheets by DSC analysis. Thermograms of the samples are presented in **Figure 5.4** and calorimetric data in **Table 5.4**. The fabrication of sheet

by thermo-moulding and quenching of PLA 4042D yields an almost amorphous sample. Annealing at 90 °C for 24 h allows for crystallizing PLA 4042D with a large melting endotherm, because of the formation of crystallites in α-form.[8o, 28] The addition of PODC speeded up the kinetics of crystallization. In fact, the sheet fabrication process yielded semi-crystalline samples despite quenching. The thermogram (**Figure 5.4**) shows furthermore cold crystallization during the heating scan. A small exotherm before the melting peak can be observed, due to the α to δ-form (former α') crystalline phase transition.[29] Moreover, the glass transition of the crystallized neat PLA 4042D is less visible, get more widen and the T_g is higher than the amorphous one. For samples containing PODC, increasing the crystallinity lead to a lowering of the T_g likely due to an enrichment in plasticizer of the amorphous phase at the expense of the crystalline one.[8r]

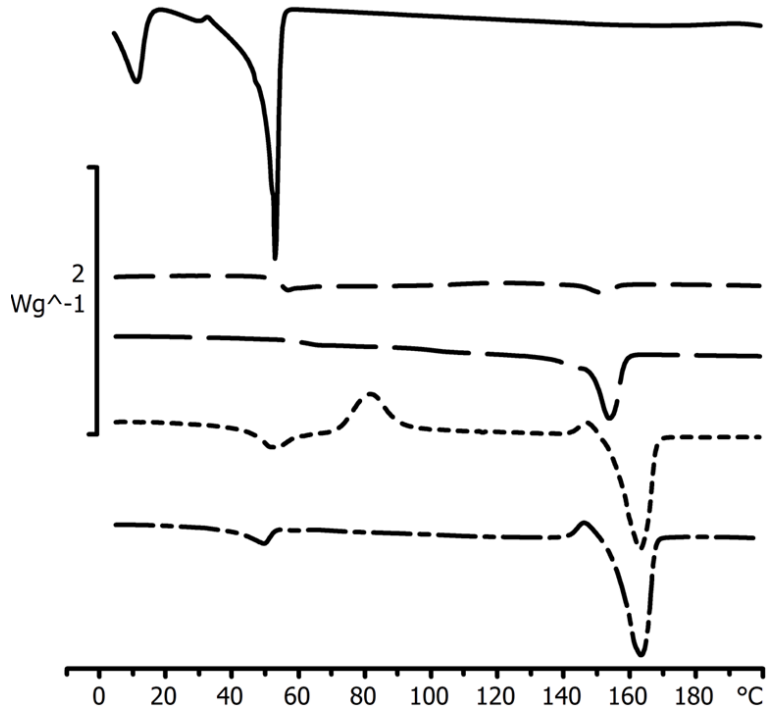

Figure 5.4 Heatflow (exo-up) of neat PODC, PLA 4042D and PLA 4042D/PODC sheets measured by DSC
(—) neat PODC ; (– –) PLA 4042D sheet quenched ;
(— —) PLA 4042D sheet quenched and annealed at 90 °C for 24 h ; (- -) PLA 4042D/PODC sheet quenched ;
(– -) PLA 4042D/PODC sheet quenched and annealed at 90 °C for 24 h

Table 5.4 Physical properties of neat PLA 4042D and PLA 4042D/PODC sheets

	Process	DSC		Tensile properties				
		χ_c *(%)*	T_g *(°C)*	**Elongation at break** (%)	**Young Modulus** (MPa)	**Stress at yield** *(MPa)*	**Elongation at yield** *(%)*	**Stress at break** *(MPa)*
PLA 4042D	Quenched	< 2	56.9 ± 0.3	6 ± 1	1,550 ± 85	57 ± 4	4.8 ± 0.1	55 ± 2
	Quenched and annealed at 90 °C for 24h	35 ± 1	60.2 ± 0.3	5 ± 2	1,710 ± 70	-	-	70 ± 6
PLA 4042D/ PODC	Quenched	20 ± 2	46.1 ± 0.4	10 ± 45	1,200 ± 115	20 ± 2	1.7 ± 0.1	19 ± 2
	Quenched and annealed at 90 °C for 24h	48 ± 2	39.8 ± 0.3	55 ± 10	1,195± 95	21 ± 1	1.8 ± 0.2	21 ± 1

Stress-strain curves of the samples are presented in **Figure 5.5** and mechanical data in **Table 5.4**. While the amorphous PLA 4042D fractures just after a yield, showing some plasticity, the crystallized one breaks before and exposes a higher rigidity. The non-annealed blend of PLA 4042D/PODC shows a close elongation at break to the fully amorphous despite a crystallinity of about 20 % and a brief peak observed just after yielding, likely due to strain-induced crystallization. Low crystallinity level has been established as being advantageous for development of crazes in semi-crystalline polymers,[30] mechanism involved in the improvement of the drawability when adding PODC.[23] It could therefore be the reason of the unchanged elongation at break properties. *A contrario*, stress at yield was lowered compared to amorphous films, presumably due to the probable enrichment in PODC of the amorphous phase over the crystallization. Moreover the most crystallized blend of PLA 4042D/PODC showed halved elongation at break compared to the non-annealed reference. In fact, the deformation of crystals in polymers requires a high energy,[31] likely far stronger than the one needed to activate crazing, which is facilitated by PODC. Therefore, crystallized parts would not be deformed, lowering the elongation at break. Contrariwise, rigidity and resilience remained similar to the non-annealed reference, regardless of the probable additional enrichment in PODC of the amorphous phase due to further crystallization. PODC phase separation due to the crystallization was further investigated by dynamical mechanical analysis.

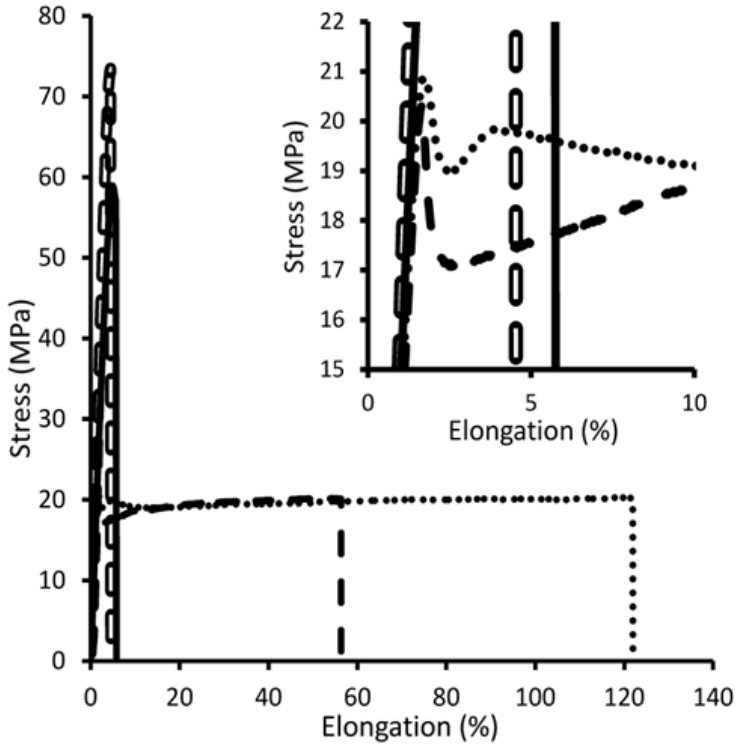

Figure 5.5 Stress-strain curves of neat PLA 4042D and PLA 4042D/PODC sheets
(—) PLA 4042D sheet quenched ; (= =) PLA 4042D sheet quenched and annealed at 90 °C for 24 h ; (• •) PLA 4042D/PODC sheet quenched ; (– –) PLA 4042D/PODC sheet quenched and annealed at 90 °C for 24 h

The evolution of the storage and loss moduli with temperature is plotted in **Figure 5.6**. PODC logically leads to a significant decrease of both the storage and loss moduli in the glassy plateau, compared to the neat semi-crystalline PLA 4042D. Increase of crystallinity of the formulated sheets induced a slight gain in both moduli in the glassy plateau. α-relaxation of formulated materials determined from the log E" peaks increased with crystallinity from 46 to 57 °C which is not consistent with the T_g determined from the DSC experiments. In fact, onsets remain similar (33 °C) but the log E" peak is broadened by crystallization. Rigidification of the amorphous phase (RAF)[32] due to reduced size of cooperative rearranging regions (CRR)[33] could explain this phenomenon. β-relaxation is seen from E" at low temperatures with semi-crystalline formulated materials but is not present with neat PLA. Increase of the crystallinity induced a diminution of the β-relaxation temperature from about

-23 to -54 °C. Decrease of the β-relaxation temperature could therefore point out an enrichment of PODC in the amorphous phase.[8t, 34]

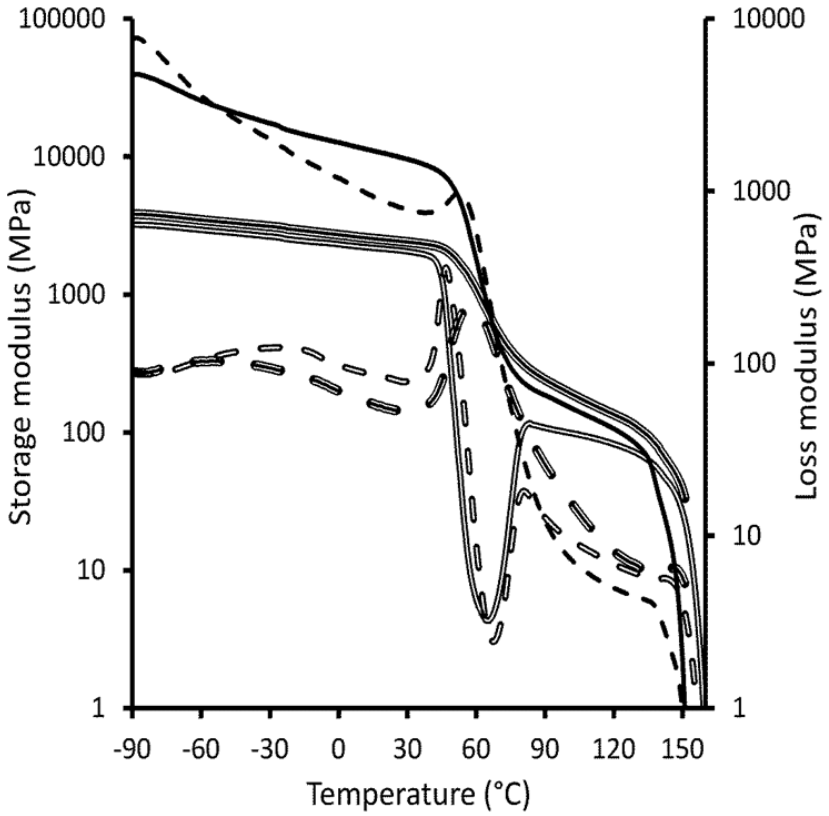

Figure 5.6 E' and E" curves of PLA 4042D and PLA4042D/PODC sheets measured by DMA (—) ; storage modulus of PLA 4042D sheet quenched and annealed at 90 °C for 24 h ; (=) storage modulus of PLA 4042D/PODC sheet quenched ; (≡) storage modulus of PLA 4042D/PODC sheet quenched and annealed at 90 °C for 24 h ; (– –) loss modulus of PLA 4042D sheet quenched and annealed at 90 °C for 24 h ; (= =) loss modulus of PLA 4042D/PODC sheet quenched and (≡ ≡) loss modulus of PLA 4042D/PODC sheet quenched and annealed at 90 °C for 24 h

5.3.6. Compliance of PLA 4060D/PODC film with requirements of Food Contact Material regulation

Suitability for food packaging of the PLA 4060D/PODC cast extruded film was evaluated with the help of normed migration testing after the European Regulation and sensorial evaluation. The films were evaluated as to the overall migration to food simulants. The food simulants were sunflower oil for fatty foods, ethanol 50 vol% for dairy products, and acetic acid 3 vol% for acidic aqueous foods and drinks. Testing at 5 °C simulates refrigerated

storage conditions, testing at 40 °C ambient storage conditions. Results are presented in **Table 5.5**. The criteria of compliance with the EU regulation required i) that the overall migration doesn't exceed 10 mg of additive leached out from 1 dm^2 packaging film (and 60 $mg.kg^{-1}$), and ii) the physical aspect of the material is not altered by the test conditions. The overall migration of additives from PLA 4060D/PODC film into the food simulants complied with the regulation in all cases, except for acidic foods and drinks at ambient conditions. Whitening of the films occurred with ethanol 50 vol% and acetic acid 3 vol% simulants at 40 °C, as shown in **Figure 5.7**. The change in physical appearance due to interaction of PLA with ethanol at 40 °C, the PLA 4060D/PODC samples failed the compliance for dairy foods stored at ambient temperature. Consequently, the blends can be approved for all types of simulated foods at refrigerated storage conditions, but only for fatty foods at ambient storage conditions.

Table 5.5 Overall migration tests in food simulants of PLA 4060D/PODC cast film

Food simulant / Temperature	Vegetable oil		Ethanol 50 vol%		Acetic acid 3 vol%	
	Overall migration *(mg/dm²)*	**Physical appearance change**	**Overall migration** *(mg/dm²)*	**Physical appearance change**	**Overall migration** *(mg/dm²)*	**Physical aspect change**
5	< 1	No	< 1	No	< 1	No
40	< 1	No	< 1	Yes	18.4	Yes

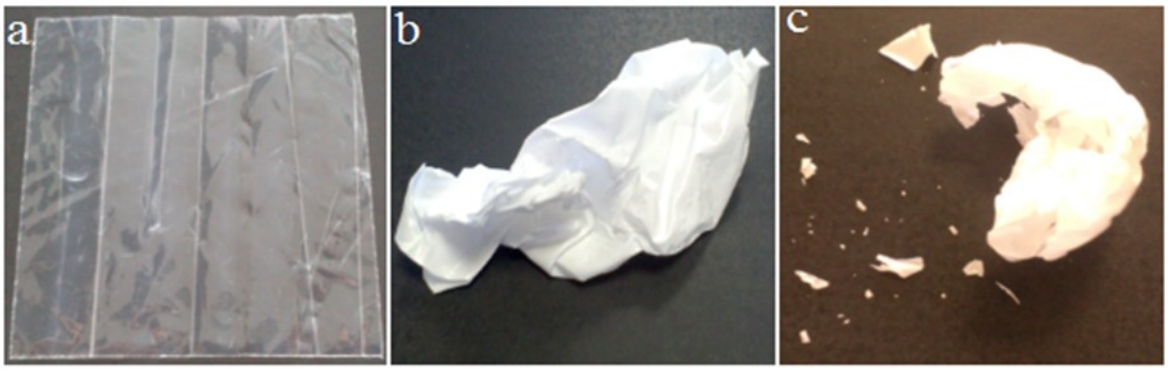

Figure 5.7 Physical aspect change of PLA 4060D/PODC cast film after testing during 10 days at 40 °C in ethanol 50 vol% and acetic acid 3 vol%

(a) PLA 4060D/PODC film reference ; **(b)** PLA 4060D/PODC film after 10 days at 40 °C in ethanol 50 vol% ; **(c)** PLA/PODC film after 10 days at 40 °C in acetic acid 3 vol%

The change in flavors or tastes from packaging to food was assessed by the Robinson test. Differences were noted on a scale between 0 and 4, *i.e.* from no taste difference to strong taste difference. Neat PLA 4060D film received an average mark of 0, whereas the PLA 4060D/PODC cast film obtained an average mark of 0.25 ± 0.79, which is not statistically different from the reference sample. No deterioration of the sensorial properties due to PLA and PLA/PODC blends was observed, which makes the films suitable for food packaging.

5.3.7. Biodegradation of the PLA 4060D/PODC cast extruded film

The biodegradability of the PLA 4060D/PODC cast film was assessed according to the EN 14855 standard. The biodegradation curve is given in **Figure 5.8**. Biodegradation of 90 % of the carbon content of PLA 4060D/PODC film compared to the reference material was obtained after 60 days. The film therefore complies with the requirements of biodegradability.

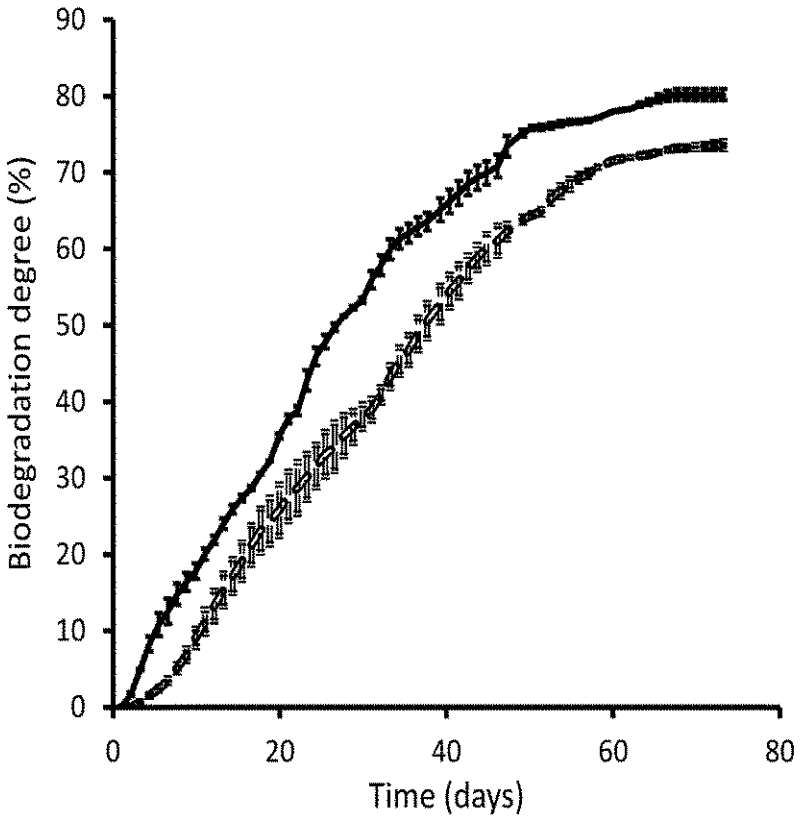

Figure 5.8 Biodegradation curves of cellulose reference and PLA 4060D/PODC cast film
(—) cellulose reference ; (= =) PLA 4060D/PODC cast extruded film

5.4. Conclusion

PODC, a natural and biodegradable by-product of oil refinery, successfully improved the elongation at break of amorphous PLA as well as the semi-crystalline one, while retaining its interesting stiffness and glassy state. Processing aid abilities were pointed out, reducing the required heating temperatures and enabling the film blowing extrusion process of PLA. Speeding up of the crystallization kinetic was also noted with an increase in the maximum degree of crystallinity. Oxygen permeability of formulated films remained close to that of neat PLA, allowing to preserve markets where PLA is already suitable for packaging. Aging behavior of films after 6 months stored at ambient conditions showed an ordinary embrittlement process with a slower decrease of mechanical properties as observed with usual plasticizers. Biodegradation of the blends was fully achieved and compliance with requirements of the food contact materials regulation was obtained for all types of simulated foods at refrigerated storage conditions and fatty food at ambient storage conditions. More, preservation of the PLA biodegradability blended with PODC would be of interest because fatty food packages are often soiled with fat prohibiting recyclability. Cheese packaging could therefore constitute an appropriate application.

Acknolewdgements

This work was financially supported by Brodart Packaging and the BIP-ADEME French project CREABioM. The authors also gratefully thank the following laboratories: Institut des Corps Gras (ITERG – Bordeaux, France), Laboratoire National de Métrologie et d'Essais (LNE – Trappes, France) and MateriaNova (Ghishlenghien, Belgium) for their technical support.

REFERENCES

1. Markarian, J., Biopolymers present new market opportunities for additives in packaging. *Plastics, Additives and Compounding* 2008, *10* (3), 22-25.

2. Tuominen, J.; Kylmä, J.; Kapanen, A.; Venelampi, O.; Itävaara, M.; Seppälä, J., Biodegradation of Lactic Acid Based Polymers under Controlled Composting Conditions and Evaluation of the Ecotoxicological Impact. *Biomacromolecules* 2002, *3* (3), 445-455.

3. Lunt, J., Large-scale production, properties and commercial applications of polylactic acid polymers. *Polymer Degradation and Stability* 1998, *59* (1–3), 145-152.

4. **(a)** Weber, C. J., Biobased Packaging Materials for the Food Industry - Status and perspectives*, Danemark* 2000.
b) Auras, R.; Harte, B.; Selke, S., An Overview of Polylactides as Packaging Materials. *Macromolecular Bioscience* 2004, *4* (9), 835-864.
(c) Lim, L. T.; Auras, R.; Rubino, M., Processing technologies for poly(lactic acid). *Progress in Polymer Science* 2008, *33* (8), 820-852.
(d) Sinclair, R. G., The Case for Polylactic Acid as a Commodity Packaging Plastic. *Journal of Macromolecular Science, Part A* 1996, *33* (5), 585-597.
(e) Vert, M.; Schwarch, G.; Coudane, J., Present and Future of PLA Polymers. *Journal of Macromolecular Science, Part A* 1995, *32* (4), 787-796.

5. **(a)** Conn, R. E.; Kolstad, J. J.; Borzelleca, J. F.; Dixler, D. S.; Filer Jr, L. J.; Ladu Jr, B. N.; Pariza, M. W., Safety assessment of polylactide (PLA) for use as a food-contact polymer. *Food and Chemical Toxicology* 1995, *33* (4), 273-283.
(b) Mauricio-Iglesias, M.; Jansana, S.; Peyron, S.; Gontard, N.; Guillard, V., Effect of high-pressure/temperature (HP/T) treatments of in-package food on additive migration from conventional and bio-sourced materials. *Food Additives & Contaminants: Part A* 2009, *27* (1), 118-127.

6. Sodergard, A.; Selin, J.-F.; Niemi, M.; Johansson, C.-J.; Meinander, K. Processable Poly(hydroxy Acids). 2003.

7. Anderson, K. S.; Schreck, K. M.; Hillmyer, M. A., Toughening Polylactide. *Polymer Reviews* 2008, *48* (1), 85-108.

8. **(a)** Labrecque, L. V.; Kumar, R. A.; Davé, V.; Gross, R. A.; McCarthy, S. P., Citrate esters as plasticizers for poly(lactic acid). *J. Appl. Polym. Sci.* 1997, *66* (8), 1507-1513.
(b) Martin, O.; Averous, L., Poly(lactic acid): plasticization and properties of biodegradable multiphase systems. *Polymer* 2001, *42* (14), 6209-6219.
(c) Baiardo, M.; Frisoni, G.; Scandola, M.; Rimelen, M.; Lips, D.; Ruffieux, K.; Wintermantel, E., Thermal and mechanical properties of plasticized poly(L-lactic acid). *Journal of Applied Polymer Science* 2003, *90* (7), 1731-1738.
(d) Ljungberg, N.; Wesslén, B., The effects of plasticizers on the dynamic mechanical and thermal properties of poly(lactic acid). *Journal of Applied Polymer Science* 2002, *86* (5), 1227-1234.
(e) Ljungberg, N.; Andersson, T.; Wesslén, B., Film extrusion and film weldability of poly(lactic acid) plasticized with triacetine and tributyl citrate. *Journal of Applied Polymer Science* 2003, *88* (14), 3239-3247.
(f) Ljungberg, N.; Wesslen, B., Preparation and properties of plasticized poly(lactic acid) films. *Biomacromolecules* 2005, *6* (3), 1789-1796.
(g) Martino, V.; Ruseckaite, R.; Jiménez, A., Thermal and mechanical characterization of plasticized poly (L-lactide-co-D,L-lactide) films for food packaging. *Journal of Thermal Analysis and Calorimetry* 2006, *86* (3), 707-712.

(h) Murariu, M.; Da Silva Ferreira, A.; Alexandre, M.; Dubois, P., Polylactide (PLA) designed with desired end-use properties: 1. PLA compositions with low molecular weight ester-like plasticizers and related performances. *Polymers for Advanced Technologies* 2008, *19* (6), 636-646.
(i) Yang, S. L.; Wu, Z. H.; Meng, B.; Yang, W., The Effects of Dioctyl Phthalate Plasticization on the Morphology and Thermal, Mechanical, and Rheological Properties of Chemical Crosslinked Polylactide. *J. Polym. Sci. Pt. B-Polym. Phys.* 2009, *47* (12), 1136-1145.
(j) Martino, V. P.; Jimenez, A.; Ruseckaite, R. A., Processing and Characterization of Poly(lactic acid) Films Plasticized with Commercial Adipates. *J. Appl. Polym. Sci.* 2009, *112* (4), 2010-2018.
(k) Lemmouchi, Y.; Murariu, M.; Dos Santos, A. M.; Amass, A. J.; Schacht, E.; Dubois, P., Plasticization of poly(lactide) with blends of tributyl citrate and low molecular weight poly(D,L-lactide)-b-poly(ethylene glycol) copolymers. *European Polymer Journal* 2009, *45* (10), 2839-2848.
(l) Wang, R. Y.; Wan, C. Y.; Wang, S. F.; Zhang, Y., Morphology, Mechanical Properties, and Durability of Poly(Lactic Acid) Plasticized With Di(Isononyl) Cyclohexane-1,2-Dicarboxylate. *Polymer Engineering and Science* 2009, *49* (12), 2414-2420.
(m) Sierra, J.; Noriega, M.; Cardona, E.; Ospina, S., Relationship between properties, citrate content and postproduction time for a plasticized polylactic acid. *ANTEC 2010 [Proceedings]* 2010.
(n) Courgneau, C.; Domenek, S.; Guinault, A.; Averous, L.; Ducruet, V., Analysis of the Structure-Properties Relationships of Different Multiphase Systems Based on Plasticized Poly(Lactic Acid). *J. Polym. Environ.* 2011, *19* (2), 362-371.
(o) Courgneau, C.; Domenek, S.; Lebossé, R.; Guinault, A.; Avérous, L.; Ducruet, V., Effect of crystallization on barrier properties of formulated polylactide. *Polymer International* 2012, *61* (2), 180-189.
(p) Jacobsen, S.; Fritz, H. G., Plasticizing polylactide—the effect of different plasticizers on the mechanical properties. *Polymer Engineering & Science* 1999, *39* (7), 1303-1310.
(q) Hu, Y.; Rogunova, M.; Topolkaraev, V.; Hiltner, A.; Baer, E., Aging of poly(lactide)/poly(ethylene glycol) blends. Part 1. Poly(lactide) with low stereoregularity. *Polymer* 2003, *44*, 5701-5710.
(r) Kulinski, Z.; Piorkowska, E., Crystallization, structure and properties of plasticized poly(l-lactide). *Polymer* 2005, *46* (23), 10290-10300.
(s) Kulinski, Z.; Piorkowska, E.; Gadzinowska, K.; Stasiak, M., Plasticization of poly(L-lactide) with poly(propylene glycol). *Biomacromolecules* 2006, *7* (7), 2128-2135.
(t) Piorkowska, E.; Kulinski, Z.; Galeski, A.; Masirek, R., Plasticization of semicrystalline poly(l-lactide) with poly(propylene glycol). *Polymer* 2006, *47* (20), 7178-7188.
(u) Pillin, I.; Montrelay, N.; Grohens, Y., Thermo-mechanical characterization of plasticized PLA: Is the miscibility the only significant factor? *Polymer* 2006, *47* (13), 4676-4682.
(v) Martino, V. P.; Ruseckaite, R. A.; Jimenez, A., Ageing of poly(lactic acid) films plasticized with commercial polyadipates. *Polymer International* 2009, *58* (4), 437-444.
(w) Kowalczyk, M.; Pluta, M.; Piorkowska, E.; Krasnikova, N., Plasticization of polylactide with block copolymers of ethylene glycol and propylene glycol. *Journal of Applied Polymer Science* 2012, *125* (6), 4292-4301.
(x) Burgos, N.; Martino, V. P.; Jimenez, A., Characterization and ageing study of poly(lactic acid) films plasticized with oligomeric lactic acid. *Polymer Degradation and Stability* 2013, *98* (2), 651-658.

9. Kern Sears, J.; Darby, J. R., *The Technology of Plasticizers*. John Wiley & Sons: New York, 1982.

10. **(a)** Regulation (EC) No 1935/2004 of the European Parliament and of the Concil of 27 October 2004 on materials and articles intended to come into contact with food and repealing Directives 80/590/EEC and 89/109/EEC. Official Journal of the European Union, 2004; pp L 338/4 - L 338/17.
(b) Commision Regulation (EU) No 10/2011 of 14 January 2011 on plastic materials and articles intended to come into contact with food. Official Journal of the European Union, 2011; pp L 12-1 - L12-89.

11. **(a)** Byrne, F.; Ward, P.; Kennedy, J.; Imaz, N.; Hughes, D.; Dowling, D., The Effect of Masterbatch Addition on the Mechanical, Thermal, Optical and Surface Properties of Poly(lactic acid). *Journal of Polymers and the Environment* 2009, *17* (1), 28-33.
(b) Hughes, P. A.; Becraft, M. L.; Opusko, S. US Patent US20070255013 A1, Polymeric blend comprising polylactic acid. 2007.

(c) McCarthy, S. P.; Gross, R. A.; Ma, W. US Patent US5883199 A, Polylactic Acid Based Blends. 1999.
(d) Li, Y.; Shimizu, H., Improvement in toughness of poly(l-lactide) (PLLA) through reactive blending with acrylonitrile-butadiene-styrene copolymer (ABS): Morphology and properties. *European Polymer Journal* 2009, *45* (3), 738-746.

12. NatureWorks Technology Focus Report: Toughened PLA. Ver.3/1/2007. (accessed 17.04.2014).

13. **(a)** Arkema presents modifier range for PLA. *Additives for Polymers* 2008, *2008* (1), 4-5.
(b) Dow introduces impact modifier for polylactic acid. *Additives for Polymers 2010* (2), 2-3.
(c) DuPont extends Biomax PLA modifier line with FDA-compliant grade. *Additives for Polymers* 2007, *2007* (7), 2.
(d) PolyOne introduces new additives for biopolymers. *Additives for Polymers* 2008, *2008* (6), 3.
(e) Brulé, B.; Fine, T.; Flat, J.J.; Yasuda, M. Composite based on polylactic acid and polyamide, having improved impact resistance, its manufacturing process and use. WO2007144543, 2007.
(f) PolyOne introduces OnCapTM BIO Impact T - Transparent impact modifier for Polylactic acid. *PolyOne Product Bulletin - Color & Additives* 2008.
(g) Galata Chemicals - Blendex Modifier Product Guide. 2010.

14. **(a)** Broz, M. E.; VanderHart, D. L.; Washburn, N. R., Structure and mechanical properties of poly(D,L-lactic acid)/poly(epsilon -caprolactone) blends. *Biomaterials* 2003, *24* (23), 4181-4190.
(b) Tsuji, H.; Yamada, T.; Suzuki, M.; Itsuno, S., Blends of aliphatic polyestersPart 7. Effects of poly(L-lactide-co-ε-caprolactone) on morphology, structure, crystallization, and physical properties of blends of poly(L-lactide) and poly(ε-caprolactone). *Polymer International* 2003, *52* (2), 269-275.
(c) Odent, J.; Raquez, J.-M.; Duquesne, E.; Dubois, P., Random aliphatic copolyesters as new biodegradable impact modifiers for polylactide materials. *European Polymer Journal* 2012, *48* (2), 331-340.

15. **(a)** Jiang, L.; Wolcott, M. P.; Zhang, J., Study of biodegradable polylactide/poly(butylene adipate-co-terephthalate) blends. *Biomacromolecules* 2005, *7* (1), 199-207.
(b) Ojijo, V.; Sinha Ray, S.; Sadiku, R., Role of Specific Interfacial Area in Controlling Properties of Immiscible Blends of Biodegradable Polylactide and Poly[(butylene succinate)-co-adipate]. *ACS Applied Materials & Interfaces* 2012, *4* (12), 6690-6701.

16. **(a)** Zhang, L.; Xiong, C.; Deng, X., Miscibility, crystallization and morphology of poly(B-hydroxybutyrate)/poly(d,l-lactide) blends. *Polymer* 1996, *37* (2), 235-241.
(b) Boufarguine, M.; Guinault, A.; Miquelard-Garnier, G.; Sollogoub, C., PLA/PHBV Films with Improved Mechanical and Gas Barrier Properties. *Macromolecular Materials and Engineering* 2012.
(c) Zhang, M.; Thomas, N. L., Blending polylactic acid with polyhydroxybutyrate: The effect on thermal, mechanical, and biodegradation properties. *Advances in Polymer Technology* 2011, *30* (2), 67-79.
(d) Gérard, T.; Budtova, T. In *PLA-PHA Blends: Morphology, Thermal and Mechanical Properties*, International Conference on biodegradable and biobased Polymers - BIOPOL 2011, Strasbourg: France, Strasbourg: France, 2011.
(e) Gerard, T.; Budtova, T.; Podshivalov, A.; Bronnikov, S., Polylactide/poly(hydroxybutyrate-co-hydroxyvalerate) blends: Morphology and mechanical properties. *eXPRESS Polymer Letters* 2014, *8* (8), 609-617.

17. **(a)** De Greyt, W., Edible Oil Refining: Current and Future Technologies. In *Edible Oil Processing*, John Wiley & Sons, Ltd: 2013; pp 127-151.
(b) De Greyt, W. F. J.; Kellens, M. J., Deodorization. In *Bailey's Industrial Oil and Fat Products,*, 6th edition ed.; Shahidi, F., Ed. John Wiley and Sons Ltd: Hoboken, New Jersey, 2005; Vol. 5.

18. NatureWorks Processing Guides. http://www.natureworksllc.com/~/media/Technical_ Resources/Processing_Guides/ProcessingGuide_Crystallizing-and-Drying_pdf.pdf.

19. Fischer, E. W.; Sterzel, H. J.; Wegner, G., Investigation of the structure of solution grown crystals of lactide copolymers by means of chemical reactions. *Colloid & Polymer Science* 1973, *251* (11), 980-990.

20. **(a)** Jamshidi, K.; Hyon, S. H.; Ikada, Y., Thermal characterization of polylactides. *Polymer* 1988, *29* (12), 2229-2234.
(b) Södergard, A.; Näsman, J. H., Stabilization of poly(l-lactide) in the melt. *Polymer Degradation and Stability* 1994, *46* (1), 25-30.
(c) Södergard, A., Stolt, M., Properties of lactic acid based polymers and their correlation with composition. *Progress in Polymer Science* 2002, *27* (6), 1123-1163.

21. Hyon, S. H.; Jamshidi, K.; Ikada, Y., Effects of residual monomer on the degradation of DL-lactide polymer. *Polymer International* 1998, *46* (3), 196-202.

22. O'Brien, R. D., *Fats and Oils : Formulating and Processing for Applications*. Third ed.; Taylor & Francis Group: 2009.

23 Ruellan, A.; Guinault, A.; Sollogoub, C.; Chollet, G.; Ait-Mada, A.; Ducruet, V.; Domenek, S., Industrial vegetable oil by-products increase the ductility of polylactide. *Express Polymer Letters* 2015, **submitted**

24. **(a)** Auras, R. A.; Singh, S. P.; Singh, J. J., Evaluation of oriented poly(lactide) polymers vs. existing PET and oriented PS for fresh food service containers. *Packaging Technology and Science* 2005, *18* (4), 207-216.
(b) Bao, L.; Dorgan, J. R.; Knauss, D.; Hait, S.; Oliveira, N. S.; Maruccho, I. M., Gas permeation properties of poly(lactic acid) revisited. *Journal of Membrane Science* 2006, *285* (1–2), 166-172.
(c) Sanchez-Garcia, M. D.; Gimenez, E.; J.M.Lagaron., Novel PET Nanocomposites of Intesrest in Food Packaging Applications and Comparative Barrier Performance with Biopolyester Nanocomposites. *Journal of plastic film & sheeting* 2007, *23*, 33-148.

25. Dorbicau, L.; Delpouve, N.; Herbinet, R.; Domenek, S.; Le Pluart, L.; Delbreilh, L.; Ducruet, V.; Dargent, E., Molecular Mobility and Physical Ageing of Plasticized Poly(lactide). *Polymer Engineering and Science* 2014.

26. Martino, V. P.; Ruseckaite, R. A.; Jiménez, A.; Averous, L., Correlation between Composition, Structure and Properties of Poly(lactic acid)/Polyadipate-Based Nano-Biocomposites. *Macromolecular Materials and Engineering* 2010, *295* (6), 551-558.

27. Pan, P.; Zhu, B.; Inoue, Y., Enthalpy Relaxation and Embrittlement of Poly(l-lactide) during Physical Aging. *Macromolecules* 2007, *40* (26), 9664-9671.

28. **(a)** Di Lorenzo, M. L., Crystallization behavior of poly(l-lactic acid). *European Polymer Journal* 2005, *41* (3), 569-575.
(b) Di Lorenzo, M. L., The Crystallization and Melting Processes of Poly(L-lactic acid). *Macromolecular Symposia* 2006, *234* (1), 176-183.
(c) Di Lorenzo, M. L., Calorimetric analysis of the multiple melting behavior of poly(L-lactic acid). *Journal of Applied Polymer Science* 2006, *100* (4), 3145-3151.
(d) Guinault, A.; Sollogoub, C.; Ducruet, V.; Domenek, S., Impact of crystallinity of poly(lactide) on helium and oxygen barrier properties. *European Polymer Journal* 2012, *48* (4), 779-788.
(e) Wasanasuk, K.; Tashiro, K., Structural Regularization in the Crystallization Process from the Glass or Melt of Poly(l-lactic Acid) Viewed from the Temperature-Dependent and Time-Resolved Measurements of FTIR and Wide-Angle/Small-Angle X-ray Scatterings. *Macromolecules* 2011, *44* (24), 9650-9660.

29. Pan, P.; Kai, W.; Zhu, B.; Dong, T.; Inoue, Y., Polymorphous Crystallization and Multiple Melting Behavior of Poly(l-lactide): Molecular Weight Dependence. *Macromolecules* 2007, *40* (19), 6898-6905.

30. Keith, H. D.; Padden Jr., F. J., Spherulitic Crystallization from the Melt. I. Fractionation and Impurity Segregation and Their Influence on Crystalline Morphology. *Journal of Applied Physics* 1964, *35*, 1270.

31. **(a)** Young, R. J.; Bowden, P. B.; Ritchie, J. M.; Rider, J. G., Deformation mechanisms in oriented high-density polyethylene. *Journal of Materials Science* 1973, *8* (1), 23-36.
(b) Young, R. J.; Bowden, P. B., Twinning and martensitic transformations in oriented high-density polyethylene. *Philosophical Magazine* 1974, *29* (5), 1061-1073.

32. Zuza, E.; Ugartemendia, J. M.; Lopez, A.; Meaurio, E.; Lejardi, A.; Sarasua, J.-R., Glass transition behavior and dynamic fragility in polylactides containing mobile and rigid amorphous fractions. *Polymer* 2008, *49* (20), 4427-4432.

33. Delpouve, N.; Saiter, A.; Mano, J. F.; Dargent, E., Cooperative rearranging region size in semi-crystalline poly(l-lactic acid). *Polymer* 2008, *49* (13–14), 3130-3135.

34. Pluta, M.; Paul, M.-A.; Alexandre, M.; Dubois, P., Plasticized polylactide/clay nanocomposites. I. The role of filler content and its surface organo-modification on the physico-chemical properties. *Journal of Polymer Science Part B: Polymer Physics* 2006, *44* (2), 299-311.

CHAPITRE 6

TABLE OF CONTENTS

ABSTRACT **212**

6.1. INTRODUCTION **213**

6.2. EXPERIMENTAL **215**

6.2.1. Materials 215
6.2.2. Processing 215
6.2.3. Physical Aging 217
6.2.4. Characterization 217
6.2.4.1. Differential Scanning Calorimetry (DSC) *217*
6.2.4.2. Tensile tests *218*
6.2.4.3. Scanning Electron Microscopy (SEM) *218*
6.2.4.4. Quantification of the PODC content *218*

6.3. RESULTS AND DISCUSSION **219**

6.3.1. Thermal and mechanical properties of PLA/PHBV/PODC blends 219
6.3.2. Effect of aging time on volume relaxation kinetic 220
6.3.3. Mechanical properties evolution upon physical aging 224
6.3.4. Deformation and fracture behavior variations during physical aging 228

6.4. CONCLUSION **231**

ACKNOWLEDGEMENT **232**

REFERENCES **233**

Chapitre 6 - Physical aging and its effect on mechanical properties of toughened PLA films

Les condensats de désodorisation d'huiles végétales, notamment celui de palme (CDHP), présentent une intéressante dualité phase soluble (plastification) et phase insoluble (phase dispersée) lorsque mélangés au polylactide au-delà du seuil de saturation. Le polylactide est d'autre part connu pour sa relaxation moléculaire rapide. De ce fait, il ne montre pas une bonne aptitude au vieillissement en général, particulièrement en ce qui concerne ses propriétés mécaniques (fragilisation, démixtion du plastifiant, etc.). Dans la littérature, l'augmentation de la mobilité moléculaire via l'accroissement du volume libre a été montrée comme accélérant la relaxation du polylactide. Nous avons souhaité étudier l'influence du condensat de désodorisation d'huile palme (formulation préalablement retenue, soit 10 %m CDHP) sur ce phénomène.

En outre, les études liées au développement industriel du projet ont montré l'efficacité du PHBV sur l'amélioration de la tenue thermomécanique d'un film PLA/CDHP. Le PHBV étant un polymère immiscible dans le PLA mais engendrant une augmentation significative de sa ductilité, nous avons étudié le vieillissement d'un matériau PLA/PHBV en comparaison des formulations PLA/CDHP et PLA/CDHP/PHBV. Pour cela, nous avons analysé leur relaxation enthalpique par DSC au cours d'un vieillissement *in situ*, et déduit des paramètres cinétiques de vieillissement. Le suivi des propriétés mécaniques au cours du temps et l'observation des mécanismes de déformation par microscopie électronique à balayage a également été réalisé.

Alexandre Ruellan[a,b,c], Jérémy Andre[d], Lidia Jimenez[d], Alain Guinault[a], Violette Ducruet[d], Sandra Domenek[b], Cyrille Sollogoub[a]

[a]*CNAM, Arts et Métiers ParisTech, CNRS, UMR 8006, Laboratoire PIMM, 151, Boulevard de l'Hopital, F-75013 Paris.*
[b]*AgroParisTech, Ingénierie Procédés Aliments, 1 avenue des Olympiades, F-91300 Massy.*
[c]*Brodart Packaging, Département R&D, 1 rue du Stand, F-10700 Arcis-Sur-Aube.*
[d]*INRA, Ingénierie Procédés Aliments, 1 avenue des Olympiades, F-91300 Massy.*

Abstract

The evolution of physical properties during aging of amorphous poly(D,L-lactide) (PLA) and blends whith poly(hydroxybutyrate-co-hydroxyvalerate) (PHBV) and/or palm oil deodorization condensate (PODC), a novel toughening agent, has been investigated. Differential scanning calorimetry (DSC) shows volume relaxation of PLA and blends, inducing increase with the aging time of both enthalpy loss (δ_H) and peak endothermic temperature (T_p) in the glass transition region. Kinetics parameters were determined: PODC appears to slow the PLA relaxation while PHBV has no significant impact. Tensile tests show that PLA and blends undergo with aging time a drastic loss of ductility and increase in rigidity. After some hours (≈ 48 h), while neat PLA turns ductile to brittle, PLA/PHBV blend retains an acceptable elongation at break (≈ 25 %) and PLA/PODC/PHBV blend exposes an important and stable ductility (≈ 130 %). Scanning electron microscopy observations of the stretched samples surfaces allow to highlight an aging induced change in the deformation mechanism. While homogenous shear deformation is predominant for unaged samples, physical aging induces a gradual change from shearing to crazing, the addition of PHBV and PODC largely promoting the crazing deformation mechanism.

Keywords: Physical aging, toughening, polylactide, PLA, poly(3-hydroxybutyrate-co-3-hydroxyvalerate), PHBV, palm oil by-product.

6.1. Introduction

Polylactide (PLA) is one of the most promising biobased and biodegradable polymer to replace traditional petroleum thermoplastic in the packaging or textile sectors.[1] PLA features advantages like ease of processing, transparency, heat-sealing capacity and satisfying rigidity at room temperature.[2] However, PLA being glassy at room temperature ($T_g \approx 60$ °C) behaves brittle because of its low entanglement density and chain stiffness[3] and possesses low heat deflection stability after passing its glass transition.[2]

In the aim to increase the ductility of PLA, plasticizers[4] and/or toughening agents[5] can be used. Ruellan et al.[6] studied recently the relationship between solubility of plasticizing molecules in the PLA matrix and ductility. They showed that vegetable oil deodorization condensates, being by-products of the vegetable oil industry, are highly efficient in increasing PLA ductility (up to 160 % of elongation at break), although merely soluble in the polymer matrix.[7] Vegetable oil deodorization condensates are mixtures containing free fatty acids and their glycerol esters, as well as unsaponifiable compounds. The high increase in PLA ductility although very low depression of T_g, stemmed from a synergistic effect of the compounds contained in the native mixtures. Crystallized compounds at measuring temperature (23 °C) allowed for efficient craze induction and therefore high elongation of PLA by multiple crazing, and liquid compounds brought about sufficient compatibility between inclusions and PLA matrix for interfacial adhesion.[7a] However, plasticizers, same as these novel biobased and biodegradable ductility agents, are inefficient for increasing thermal stability of PLA upon heating over glass transition.

A second means to improve ductility and also thermal stability is blending of PLA with polymers featuring higher thermal stability.[8] In the aim of retaining interesting environmental features of PLA, namely biobased raw materials and biodegradability, polyhydroxybutyrates (PHAs), which are aliphatic polyesters obtained by microbial fermentation, have been already

largely employed.[9] Among PHAs, the use of poly(3-hydroxybutyrate-co-3-hydroxyvalerate) (PHBV), which is a highly crystalline and brittle polymer with a glass transition temperature at around 0 °C (depending on the content in 3-hydroxyvalerate monomer) yielded increased ductility of PLA/PHBV blends[8b, 9a, 9f] at approximately 10 wt% PHBV. This effect was obtained although PLA/PHBV blends of polymers with high M_w are immiscible[8b, 9a, 10] and PHBV was highly crystallized.[8b, 9a, 9f, 11] The supplementary use of plasticizers, such as polyethylene glycol, in the PLA/PHBV blends improved further toughness and impact strength of PLA/PHBV blends.[12] The use of both plasticizer and PHBV seems therefore be interesting for increasing PLA ductility and heat stability beyond glass transition.

However, PLA is very sensitive to physical aging,[13] diminishing its ductility[14] and reducing its enzymatic degradation ability[15] because of changes in molecular conformation.[16] Hence, Hassouna et al.[17] noticed cold crystallization during physical aging leading to an enrichment in plasticizer of the amorphous phase. Dobricau et al.[18] showed that the plasticizing of PLA accelerated the structural relaxation in the glassy state by one order of magnitude, which yields quicker physical aging kinetics. Rasal et al.[19] showed that physical aging of PLA/poly(3-hydroxyhexanoate-co-3-hydroxybutyrate) blends decreased significantly the toughness of the blend. Wang et al.[20] observed the importance of the interfacial adhesion on aging behavior of PLA/starch blends. Gerard[21] investigated the physical aging of PLA/PHBV blends. He showed a decrease in aging kinetics of PLA upon addition of PHBV. His hypothesis is that the nodular distribution of PHBV inside the PLA matrix hindered the volume relaxation and thereby delayed the effects of physical aging on mechanical properties and enthalpic relaxation. Investigating the evolution of physical properties of polylactide formulations during physical aging is therefore of academic and practical interest for predicting the behavior of PLA films stored at ambient conditions, which are generally below but close to glass transition.

Therefore the effect of blending PLA with PHBV and a novel biobased and biodegradable toughening agent, palm oil deodorization condensate (PODC),[7] on its thermal and mechanical properties was studied. Furthermore, the influence on polylactide physical aging of PODC and PHBV through thermal, mechanical and morphology observations was investigated.

6.2. Experimental

6.2.1. Materials

Amorphous polylactide (PLA 4060D) containing 89 ± 1 % L-lactide and 11 ± 1 % D-lactide units (according to the datasheet), making it unable to crystallize under common processing conditions,[1, 22] was purchased from NatureWorks (U.S.A.). Semi-crystalline poly(hydroxybutyrate-co-hydroxyvalerate) (PHI 002) containing 97 % hydroxybutyrate and 3 % hydroxyvalerate units (according to the datasheet) was purchased from Natureplast (France). Average molecular weights of PLA 4060D and PHI 002 obtained from SEC measurements are respectively M_w = 238,000 g.mol^{-1} and M_w = 517,000 g.mol^{-1}. Palm oil deodorization condensate (PODC) was supplied by ITERG (Bordeaux, France). Specifications of the palm oil condensate employed are given in **Table 6.1**.

6.2.2. Processing

In order to remove water traces prior to the melt blending process, PLA 4060D and PHI 002 were dried respectively at 60 °C and 80 °C for 24 hours under dried air using a Motan 100 L Dryer. Melt blending of 90 wt% PLA 4060D with 10 wt% PHI 002 was performed using a corotating twin screw extruder (Thermo Haake Ptw 16-40D) with a screw diameter of 16 mm and a length to diameter ratio (L/D) 40:1. The twin-screw rotation speed was set at 300 rpm and the temperature profile was 170/180/185/185/180/170/170 °C along the extrusion flow. Output was 1 kg.h^{-1}. Melt blending of PLA 4060D with PODC with or without PHI 002 was performed using a corotating twin screw extruder (Dr. Collin) with a screw diameter of 35

mm and a length to diameter ratio (L:D) 56:1. Liquid addition of the PODC was done using a Robatech PuMelt D280 pump heated at 70 °C. The [90 wt% PLA 4060D + 10 wt% PODC] blend was performed at a twin-screw rotation speed of 250 rpm and a temperature profile being 65/180/180/180/180/180/180/170/170/160/150/140/140/140/140 °C along the extrusion flow. Addition of the PODC was carried out in the 9th zone of the extruder. Output was 10 kg.h^{-1}. The [90 wt% (PLA 4060D + 10 wt% PODC) + 10 wt% PHI 002] blend was carried out in one single step. The twin-screw rotation speed was set at 250 rpm and the temperature profile was 65/195/195/160/160/155/155/155/170/170/165/160/150/150/150 °C along the extrusion flow. Addition of the PODC was carried out in the 5th zone and addition of the PHI 002 in the 9th zone of the extruder. Output was 11.1 kg.h^{-1}. Cooling of the extruded strands before granulation was carried out under air. The obtained pellets were stored in hermetic sealed metalized bags to avoid rehydration.

Table 6.1 Composition of the PODC

	Type	**Content** *(%)*
Glyceride Composition	Free Fatty Acids	95.4
	Mono Glycerides	1.7
	Di Glycerides	2.2
	Tri Glycerides	0.7
Water		0.16

	Usual Name	**Formula**	**Content** *(%)*
Fatty Acid Composition	Lauric Acid	C12:0	0.4
	Myristic Acid	C14:0	1.3
	Palmitic Acid	C16:0	49.8
	Palmitoleic Acid	C16:1 cis	0.2
	Stearic Acid	C18:0	4.1
	Oleic Acid	C18:1 cis	35.0
		C18:1 trans	0.2
	Linoleic Acid	C18:2 cis	7.7
		C18:2 trans	0.1
	Linolenic Acid	C18:3 cis	0.3
	Arachidic Acid	C20:0	0.3
	Eicosenoic Acid	C20:1 cis	0.1
	Unidentified	-	0.7

Films of about 0.8 mm thickness were processed using a single screw extruder (Scamex Rheoscam), mounted with a screw of 20 mm diameter and a length to diameter ratio (L/D) 12:1, and a flat die of 40 mm width and 1 mm thickness. For the neat PLA film, the temperature profile was 180/180/180/180/190 °C and the twin-screw rotation speed was set at 105 rpm. Output was 1 $kg.h^{-1}$. For the PLA/PHBV film, the temperature profile was 180/180/190/185/180 °C and the twin-screw rotation speed was set at 105 rpm. Output was 1.1 $kg.h^{-1}$. For the PLA/PODC film, the temperature profile was 175/160/155/160/160 °C and the twin-screw rotation speed was set at 105 rpm. Output was 1.0 $kg.h^{-1}$. For the PLA/PODC/PHBV film, the temperature profile was 190/185/180/165/165 °C and the twin-screw rotation speed was set at 115 rpm. Output was 1.0 $kg.h^{-1}$. Films were stretched and cooled with chill rolls.

6.2.3. Physical Aging

Physical aging was carried out directly in the DSC under nitrogen (50 mL.min-1) at a fixed distance from T_g: $T_{aging} = T_g - 15$ °C for each formulation. The resulting aging temperatures are thus $T_{aging} = 40 \pm 2$ °C for the PLA and PLA/PHBV samples and $T_{aging} = 32 \pm 2$ °C for the PLA/PODC and PLA/PODC/PHBV samples. Physical aging times varied from 0 to 100 h.

6.2.4. Characterization

6.2.4.1. Differential Scanning Calorimetry (DSC)

DSC analyses were performed using a Mettler Toledo DSC1 STARe System under nitrogen atmosphere (50 $mL.min^{-1}$) in 40 µL standard Aluminum pans (Mettler Toledo). Calibration of the device was done using Indium and Zinc standards. Calorimetric scans were perform at 10 $°C.min^{-1}$ from -10 to 200 °C for obtaining glass transition and crystallization signals of PLA and PHBV. The crystallinity degree of PHBV was calculated from the melting enthalpy of the PLA/PHBV samples which was corrected for the effective weight content in PHBV and using

a melting enthalpy of PHBV crystals of 109 $J.g^{-1}$.[23] For aging studies, samples were rejuvenated by heating over glass transition and then quenched to aging temperature (T_{aging} = T_g – 15 °C), where they were held for different durations. After aging, samples were cooled to 0 °C and a heating scan from 0 to 85 °C at 10 °C.min^{-1} was performed. Samples of about 5 mg were used.

6.2.4.2. Tensile tests

Tensile properties were investigated at 23 °C, a relative humidity (RH) 50 ± 10 % and at a cross-head speed of 5 mm.min^{-1}, using an universal tensile machine (Instron model 4301) equipped with a load cell 1,000 ± 1 N, without using an extensometer. The dog bone shaped samples (ISO 527-2 type 5A) were directly cut from aged materials. Prior to tensile testing, samples were conditioned at 23 °C and 50 ± 10 % RH for about 15 minutes. Each mechanical characteristic value is an average of 5 measurements.

6.2.4.3. Scanning Electron Microscopy (SEM)

Morphology of samples stretched until failure was visually observed with SEM (Hitachi 4800 II). Observations were directly conducted on the longitudinal surface of the dog bone shaped samples without any previous preparation.

6.2.4.4. Quantification of the PODC content

PODC content of aged PLA/PODC and PLA/PODC/PHBV films was estimated from thermogravimetric analyses[7b] using a thermobalance (TA Instruments Q500) from 25 to 450 °C under nitrogen atmosphere (40 mL.min^{-1}) at 10 °C.min^{-1} on samples of about 4 mg. Prior to measurements, weight calibration of the device was achieved using calibration weights and temperature calibration by an external thermometer and the Curie point of Nickel. The chosen comparison temperature at which the PODC amount was estimated into samples was 250 °C. It is based on the fact that measurements on components (*i.e.* neat PODC, neat PLA 4060D

and neat PHI 002) show that a large amount of PODC is already volatilized while only a very low weight loss for PLA 4060D and PHI 002 is observed. Thus, the following calculation **(6.1)** was applied to estimate the PODC content in samples. Experiments were carried out in triplicate.

$$\text{PODC wt\%} = \frac{\left(\text{PLA/PODC/PHBV}_{\text{weight loss}}\right)_{(t)} - 0{,}9*\left(\text{PLA/PHBV}_{\text{weight loss}}\right)_{(t)}}{\left(\text{PODC}_{\text{weight loss}}\right)_{(t)}} * 100 \qquad \textbf{(6.1)}$$

where PODC wt% is the PODC weight content in the formulation and $\text{PLA/PODC/PHBV}_{\text{weight loss}}$, $\text{PLA/PHBV}_{\text{weight loss}}$ and $\text{PODC}_{\text{weight loss}}$ are the relative weight loss of the PLA/PODC/PHBV and PLA/PHBV blends and the neat PODC at 250 °C, respectively.

6.3. Results and Discussion

6.3.1. Thermal and mechanical properties of PLA/PHBV/PODC blends

Table 6.2 compares the thermal and mechanical properties of PLA, PLA/PODC, PLA/PHBV and PLA/PODC/PHBV blends.

Table 6.2 Mechanical and thermal properties of PLA, PLA/PODC, PLA/PHBV and PLA/PODC/PHBV blends

Film	**Storage**	**Yield stress** *(MPa)*	**Elongation at break** *(%)*	**Young modulus*** *(MPa)*	**ΔH_m (PHBV)** *($J.g^{-1}$))*	**χc** ***(PHBV)*** *(%)*
PLA**	1 week at 23 °C	56 ± 4	17 ± 4	1,620 ± 80	-	-
	1 month at 40 °C	61 ± 3	6 ± 1	1,800 ± 30	-	-
PLA + PODC**	1 week at 23 °C	27 ± 3	135 ± 25	1,330 ± 50	-	-
	1 month at 40 °C	n.m.	n.m.	n.m.	-	-
PLA + 10 wt% PHBV	1 week at 23 °C				0.3± 0.2	3 ± 2
	1 month at 40 °C	48 ± 1	35 ± 5	1,540 ± 50		
90 wt% [PLA + 10 wt% PODC] + 10 wt% PHBV	1 week at 23 °C	24 ± 3	105 ± 15	1,490 ± 75	4 ± 1	41 ± 10
	1 month at 40 °C	30 ± 1	125 ± 15	1400 ± 15		

n.m.: not measurable

*apparent Young modulus measured without extensometer

**samples made according to material and methods from Ref.[7b]

If neat PLA displays a low elongation at break, PLA/PHBV (90 wt% / 10 wt%) blends present clearly a ductile behavior. Such gain of ductility in PLA/PHB(V) blends for compositions containing a small amount of PHB(V) (20 wt% or less), has been observed by several authors[9a, 9h, 9j] and is generally attributed to an optimal size and fine distribution of the

immiscible PHB(V) particles in the PLA matrix, acting as toughening agents, as will be discussed later. Adding PODC in a PLA/PHBV blend allows to obtain an even greater elongation at break. It seems that PHBV, dispersed in PLA as small nodules (around 100 nm to several microns diameter as can be seen in **Figure 6.7**), can hardly crystallize. This confinement effect has been observed by several authors.[9c] Still, when PODC is added, PHBV crystallization is possible certainly due to a nucleation and/or plasticizing effect. Consequently, PHBV has a degree of crystallinity superior to 40 % in PLA/PHBV/PODC blends, which induces an improvement in thermal stability of this ternary blend. This stability is evidenced by the good aspect of an extruded film after one month of storage at 40 °C, compared to the blend without PHBV (PLA/PODC) (**Figure 6.1**).

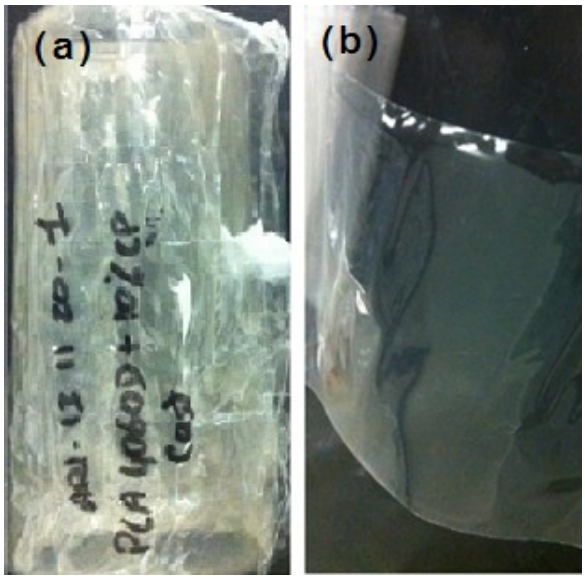

Figure 6.1 Cast extruded films **(a)** [PLA + 10 wt% PODC] and
(b) [90 wt% (PLA + 10 wt% PODC) + 10 wt% PHBV] stored at 40°C during one month

6.3.2. Effect of aging time on volume relaxation kinetic

DSC heating thermograms of formulations at different aging times are shown in **Figure 6.2**. For all formulations, the area of the endothermic peak and the peak temperature value increase with the aging time. A higher glass transition temperature means a lower free volume. Even if the polymer chains are frozen below T_g, the segmental mobility allows a volume relaxation.[14]

More energy is therefore needed with the aging time to turn the polymer from the glassy to rubbery state. The enthalpy corresponds to the energy needed by the glass to reach the thermodynamic equilibrium.

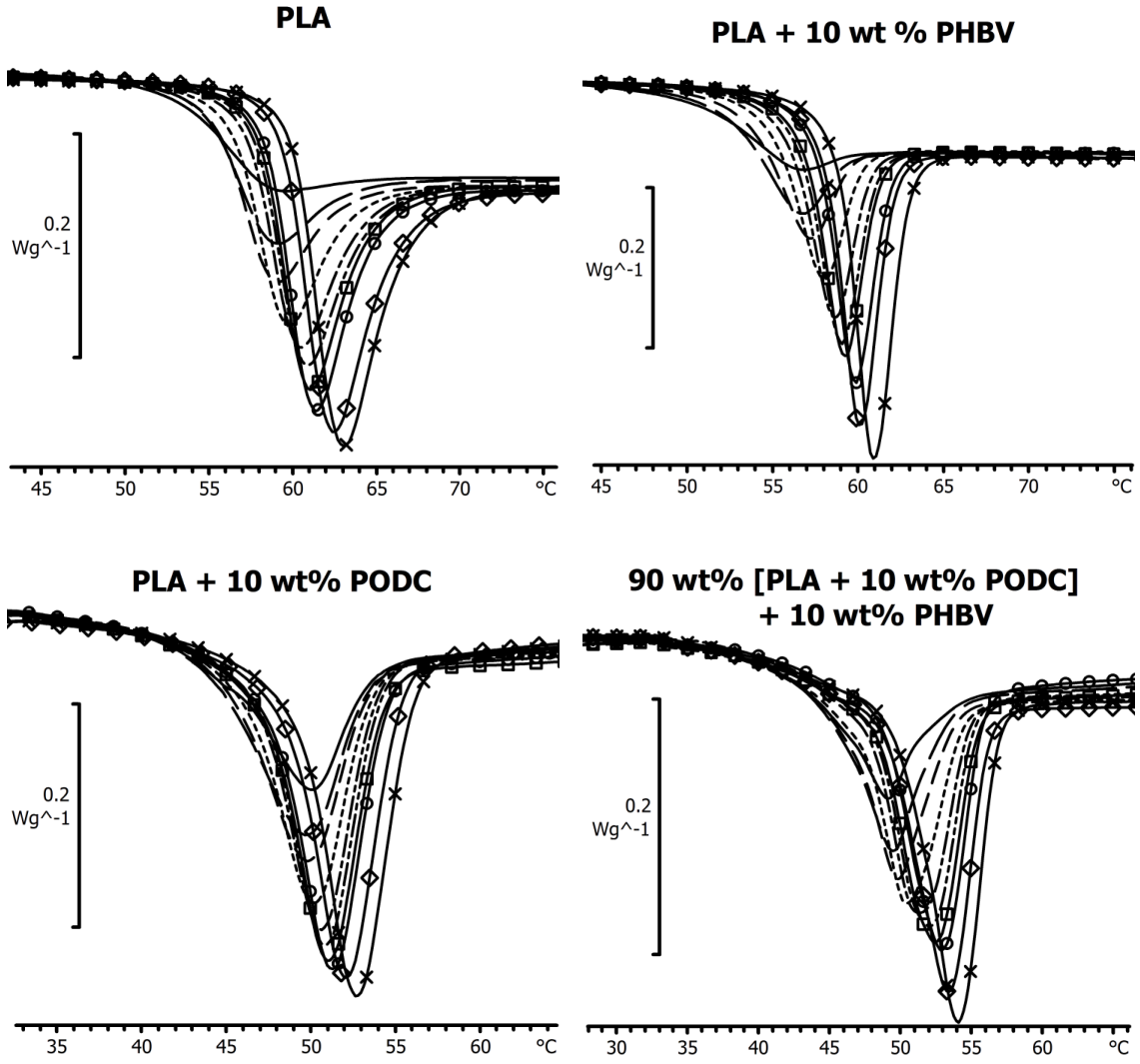

Figure 6.2 DSC heating scans of PLA and PLA blends after physical aging at T_g -15 °C for different times (—) 0 h ; (— —) 1 h ; (– –) 2 h ; (- - -) 5 h ; (– -) 10 h ; (– - -) 15 h ; (⊟) 20 h ; (⊖) 30 h ; (⍜) 50 h ; (X) 100 h

Pan et al.[14] studied the physical aging of poly(L-lactide) and poly(D,L-lactide) under comparative conditions. Similar volume relaxation behavior was observed. The glass transition of the PHBV is about 0 to 5 °C and is generally weak because of the high crystallinity degree of the polymer. The small decrease of the T_g of PLA phase in PLA/PHBV blends can be attributed to the compatibility of this blend. Besides, blends of PLA and PHBV having high molecular weights are immiscible.[10, 24] Therefore, the glass transition observed

from 45 to 65 °C can be attributed to the PLA fraction. PODC is partially miscible in PLA,[7] the glass transition is shifted to lower temperatures because of the plasticization effect. Moreover, PODC contains some fats which melting point is in the same range of temperature as the PLA glass transition. Therefore, the fats endothermic melting peak is concomitant with the endothermic peak of the enthalpy recovery of PLA during glass transition.[7] In order to be able to characterize the PLA in the two samples containing PODC, the content was controlled to be constant with the aging time. Results are presented in **Figure 6.3**. Note that contents are lower than 10 wt%, likely due to volatilization of PODC during polymer processing.[7]

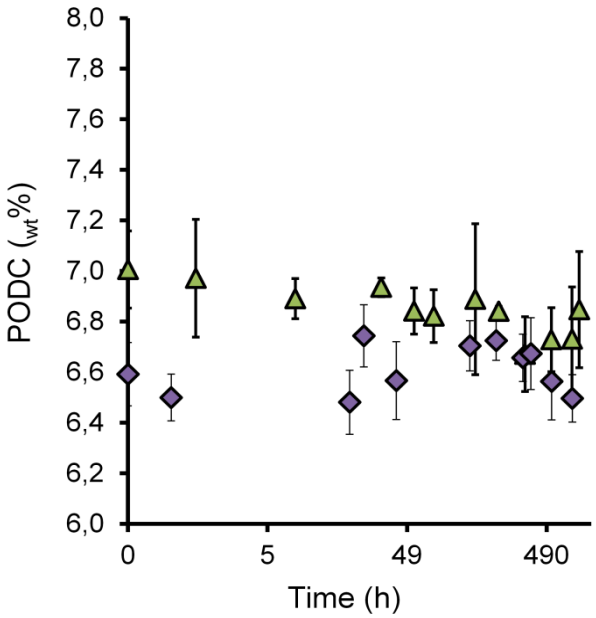

Figure 6.3 PODC contents of PLA/PODC and PLA/PHBV/PODC films determined from thermogravimetric analyses in function of the aging time
(◊) PLA/PODC ; (Δ) PLA/PODC/PHBV

Based on the DSC curves exposed in **Figure 6.2**, the enthalpy loss and the endothermic peak temperature are plotted in function of the logarithm of the aging time. Results are shown in **Figure 6.4**. Enthalpy loss is obtained from the area difference between the DSC curves of annealed reference and the aged samples.[14, 25] The enthalpy of fusion of fats from PODC is therefore ignored since it has been controlled to be constant with aging time. For all the formulations, both the enthalpy loss and the endothermic peak temperature increase linearly

with the logarithm of the aging time as depicted for neat poly(L-lactide).[14] The relaxation rate of the different formulations was determined from equation **(6.2)**:

$$\beta_H = [\partial \delta_H / \partial (\log\ t_a)]_{q_1, q_2, T_a} \quad \textbf{(6.2)}$$

where β_H is the relaxation rate in $J.g^{-1}$ per decade, δ_H the enthalpy loss in $J.g^{-1}$, t_a the aging time, q_1 the cooling rate in $°C.min^{-1}$, q_2 the heating rate in $°C.min^{-1}$ and T_a the aging temperature. q_1 and q_2 were fixed at 10 $°C.min^{-1}$. T_a was different depending on the presence of PODC but was set to $T_a = T_g - 15$ °C for all formulations. Results are shown in **Table 6.3**.

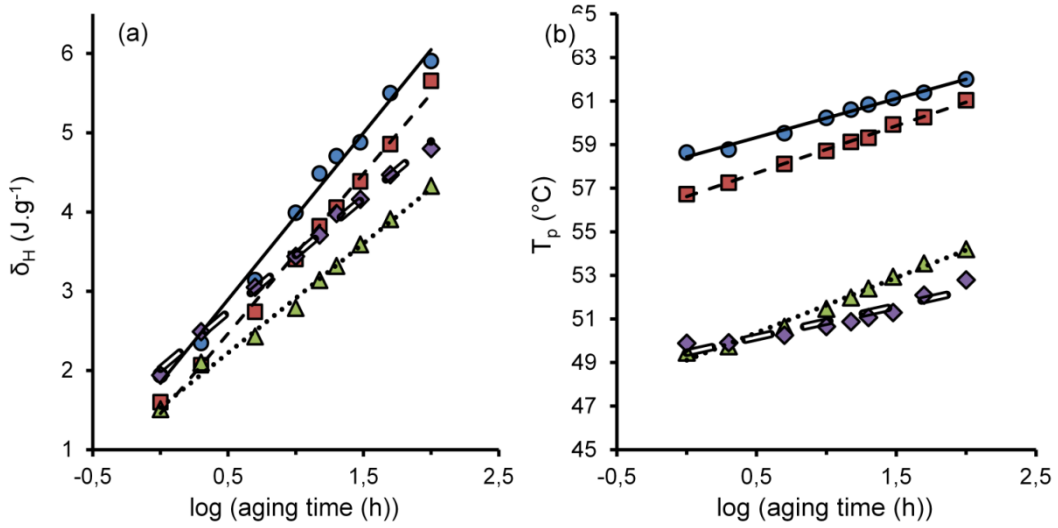

Figure 6.4 Dependence of **(a)** Enthalpy loss (δ_H) and **(b)** Peak temperature (T_p) during physical aging of neat PLA, PLA/PODC, PLA/PHBV and PLA/PODC/PHBV films at $T_a = T_g - 15$ °C as a function of log ($_{\text{aging time (h)}}$)
(○) PLA ; (□) PLA/PHBV ; (Δ) PLA/PODC/PHBV ; (—) linear square fit of PLA ;
(– –) Linear square fit of PLA/PHBV ; (• •) linear square fit of PLA/PODC/PHBV

Table 6.3 Volume relaxation kinetic parameters of PLA, PLA/PHBV, PLA/PODC and PLA/PODC/PHBV

Formulation	**Enthalpy loss relaxation kinetic**		**Peak temperature relaxation kinetic**	
	β_H *($J.g^{-1}$ per decade)*	**Correlation coefficient**	**$\partial T_p/\partial(\log t_a)$** *(°C per decade)*	**Correlation coefficient**
PLA	2.10	0.991	1.78	0.988
PLA/PHBV	2.03	0.995	2.16	0.996
PLA/PODC	1.34	0.996	1.43	0.901
PLA/PODC/PHBV	1.38	0.993	2.52	0.988

The PLA 4060D relaxation rate is slightly higher than the one obtained for poly(L-lactide) (1.77 $J.g^{-1}$).[14] PHBV does not modify (in a significant way) the relaxation rate of PLA 4060D. It is likely due to the immiscibility of both polymers,[10, 24] the segmental mobility of polylactide is therefore not altered. On the opposite, adding PODC, which is partially miscible with PLA and decreases T_g, induces a reduction of the relaxation rate, whatever the presence of PHBV. This result seems contradictory with Dobircau et al.[18] who observed an accelerating effect of plasticizers on the molecular mobility in the glassy state, reducing the time needed for cooperative motions due to the breaking of interactions between polymer chains. It seems thus that the miscible part of PODC, acting as a plasticizer, increases the molecular mobility and induces a decrease of the T_g. When the miscibility limit is reached, the immiscible part of PODC forms micrometric aggregates, as observed in our previous studies.[7] We can assume that these aggregates have strong polar interactions with macromolecular chains, therefore hampering segmental motions and are responsible for the slower kinetics of aging. Those polar interactions prevent as well the immiscible PODC from migrating to the film surface,[7b] as it was observed for other plasticizers presenting high compatibility with PLA matrix.[17]

6.3.3. Mechanical properties evolution upon physical aging

Tensile properties of PLA, PLA/PHBV and PLA/PODC/PHBV materials were measured at different aging times from 0 to 750 h stored at $T_a = T_g - 15$ °C. PLA/PODC mechanical properties were already investigated stored in ambient conditions for 6 months.[7b] Typical stress/strain curves are shown in **Figure 6.5** and the **Figure 6.6** plots the evolution of the elongation at break, tensile modulus and yield stress as a function of aging time.

The effect of physical aging on the stress-strain curves for all the formulations is substantial. All the unaged specimens present a ductile behavior and can elongate to more than 250 % of their initial length. During aging, all the samples expose a decrease of the ductility, more or less rapid and pronounced depending on the formulation.

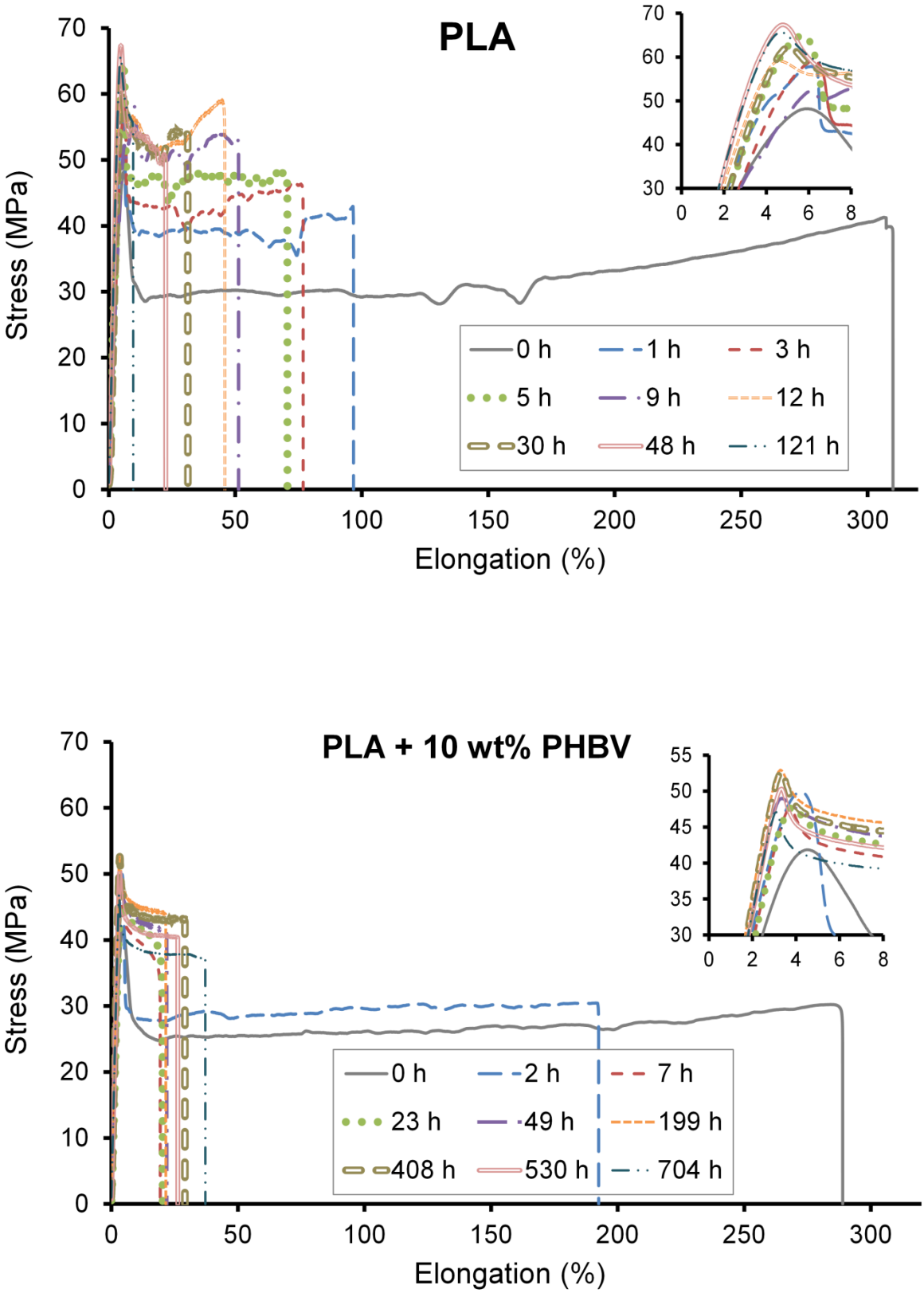

Figure 6.5 Typical stress/strain curves of neat PLA, PLA/PHBV and PLA/PODC/PBHV films upon physical aging

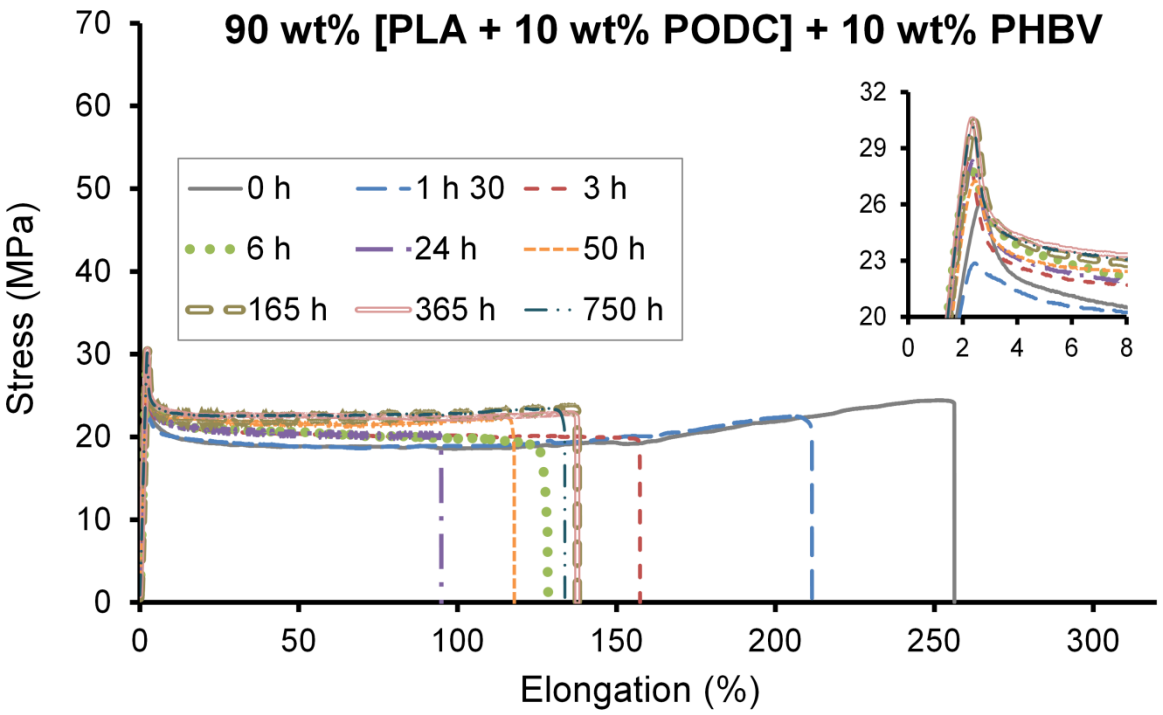

Figure 6.5 Typical stress/strain curves of neat PLA, PLA/PHBV and PLA/PODC/PBHV films upon physical aging (continued)

The ductility of neat PLA constantly decreased to the well-known ≈ 5 % elongation at break, turning brittle over 48 h. Meantime, as depicted by Pan et al.,[14] rigidity, yield stress and stress at break increased. This embrittlement, as classically stated in glassy polymers,[26] is linked with the densification and the related decrease of molecular mobility and of free volume occurring during physical aging. The densification is correlated with an increase in glass transition temperature, of several degrees as observed for PLA (**Figure 6.4b**).

Like for neat PLA, aging leads, for PLA/PHBV blends, to a decrease of ductility and an associated increase in modulus and stress yield. This aging-induced evolution seems nevertheless to stop around 20 h aging. Similar results were obtained for PLA/PHBV (90 wt% / 10 wt%) blends, by Gerard et al.,[9j] who observed a dramatic decrease of the elongation at break from 200 % to 20 % in one month. However, in their case, this decrease of ductility

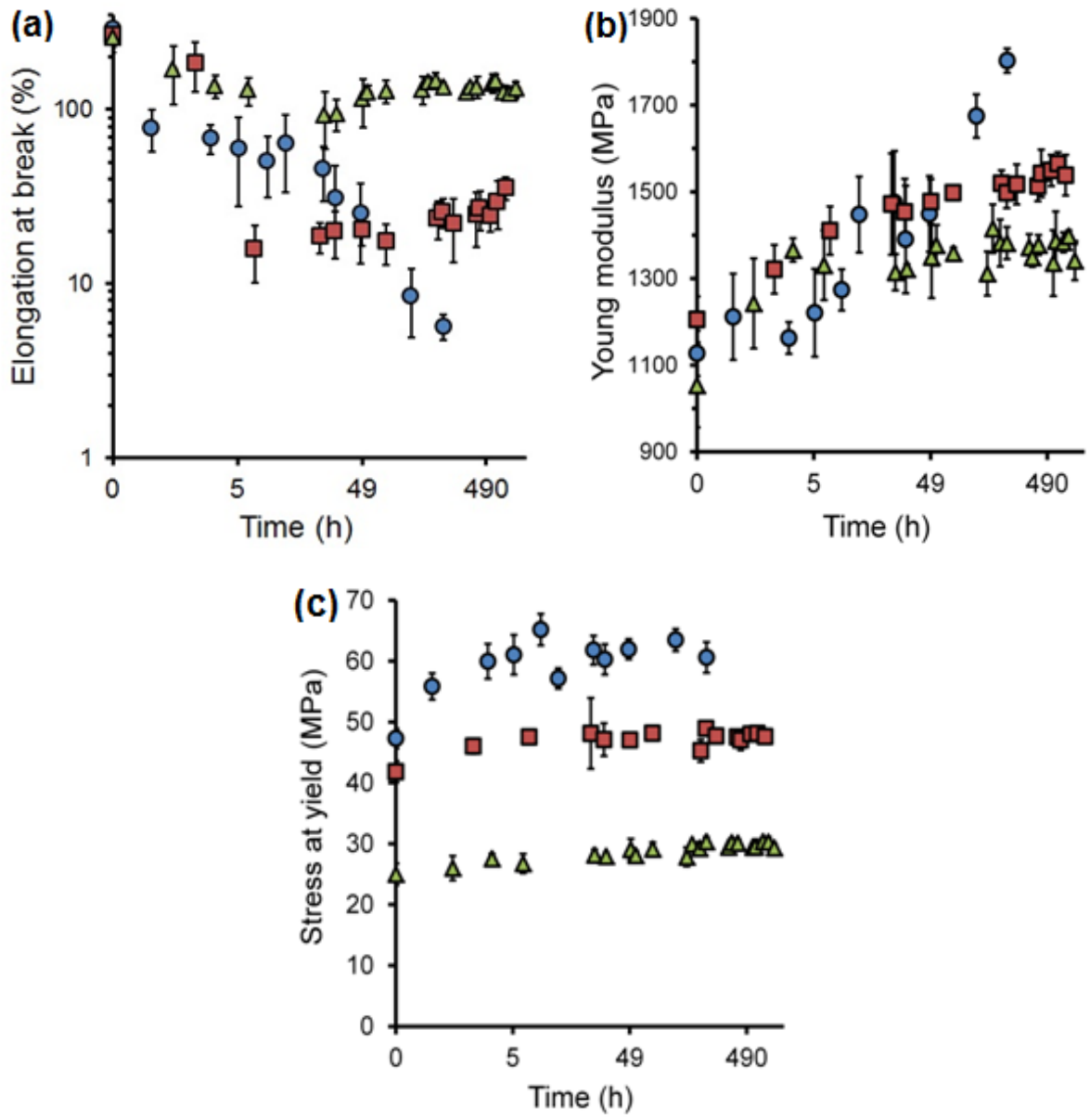

Figure 6.6 (a) Elongation at break, **(b)** Young modulus, **(c)** Stress at yield
(○) PLA ; (□) PLA/PHBV ; (Δ) PLA/PODC/PHBV

occurs more slowly since, after 14 days, the elongation at break is still around 50 %, which can be certainly explained by the fact that their aging temperature (room temperature) is lower than in our case (40 °C). Blending 10 wt% of PHBV with PLA eventually allows to retain ≈ 25 % elongation at break, even on 750 h aged samples. Adding PODC to PLA/PHBV blend induces a slowdown and a limitation in the decrease of the elongation at break, certainly correlated with the smaller relaxation rate. The elongation at break for long aging times stagnates at around 150 %, presenting the highest ductility. Conversely, Young's modulus and

stress at yield reach values much smaller than for neat PLA or PLA/PHBV blend, which indicates the effective plasticizing effect of PODC.[7]

6.3.4. Deformation and fracture behavior variations during physical aging

The SEM observation of the longitudinal surface of the samples after tensile tests allows to follow the aging-induced evolution of the deformation and failure modes. The SEM micrographs, obtained at different aging times for the three formulations, are exposed in **Figure 6.7**. While SEM is not adapted to observe shear bands, it allows to analyze the craze and crack microstructures, their dimension and orientation.

The unaged neat PLA sample exhibits homogeneously plastic deformed surface, presumably by shear yielding. Some rare cracks perpendicularly to the stretching direction are visible, originated in pre-existing flaws or defects. After several hours of aging, a mixed mode of deformations, involving both crazing and shear banding, appears. Under these conditions, craze initiation and crack propagation are highly influenced by large plastic strains induced by band shearing: large crack-like features ("fissures") are visible and appear orientated along shear bands (aging time of 12 h). Further aging induces a progressive embrittlement with appearance of cracks at ≈ 90 ° to the stretching direction, typical for a craze initiated brittle failure.

It is widely known that PLA/PHBV blends are immiscible and that blending 10 % PHBV in PLA leads to small (100 nm to several μm) PHBV nodules dispersed in the PLA matrix. Those small nodules are visible on the SEM micrograph of the unaged deformed PLA/PHBV samples, which exhibit, like neat unaged PLA, homogenous plastic deformation. Aging induces an embrittlement similar to neat PLA, but leads to the appearance of more numerous, thinner and shorter cracks. It seems that dispersed particles of PHBV act as crazing initiators and promote multiple crazing delaying the ultimate fracture of the material. This toughening

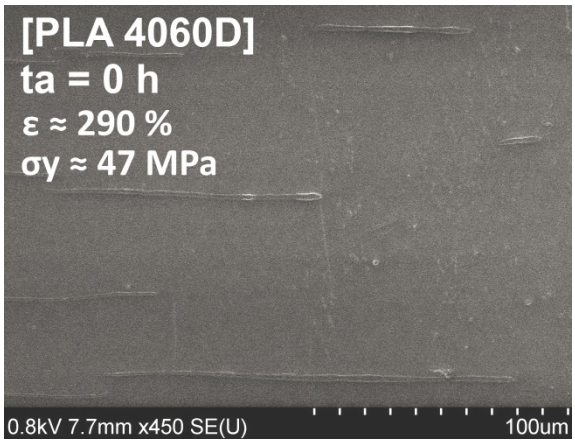
[PLA 4060D]
ta = 0 h
ε ≈ 290 %
σy ≈ 47 MPa
0.8kV 7.7mm x450 SE(U)
100um

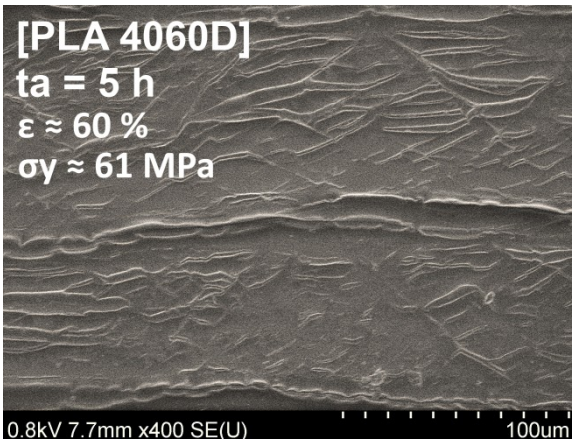
[PLA 4060D]
ta = 5 h
ε ≈ 60 %
σy ≈ 61 MPa
0.8kV 7.7mm x400 SE(U)
100um

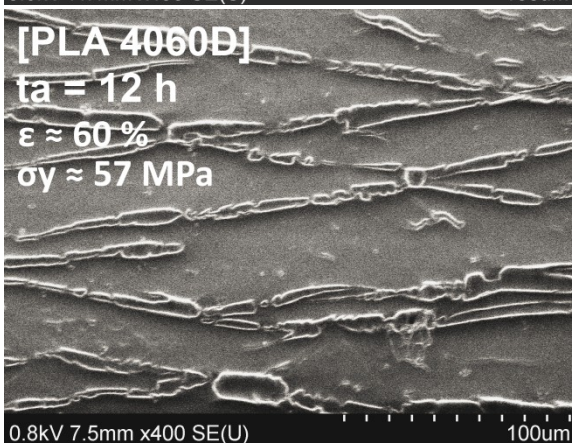
[PLA 4060D]
ta = 12 h
ε ≈ 60 %
σy ≈ 57 MPa
0.8kV 7.5mm x400 SE(U)
100um

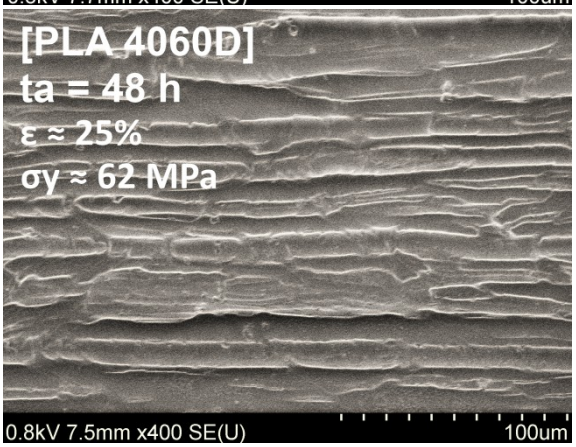
[PLA 4060D]
ta = 48 h
ε ≈ 25%
σy ≈ 62 MPa
0.8kV 7.5mm x400 SE(U)
100um

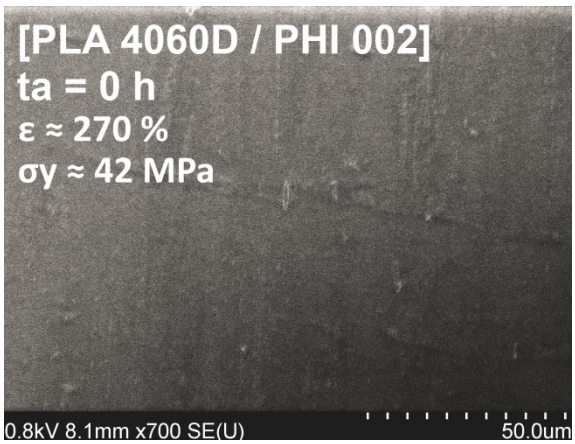
[PLA 4060D / PHI 002]
ta = 0 h
ε ≈ 270 %
σy ≈ 42 MPa
0.8kV 8.1mm x700 SE(U)
50.0um

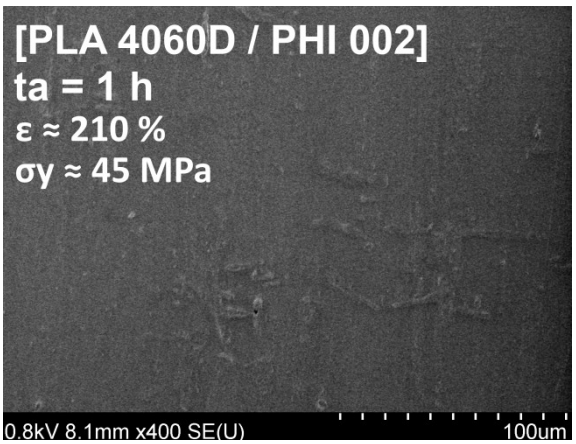
[PLA 4060D / PHI 002]
ta = 1 h
ε ≈ 210 %
σy ≈ 45 MPa
0.8kV 8.1mm x400 SE(U)
100um

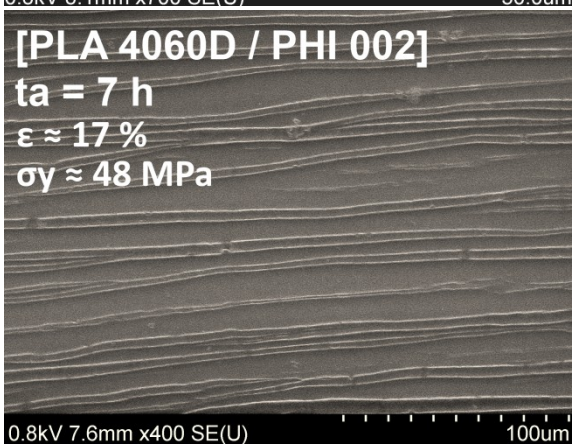
[PLA 4060D / PHI 002]
ta = 7 h
ε ≈ 17 %
σy ≈ 48 MPa
0.8kV 7.6mm x400 SE(U)
100um

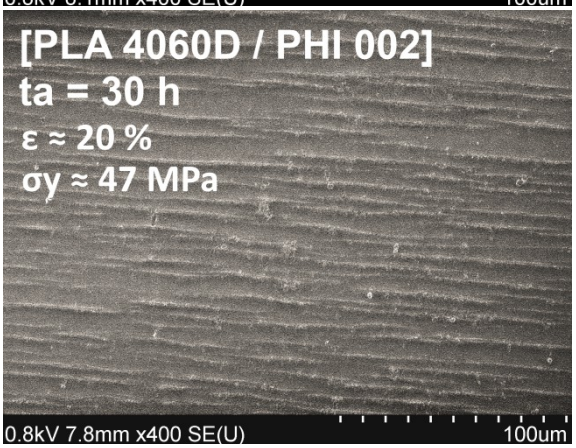
[PLA 4060D / PHI 002]
ta = 30 h
ε ≈ 20 %
σy ≈ 47 MPa
0.8kV 7.8mm x400 SE(U)
100um

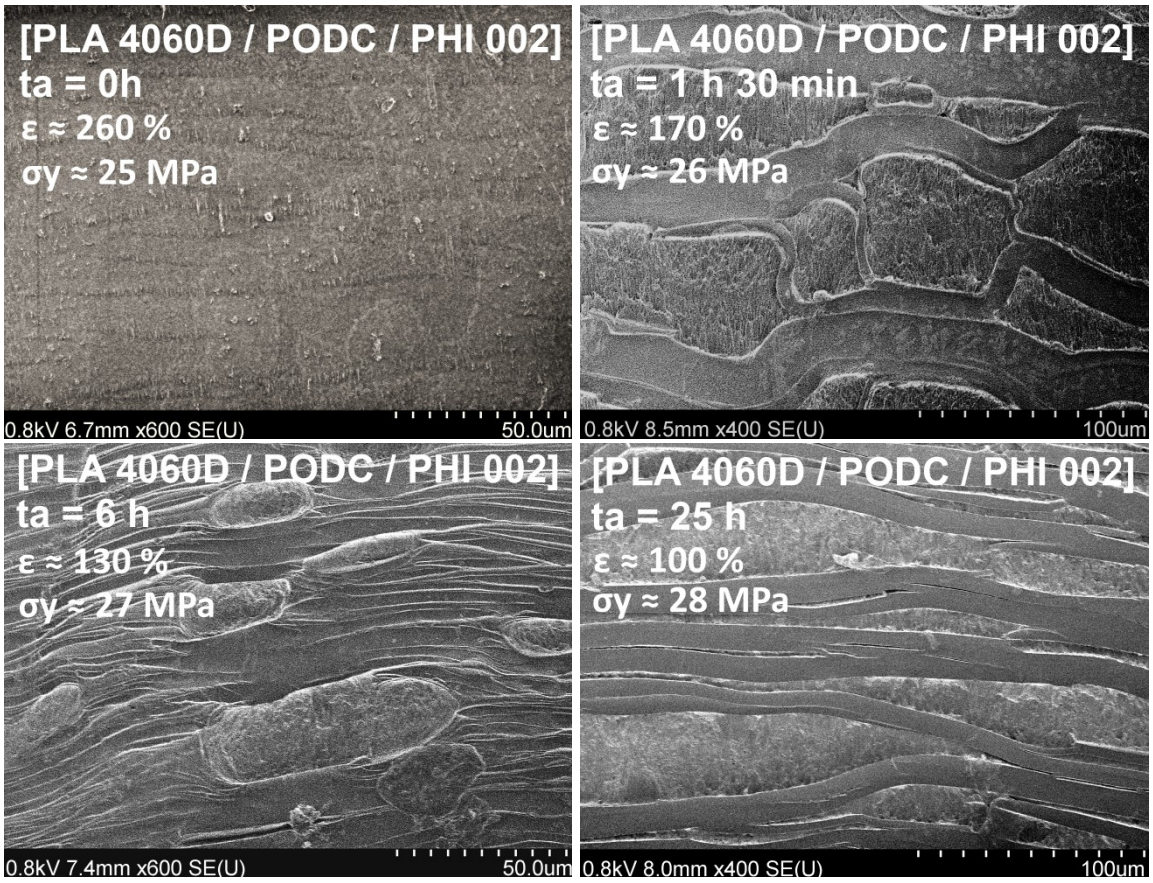

Figure 6.7 SEM micrographs of the surface of stretched until breakage samples

Drawing direction: vertical

Note that spheroidal items observed on SEM pictures of drawn aged materials containing PODC (here above) are big cracks exposing fibrils. Cracks are observable with the naked eye in figure **S4.7**.

mechanism is well-known in rubber toughening[27] and has also been observed for PLA/PHBV blends by Bartczak et al.[28] As a consequence, the adding of PHBV allows PLA to retain ≈ 25 % elongation at break, even on 750 h aged samples (**Figure 6.5** and **6.6**).

It was shown in previous studies that the PODC significantly improves the PLA ductility[7] by: 1) enhancing cavitation likely because of the important contrast between mechanical properties of the matrix and dispersed domains acting as flaws[29] and 2) extensively increasing the maximum size of cracks through easing of fibril formation probably due to plasticizer abilities.[30] Miscibility limit of PODC in PLA was already reached at 5 wt%. It was also observed that the non-miscible part appears as inclusions in the PLA. SEM micrographs of unaged PLA/PODC/PHBV samples show the presence of PHBV nodules and PODC

inclusions on the deformed surface. After one hour, relaxation of the macromolecules through physical aging increases the rigidity of the material (**Figure 6.6**) and thus enables cavitation (**Figure 6.7**). The mobility of the matrix induced by the miscible PODC allows a plastic deformation around inclusions (PHBV and/or PODC non-miscible inclusions) and the formation of big cracks exposing fibrils. With the aging time, we observe that cracks become thinner and wider indicating an embrittlement process induced by the physical aging.

6.4. Conclusion

Physical aging plays an important role in determining the long terms performance of polymers, especially PLA, whose T_g is close to ambient temperature. It is besides quite important to follow the stability over time of PLA toughened with different additives (PHBV and/or PODC) since phenomena like segregation or migration of additives can occur during physical aging. It was shown that physical aging induces a substantial decrease of the ductility within the first aging hours and that stagnation is reached after 48 hours for the formulated samples. For all the systems studied here, physical aging leads to promote brittle behavior by removing plastic deformation. This embrittlement process is associated with change of the deformation mechanisms. While homogenous shear deformation is predominant for unaged samples, physical aging leads to crazing mechanism, the density of crazes formation depending on the samples formulation (PHBV and/or PODC).

Considering long term performances, it seems that PLA/PHBV/PODC blends are the most promising materials for the toughening of PLA. Indeed, for these blends significant improvement in the strain at break was observed, along with a limited depression of the Young modulus and the stress at yield in comparison to neat PLA, as well as an improved thermal stability.

Acknowledgement

This work was financially supported by Brodart Packaging and the BIP-ADEME French project CREABioM. The authors also gratefully thank the laboratory Institut des Corps Gras (ITERG – Bordeaux, France) for its technical support. The authors acknowledge sincerely Prof. B. Fayolle for helpful discussions and valuable remarks that have much improved the manuscript.

REFERENCES

1. Auras, R.; Harte, B.; Selke, S., An Overview of Polylactides as Packaging Materials. *Macromolecular Bioscience* 2004, *4* (9), 835-864.

2. Domenek, S.; Courgneau, C.; Ducruet, V., Characteristics and applications of PLA. In *Biopolymers: Biomedical and Environmental Applications*, Kalia, S.; Averous, L., Eds. John Wiley & Scrivener Pub.: 2011; pp 183-223.

3. **(a)** Yang, X.; Kang, S.; Hsu, S. L.; Stidham, H. D.; Smith, P. B.; Leugers, A., A Spectroscopic Analysis of Chain Flexibility of Poly(lactic acid). *Macromolecules* 2001, *34* (14), 5037-5041.
(b) Kang, S.; Zhang, G.; Aou, K.; Hsu, S. L.; Stidham, H. D.; Yang, X., An analysis of poly(lactic acid) with varying regio regularity. *The Journal of Chemical Physics* 2003, *118* (7), 3430-3436.

4. Ruellan, A.; Ducruet, V.; Domenek, S., Plasticization of Poly(lactide). In *Poly(lactic acid) Science and Technology: Processing, Properties, Additives and Applications*, The Royal Society of Chemistry: 2015; pp 124-170.

5. Liu, H. Z.; Zhang, J. W., Research Progress in Toughening Modification of Poly(lactic acid). *J. Polym. Sci. Pt. B-Polym. Phys.* 2011, *49* (15), 1051-1083.

6. Ruellan, A.; Guinault, A.; Sollogoub, C.; Ducruet, V.; Domenek, S., Solubility Factors as Screening Tools of Biodegradable Toughening Agents of Polylactide. *J. Appl. Polym. Sci.* 2015, *Special Issue: Manufacturing of Advanced Biodegradable Polymeric Components*.

7. **(a)** Ruellan, A.; Guinault, A.; Sollogoub, C.; Chollet, G.; Ait-Mada, A.; Ducruet, V.; Domenek, S., Industrial vegetable oil by-products increase the ductility of polylactide. *Express Polymer Letters* 2015, ***submitted***.
(b) Ruellan, A.; Gratia, A.; Guinault, A.; Sollogoub, C.; Chollet, G.; Ducruet, V.; Domenek, S., Biobased and biodegradable by-product of oil industry as toughening agent of polylactide. *J. Appl. Polym. Sci.* 2015, ***intended*.**

8. **(a)** Odent, J.; Raquez, J.-M.; Duquesne, E.; Dubois, P., Random aliphatic copolyesters as new biodegradable impact modifiers for polylactide materials. *European Polymer Journal* 2012, *48* (2), 331-340.
(b) Nanda, M. R.; Misra, M.; Mohanty, A. K., The Effects of Process Engineering on the Performance of PLA and PHBV Blends. *Macromol. Mater. Eng.* 2011, *296* (8), 719-728.

9. **(a)** Boufarguine, M.; Guinault, A.; Miquelard-Garnier, G.; Sollogoub, C., PLA/PHBV Films with Improved Mechanical and Gas Barrier Properties. *Macromol. Mater. Eng.* 2013, *298* (10), 1065-1073.
(b) Tri, P. N.; Domenek, S.; Guinault, A.; Sollogoub, C., Crystallization behavior of poly(lactide)/poly(-hydroxybutyrate)/talc composites. *J. Appl. Polym. Sci.* 2013, *129* (6), 3355-3365.
(c) Zhang, L. L.; Xiong, C. D.; Deng, X. M., Miscibility, crystallization and morphology of poly(beta-hydroxybutyrate)/poly(d,l-lactide) blends. *Polymer* 1996, *37* (2), 235-241.
(d) Zhang, M.; Thomas, N. L., Blending polylactic acid with polyhydroxybutyrate: The effect on thermal, mechanical, and biodegradation properties. *Advances in Polymer Technology* 2011, *30* (2), 67-79.
(e) Zembouai, I.; Kaci, M.; Bruzaud, S.; Benhamida, A.; Corre, Y. M.; Grohens, Y., A study of morphological, thermal, rheological and barrier properties of Poly(3-hydroxybutyrate-Co-3-Hydroxyvalerate)/polylactide blends prepared by melt mixing. *Polym. Test.* 2013, *32* (5), 842-851.
(f) Gerard, T.; Budtova, T., Morphology and molten-state rheology of polylactide and polyhydroxyalkanoate blends. *Eur. Polym. J.* 2012, *48* (6), 1110-1117.
(g) Noda, I.; Satkowski, M. M.; Dowrey, A. E.; Marcott, C., Polymer alloys of Nodax copolymers and poly(lactic acid). *Macromol. Biosci.* 2004, *4* (3), 269-275.
(h) Ma, P.; Spoelstra, A. B.; Schmit, P.; Lemstra, P. J., Toughening of poly (lactic acid) by poly (β-hydroxybutyrate-co-β-hydroxyvalerate) with high β-hydroxyvalerate content. *European Polymer Journal* 2013, *49* (6), 1523-1531.

(i) Corre, Y. M.; Bruzaud, S.; Audic, J. L.; Grohens, Y., Morphology and functional properties of commercial polyhydroxyalkanoates: A comprehensive and comparative study. *Polym. Test.* 2012, *31* (2), 226-235.
(j) Gerard, T.; Budtova, T.; Podshivalov, A.; Bronnikov, S., Polylactide/poly(hydroxybutyrate-co-hydroxyvalerate) blends: Morphology and mechanical properties. *eXPRESS Polymer Letters* 2014, *8* (8), 609-617.

10. Ferreira, B. M. P.; Zavaglia, C. A. C.; Duek, E. A. R., Films of PLLA/PHBV: Thermal, morphological, and mechanical characterization. *Journal of Applied Polymer Science* 2002, *86* (11), 2898-2906.

11. Modi, S.; Koelling, K.; Vodovotz, Y., Assessing the mechanical, phase inversion, and rheological properties of poly- (R)-3-hydroxybutyrate-co-(R)-3-hydroxyvalerate (PHBV) blended with poly-(L-lactic acid) (PLA). *Eur. Polym. J.* 2013, *49* (11), 3681-3690.

12. Wang, S. A.; Ma, P. M.; Wang, R. Y.; Wang, S. F.; Zhang, Y.; Zhang, Y. X., Mechanical, thermal and degradation properties of poly(d,l-lactide)/poly(hydroxybutyrate-co-hydroxyvalerate)/poly(ethylene glycol) blend. *Polym. Degrad. Stab.* 2008, *93* (7), 1364-1369.

13. Celli, A.; Scandola, M., Thermal properties and physical ageing of poly (l-lactic acid). *Polymer* 1992, *33* (13), 2699-2703.

14. Pan, P.; Zhu, B.; Inoue, Y., Enthalpy Relaxation and Embrittlement of Poly(l-lactide) during Physical Aging. *Macromolecules* 2007, *40* (26), 9664-9671.

15. Cai, H.; Dave, V.; Gross, R. A.; McCarthy, S. P., Effects of physical aging, crystallinity, and orientation on the enzymatic degradation of poly(lactic acid). *Journal of Polymer Science Part B: Polymer Physics* 1996, *34* (16), 2701-2708.

16. **(a)** Pan, P.; Zhu, B.; Dong, T.; Yazawa, K.; Shimizu, T.; Tansho, M.; Inoue, Y., Conformational and microstructural characteristics of poly (L-lactide) during glass transition and physical aging. *The Journal of chemical physics* 2008, *129* (18), 184902.
(b) Zhang, T.; Hu, J.; Duan, Y.; Pi, F.; Zhang, J., Physical Aging Enhanced Mesomorphic Structure in Melt-Quenched Poly(l-lactic acid). *The Journal of Physical Chemistry B* 2011, *115* (47), 13835-13841.

17. Hassouna, F.; Raquez, J.-M.; Addiego, F.; Toniazzo, V.; Dubois, P.; Ruch, D., New development on plasticized poly(lactide): Chemical grafting of citrate on PLA by reactive extrusion. *European Polymer Journal* 2012, *48* (2), 404-415.

18. Dobircau, L.; Delpouve, N.; Herbinet, R.; Domenek, S.; Le Pluart, L.; Delbreilh, L.; Ducruet, V.; Dargent, E., Molecular mobility and physical ageing of plasticized poly(lactide). *Polym Eng Sci* 2015, *55*, 858-865.

19. Rasal, R. M.; Hirt, D. E., Toughness decrease of PLA-PHBHHx blend films upon surface-confined photopolymerization. *Journal of Biomedical Materials Research Part A* 2009, *88A* (4), 1079-1086.

20. Wang, H.; Sun, X.; Seib, P., Properties of poly(lactic acid) blends with various starches as affected by physical aging. *Journal of Applied Polymer Science* 2003, *90* (13), 3683-3689.

21. Gérard, T. Elaboration and characterization of multiphasic polylactide (PLA) and polyhydroxyalkanoates (PHA) multiphasic blends. Ecole Nationale Supérieure des Mines de Paris, 2013.

22. NatureWorks Processing Guides.
http://www.natureworksllc.com/~/media/Technical_Resources/Processing_Guides/ProcessingGuide_Crystallizing-and-Drying_pdf.pdf. (Accessed on September 2014)

23. Scandola, M.; Focarete, M. L.; Adamus, G.; Sikorska, W.; Baranowska, I.; Swierczek, S.; Gnatowski, M.; Kowalczuk, M.; Jedlinski, Z., Polymer blends of natural poly(3-hydroxybutyrate-co-3-hydroxyvalerate) and a synthetic atactic poly(3-hydroxybutyrate). Characterization and biodegradation studies. *Macromolecules* 1997, *30* (9), 2568-2574.

24. **(a)** Gérard, T.; Budtova, T. In *PLA-PHA Blends: Morphology, Thermal and Mechanical Properties*, International Conference on biodegradable and biobased Polymers - BIOPOL 2011, Strasbourg: France, Strasbourg: France, 2011.
(b) Blümm, E.; Owen, A. J., Miscibility, crystallization and melting of poly(3-hydroxybutyrate)/ poly(l-lactide) blends. *Polymer* 1995, *36* (21), 4077-4081.
(c) Koyama, N.; Doi, Y., Miscibility of binary blends of poly[(R)-3-hydroxybutyric acid] and poly[(S)-lactic acid]. *Polymer* 1997, *38* (7), 1589-1593.

25. Lixon Buquet, C.; Hamonic, F.; Saiter, A.; Dargent, E.; Langevin, D.; Nguyen, Q. T., Physical ageing and molecular mobilities of sulfonated polysulfone for proton exchange membranes. *Thermochimica Acta* 2010, *509* (1–2), 18-23.

26. Volynskii, A. L.; Efimov, A. V.; Bakeev, N. F., Structural aspects of physical aging of polymer glasses. *Polym. Sci. Ser. C* 2007, *49* (4), 301-320.

27. **(a)** Wu, S., Phase structure and adhesion in polymer blends: A criterion for rubber toughening. *Polymer* 1985, *26* (12), 1855-1863.
(b) Borggreve, R. J. M.; A Gaymans, R. J.; A Schuijer, J.; A Ingen Housz, J. F., Brittle-tough transition in nylon-rubber blends: effect of rubber concentration and particle size. *Polymer* 1987, *28* (9), 1489-1496.
(c) Muratoglu, O. K.; Argon, A. S.; Cohen, R. E.; Weinberg, M., Toughening mechanism of rubber-modified polyamides. *Polymer* 1995, *36* (5), 921-930.
(d) van Dommelen, J. A. W.; Brekelmans, W. A. M.; Baaijens, F. P. T., Micromechanical modeling of particle-toughening of polymers by locally induced anisotropy. *Mechanics of Materials* 2003, *35* (9), 845-863.

28. Bartczak, Z.; Galeski, A.; Kowalczuk, M.; Sobota, M.; Malinowski, R., Tough blends of poly(lactide) and amorphous poly([R,S]-3-hydroxy butyrate) – morphology and properties. *European Polymer Journal* 2013, *49* (11), 3630-3641.

29. Fond, C.; Lobbrecht, A.; Schirrer, R., Polymers toughened with rubber microspheres: an analytical solution for stresses and strains in the rubber particles at equilibrium and rupture. *Int J Fract* 1996, *77* (2), 141-159.

30. **(a)** Dettenmaier, M.; Kausch, H., Intrinsic crazes in polycarbonate: Phenomenology and molecular interpretation of a new phenomenon. In *Crazing in Polymers*, Springer Berlin / Heidelberg: 1983; Vol. 52-53, pp 57-104.
(b) Kramer, E.; Berger, L., Fundamental processes of craze growth and fracture. In *Crazing in Polymers Vol. 2*, Kausch, H. H., Ed. Springer Berlin Heidelberg: 1990; Vol. 91/92, pp 1-68.

CONCLUSION GENERALE

& PERSPECTIVES

Conclusion générale

L'amélioration de la ductilité du polylactide revêt une grande importance dans le développement de nouvelles applications, notamment au sein du marché de l'emballage alimentaire. Jusqu'alors, de nombreuses études, principalement ces quinze dernières années, ont apporté des avancées significatives qui permettent aujourd'hui au PLA d'être utilisé comme gobelet plastique, couverts jetables, films agricoles, fibres non tissées, bouteilles d'eau, emballages de légumes, etc. Pour cela, deux techniques ont majoritairement été utilisées, la plastification ou/et la dispersion d'éléments immiscibles tels que des modifiants aux chocs ou autres particules adéquates. Bien souvent, ces solutions n'ont pas permis de conserver l'entièreté de l'origine biologique renouvelable du matériau final, en ce sens que les additifs sont généralement issus de la pétrochimie. D'autre part, la biodégradabilité du PLA s'avère un atout majeur, au-delà même de l'aspect écologique évident. En effet, la désintégration contrôlée d'un tel matériau peut ouvrir de nouvelles perspectives, notamment son utilisation dans le domaine de l'agriculture pour des applications à fin de vie programmée. L'originalité de cette étude réside donc dans l'intransigeance pour le développement d'un produit entièrement biosourcé et biodégradable selon la norme EN 13432. Enfin, dans le cas d'un contact direct avec les aliments, dans la mesure où l'aptitude au contact alimentaire est bien entendu requise, le choix des additifs est d'autant plus restreint.

Afin de développer une telle solution, répondant notamment au cahier des charges du groupe Brodart, porteur du projet dont la spécialité est la transformation de films souples pour l'emballage alimentaire, les recherches ont été réalisées en plusieurs étapes. Outre les études bibliographiques initiales, les expériences ont notamment exploré l'utilisation d'additifs biosourcés biodégradables potentiellement plastifiant et disponibles commercialement, tels que le Polysorbid® 37 ou le squalène. Au regard des propriétés thermomécaniques

développées, notamment rapportées aux solubilités calculées et la comparaison des effets obtenus en utilisant des plastifiants pétrochimiques connus, nous avons défini un profil physicochimique adéquat. Ainsi, le DOA et le squalène ont montré la possibilité d'obtenir d'importants allongements à la rupture tout en conservant une rigidité acceptable et la vitrosité à température ambiante du PLA. Leur solubilité partielle dans le PLA en a été jugée comme responsable, particulièrement grâce à la combinaison des effets de plastification et de cavitation/craquelage. Il est également apparu par l'étude du PEG 400 l'importance de croiser les modèles de calcul de solubilité pour obtenir une indication plus fiable.

Au démarrage du projet, l'industrie de l'huilerie alimentaire a été ciblée comme générant un grand nombre de coproduits faiblement valorisés et potentiellement intéressants. Forts des études bibliographiques sur l'utilisation de la biomasse comme plastifiants et de nos résultats sur les mécanismes de déformation développés en fonction de la solubilité de l'additif, l'utilisation de coproduits non purifiés a été privilégiée. En effet, deux solutions de valorisation sont généralement possibles : l'isolement d'une molécule d'intérêt ou l'utilisation entière du coproduit généralement hétérogène. Les condensats de désodorisation d'huile végétale, présentant globalement une composition qualitative fixe (acides gras libres, mono, di et triglycérides, stérols et autres composés hydrocarbonés tels que le squalène) mais quantitativement variable, se sont avérés efficaces pour accroitre l'élongation à la rupture du PLA. Parmi ces derniers, les condensats de désodorisation d'huile de palme, très riches en acides gras libres, ont permis d'obtenir jusqu'à 180 % de déformation du PLA par rapport à sa dimension initiale, tandis que sa rigidité n'est diminuée que d'environ 35 % et sa température de transition vitreuse reste supérieure à 40 °C. Les acides gras libres avaient déjà été testés comme molécules plastifiantes du PLA, sans résultat probant. Au cours de nos expériences, il s'est avéré que la combinaison d'acides gras libres solides et liquides à température ambiante, en fonction de la longueur et du degré d'insaturation de leur chaine alkyle, ainsi que

l'hétérogénéité de composition, notamment la présence de glycérides, permettent de développer une ductilité significative. La solubilité limitée des composés provoquant, d'une part la plastification partielle du PLA, d'autre part la répartition des contraintes mécaniques au travers d'un mécanisme de cavitation/craquelage a été, là encore, mise en avant. En outre, il a été observé que les fonctions acides des acides gras libres entrainent une réduction sensible de la masse molaire du PLA, vraisemblablement par acidolyse des groupements esters, sans que cela ne conduise à une diminution significative de propriétés d'usage.

L'addition de condensats de désodorisation d'huile, notamment de palme (CDHP), améliore également la procéssabilité du PLA, à condition que le taux d'incorporation ne soit pas trop élevé (≈ 15 %m). La diminution des températures d'extrusion, rendue possible par l'action conjointe de la plastification et de la lubrification engendrées par le coproduit, permet de mettre en oeurve un film de PLA sur une ligne de gonflage de gaine à l'échelle semi-pilote. La formulation avec le CDHP a également été menée par extrusion bivis sur une machine de taille semi-industrielle (⌀vis = 35 mm) montrant une excellente stabilité du procédé. Les propriétés physicochimiques de films fins de PLA contenant 10 %m de CDHP, réalisés par extrusion de film à plat et gonflage de gaine, ont été étudiées. Malgré la faible épaisseur des films (≈ 25 mm), le mécanisme d'augmentation de la ductilité par endommagement reste parfaitement efficace. Une légère infériorité d'élongation à la rupture des films obtenus par gonflage de gaine ($\varepsilon \approx 90$ %) par rapport aux films extrudés à plat ($\varepsilon \approx 130$ %) a néanmoins été observée, sans que l'on en identifie la cause (biorientation, défauts physiques liés au gonflage, etc.). L'évolution des propriétés thermomécaniques des films a été contrôlée après 6 mois de stockage en conditions ambiantes. La fragilisation classique du PLA a été constatée, à un rythme toutefois plus lent que rapporté pour les matériaux formulés avec des plastifiants usuels. Les propriétés barrière à l'oxygène des films PLA formulés avec 10 %m de CDHP ne montrent également pas/peu de différence par rapport à un film vierge. Néanmoins, le CDHP

engendre une modification significative de la cristallisation du PLA. La comparaison de deux plaques de PLA grade semicristallin, mises en œuvre à 190 °C puis immédiatement trempées dans l'eau froide, montre que celle contenant 10 %m de CDHP affiche déjà une cristallinité d'environ 20 % tandis que celle n'en contenant pas est restée amorphe. De plus, après un recuit à 90 °C pendant 24 h, celle formulée avec le CDHP présente une cristallinité d'environ 48 % alors que l'autre stagne à un taux de 35 %. Les propriétés plastifiantes de la partie miscible du CDHP couplées à des effets nucléants possibles de la fraction insoluble pourraient être à l'origine de tels résultats. Enfin, les propriétés d'usage telles que l'aptitude au contact alimentaire en conditions de stockage réfrigérées ou ambiantes, ainsi que la biodégradabilité, ont été vérifiées par un organisme certificateur (L.N.E). Le conditionnement d'aliments gras, acides et produits laitiers serait possible en environnement réfrigéré, tandis que seul l'emballage de produits gras serait accepté en conditionnement à température ambiante.

L'influence du CDHP sur les propriétés de vieillissement du PLA, notamment sa relaxation enthalpique et l'évolution des mécanismes de déformation mécanique, a été étudiée en comparaison aux effets du PHBV, polyester immiscible dispersé sous forme nodulaire connu pour améliorer la ductilité du PLA. Il est apparu que malgré la plastification engendrée par le CDHP, la vitesse de relaxation enthalpique est diminuée. *A contrario*, le PHBV qui est immiscible dans le PLA mais présent sous forme de nodules de petite taille (submicronique) n'altère pas cette propriété. L'observation de l'évolution des mécanismes de déformation en traction uniaxiale montre que le PLA passe d'un mécanisme ductile (bandes de cisaillement) à fragile (craquelage et fractures) sous 48 h. Pendant ce temps, l'élongation à la rupture diminue drastiquement de 300 à 15 % et la rigidité est multipliée par 1,5. L'ajout de PHBV sous forme nodulaire submicronique et micrométrique ne semble pas modifier la cinétique de vieillissement court, mais après environ 12 h, les propriétés mécaniques stagnent et le matériau conserve une élongation à la rupture d'environ 25 %. L'observation de la surface des

échantillons déformés montre l'apparition d'un grand nombre de petites craquelures, probablement nucléées et stoppées par les particules de PHBV. Enfin, le CDHP semble rapidement provoquer (sous 1,5 h) l'apparition d'immenses craquelures exposant des fibrilles de PLA. La diminution des propriétés mécaniques stoppe rapidement après 5 h et le matériau conserve une ductilité d'environ 130 %. Notons que la forme des craquelures évolue sensiblement avec le temps, passant d'une géométrie sphéroïdale à elliptique.

Enfin, ce projet de recherche à permis à la société Brodart de co-développer la formulation d'un film correspondant en partie au cahier des charges initialement établi, notamment pour l'emballage de fromage, et d'être co-dépositaire d'un brevet auprès de l'Institut National de la Propriété Industrielle (INPI) depuis mars 2014. Les compétences de transformateur de la société Brodart, en particulier liées au complexage de films souples, vont alors être déployées afin d'orienter les propriétés du matériau développé vers l'emballage souhaité, permettant en outre au groupe de communiquer activement sur sa très forte volonté d'innovation.

Perspectives

Les perspectives de ce travail sont nombreuses en raison 1) des hypothèses et pistes de recherche qu'il a permises d'ouvrir et 2) des multiples étapes restantes avant une mise sur le marché éventuelle.

Premièrement, l'influence des condensats de désodorisation sur le comportement de déformation mécanique du PLA via un mécanisme d'endommagement a été observée comme gouvernée par plusieurs facteurs. D'une part, la solubilité partielle de l'additif semble déterminante, le couple PLA/condensats de désodorisation pourrait être spécifique. Ainsi, il serait intéressant d'investiguer l'effet de ces coproduits sur d'autres matrices polymères vitreuses et disposées au craquelage telles que le polystyrène ou le polycarbonate. D'autre part, l'action synergique des composés solides et liquides sur la ductilité du PLA reste mal comprise. Il semble légitime de s'interroger sur le comportement mécanique à basse température des matériaux additivés, typiquement sous la température de fusion de l'acide oléique (≈ 12 °C), composé majoritaire de la fraction liquide. Cette étude permettrait de distinguer le rôle de l'état physique (liquide ou solide) de celui de la morphologie de la phase dispersée, c'est à dire nodulaire (acide oléique C18:1) ou allongée « type batonnets » (acide palmitique C16:0). Ensuite, l'hétérogénéité de composition a été constatée comme bénéfique à la ductilité sans que nous n'en comprenions la cause. Les élongations à la rupture obtenues grâce au condensat de désodorisation d'huile de palme, coproduit naturel complexe, ont toujours été supérieures à celles mesurées lors de l'ajout de compositions artificielles mimétiques simplifiées. La diversité des structures moléculaires permettrait-elle d'augmenter la miscibilité totale de l'additif et ainsi d'assurer une meilleure compatibilité avec la matrice, paramètre primordial pour le développement des mécanismes de cavitation/craquelage ? Enfin, le ralentissement de la relaxation enthalpique du PLA lors de l'addition de condensat

de désodorisation d'huile, notamment de palme, a été mis en évidence. Des études complémentaires sont nécessaires pour déterminer les mécanismes à l'origine de ce phénomène, en particulier l'étude des interractions polaires. Pour cela, des mesures comparatives par analyse mécanique dynamique (DMA) entre un PLA amorphe additivé ou non avec du CDHP, afin d'observer les transitions secondaires, ou encore des analyses par spectroscopie diélectrique, pourraient fournir de précieuses informations.

Deuxièmement, d'importantes actions doivent être réalisées pour fianliser le projet avant une commercialisation éventuelle. Dans l'optique d'un développement industriel, le volume requis des condensats de désodorisation serait important et un approvisionnement stable necessaire. Il est alors primordial d'étudier leur composition en fonction des différents procédés d'obtention, de la saison, de l'usine, de la variabilité de la biomasse, etc. Ensuite, la rédaction d'un cahier des charges des coproduits, afin de mettre en place un suivi qualité, serait indispensable. En outre, le traitement des questions réglementaires, notamment les nécessités pour inscrire les coproduits sur la liste positive des additifs pour matériaux au contact des aliments, reste en suspens. Concernant la mise en œuvre, il faut encore valider l'extrudabilité à plat et/ou gonflage de gaine de larges laizes (> 50 cm) de films fins. En outre, l'extrusion de plaques, leur thermoformage et l'analyse de leurs propriétés seraient également à investiguer et permettraient d'ouvrir potentiellement de nouveaux marchés, notamment celui des barquettes alimentaires. Ensuite, le complexage des films fins développés avec d'autres matériaux n'a pas encore été étudié. Il peut être réalisé avec une colle contenant ou non un solvant, il faudrait donc définir la technique à privilégier afin de ne pas altérer les propriétés du film. Enfin, la conservation de la rigidité du PLA, associée à l'obtention d'une nouvelle tolérance aux déformations mécaniques, permettent au film additivé de conserver le pli. Il reste toutefois à définir la forme du packaging et réaliser des essais d'emballage et conditionnement des aliments concernés.